WELDING Journal

May 2007

- Advances in Laser Technology
- EB Welding the F-14
- Stainless Steel Welding
  - Unique Structures
  - Problem Solving

PUBLISHED BY THE AMERICAN WELDING SOCIETY TO ADVANCE THE SCIENCE, TECHNOLOGY AND APPLICATION OF WELDING AND ALLIED JOINING AND CUTTING PROCESSES, INCLUDING BRAZING, SOLDERING, AND THERMAL SPRAYING


100 YEARS OF HARD WORK.
AND THAT'S JUST THE START.
When you've been around for a century, you learn a thing or two. Most importantly, that our customers' overall productivity relies on the wire innovations we create. We solve problems and deliver solutions, to make things easier on your end.
WE'RE SOLID WIRE EXPERTS, WITH A JOB TO DO.
National Standard
100 YEARS
Established 1907
©2007 National Standard, A Heico Wire Group Company.
NS
NATIONAL STANDARD
A HEICO WIRE GROUP COMPANY
WWW.NATIONALSTANDARD.COM 1.800.777.1618
Circle No. 44 on Reader Info-Card


Built TOUGH in USA by CMI for Welders around the WORLD.
Weld with the BEST
Forget the REST!
Your best source for Semi-Automatic and Automatic MIG welding guns: including air and water cooled, Push-Pull, and Smoke Extractor.
With us, customer support comes first: from custom designed MIG guns and consumables to rapid delivery.
Call us today to experience the best.
1-800-530-0032
CMI 400A MADE IN U.S.A.
Push-Pull MIG Guns for Aluminum & Stainless Steel Welding.
"Save time and money by connecting a CMI Push-Pull to your existing wire feeder."
CM INDUSTRIES® INC.
505 Oakwood Rd. Lake Zurich, Illinois 60047
PH. 847-550-0033 FX. 847-550-0444
CMINDUSTRIES.COM EMAIL: SALES@CMINDUSTRIES.COM

CONTENTS

May 2007 • Volume 86 • Number 5

Features

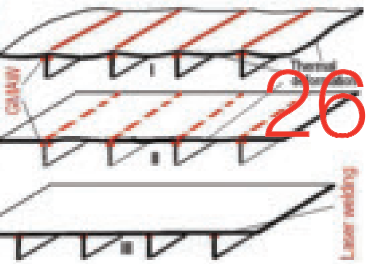

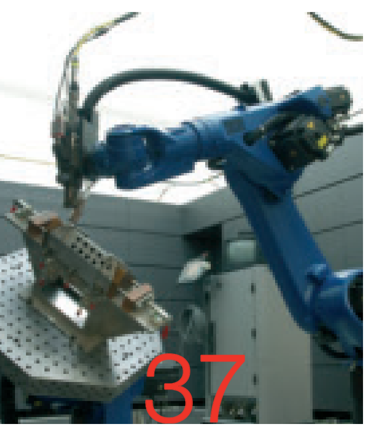

Welding Research Supplement

Cover photo: The three spires of the U.S. Air Force Memorial as seen overlooking Arlington National Cemetery. (Photo courtesy of TMR Consulting; Catherine Houska, photographer.)

AWS Web site *http://www.aws.org*

Departments

Welding Journal (ISSN 0043-2296) is published monthly by the American Welding Society for $120.00 per year in the United States and possessions, $160 per year in foreign countries: $7.50 per single issue for AWS members and $10.00 per single issue for nonmembers. American Welding Society is located at 550 NW LeJeune Rd., Miami, FL 33126-5671; telephone (305) 443-9353. Periodicals postage paid in Miami, Fla., and additional mailing offices. **POSTMASTER:** Send address changes to Welding Journal, 550 NW LeJeune Rd., Miami, FL 33126-5671.

U.S. Steel to Acquire Lone Star Technologies

United States Steel Corp., Pittsburgh, Pa., and Lone Star Technologies, Inc., Dallas, Tex., have entered into a definitive agreement where U.S. Steel will acquire Lone Star, a manufacturer of welded oilfield tubular goods, for $67.50 per share in cash.

U.S. Steel expects that the acquisition will strengthen its position as a producer of tubular products for the energy sector and will create North America's largest tubular producer. In addition, the transaction will broaden the company's energy product offerings by joining its predominantly seamless tubular business with Lone Star's complementary welded tubular business. Following the transaction, U.S. Steel will have annual North American tubular manufacturing capability of approximately 2.8 million tons.

The company projects that the combination with Lone Star's operations will generate annual pretax operating revenues in excess of $100 million by the end of 2008.

Airgas Agrees to Purchase Linde's U.S. Packaged Gas Business

Airgas, Inc., Radnor, Pa., recently announced a definitive agreement to acquire a significant part of the U.S. packaged gas business of Linde AG for $310 million in cash, to be financed under its revolving credit facility.

The operations to be acquired include branches, warehouses, packaged gas fill plants, and other operations involved in distributing packaged industrial and specialty gases and related equipment. The business includes 130 locations in 18 states, with more than 1400 employees. It generated $346 million in revenues and $36 million in earnings before interest, taxes, depreciation and amortization in the year ended December 31, 2006. Approximately 50% of the revenues were from gas sales and cylinder rentals, with the remainder from sales of welding equipment and supplies.

Upon closing, Airgas also intends to sell 17 of the acquired packaged gas facilities in the Carolinas, southern Virginia, and eastern Georgia to National Welders Supply Co., Inc., a joint venture between Airgas and the Turner family of Charlotte, N.C.

BAE Systems Awarded Multi-Ship Navy Destroyer Maintenance Contract

BAE Systems has been awarded a multi-ship, multi-option (MSMO) contract to maintain all Destroyer (DDG-51) Class ships homeported or visiting San Diego, Calif. The five-year contract includes execution planning, drydocking, and pierside maintenance, repair, and alteration work for 17 ships, if all options are exercised.

The first major repair availability on the contract will begin this June, with work on the *USS Howard* (DDG-83).

The award is a follow-on to San Diego's existing Destroyer MSMO contract. All work will be performed at the company's San Diego Ship Repair facility and will be completed by 2011.

Northwest Pipe Co. to Supply $12 Million of Pipe, Fittings

Northwest Pipe Co., Portland, Ore., has recently received a verbal commitment to be pipe supplier to Western Summit Constructors, Inc., of Denver, Colo., for the city of Aurora, Colo.

The company will supply pipe and fittings ranging from 10 through 72 in. diameter valued at approximately $12 million for an engineered and custom-fabricated piping system to be installed in the Utility Corridor and Yard Piping project. The pipe is expected to be manufactured in the company's Denver, Colo., division, and the majority of the fabricated items will be completed in Monterrey, Mexico. Delivery is scheduled to begin in the third quarter of this year.

WELDING Journal

Publisher *Andrew Cullison*

Editorial
Editor/Editorial Director *Andrew Cullison*
Senior Editor *Mary Ruth Johnsen*
Associate Editor *Howard M. Woodward*
Assistant Editor *Kristin Campbell*
Peer Review Coordinator *Erin Adams*

Publisher Emeritus *Jeff Weber*

Graphics and Production
Managing Editor *Zaida Chavez*
Senior Production Coordinator *Brenda Flores*

Advertising
National Sales Director *Rob Saltzstein*
Advertising Sales Representative *Lea Garrigan Badwy*
Advertising Production Manager *Frank Wilson*

Subscriptions
acct@aws.org

American Welding Society
550 NW LeJeune Rd., Miami, FL 33126
(305) 443-9353 or (800) 443-9353

EDITORIAL

RWMA Enters a New Era

An era is a segment of time that has distinct differences from other time periods. A new era has begun for the Resistance Welding Manufacturers Alliance (RWMA): the final stages of its reorganization will be completed in the coming year. The rebirth of the RWMA — with it becoming a vital asset in today's marketplace — will define this era. In the past, we have seen troubled companies that have not only been able to restructure themselves, but have exceeded their previous position in the marketplace. They have managed to do this by realizing that the assets they offer the market — defined and constrained by their resources — do not have to remain the same in the future; change is possible. A well-known, but very descriptive, example is that of Harley Davidson Motor Co. It was nearly forced to exit from the business of manufacturing motorcycles until the Harley employees defined the company's weaknesses and strengths. They studied the company's position not only with regard to the market at that time, but its potential for the future, then capitalized on opportunities with regard to market changes occurring at the time of the transition. The company relied on the strength and knowledge of the people involved to make accurate decisions and to rapidly put the changes in place.

The RWMA is in the midst of its own defining era. The first phase has consisted of merging into the AWS organization. Prior to RWMA's venture with AWS, it had become clear that the stagnation of growth in membership was due, to some degree, to the high cost of operating as an independent institution. With the reduction in cost, which the RWMA has been able to pass on to its current and potential members, as well as an increase in benefits, membership has been propelled upward at a manageable rate. Now that its financial footing is strong, the RWMA has embarked on the second phase: solidifying its presence in the metals joining marketplace as a valuable and progressive asset. As with the associates at Harley Davidson, the requirements are grueling, but the rewards will far outstrip them over the long run. An initial evaluation of the assets within reach of the RWMA and the current/future needs of the market has been completed. During this evaluation, a diverse panel took a realistic view of the current and projected market conditions.

The culmination of stepping into this new era begins with putting together a team of forward-thinking professionals to refine and implement a working program. Anyone in the metals joining industry who believes he or she can adapt to a fluid system geared toward managing the future in metals joining, should contact Susan Hopkins at (800/305) 443-9353, ext. 295, to see if your firm qualifies to participate.

In conclusion, I would like to say that from my own observations of companies in the resistance welding arena, those that take those changes in the marketplace that they may or may not have control of and mold them to benefit their institution are the leaders in their fields.

Michael Simmons
Chair, Resistance Welding Manufacturers Alliance (RWMA)

Grainger Presents Donation to Hobart Institute to Help Address Growing Shortage of Skilled Welders

The Hobart Institute of Welding Technology has received a $5000 donation from Grainger. In the picture, Andre Odermatt of Hobart (left) is shown with Octavia Matthews of Grainger.

Grainger, a national supplier of facilities maintenance supplies to businesses, recently donated $5000 to the Hobart Institute of Welding Technology (HIWT), Troy, Ohio. This contribution will be used to help the program purchase equipment for its classrooms and learning labs.

"We're proud to invest in the young people who will help fill the growing demand for skilled welders and other trade workers in our country," said Octavia Matthews, Grainger's Regional Branch Services vice president.

In fact, manufacturers across the United States are reporting a dire shortage of skilled tradespeople, including welders, electricians, and machinists. The American Welding Society predicts that by 2010, demand for skilled welders may outpace supply by about 200,000.

The HIWT, through specialized training and certification programs, is helping address this shortage by preparing young people for successful careers in welding.

"On behalf of the Board of Directors and staff of Hobart Institute, we're grateful to Grainger for this contribution that will have a direct influence on the training that our students receive," said Andre Odermatt, chairman of the Board and president.

Welding Highlighted in *Modern Marvels* TV Episode

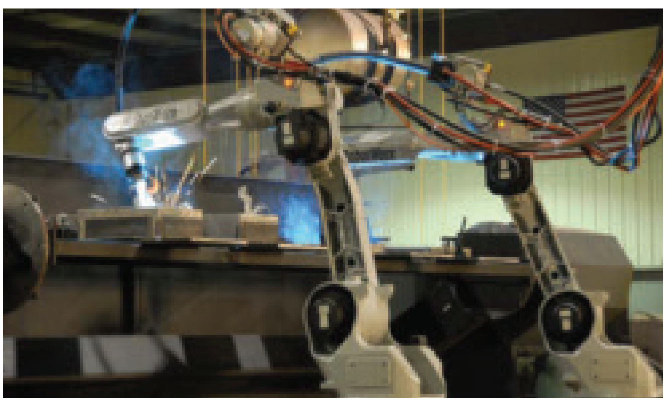

For the television show Modern Marvels: Welding*, RobotWorx was chosen to demonstrate industrial robotic welding. Displayed in the photograph are two Motoman UP6 XRC robots on a Motoman ArcWeld 6200. They are arc welding in tandem.*

Modern Marvels, a History Channel television series dedicated to the scientific innovation behind everyday items, will broadcast on May 9 an episode focused on welding. The episode, *Modern Marvels: Welding*, will cover the history, science, and technology of welding, and provide an overview of various welding methods, including shielded metal arc welding, gas metal arc welding, gas tungsten arc welding, resistance welding, explosion welding, underwater welding, welding in steel erection, automotive robotic welding, and more. In addition, the program will feature interviews of welding professionals in various capacities, including ironwork, technology, research, and engineering.

The American Welding Society, along with a selection of companies across the nation, assisted the History Channel in the production of this film, and several will be featured throughout. These include the following: Lincoln Electric Co., a welding and cutting products manufacturer based in Cleveland, Ohio; RobotWorx, a robotics integrator based in Marion, Ohio; Dynamic Materials Corp., a provider of explosion-welded clad metal plates based in Boulder, Colo.; and Global Industries, an offshore construction and engineering services company based in Sulphur, La.

The show's film crew visited with executives from RobotWorx to talk about robotic welding processes and the future of that industry. Because robots offer safe, high-quality, and affordable welds, president and owner Keith Wanner said that he expects a shift in the way of robotic welding is viewed in the future.

"I think what is going to change is people's acceptance of robots in the field," Wanner said. "As companies realize the benefits they offer, robots are becoming common manufacturing tools."

AWS Calls for Nominations for Fifth Annual Image of Welding Awards

The American Welding Society (AWS), Miami, Fla., is seeking nominations for its fifth annual Image of Welding Awards.

The awards are issued in seven categories, and the winners will be announced at the Image of Welding Awards ceremony to be held on November 12 during the FABTECH International & AWS Welding Show at McCormick Place, Chicago, Ill.

In addition, the awards recognize individuals and organizations that have shown exemplary dedication to promoting the image of welding in their communities.

The awards categories are as follows: Individual; Section (AWS local chapter); Large Business (200 or more employees);

Small Business (less than 200 employees); Distributor (welding products); Educator; and Educational Facility.

"Raising public awareness about welding is vital to creating a positive image for the industry," said Jim Horvath, chair of the AWS Image of Welding Subcommittee. "Every year, welding professionals triumph in inspiring young adults to join the field... honoring those who are driving real improvements for this industry encourages others to get involved."

Nominations will be judged by the Welding Equipment Manufacturers Committee (WEMCO), a standing committee of AWS that is composed of executives from welding industry suppliers to promote the welding equipment market.

To nominate an individual or organization for an award, please send a written explanation of the nominee's qualifications, along with your name, phone number, email, and mailing address, to Adrienne Zalkind at *azalkind@aws.org* or by postal mail to AWS Image of Welding Awards, 550 NW LeJeune Rd., Miami, FL 33126. The deadline for submissions is August 15.

Noble Signs Agreement with Arcelor Mittal

Noble International, Ltd., Warren, Mich., has recently signed a share purchase agreement with Arcelor Mittal to combine its TBA Arcelor laser-welding operations into Noble.

Arcelor Mittal will receive 9.375 million shares of Noble's common stock, at a price of $18 per share, with the balance in the form of cash, assumption of certain TBA obligations, and a subordinated note. The total value of the transaction is approximately $300 million.

At closing, Noble will operate a total of 22 manufacturing facilities. Noble and Arcelor Mittal will enter into a shared services and steel supply agreement to support the company's European operations. Additionally, Noble will have access to Arcelor Mittal's research and development efforts and the companies will work together to develop new products and applications.

The agreement also provides for the acquisition of the Powerlasers business of Dofasco, Inc., a Canadian subsidiary of Arcelor Mittal, in a separate transaction if and when it is available for sale.

The companies contemplate closing the TBA transaction during this summer.

American Iron and Steel Institute Selects the Pontiac Solstice for Award

The American Iron and Steel Institute (AISI), Detroit, Mich., has selected the product engineering and manufacturing team of the Pontiac Solstice for its inaugural Great Designs in Steel Automotive Excellence Award for the innovative and cost-effective use of advanced high-strength steels.

This award recognizes individuals or teams from automaker, supplier, and academic ranks who embrace innovation and make significant contributions to the advancement of steel in the automotive marketplace.

Award candidates were limited to presenters from the organization's Great Designs in Steel Seminar in 2006 and were rated in several categories. The Pontiac Solstice presentation was given by Warren Parsons and David Friddell of the General Motors Product and Manufacturing Engineering Operations Group.

According to AISI, new advanced high-strength steels offer significant weight savings and improved crash resistance. The Solstice uses several new steels and processing technologies, including sheet-hydroforming of outer body panels, to achieve class A surface quality and an eye-catching design at a lower cost than other materials. The Solstice roadster is also the first vehicle to incorporate dual-phase steel — a predominant advanced high-strength steel grade — into its hydroformed structure, consisting of dual-phase 600 grade tubes.

Shown above is the 2006 Pontiac Solstice. The product engineering and manufacturing team of this car has been selected by the American Iron and Steel Institute for its inaugural Great Designs in Steel Automotive Excellence Award.

— continued on page 113

Arcaloy stainless steel electrode (bare wire, rod and covered) products are manufactured under a carefully administered quality control program developed through years of experience. Since all Arcaloy products are produced under the ASME umbrella, the quality built into every product is consistent, time after time. Fabricators have learned to rely on Arcaloy stainless steel for exceptional results, guaranteed. Arcaloy offers:

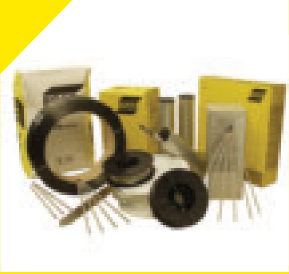

+ Engineered solutions
+ High productivity with maximum efficiency
+ Producible to exacting customers specifications
+ Unmatched reliability and consistency

Whatever your filler metal requirements, ESAB has the products you need and the quality you can trust.

GREAT THINGS HAPPEN WHEN YOU PUT US TO WORK
esabna.com + 1.800.ESAB.123

ESAB®
ESAB Welding & Cutting Products

Circle No. 30 on Reader Info-Card

European Union Imposes Duties on Chinese Welding Electrodes

The European Union (EU) recently imposed five-year tariffs on welding products from China to shield Austria's Plansee Metall GmbH from cheaper imports. The duties of as much as 63.5% on tungsten electrodes punish Chinese exporters for selling in Europe at below domestic prices or below the cost of production, a practice known as "dumping."

The aim is to "restore a level playing field that had been distorted by unfair trade practices," the 27-nation European Union said in a decision in March.

Plansee Metall GmbH, which produces more than half the EU's output of tungsten electrodes, suffered "heavy price pressure" and "injury" as a result of imports from China, the European Commission said in September 2006 when it imposed provisional tariffs.

Under EU practices, the commision can impose provisional antidumping duties for six months and the EU's national governments can turn those measures into "definitive" five-year levies at the same or different rates.

Canadian College Offers Extra Welding Classes to Meet Industry Demands

Industry's need for more welders drove Malaspina to add more welding classes

Malaspina University-College, Nanaimo, BC, Canada, recently began offering an extra Level C welding program to meet industry demand for trained welders.

"There are lots of good paying jobs for welders, especially in northern British Columbia and Alberta," said Dan Lines, associate dean of Trades & Applied Technology at Malaspina. The seven-month program leads to Industry Training Authority qualification as a Level C welder.

Chad Witczak, fabrication supervisor for Madill Equipment Canada, said there are plenty of jobs in mills and the oil patch for those willing to move to northern BC or Alberta. "From what I'm hearing, everything's booming out there right now," he said.

Lincoln Electric Acquires Electrode Manufacturer in Poland

Lincoln Electric Holdings, Inc., recently acquired SPAWMET Sp. z.o.o., a privately held manufacturer of covered electrode products headquartered near Katowice, Poland. SPAWMET's annual sales are approximately $5 million.

"This acquisition provides Lincoln with an excellent portfolio of stick electrode products, which will help us pursue our growth strategy for the distribution markets in Eastern Europe," said John M. Stropki, Lincoln's chairman and chief executive officer. "Moreover, the extensive distribution network of SPAWMET will enhance Lincoln's overall market position in Poland."

Synova Licenses Water Jet-Guided Laser Technology to Japanese Manufacturer

Synova, Lausanne, Switzerland, recently announced a licensing agreement with Kataoka Corp. under which the Japanese laser equipment maker will integrate Synova's proprietary Laser MicroJet® technology into its laser-processing systems sold exclusively in Japan. The collaboration also includes the opening of a joint micromachining center at Kataoka's Kuze facility in Kyoto that will serve as a manufacturing site for the company's new Laser MicroJet-integrated systems, as well as a demonstration, service, and support facility.

Synova's equipment combines a laser beam and a water jet so that a hair-thin water jet guides the laser beam. The technology creates a laser beam that is completely reflected at the air-water interface, similar in principle to an optical fiber. The water jet also cools the material surface for protection against thermal damage.

Kataoka produces YAG laser equipment for welding, cutting, and microprocessing applications.

North American Safety Products to Sell Italian-Made Perimeter Guarding Systems

SATECH perimeter guarding systems such as this one are now available to customers in the United States, Mexico, and Canada through North American Safety Products.

SATECH Safety Technology S.p.A., Milan, Italy, recently signed an agreement with North American Safety Products, Inc., Frankfort, Ill., to supply its modular perimeter guarding systems to customers in the United States, Canada, and Mexico. The products include a comprehensive range of panels, posts, access doors, brackets, and accessories.

The company's perimeter guarding options are easy to install. Comprehensive choices of hinged, sliding, and rise and fall access gate designs are available to fulfill a wide variety of machine access requirements.

BY DAMIAN J. KOTECKI

Q: How can submerged arc flux for welding stainless steel or nickel-based alloys be classified for purposes of a welding procedure specification (WPS) or procedure qualification record (PQR)?

A: There is no AWS filler metal specification that considers classification of submerged arc fluxes for welding stainless steels or nickel-based alloys. AWS classification of fluxes for welding of carbon steel is addressed by the AWS A5.17 specification, and classification of fluxes for welding of low-alloy steels is addressed in the AWS A5.23 specification. Both of these specifications classify flux by deposit mechanical properties (strength and toughness) with a specific wire, but these considerations, which are critical for carbon steel and low-alloy steel weldments, are usually of secondary importance at best when welding stainless steels or nickel-based alloys. As a result, the classification system used in the AWS A5.17 and A5.23 specifications is considered by the AWS A5 Committee on Filler Metals and Allied Materials as useless for stainless steel and nickel-based alloys.

For submerged arc welding of stainless steels and nickel-based alloys, the most important concerns, rather than mechanical properties, involve the chemical composition of the deposit. In particular, recovery of chromium and carbon in the weld metal is critical.

For applications chiefly concerned with corrosion resistance at or near ambient temperature, it is usually desirable to avoid carbon pickup from the flux. In general, it can be safely said that fluxes specifically designed for stainless steel welding, and advertised by their manufacturer as such, will not produce significant carbon pickup in the deposit as compared to the carbon content of the electrode. However, it is not uncommon to apply a flux that was originally designed for carbon steel or low-alloy steel to stainless steel welding or even to nickel-based alloy welding. It happens that many fluxes designed for carbon steel and low-alloy steel, usually those that are metallurgically basic (low in SiO_2), have attractive welding characteristics with stainless steel also. It can be attractive to the fabricator to use such flux for stainless or even for a nickel-based alloy because the fabricator need not inventory a special flux for the high alloys. Then it becomes important to inquire of the flux manufacturer whether or not the flux will produce carbon pickup when used with a high-alloy electrode.

A different picture emerges when a stainless steel or nickel-based alloy weldment is intended for high-temperature service. In this situation, carbon is a highly desirable alloying element because formation of chromium and other alloy carbides improves creep resistance. Then preservation of the normally high carbon content of the electrode when it transfers into the weld metal is important. Some SAW fluxes, usually those described as metallurgically acid (high in SiO_2), can significantly reduce the carbon content of the weld metal as compared to that of the electrode, which would generally be undesirable for high-temperature service. There are also fluxes containing carbonates or other carbonaceous compounds which can add carbon to the high-alloy deposit as compared to the carbon content of the electrode.

Preservation of chromium from the electrode to the deposit is also important, for maintenance of desired ferrite content, for corrosion resistance at temperatures at or near ambient, and for oxidation resistance at high temperatures. There are fluxes, usually metallurgically acid, which remove chromium from high-alloy weld metal. There are other fluxes, usually metallurgically basic, which pretty well preserve the chromium in the electrode — a loss of on the order of 1% might be expected. And there is a third group of fluxes, often described as “chromium-compensating,” which contain metallic chromium or ferro-chromium particles within the flux particles. This third group of fluxes can produce weld metal with significantly more chromium content than that of the electrode used to make the weld.

On more than one occasion, I have proposed to the AWS A5D Subcommittee that it develop a classification system for fluxes for stainless steel and nickel-based alloys based upon recovery of chromium and carbon. But the committee rejected the suggestion as being unnecessarily complicated and unlikely to lead to any degree of flux interchangeability for a WPS or a PQR. So, in the AWS system, you are left with having to write your WPS and PQR using the flux trade name as an essential variable. If you change the flux trade name, you must develop a new WPS and a new PQR.

An alternative to classification (or lack thereof) according to AWS may be found in the international standard ISO 14174, *Welding consumables — Fluxes for submerged arc welding — Classification.* This standard classifies SAW fluxes according to chemical makeup of the flux and applications for the flux. The chemical makeup of the flux is indicated by a symbol chosen by the manufacturer of the flux to indicate a rather loose composition range, such as “AB” for an aluminate-basic flux containing at least 20% Al_2O_3, at least 22% CaF_2, and at least 40% Al_2O_3 + CaO + MgO, or “CS” for a calcium-silicate flux containing at least 15% CaO + MgO and at least 55% CaO + MgO + SiO_2. But there is no indication of what constitutes the remainder of the flux. A “Class 1 flux” is suitable for carbon steels and low-alloy steels, a “Class 2 flux” is suitable for stainless steels, nickel-based alloys and some hardfacing applications, a “Class 3” flux is suitable for hardfacing only and adds alloying elements, and a “Class 4 flux” is suitable for both Class 1 and Class 2 applications. ISO 14174 doesn’t in any quantitative way address recovery of carbon or chromium, so its utility for high-alloy weld metals is somewhat limited.

Another possibility is to look to the European standard EN 760:1996, *Welding consumables — Fluxes, for submerged arc welding — Classification,* upon which ISO 14174 was based. Besides the chemical makeup of the flux and the applications for the flux, this classification system includes a nonmandatory indication of the metallurgical behavior of the flux. The symbols given for metallurgical behavior in this standard seem best geared toward describing what happens to Mn and Si content in carbon steel and low-alloy steel weld metal. If applied to stainless steel or nickel-based alloys, it would apply the symbol “1” for loss of over 0.7% Cr, symbol “2” for loss of 0.5 to 0.7% Cr, symbol “3” for loss of 0.3 to 0.5% Cr, symbol “4” for loss of 0.1 to 0.3% Cr, symbol “5” for loss of 0.1 to gain of 0.1% Cr, symbol “6” to gain of 0.1 to 0.3% Cr, symbol “7” to gain of 0.3 to 0.5% Cr, symbol “8” to gain of 0.5 to 0.7% Cr, and symbol “9” to gain of more than 0.7% Cr. Practically, however, this does not provide much differentiation among fluxes with which I am familiar, because all fluxes that are not chromium-compensating produce loss of nearly 1% Cr, or considerably more, when used with stainless steel or nickel-based alloy wires, while chromium-compensating fluxes produce more like 1% Cr gain. So, both acidic and basic fluxes would get the symbol “1” for chromium loss over 0.7%, and chromium-compensating fluxes would get the symbol “9” for more than 0.7% Cr gain. But there would be no fluxes in between symbol “1” and symbol “9”. I don’t find that very useful.

Evidence of lack of commercial usefulness of the EN 760 metallurgical behavior symbols is provided by the deletion of this provision when EN 760 was adopted as ISO 14174:2004, and my observation that even the European suppliers of fluxes for submerged arc welding of stainless steels and nickel-based alloys do not seem to use these metallurgical behavior symbols in their trade literature. The condition of EN 760 was reviewed by CEN TC121 SC3 (the European committee responsible for that standard) in March 2006, and the committee decided to make no revision for the present, but to see what, if anything, ISO TC44 SC3 does with regard to possible revision of ISO 14174 — ISO review of that standard is due to take place in 2007.

The Japanese standard JIS Z 3324, *Stainless steel solid wires and fluxes for submerged arc welding,* offers classification possibilities for fluxes for submerged arc welding of stainless steels. The flux classification, however, is only based on whether the flux is fused or bonded (agglomerated), and, if bonded, whether the flux changes the alloy type from the wire to the deposit (e.g., by adding Nb (Cb) through the flux, a 308-type wire can be converted into a 347-type deposit). Again, there is no possibility of indicating interchangeability of fluxes.

In conclusion, there appears to be no classification system for submerged arc fluxes for stainless steel or nickel-based alloys that would provide any degree of interchangeability for use in a WPS or in a PQR. And there appears to be nothing looming on the horizon that is likely to change that situation in the foreseeable future. You can only write your WPS or PQR around the trade name of the flux, which requires a new WPS and PQR whenever you change flux.♦

DAMIAN J. KOTECKI is technical director for stainless and high-alloy product development for The Lincoln Electric Co., Cleveland, Ohio. He is a past president of the American Welding Society, a vice president of the International Institute of Welding, a member of the A5D Subcommittee on Stainless Steel Filler Metals; D1 Committee on Structural Welding, D1K Subcommittee on Stainless Steel Welding; and a member and past chair of the Welding Research Council Subcommittee on Welding Stainless Steels and Nickel-Base Alloys. Questions may be sent to Dr. Kotecki c/o Welding Journal, 550 NW LeJeune Rd., Miami, FL 33126; or e-mail to Damian_Kotecki@lincolnelectric.com.

American Welding Society

Friends and Colleagues:

The American Welding Society established the honor of *Counselor* to recognize individual members for a career of distinguished organizational leadership that has enhanced the image and impact of the welding industry. Election as a Counselor shall be based on an individual's career of outstanding accomplishment.

To be eligible for appointment, an individual shall have demonstrated his or her leadership in the welding industry by one or more of the following:

- Leadership of or within an organization that has made a substantial contribution to the welding industry. The individual's organization shall have shown an ongoing commitment to the industry, as evidenced by support of participation of its employees in industry activities.

- Leadership of or within an organization that has made a substantial contribution to training and vocational education in the welding industry. The individual's organization shall have shown an ongoing commitment to the industry, as evidenced by support of participation of its employees in industry activities.

For specifics on the nomination requirements, please contact Wendy Sue Reeve at AWS headquarters in Miami, or simply follow the instructions on the Counselor nomination form in this issue of the *Welding Journal*. The deadline for submission is July 1, 2007. The committee looks forward to receiving these nominations for 2008 consideration.

Sincerely,

Alfred F. Fleury
Chairman, Counselor Selection Committee

Circle No. 58 on Reader Info-Card

AWS Joining Dissimilar Metals Conference
Orlando, Florida • Grosvenor Resort
May 22–23, 2007

One of the most discussed topics and sources of misunderstanding involves joining dissimilar materials by welding. Vendors probably receive more phone calls with questions on this subject than any other. The traditional codes are nearly silent on the issue. Many design, shop, or field organizations do not have—or have lost—expertise in this area.

This conference will address issues including material properties, weld properties, preheat/post-weld heat treatment, corrosion, the use of transition joints, service conditions, and practical considerations.

Even the most difficult-to-weld of all material combinations—steel to aluminum—has been welded satisfactorily using such techniques as explosion welding and magnetic pulse welding. New chemistries are coming to the aid of existing filler metals, making them more amenable to dissimilar metals welding. Filler metals based on nickel-base superalloy chemistries are also meeting the challenge. Advances in brazing technology are taking care of a host of metallurgical problems as well.

The problems are there, but so are the solutions.

The conference keynote address will be presented by Dr. Thomas Eagar from MIT, a noted expert in this most difficult area of welding.

Keynote address:
Dealing with Diversity in the Joining of Dissimilar Metals
Thomas W. Eagar, Professor, MIT, Cambridge, MA

"As product life cycles increase, and the need for fuel-efficient lightweight structures increases, designers are specifying both higher strength metals, as well as a greater diversity of metals. Fabrication of these structures in an economically efficient manner poses significant challenges, as our favored fusion welding processes are simply not practical (or possible) for many of these combinations of metals. Meeting these challenges requires both greater expertise of the fabrication engineer but also earlier involvement in the product design process."

Dissimilar Metal Weld Failures Involving Grade 91 Steel
Jeff Henry, Structural Integrity Associates, Inc., Chattanooga, TN

Advances in Friction Stir Welding and Application to Dissimilar Metal Joining
William J. Arbegast, NSAF Center for Friction Stir Processing, and Advanced Materials Processing and Joining Center, Rapid City, SD

Large-Area Soldering and Brazing of Dissimilar Materials with a Novel Heat Source
Dr. Timothy P. Weihs, Reactive NanoTechnologies, Inc., Hunt Valley, MD

CSC-Controlled Short Circuit Transfer – A New GMAW Process That Solves Old Weld Problems
Tom Rankin, ITW Jetline Engineering, Irvine, CA

Tensile Properties Evaluation of Dissimilar Welds in AL-6XN, DH-36, and A514 Gr. 2 Plate
Kim Tran, Surface Warfare Center Carderock Division (NSWC-CD), West Bethesda, MD

Magnetic Pulse Welding: Design and Analysis
Dr. James R. Dydo, Advanced Computational and Engineering Services, LCC (ACES), Gahanna, OH

Prediction of DMW Microsturctures
Dr. Damian J. Kotecki, The Lincoln Electric Company, Cleveland, OH

Explosion Welding – A Highly Versatile Welding Technology
John G. Banker, DMC Clad Metal, Boulder, CO

Alternative Filler Materials for DMWs Involving P91 Materials
Kent Coleman, Electric Power Research Institute, Charlotte, NC

Ultrasonic Welding of Dissimilar Metals
Dr. Karl Graff, Edison Welding Institute, Columbus, OH

The Way We Were – NDE from the Beginning
Mike Turnbow, Tennessee Valley Authority, Chattanooga, TN

Applications of Dissimilar Joint Metallurgy in the Chemical Process Industry
David Oulton, NOVA Chemicals (Canada) Ltd, Ontario, Canada

Inertia Friction Welding
Al Wadleigh, Interface Welding, Carson, CA

Conference price is $550 for AWS members, $680 for nonmembers. To register or to receive a descriptive brochure, call (800) 443-9353 ext. 223, (outside North America, call 305-443-9353), or visit www.aws.org/conferences

Electron Beam Welding System Features Lean Design

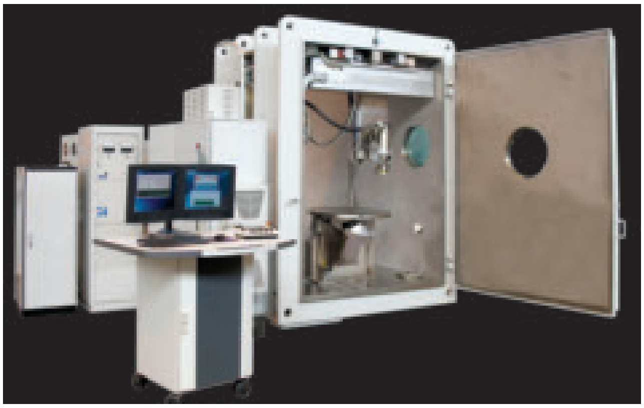

The NG1 — New Generation electron beam welding system features many improved system elements. The PC-based control system takes advantage of the company's experience using integrated CNC motion and process controls. With the capability of more than 10 axes of motion control, the system synchronizes the process parameters tightly. Capabilities include process monitoring with data acquisition, networking, and off-line programming. Open architecture allows for easy upgrading. The easy-to-use operator interface has pull-down menus and color graphics. System diagnostics, hard drive, and three levels of program access for security are included. In addition, the company's electron beam gun package provides an improved, narrow beam geometry that produces depth-to-width ratios and operational stability. Requiring little maintenance, the electron beam filaments can be changed out in 10 min at the end or beginning of any chamber cycle. The viewing system features high-resolution, precision gun optics with CCD camera and monitor. Optic focus, shutter and iris controls, and an electronic adjustable crosshair are built-in. A laser height measurement system can be implemented to provide automatic gun-to-work distance detection. Also, the solid-state power supply is designed to be a smaller unit that operates more efficiently. The design provides improved current and voltage quality as well as improved weld quality. The product's smaller footprint requires less shop space. The company has further provided the electron beam welding system with a more compact and flexible vacuum system, and made the entire unit easier to maintain.

Sciaky, Inc. **100**
4915 W. 67 St., Chicago, IL 60638

Pulsed Solid-State Laser Optimized for Cutting, Welding Applications

The TruPulse laser is a fully optimized successor to the HL line of TRUMPF lasers. The burst function allows the average power to be briefly exceeded and increases the pulse frequency, thereby reducing the welding cycle. Quasi-continuous seam welds are possible with longer pulses of up to 50 ms. The maximum mean power and pulse energy, focusability, and beam quality can also be adjusted depending on the requirements of the application area. A removable touch-screen control panel with turn-push knob is a feature to simplify setting output parameters. The product's solid-state laser's average power also ranges from 20 to 150 W at a maximum pulse power of up to 10 kW. Focused spot sizes from 50 to 300 μm are possible due to the wide range of fiber-optic cables available and processing optics. With a selectable pulse width between 0.2 and 50 ms, and pulse energies from 0.2 to 90 joules, the user has maximum flexibility for a wide range of applications from microwelding to joining of aluminum, stainless, platinum, or nitinol.

TRUMPF Power Tools **101**
111 Hyde Rd., Farmington Industrial Park
Farmington, CT 06032

Welding Machine Contains Seven-Tap Control Knob

The Handler® 187 GMA welding machine offers a seven-tap voltage selection control. Combined with this feature, better inductance enables the machine to provide better arc starts, smoother arc performance, create less spatter for less cleanup, and create weld beads with a professional appearance. According to the company, anyone welding stainless steel will especially notice beads with a flatter crown and good wet out at the toes of the weld. The product provides an extremely stable arc when welding steel as thin as 24-gauge while maintaining this performance on materials up to $\frac{5}{16}$ in. thick. The machine weighs 68 lb and has a welding output range of 25 to 185 A. It operates on standard 230/240-V power and accommodates a 4- or 8-in. spool of wire. A dual-groove drive roll accommodates 0.023–0.035 in. wire diameters. The machine is designed for welding with 0.023–0.035 in. mild steel or stainless steel, 0.030–0.045 flux cored, or 0.030–0.035 in. aluminum welding wires.

Hobart Welding Products **102**
PO Box 100, Lithonia, GA 30058

Ruby Grain Wheels Increase Productivity

The line of ruby surface grinding wheels is for fast material removal and strong form-holding capabilities. Ruby aluminum oxide (RA) grain is a tough, sharp, friable abrasive engineered for grinding all tool steels. Designed for fast material removal rates and reduced cycle times, these wheels increase productivity and require fewer dressing intervals. They are available in 7 to 14 in. diameters.

CGW-Camel Grinding Wheels **103**
7525 N. Oak Park Ave., Niles, IL 60714

Dust Collector Offers Big Capacity in Small Package

The Model RP-1 Twister™ is a compact dust collector with 1000 ft^3/min performance. It features cartridge collection with a cyclonic drop-out design, 99.999% efficient fire-retardant cartridge filter, and quiet operation. The dust collector measures 18.5 in. in diameter and 63.5 in. high, and also features the company's Roto-Pulse™ cartridge cleaning system.

It is designed to work in typical applications to remove grinding dust and welding smoke and fumes.

Micro Air **104**
PO Box 1138, Wichita, KS 67201

Finishing Tool Performs Consistently on Irregular Part Patterns

VersaFinish™ is an axially compliant finishing tool suited for robotic and automated material finishing operations on aluminum, plastic, steel, etc. The robust, low-speed, high-torque finishing tool has a "floating" motor and spindle arrangement that provides the finishing tip's axial compliance to perform consistently on irregular part patterns. The product, mounted to a robot or CNC machine, has a vane-type air motor with gear reduction. Remotely adjusted air pressure controls maintain a constant axial force on the floating spindle. The rotating spindle is equipped with a ⅜-in. chuck to hold a variety of finishing devices. The motor maintains a working spindle speed of 2600 rev/min, and the compliance force is 3.2–16.7 lb at air supply pressure of 5–60 lb/in.^{2}. The entire tool weighs 7.25 lb and requires 390 W of power.

ATI Industrial Automation **105**
Pinnacle Park, 1031 Goodworth Dr., Apex, NC 27539

Stainless Steel Electrode Useful for Seawater Applications

The company has introduced a flux cored electrode designed to weld duplex stainless steels. This all-position stainless steel wire, Select 2209-AP, exhibits high strength with corrosion resistance, especially to pitting from chlorides in seawater. It provides a stable arc with low spatter. The slag removes easily to enhance productivity, and the weld bead is shiny, smooth, and silvery. The product is well suited for welding stainless steels such as 22% chromium, 5% nickel, and 2% molybdenum-nitrogen types. It is also formulated for welding similar materials in a broad range of demanding applications.

Select-Arc, Inc. **106**
PO Box 259, Fort Loramie, OH 45845-0259

Manual Cold Saw Cuts Round, Square Shapes

The variable-speed Model C315/350V manual cold saw is designed to meet the need for a powerful, single-phase saw offering infinite control over blade speed. The saw uses a solid hinge-type design. A double vise assembly, with a 6¼ in. maximum opening, provides holding power on both sides of the cut for burr-free operation. Additionally, the saw features a 14-in. HSS blade, a three-phase TEFC motor, variable blade speeds from 24 to 105

rev/min, totally enclosed transmission, 24-V controls, and built-in flood coolant. The machine is also capable of cutting round shapes up to 4 in. in diameter at 90 deg and 3¾ in. in diameter at 45 deg; square and rectangular shapes up to 3¾ × 5 in. at 90 deg; and 3¾ × 3¾ in. at 45 deg.

Kalamazoo Machine Tool **107**
6700 Quality Way, Portage, MI 49002

In the April 2007 Welding Journal*, the following item from ELCo Enterprises, Inc., was featured in the New Products section on page 27, but its picture was not clear. This is the correct version.*

Wire Dispensing System Optimizes Production Time

The Non-Stop™ wire dispensing system, constructed with heavy-duty extruded aluminum, utilizes a process that joins the end wire from an empty drum with the start wire of the next full drum, eliminating downtime for wire changeover and optimizing production time. A smooth operating wire guide arm handles the wire transfer during the automatic change, with no manual operator action required. The system works with either one or two station robotic cells (two or four drums), and it is available for both 500- and 1000-lb Accu-Pak drums.

ELCo Enterprises, Inc. **108**
5750 Marathon Dr., Jackson, MI 49201

Glove Reduces Hand Fatigue

A leather palm and Kevlar® knit construction are combined to make the company's Kevlar LEA Series glove a choice for assemblers and fabricators. The result is a more comfortable, seamless knit glove that reduces chafing and hand fatigue while providing the kind of puncture, abrasion,

— continued on page 111

Investigating Fiber Lasers for Shipbuilding and Marine Construction

Laser beam technology promises both quality and cost advantages compared with the current arc welding processes

BY H. OZDEN

Currently, many ships are prefabricated as a number of individual sectional and modular construction units, and then assembled on the slipway partially in the water — Fig. 1. For the manufacturing of sectional and modular constructions of marine structures, the application of laser beam welding technology proves to be very favorable due to combined welding and cutting automation with the laser beam technique. Thus, productivity could be greatly improved with this technology compared with the arc welding method.

In shipbuilding, using fiber laser technology, the components can be joined together without welding edge preparation and pre- or postweld heat treatments. The resulting joints are more economical and are of better quality than arc welded joints. The laser produces a narrow weld joint with a small heat-affected zone (HAZ) compared with arc welding, plus there are no weld defects caused by arc blow or electrode wear, which can occur during conventional arc welding methods.

With fiber lasers, new welded structure designs can be realized that were not possible before. With arc welding, heat distortion and deformation often appear in the panels because of the high heat input. Laser welding of the same parts produces minimal heat distortion. The laser permits welding of pipes with a number of joint configurations, especially in underwater applications.

High-power fiber lasers with high beam quality and high efficiency are available for material processing, particularly for welding and cutting. High-power fiber lasers can weld thick sheet metals with very high speed (about 5 m/min) and on one side up to a wall thickness of 15 mm, and they can be welded bilaterally up to 30 mm economically with acceptable quality (Refs. 1–5).

The high-quality steels and light metals alloyed with Al, Mg, and Ti, which present various problems when welded with the conventional methods, can be easily welded with the laser beam technique. Thus, the unladen weight of ships is decreased, and production and operating costs as well as production times are reduced. For the manufacturing and/or building of sectional and modular constructions of marine structures, the application of laser technology proves as favorable, because laser beam welding and cutting can be combined and automated very well with each other.

However, for an economic evaluation of the laser beam-welded constructions, knowledge is necessary for the correlation among welding parameters, joining geometry, and fatigue strength characteristics of the materials used. The advancement of the high-power laser technology for welding of construction units in the I-butt jointconnection with joint columns can give new impulses to the welding technique. For example, the application of laser beam welding in ships, plants, and other steel buildings as well as in the offshore technology can spread rapidly. The laser beam connecting methods make newer construction techniques for ships and other marine structures possible (Refs. 1–5).

Comparison of Laser Beam Welding with Other Technologies

The advantages of laser beam welding in relation to conventional welding methods can be summarized as follows.

1. Materials Advantages

- Minimum, concentrated, point-shaped heat entry; hence, deep and slim zones of fusion with narrow HAZ — Fig. 2.
- High-melting metals are weldable due to the high power density.
- Reduction of microcracks
- Liquation by rapid cooling
- Suitability for joining numerous materials with different characteristics as well as material combinations
- Highly reactive as well as very pure materials are weldable under inert gas or vacuum
- Smooth joint surfaces; therefore, finishing is mostly unnecessary
- Decreased chemical changes such as small burn-up of alloying elements
- Fine-grained, generally defect-free joints with more favorable mechanical and technological characteristics can be made.

2. Construction Advantages

- High strength of the weld material and the HAZ (approximately the same strength of the base metal)
- Small residual stresses, small thermal distortion — Fig. 3.
- Accurately controllable with reproducible weld depths
- Production of narrow welded joints and small spot welds
- Production of the current-conducting

H. OZDEN (huseyin.ozden@ege.edu.tr) *is a professor in the Mechanical Engineering Dept., Ege University, Bornova, Izmir, Turkey.*

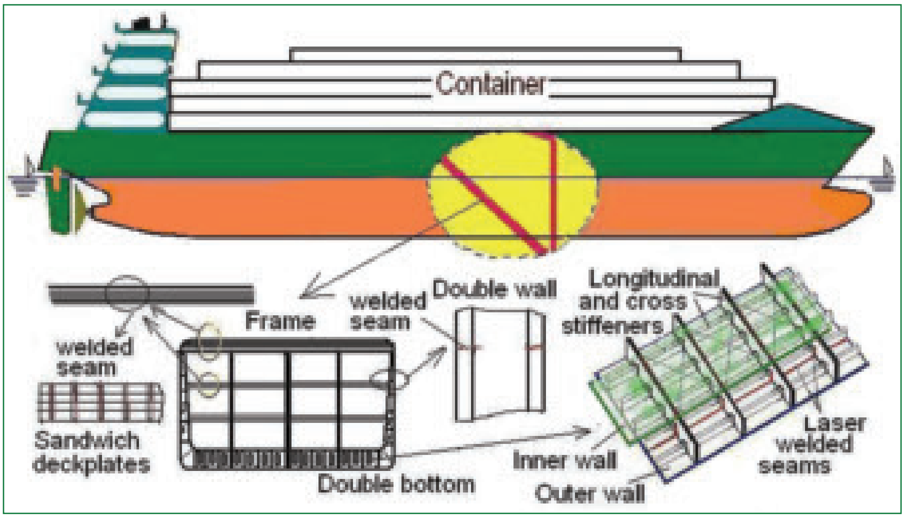

Fig. 1 — Schematic presentation of the shipbuilding units that are suitable for laser beam welding (not to scale).

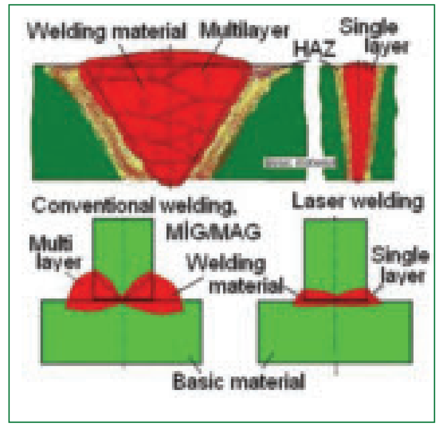

Fig. 2 — Comparison of joints welded with gas metal arc and laser beam welding.

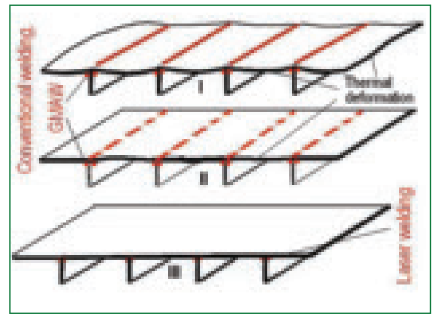

Fig. 3 — Comparison of the thermal deformations to metal plates resulting from gas metal arc welding vs. laser beam welding.

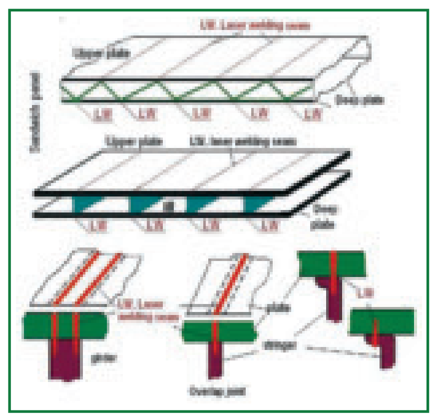

Fig. 4 — Laser beam welded sandwich panels featuring overlap joints.

connections of metals

- Production of connecting kinds that is not possible or is uneconomical with conventional welding methods such as welding below-deck sheet metals of ships and marine structures — Fig. 4.
- Manufacturing of sheet metals with thicknesses up to 15 mm faster and more economically than by welding methods with multilayer technology
- Smaller transition radius between the workpiece and the welded joint, and thus, more favorable fatigue resistance
- Suitability for welding of heat-sensitive construction units,
- Welding by transparent materials is possible.

3. Manufacturing Advantages

- Because of noncontact welding, tool wear does not occur
- Higher welding speeds offer much shorter welding times than with conventional welding methods
- Higher degree of automation and mechanization is possible
- Possibility for the combination of welding, cutting, and machining processes
- Higher reliability and reproducibility than with conventional methods
- Suitability of process control for quality increase is available in real time
- New and economical connection techniques in shipbuilding such as welding in ships with double walls
- Application in underwater welding under hyperbaric chamber gas conditions
- Property accessibility by large work distance and/or by inlet and focusing of the beam over long distance (fiber cables) in hard-to-access places
- Work in various atmospheres such as air or inert gas depending upon requirements (e.g. material ones)
- Larger flexibility using movable optics or fiber cables
- Supply of several work terminals over a multiplexer with fiber optics is possible (time-sharing operation)
- The parts to be joined require only a small clamping force
- Short warming-up and cooling times make short cycle times possible
- Little or no pollution of the environment.

4. Disadvantages

The following are some of the disadvantages of laser beam welding. The relatively narrow welds can lead to unacceptable weld joint failures, such as joints falling or burning notches. A further disadvantage in the application of the laser welding at the thick sheet metal connections is the occurrence of hot cracks and pores. With increasing joint depth and plate thicknesses, the frequency of the micropores increases due to the fast cooling and narrowed deep welding caverns, because degassing from the melting pool is hindered. Further, in laser beam welding, a multiplicity of factors such as laser beam characteristic values, welding process parameters, and material properties are present, which affect the reliability and the reproducibility of the welding results. Sufficient knowledge on the influence of the parameters on the mechanical technological characteristics of the thick sheet metal connections is still pending. The precise positioning of the laser beam in welding is a disadvantage.

Laser Beam Plants for Welding in Shipbuilding

The laser beam is a monochromatic light, i.e., it radiates with a characteristic wavelength of the respective beam source. Depending upon the laser-active medium, the laser beam can be ultraviolet, green, blue, red, or infrared. Depending upon the structure and kind of the beam source, the laser can radiate steadily or emit extremely short pulses. Nowadays, the following laser beam welding devices are used in shipyards, e.g., CO_2 laser with power performance $P = 40$ kW and wavelength $\lambda = 10.6$ µm; Nd:YAG laser with $P = 10$ kW, $\lambda = 1.064$ µm, and $\eta = 3\%–10\%$, as well as fiber laser with $P = 20$ kW, $\lambda = 1.070$ µm, and $\eta = 30\%$.

Depending on the laser type, the light beam is delivered, without loss, to the weld site using a mirror-and-lens system or light cables. (Ten-mm-diameter fiber-optic

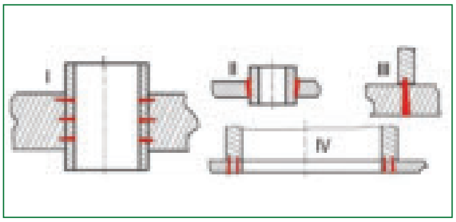

Fig. 5 — Plate-pipe joints suitable for laser beam welding (one-sided accessibility).

cable or beam fiber cable.) Laser beam delivery to the weld area with a beam cable depends on the wavelength of the laser beam. For example, the beam delivery of Nd:YAG lasers (short wavelengths) use a beam cable, and the beam delivery of CO_2 lasers use mirror systems.

The absorption and reflection characteristics of the obtained beam depend on the material and the wavelength of the beam. For example, Nd:YAG laser beam (λ = 1.06 μm) is absorbed more than the CO_2 laser beam and is reflected from materials less than CO_2 laser beams. There are different absorption characteristics for different materials; for example, absorption of the laser beam by aluminum is less than by iron and steel.

Currently one-side steel sheets with a thickness of 15 mm and double-side thick sheets with a thickness of 30 mm are welded without joint preparation. The developments of mobile, more compact fiber laser beam plants for welding and cutting are occurring rapidly.

High-Power Fiber Laser

Fiber lasers combine the advantages of diode-pumped solid-state lasers (Nd:YAG lasers) in an outstanding way with those from transverse electromagnetic waves. Fiber lasers offer high-power outputs with distinguished jet quality at the same time. The state of the art constantly changes with innovations in technology and with higher speeds. The laser welding machines are becoming more efficient and less expensive. Thus, laser beam welding and cutting of thick sheet metals in shipbuilding and marine engineering is becoming more attractive. The newest fiber lasers are able to do jobs that previously required a CO_2 laser.

Very good results have been obtained regarding flexibility and reliability using a 17-kW fiber laser (Ref. 5). The most important advantages of the fiber lasers compared with CO_2 and Nd:YAG lasers can be summarized as follows (Refs. 1–5). High output powers, excellent beam quality, electrical efficiencies above 25%, high flexibility, maintenance-free operation, simple operation, truly mobile system for service under field conditions, small size and weight, complete building method, and low purchase prices.

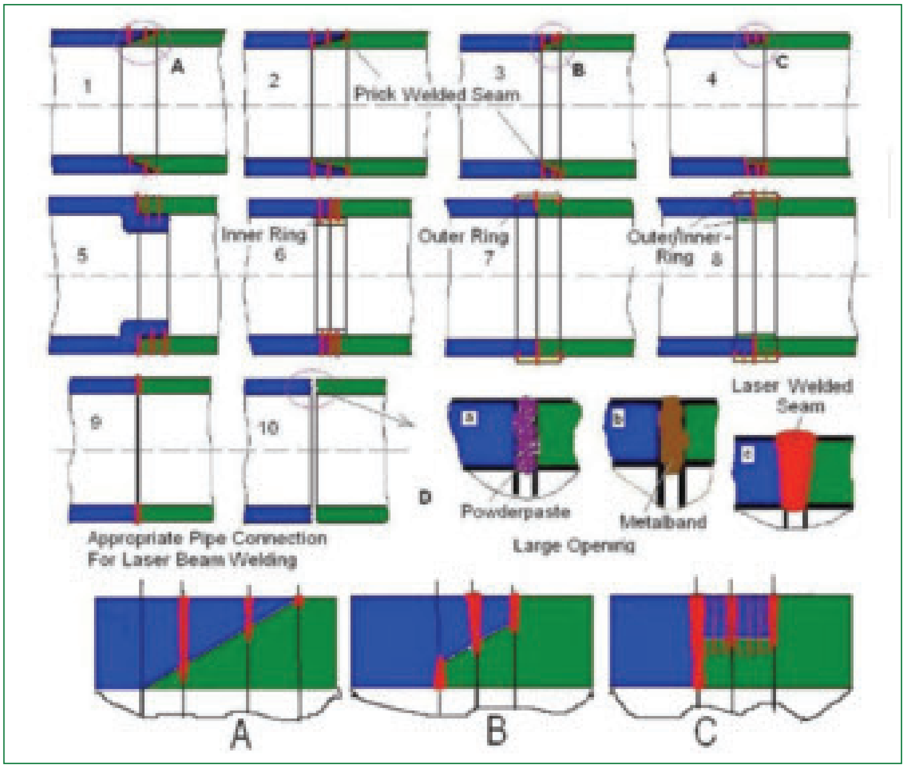

Fig. 6 — Typical pipe connections used in onshore and offshore applications (not to scale).

In the near future, it is expected that the conventional welding methods used in shipyards will be replaced with Nd:YAG and ytterbium laser procedures due to their low initial costs, mobility characteristics, and higher-power performance by which the thick sheet metals can be welded. The following tasks of the development are to be solved for the laser welding in shipbuilding and marine structures.

Development Trends of Laser Beam Welding in Shipbuilding and Marine Structures

Additionally, the following development phase tasks have to be solved for the application of laser beam welding in shipbuilding and marine structures.

Construction and joining techniques still require smaller tolerances in laser welding. Figures 5, 6 show schematic presentations of possible pipe connections in the onshore and offshore applications.

- Parameter studies for laser welding of thick sheet metal joints and material combinations are still missing.
- An interactive computer-aided database for the selection of optimal laser beam parameters has to be created.
- Investigations on the mechanical behavior of thick sheet metal welds and material combination joints performed by the laser beam method are lacking.
- The ability to bridge root openings using welding rod and filler metals such as wire, powder, powder paste, or band-stripe should be optimized.
- Fatigue strength characteristics of laser beam welded thick sheet metal joints should be determined.
- Laser systems should be more flexible and portable.
- Welding of coated surface joints is limited.
- The new techniques for improving laser beam welding efficiency should be developed (for example, preheating, absorbant coatings, etc.).

In summary, some suggestions for improving laser beam welding are as follows:

A combination laser beam should be developed that can penetrate solid materials and liquid mediums without breaking off, and can focus in the required welding or burning place — Fig. 7. Here, by using Lens 1, the concentrated laser beam I with suitable wave characteristics is accelerated and concentrated once again. By means of the focusing Lens 2, the enriched beams are focused on the burning place or joint to be welded, without significant breaking off or back reflections. The burning place can be adjusted in such a way that it can be radiated so long as no evaporation of the weld pool arises. After the solidification of the pool, a fixed joint results. Here, the pulsating laser beam could contribute to additional improvements such as deep welding without significant evaporation of the additive elements. The pulsations can contribute to the mixing of narrow melting and facilitate degassing as

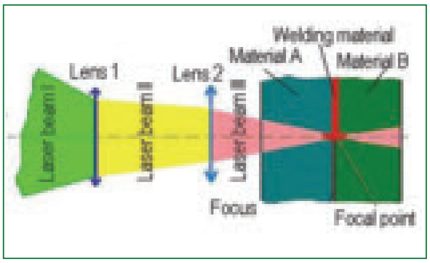

Fig. 7 — Graphic depicting the covered laser welding principle.

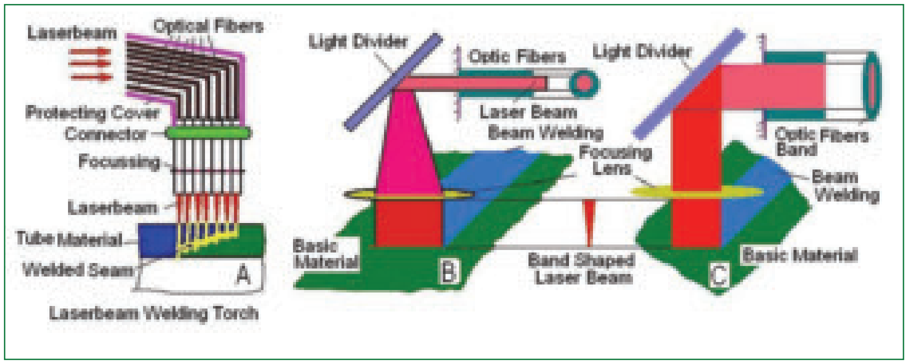

Fig. 8 — Graphic presentation of the broad-band laser beam burner principle.

in welding plastics, in which a similar procedure is already used successfully. This method can bring many further advantages in shipbuilding.

Figure 8 presents a further consideration in principle. The light-beam burner is intended for welding broader buildup joints and constructions with larger and variable joint columns. The light burner can be assembled from several individual light-beam burners, which are easily dissassembled again. Each individual burner is connected with individual light conductors that transfer laser radiation on the focusing lens of the burner. The burning depth can be selected by the individual lenses optionally. The light conductor could function here as power cable, as it is usual in the conventional arc welding method. In the other case, the light conductor transfers the produced laser beam into the housing of the laser burner. By the light distributors, the light is transmitted to the focusing lens; from there, the light beam is adjusted as band-shaped for welding. The same can be implemented with the accordingly formed light conductor. A further possibility is to produce the laser light in the burner by the lenses in three dimensions as a broader shaped laser beam.

Conclusions

High-power fiber laser beam technology opens numerous new work perspectives. Although applications for laser beam welding and cutting are still in the development stages, the laser beam welding method possesses many advantages in material processing as discussed in this article. It is regarded as the wear-free multitool of the century. Indeed, the substantial advantages of laser beam welding is the production of joints without joint preparation as well as without the need for pre- and postweld treatment of the parts.

With future improvements to the laser beam performance, beam quality, and efficiency, the laser beam welding and cutting of thick sheet metals will become more attractive in shipbuilding and marine engineering. The current problems in the production of thick sheet metal joints are solvable. By applying new techniques and performing suitable constructions for the laser beam method and with selection of optimal process variables, good welding results will be obtained.♦

References

1. *Laser Tools,* Trumpf. 2006. In German. Vogel Buchverlag, D.-Würzburg.

2. Sumpf, A., and Jasnau, U. 2005. Usage of fiber lasers as mobile beam source in the shipbuilding industry. I. Intern, Fraunhofer Workshop, *Fiberlaser*, Dresden, Germany.

3. Jasnau, U., and Schmid, C. 2006. Fiber laser cutting of thick metal sheets. 2. Intern, Fraunhofer Workshop, *Fiberlaser*, Dresden, Germany.

4. Verhaeghe, G. 2005. The fiber laser — a newcomer for material welding and cutting. *Welding Journal* 84(8): 56–60.

5. Thomy, C., Vollertsen, F., and Seefeld, T. 2005. Welding with high-power fiber laser. In German. *Laser Journal,* No. 3, pp. 28–31.

Stainless Steel Welding Soars to New Heights

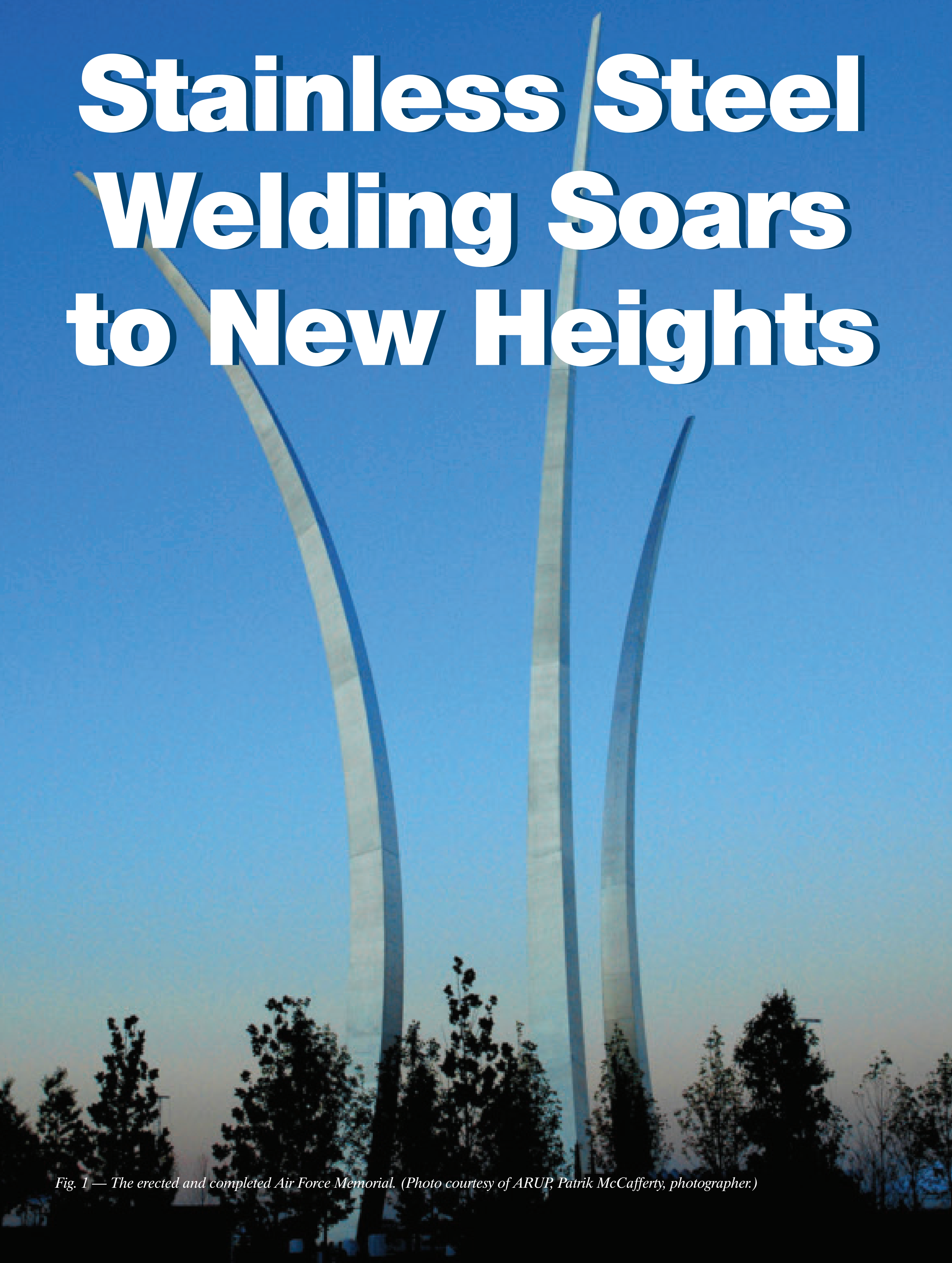

Fig. 1 — The erected and completed Air Force Memorial. (Photo courtesy of ARUP, Patrik McCafferty, photographer.)

High-quality stainless steel welds were critical to achieving the designer's long-term structural integrity and aesthetic goals

BY RON STAHURA AND CATHERINE HOUSKA

Gracefully curving, triangular, Type 316L stainless steel spires form the centerpiece of the new United States Air Force Memorial, which was dedicated in October 2006. Rising from a hill in Arlington National Cemetery and overlooking the Pentagon, the Air Force Memorial's three spires are a highly visible addition to the Washington skyline. This spectacular memorial honors the men and women of the U.S. Air Force and its heritage organizations while symbolizing its three core values — integrity, service, and excellence — and its total force, which encompasses the active duty, reserve, and guard forces. Its shape emulates the "bomb-burst" flying formation made famous by the Thunderbirds — Fig. 1.

High-quality welds were a critical aspect of achieving the designer's long-term structural integrity and aesthetic goals. Innovative weld fixturing (Fig. 2) and careful attention to joint detailing, specification, welding, and inspection were necessary to bring this world-class monument from concept to successful completion.

The Project

There were many challenging aspects to the design and construction of the Air Force Memorial, and all stem from the necessity of achieving the desired aesthetic impression under all light conditions while ensuring the structural integrity necessary for long service life. Designed by world-renowned architect James Ingo Freed of Pei Cobb Freed, the three stainless steel spires appear seamless as they rise to touch the sky and reach heights of 200, 230, and 270 ft above the ground.

Kyle Johnson, senior associate, Pei Cobb Freed & Partners, described the importance of the aesthetic appearance of the stainless steel welds as follows: "The design envisioned by architect James Ingo Freed required that the spires appear seamless and monolithic, rather than "assembled." In order to achieve this appearance, it was important that the welds be ground flush and finished to match the adjacent glass bead-blasted surfaces, so as to be virtually invisible."

The slender, curved unsupported shapes of the stainless steel spires make them sensitive to wind loading, which makes weld integrity critical, and extensive structural modeling was necessary — Fig. 3. Leo Argiris of ARUP, the consulting engineering firm involved with the project, commented, "The Air Force Memorial's cantilevered, curved spires are subject to dynamic excitations in all wind conditions. An internal damping system consisting of ball-in-box impact dampers (Fig. 4) was installed to minimize this dynamic behavior. As a memorial structure, the design life of the structure was important. In order to extend this life, all the welds were detailed to maximize their fatigue performance. These cyclically loaded welds had to be perfect and blended flush with the surrounding plate. Weld discontinuities such as incomplete fusion, cracking, or porosity could lead to catastrophic failure making high-quality welding and 100% visual and nondestructive inspection critical to the spires' long-term performance."

Tight dimensional tolerances were necessary to achieve the graceful shapes and smooth assembly, which made movement control during all stages of welded fabrication critical. Low-sulfur Type 316L stainless steel (≥ 0.005%) plate was specified for improved corrosion resistance and aesthetic appearance, which made it necessary to also use matching low-sulfur welding wire. The spires were fabricated from 380 tons of 0.75-in.-thick, low sulfur, Type 316L plate from Outokumpu Plate and 4 tons of matching welding wire from Avesta Welding.

The spires are partially filled with concrete to counterbalance their curved shapes and provide added stability, making the addition of internal stiffeners and rebar necessary — Fig. 5. The dampers and their supporting structures were also welded in place. Because of the need to closely control the shape of the spires and produce high-quality, well-blended welds, most of the fabrication was done in shop by Mariani Metal, Etobicoke, Ont., Canada, but with field erection and welding done by Cianbro, Pittsfield, Maine.

The Specifications

The design team realized that tight project specifications were necessary to communicate project requirements and establish tight process controls. ASTM specifications were used to define and to tighten stainless steel plate chemistry and flatness requirements. For example, ASTM A240 was used to establish the plate chemistry and property requirements, and it was further tightened to limit sulfur content (≤ 0.005%). ASTM A480 was used to define dimensional tolerance requirements, and its flatness requirements were tightened to meet project requirements, limiting the maximum deviation from flatness across the entire length and width of each plate to ⅛-in. ASTM A967 and A380 were also used to define surface chemical cleaning and surface preparation expectations.

AWS D1.6, *Structural Welding Code — Stainless Steel*, was used to establish requirements for welder qualification and procedural and inspection requirements. AWS welding consumable specifications (A5.4, A5.9, and A5.22) were specified and tightened to limit the filler metal sulfur content (≤ 0.005%). In addition, it was stipulated that all welds were to be ground flush in order to minimize stress concentrations, increase fatigue life, and as the first step in achieving a seemingly seamless memorial. Furthermore, to ensure that adjacent welded plate surfaces were flush to eliminate stress risers and aesthetic requirements, the fabricator had to maintain ± 1⁄16-in. adjoining plate surface tolerance requirements. The inspectors were certified in accordance with the requirements of AWS QC1, *Standard for AWS Certification of Welding Inspectors*.

Because the wind produces continuous cyclical loading, structural performance of the welds was critical. All complete joint penetration and partial penetration welds were subject to 100% visual inspection. In addition, all welds were inspected using dye penetrant and either ultrasonic or radiographic examination. The comprehensive requirements defined in AWS D1.6 were an invaluable tool to the architects, structural engineers, and metallurgists on the design team because it comprehensively covers welding requirements.

Development

Many factors influenced the selection of welding consumables for the application. Most of the welding was done under shop conditions, although field welding

*RON STAHURA (*ron.stahura@avestawelding.com*) is regional manager, Avesta Welding, LLC, Orchard Park, N.Y., and CATHERINE HOUSKA is senior development manager, TMR Consulting, Pittsburgh, Pa.*

Fig. 2 — To ensure an accurate fit, fixtures were utilized during fabrication. (Photo courtesy of Avesta Welding, LLC, Ron Stahura, photographer.)

Fig. 3 — A general layout of the 230-ft-tall spire #2. (Illustration courtesy of Mariani Metal.)

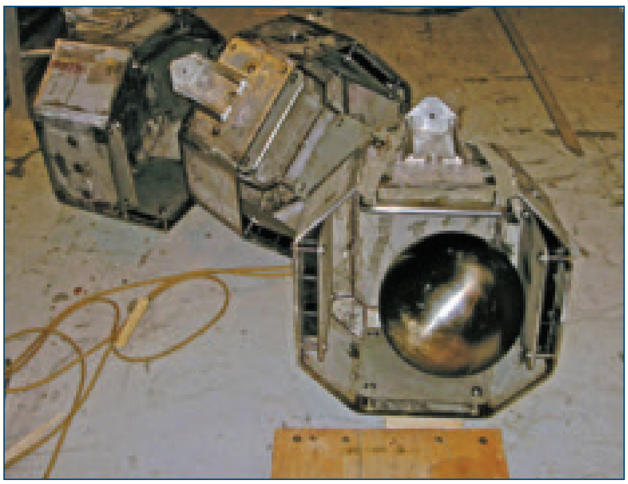

Fig. 4 — Six damper boxes containing a 20-in. steel ball were installed in each spire. (Photo courtesy of Mariani Metal, Len Barnes, photographer.)

was performed during the erection phase. The 316L stainless plate had to be welded with a high-deposition process, capable of producing repeatable, high-quality weld deposits. Mariani Metal's technical welding team had experience in welding stainless steel, but the enormous scope of this project with regard to physical size, lineal feet of weld, joint configurations, aesthetics, and quality assurance presented unique challenges.

After reviewing several welding processes and developing mock-ups (Fig. 6), the decision was made to focus on gas shielded flux cored arc welding (FCAW-G) as the primary welding process for this project. The consumable of choice was ⅟₁₆-in. E316LT0-1 gas shielded flux cored wire. This product is ideal for projects requiring high metal deposition rates. In-shop conditions of 11.5 lb/h were easily achieved in the flat and horizontal positions. The flux, which enhances the arc characteristics, contains slag-forming compounds and alloying elements. The weld metal chemistry had a restricted sulfur content (≤ 0.005%), and Avesta Welding was able to supply a single batch lot meeting this requirement.

The composition of the gas shielded flux cored wire was specifically formulated to ensure the correct chemical composition of the weld, good mechanical properties, and optimum welding arc characteristics. Len Barnes, fabrication project manager, Mariani Metal, stated: "The weld bead appearance was very good with virtually no spatter. Since cosmetics were very important on this job, this was monitored closely."

During the initial phase of welding the prototypes, different shielding gases were evaluated. Typically, a 75% argon/25% CO_2 or 100% CO_2 were used with good results. Len Barnes commented, "Since Mariani's facility is capable of mixing its own gas component ratios, we experimented with different combinations and settled on 60% argon/40% CO_2. It produced optimal arc characteristics for this application."

Equipment

In evaluating the welding equipment needed for this job, it became evident that they could primarily use existing capabilities with some minor modifications. Constant voltage power supplies were used since flux cored wire used in combination with an external shielding gas provides exceptional arc characteristics. This eliminated the need for high-technology equipment. The existing wire feeders were simply fitted with unique air-cooled torches specially designed by PAC-MIG, Inc., Wichita, Kans., to withstand the amperage requirements and high duty cycles, while keeping in mind operator comfort during long-duration welds. Knurled ⅟₁₆-in. feed rolls were fitted for optimal wire feed speed control.

Automation was used to reduce welder fatigue and maximize arc-on time. A torch was mounted on portable tractors that traveled on tracks held in place with suction cups. The use of suction cups also eliminated the possibility of surface damage.

Weld Joints

The joint configurations had a narrow footprint to meet aesthetic requirements and minimize the amount of weld filler

Fig. 5 — The interior of a modular section showing stiffeners that were welded to the anchor studs. (Photo courtesy of Avesta Welding, LLC, Ron Stahura, photographer.)

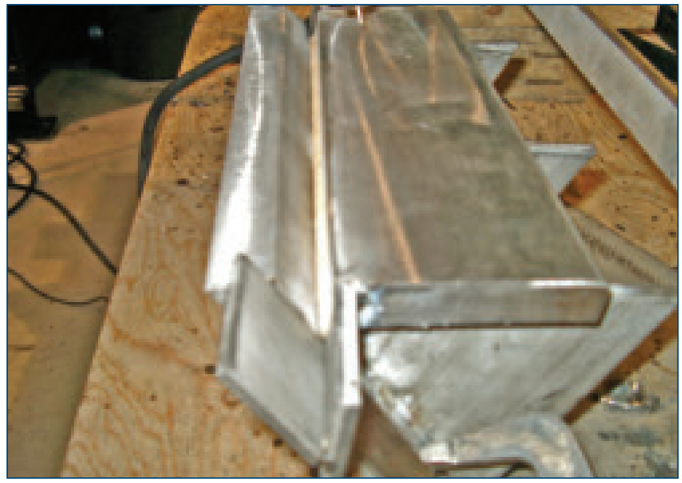

Fig. 6 — Exterior corner joint prepared during weld procedure development. (Photo courtesy of Avesta Welding, LLC, Ron Stahura, photographer.)

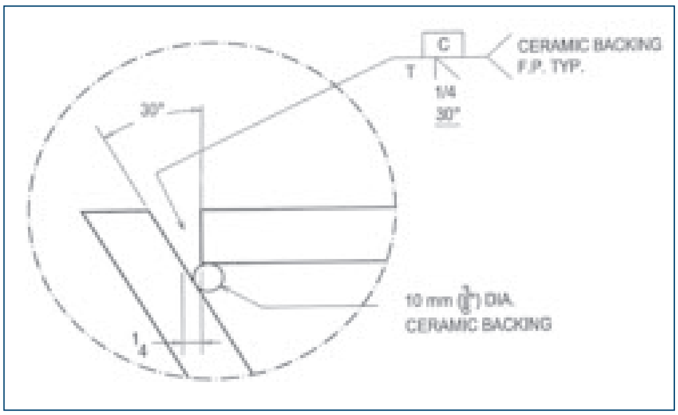

Fig. 7 — Outline of the three exterior spire corner joints. (Illustration courtesy of Mariani Metal.)

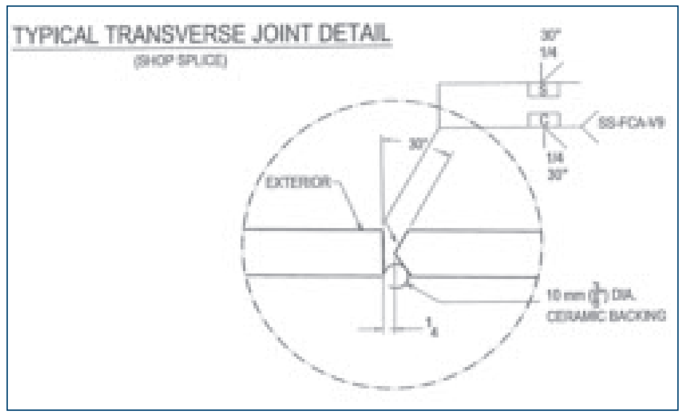

Fig. 8 — Outline of the numerous transverse welds that were used to join each plate in shop and modular section during field erection. (Illustration courtesy of Mariani Metal.)

metal, but this made welding more challenging. Several joint designs were considered, and Figs. 7 and 8 show the configurations selected. The corner- and butt-joint welds were all complete penetration — Fig. 9. Since 100% weld radiographic or ultrasonic inspection was required, procedures were submitted, as mandated per AWS D1.6, to ensure consistent results.

During development of the weld parameters, incomplete fusion and surface imperfections were observed in the root welds. A technical team from Avesta Welding worked closely with Mariani Metal to identify the problem and ensure the product was performing to the project's high standards. The problem was identified and 0.045-in.-diameter wire was used in the root pass. This was applied manually due to accessibility limitations, tight fitup, and the use of ceramic backing bars. In order to gain full access to this narrow groove configuration and maintain a proper 0.75-in. electrode extension, tapered contact tips and nozzles were used.

Excessive electrode extension would result in loss of working voltage and shielding gas coverage, which could induce atmospheric contamination. All of the consecutive passes were automated, utilizing the torch-mounted tractor. These subsequent automated welding steps increased efficiency and produced consistent welds throughout the project.

Stud Welding

Arc studs (concrete anchor type) were welded to the interior spire walls. The 12,000 low-sulfur Type 316L stainless steel studs were 0.75 in. diameter by 8 in. long. The arc stud welding method minimizes the heat-affected zone, ensures 100% penetration of the stud face, and reduces the possibility of distortion marks on the exterior surface. The parameter settings for the welding current were 1480 A, and the arc-on time was 0.8 s. Internal stiffeners were then welded to the studs to maintain structural rigidity. This required two fillet welds on each stud, so there were a total of 24,000 individual welds. All were completed in accordance with AWS D1.6, section 7, stud welding requirements.

Distortion Control

Because of the project's very tight tolerances, minimizing distortion by maintaining tight joint fitup was a significant concern throughout the project. One important aspect of achieving this goal was constant monitoring of the heat input and interpass temperatures. Temperature control is a critical aspect of minimizing distortion and limiting adverse metallurgical effects.

Due to physical property differences, management of the distortion of austenitic stainless is different from carbon steels and requires some adjustment in fabrication procedures. Specifically, stainless steel's heat conductivity is lower than that of carbon steel, and its coefficient of thermal expansion is higher. Barnes indicated, "We did not exceed interpass temperatures of 200°F to ensure that distortion was limited." Temperature was monitored using accurate electronic

Fig. 9 — Cross-sectional view of welded corner joint. (Courtesy of Mariani Metal, Len Barnes, photographer.)

Fig. 10 — During the erection phase, 40-ft sections were successfully welded together. The blue outer wrapping protects the exterior finish. (Photo courtesy of Avesta Welding, LLC, Ron Stahura, photographer.)

Fig. 11 — The modular section is hoisted for chemical treatments to clean and pickle prior to glass bead blasting. (Photo courtesy of Avesta Welding, LLC, Ron Stahura, photographer.)

indicating devices. In addition to increased accuracy, this eliminated a quality control step because foreign products were not introduced into the weld or heat-affected zone.

The average welding parameters were 275 in./min wire feed speed (260 A), 30 V (at 0.75-in. electrode extension), and the deposited weld travel speed rate was 13 in./min. The average heat input for the flux cored welding process was 36 kJ/in., which is well within the typical range that would be considered appropriate. To calculate heat input in kJ/in., the following formula applies.

$$\text{Heat Input} = \frac{A \times V \times 60}{S \times 1000}$$

where A = current (amps)

V= voltage (volts)

S= travel speed (in./ min)

$$\frac{260 \times 30 \times 60}{13 \times 1000}$$

Field Welding

Developing segment erection and field welding procedures for this one-of-a-kind project created interesting challenges for Cianbro Construction — Fig. 10. Each prefabricated section brought to the site was about 40 ft long. Working enclosures were necessary to shield each weld area from weather conditions during fabrication and surface finishing. Because the gas shielded flux cored process was used, air movement had to be minimized and welding could not occur if there was exposure to moisture.

Furthermore, chemical pickling of the weld areas was necessary to restore corrosion resistance and dull the finish. On a project of this scale, chemical treatments must be enclosed since the pickling product cannot be applied if there is direct sunlight or exposure to moisture, and it was necessary to have controlled collection of the rinse water used to remove the acid-based pickling product.

The field welding had to be done in the horizontal position, which required different procedures. In shop conditions, all of the fabrications were arranged in the favorable flat position. During the erection phase, this was no longer possible and fitup adjustments were necessary. The Avesta Welding technical team worked closely with Cianbro to develop field welding procedures, and it was determined that 0.045-in., 316LT1-1 all-position flux cored wire was the most appropriate choice. This product's smaller weld pool, combined with faster freezing arc characteristics, provided greater control of the molten weld pool. While gravity creates a whole new array of challenges, there is usually a welding consumable engineered for the application.

Because the joint configuration had to be welded from both sides, a planned sequence of weld passes was applied to the internal and external faces to minimize distortion. Prior to welding, temporary holding brackets and tack welds were put in place to ensure alignment throughout the welding process. Tight alignment was critical if the project was to achieve a visually seamless surface after welding and surface finishing. The result was a very effective distortion control plan.

Cleaning

In accordance with AWS D1.6, *Structural Welding Code — Stainless Steel*, section 5.2.1.1, surfaces on which weld metal is to be deposited must be clean and free from organic contaminants and surface oxides prior to welding. Hydrocarbons or sulfur-bearing products can have detrimental effects to stainless steel weld deposits. This cleaning was also done in accordance with ASTM A380 and A967. Standard procedures for cleaning between passes on single and multipass welds were also followed. Stainless steel wire brushes or grinding with wheels dedicated to stainless steel processing were used to remove any slag or heat oxide.

Because of aesthetic requirements, weld blending was a paramount concern. During shop fabrication, welds were ground flush with the surrounding plate surfaces. A 50-grit finish was applied to match the directionality of the ground finish on the surrounding plate. Then the entire section was cleaned to remove any fingerprints, dirt, and oils prior to the pickling process.

Each 40-ft-long, shop-fabricated segment was then chemically pickled to ensure restoration of the stainless steel's corrosion resistance and to dull the surface so that aesthetic goals could be achieved — Fig. 11. Because of the size of the fabrications, Avesta Welding's Red One™ spray pickling gel was applied to about 53,000 square feet of the entire exterior surface. This product was preferred because it was capable of producing the desired performance under the wide range of production temperatures.

The use of a gel product permitted rapid uniform coverage, which improved control over the pickling process and final appearance. This was done in accordance with ASTM A380. Deionized water was used to wash off the residual chemical pickling product. This cleaning prevented mineral staining of the surface, which could otherwise occur if potable water containing more than 200 ppm solids were used. The final finishing step was glass bead blasting. If there had been dirt accumulation or fingerprinting between pickling and bead blasting, the surface was cleaned prior to the final finishing step.

The same grinding, chemical pickling, and glass bead finishing steps were used to blend in the field welds after shielding the surrounding surfaces. Because glass bead blasting dents but does not remove the surface, the final finish should retain the corrosion performance advantage of chemical pickling.

Conclusions

Due to the complexity and unique characteristics of the Air Force Memorial fabrication process, innovative techniques were necessary. Close supplier, fabricator, and design team cooperation was needed during development and fabrication to meet the unusual tolerance, structural, and aesthetic requirements of this project. Maximum use and tightening of existing specifications in combination with stringent inspection were critical to achieving success.◆

Acknowledgments

The authors would like to acknowledge the assistance of Mariani Metal, the Air Force Memorial Foundation, ARUP, and Pei Cobb Freed.

Works Consulted

Avesta Welding Manual: Practice and Products for Stainless Steel Welding. Martin Larén, editor, Avesta Welding AB.

Laser Beam Welding: Benefits, Strategies, and Applications

Technology, such as thin disk lasers, is making lasers more attractive for welding applications

BY HOLGER SCHLUETER

Over the last two decades, laser beam welding has become established as an economically sound and high-quality joining process ideal for many industrial applications. Welding with laser technology offers a number of advantages over conventional welding methods. It improves efficiency, simplifies handling, provides high quality, and laser-welded parts require less refinishing.

These advantages are a result of focused energy input, narrow heat-affected zone, and minimal distortion of the workpiece. Laser welding also offers higher productivity due to high welding speeds, process reliability, and good accessibility.

Repeatability is also an important strength of laser welding. The laser welding process is almost always highly automated and often accompanied with online process control. This control gives highly repeatable results and makes manufacturers less dependent on workers' experience.

Good Part Fitup Required

If laser welding offers so many benefits, why is it still used mostly in high-volume applications such as automotive production or appliance manufacturing? Getting started in laser welding requires a substantial investment of time, money, and resources. A thorough understanding of the risk and the benefits at the management level is mandatory.

Cost-effective laser welding demands workpieces designed in a manner that is compatible with laser technology. Some of the aspects to consider include the part design and fixture construction. Proper design (Fig. 1) and positioning results in high-quality welds that require little or no finishing operations. For example, when processing sheet metal components, secondary processes such as flattening and grinding are not usually necessary and cycle times per piece and costs are significantly reduced.

Along with laser-compatible design of workpieces, the fixture construction plays an important role. Some components lend themselves to laser-friendly geometries, which make it possible to include fixture features in the workpiece itself, or at least mean that only simple fixtures are required. Fixtures can often be inexpensively made from laser-cut sheets.

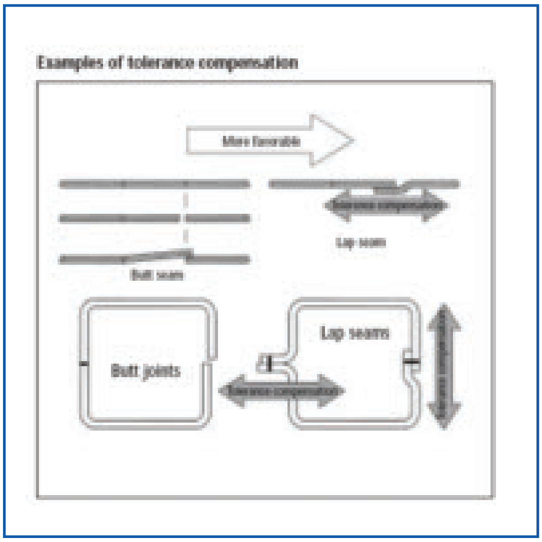

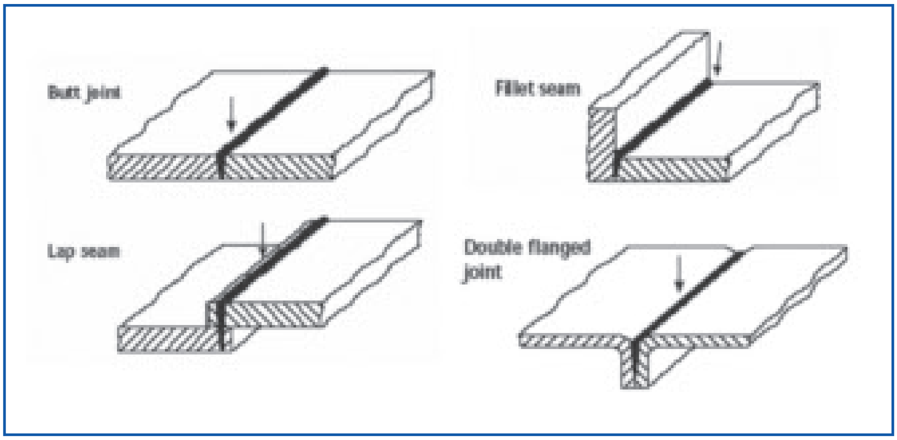

Fig. 1 — Typical welding geometries and strategies to reduce the requirements on edge preparation and parts tolerance.

HOLGER SCHLUETER is vice president, laser, TRUMPF, Inc., Farmington, Conn.

Fig. 2 — *The beam quality of the thin disk laser enables remote welding with a 2-D scanner focus optic.*

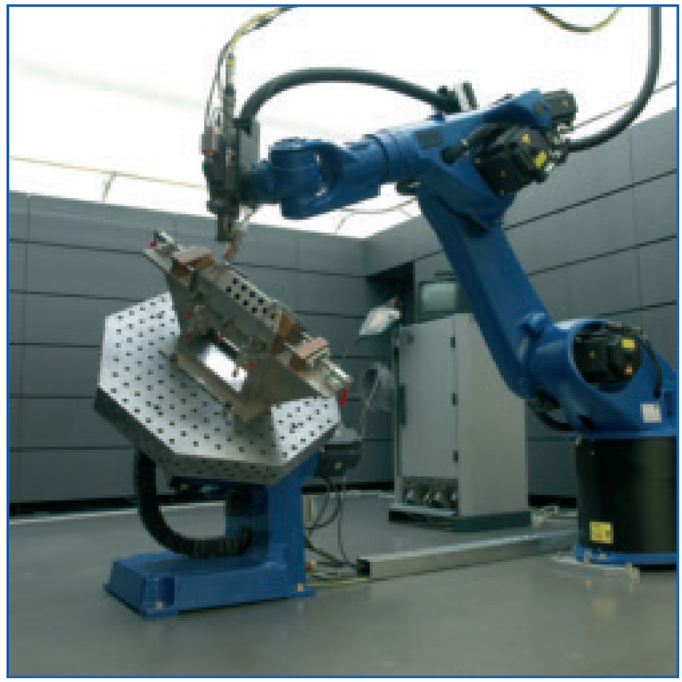

Fig. 3 — Components of a robotic laser welding cell: welding head with laser optics, process camera and sensors, fixture, positioner, welding cabin and exhaust, and robot.

3-D Programming

A particular challenge in the laser process is the fact that the weld joint occasionally follows a complex three-dimensional contour. From a process standpoint, it is important to consider that the speed of the welding head might depend on the local radius of curvature. In such cases, a feedback loop between laser power and welding speed is mandatory to control the penetration depth and prevent joint failure.

Complex three-dimensional programming is needed for parts with complex path geometry. Fortunately, modern tools like teach-in panels and offline 3-D graphic visual programming software make this task much easier, although it does require high-level training and qualification.

In many cases, only minor changes in part design are needed to transition them from challenging to laser friendly. In such cases, an iterative redesign of the part, fixture, and welding strategy might be necessary. Control over the part design is necessary, but can pose a logistical hurdle for job shops and contract manufacturers. While every part requires special fixtures and programming, it is not always possible to convince a customer of the need to redesign a part for laser welding. This is where much of the disappointment in the "new, highly productive" laser process can arise. Therefore, a close connection between the welding, the programming, and the part design is key for a successful implementation of the laser process for welding applications.

Creating a Laser Champion

To help ensure success early in the process, appoint, shepherd, and empower someone to serve as the process champion. History and experience show a process champion can have a dramatic effect on production quality and quantity.

Selecting a laser champion is the first part of the process. The most successful laser champion is ideally an engineer (welding, mechanical, or has the practical experience of an engineer), has an interest or passion for laser technology, will be around for awhile (or at least who is capable and suited to pass the baton), is teachable and trainable, can teach others, and has a desire to share information with others.

There are many courses that would benefit the champion and ultimately the success of the laser welding manufacturing process. Such courses include topics on laser safety, the basics of laser welding, basics of metallurgy, statistical process control, etc. The biggest challenge to managers in this regard is to justify both the financial and time costs associated with the training process, but to ignore or downplay this essential aspect is to allow the less than excellent to permeate the process.

The Components of a Laser Welding System

The majority of industrial welding applications use CO_2 and solid-state lasers such as the thin disk laser. The choice between a CO_2 or a solid-state laser needs to be made on a case-by-case basis and requires knowledgeable partners in the analysis of the entire system layout and its impact on cost, flexibility, and performance.

We will focus on the thin disk laser with its versatile fiber-optic beam delivery. The laser medium of a thin disk laser is a synthetic yttrium aluminum garnet (YAG) crystal. Embedded in the crystal lattice are the ions of a laser-active medium such as ytterbium (Yb).

The higher beam quality attainable with the diode-pumped thin disk laser is primarily a function of the ability to dissipate heat from the lasing medium. The Yb:YAG disk (roughly 14 mm diameter by 0.15 mm thick) is mounted to a water-cooled block (heat sink). Since the disk is face surface-mounted to the block and because the disk is very thin (i.e., high area to lasing medium volume ratio), cooling is extremely efficient and results in a nearly negligible thermal gradient. In the laboratory, such a disk can run at 5 kW of cw output power. These disks are operated at a guaranteed output of 2 kW per disk at the workpiece.

The beam quality of a laser affects four parameters: focus diameter, depth of focus, working distance, and raw beam diameter. The effects of good focusability include

• **Small focus spot diameter.** The smaller the focus spot, the higher the power density on the workpiece. There is a threshold power density for deep penetration welding. Deep penetration welding allows greater penetration and speed than conventional heat conduction welding. Therefore, it is important to reach at least this power density for most applications.

• **Greater working distance.** The working distance is the distance between the processing optics and the workpiece. The beam quality of the thin disk laser enables these power densities even at a working distance of 50 cm, and thereby enables remote welding where the laser beam is steered onto the workpiece remotely, using a 2-D scanner system.

• **Greater depth of focus.** A greater depth of focus enables accurate processing of thick sheets while expanding the tolerance limits for adjustment of the working distance.

• **Small optics diameter.** A small raw beam diameter enables more compact design of the processing optics.

Finding the optimum focus spot for each individual process is crucial for obtaining good laser processing results. The beam quality of the disk laser combined with the modularity of the fiber delivery and processing optics make it possible to select the appropriate beam quality at the workpiece and, with it, the appropriate focus spot diameter for particular tasks.

The Focusing Optic and Fiber Delivery

The beam emitted from a thin disk laser has a wavelength of around 1 μm, putting it within the near-infrared spectral band. As a result, optical components constructed of glass and fiber-optic laser cables can be used for beam delivery. Fiber optic laser cables can carry multi-kW cw laser power over several hundreds of meters without notable loss, enabling the use of thin disk lasers in a variety of locations. The laser beam is focused into the cable and collimated after it exits the fiber so that it is parallel again. Focusing optics are then used to focus the beam at the desired point on the workpiece.

Modern laser systems, such as the thin disk laser, can provide uptime of around 99% or more, even at power levels of 8 kW for solid-state lasers and up to 20 kW for CO_2 lasers. These modern laser sources have design concepts that allow easy exchange of components in the field. One particular example is the quick exchange mechanism for diode laser modules on TRUMPF's thin disk laser. Maintenance can be performed by trained operators on the shop floor.

Beam parameters are standardized and closed-loop controlled, so that a process developed on a specific laser system can be transferred to a different laser system. Due to their flexible beam delivery and integration into other systems, thin disk lasers are often used in robot-aided manufacturing processes.

There are many different options available for the focusing optics. Modern focusing optics can be equipped with process control (sensors and cameras), closed feed-back loops that ensure the automatic laser power control, wire feeders, even scanner optics for remote welding applications.

The economical success of a new laser welding application is clearly linked to the choice of the right system integrator.

System Integration

There are many choices for laser welding system setups. Choices include a robot-based laser welding cell with a fiber delivered thin disk laser, gantry-based systems, systems optimized for linear welds or circular welds, and even scanner welding systems for remote welding. It is very important to find a system integrator partner that can support your needs in the layout of the system and integrate all the different components into a maintainable and reliable system. The reliability and accuracy of all the components of the system solution determine the success of the application. Often the laser is at the center of attention. However, the modern laser sources hardly ever pose the greatest financial or reliability risk. The fixture and part fitup tolerances, beam delivery fiber management, the optical system, and the programming of the motion system are often more important factors in determining the success or failure of a laser welding application.

The remote welding process has become an important joining method at many car manufacturers. In this case, a laser welding head with a scanner is attached to a robot and creates small welds remotely — Fig. 2. This enables welding operations up to 8 times more productive than traditional resistance spot welding.

The economical success of a new laser welding application is clearly linked to the choice of the right system integrator. It is beneficial if the integrator has access to the most modern components in the following fields:

• Laser — access to multi-kW high-power solid-state laser and modern fast-axial-flow CO_2 laser technology.

• Optics — 2-D and 3-D scanner optics, welding optics with integrated process control and optional wire feeder, specialty optics for optimized weld geometries.

• Beam delivery — fiber delivery cables that enable exchange in the field in the case of required maintenance. Fast plug-and-play technology to switch fibers between workstations and lasers. Fiber delivery cables and beam switches that have proven performance at power levels greater than 4 kW.

• System components and motion systems — robot cells (Fig. 3), 5-axis gantry welding systems, linear and rotary welding systems, off-line programming, teach in concepts, fixture design capabilities.

• Process competency — application laboratory with different lasers and delivery systems, access to a metallurgical laboratory, online process control equipment, design capabilities and training classes.

Conclusion

The thin disk laser is gaining strength as a welding option based on its ability to address market requirements regarding power, beam quality, and price. With many installations in the demanding automotive sector, disk lasers are industrially proven, offer excellent performance and flexibility, and are field maintainable and repairable by trained customer maintenance personnel, all of which are demanded by industrial users of lasers in production welding.

Laser welding offers many advantages over conventional processes. The keys to successful implementation involve criteria for the part to be welded (factors such as fitup, cleanliness, fixturing, etc.) and also wise and informed selection of laser manufacturer and/or integrator. Beyond component and equipment considerations, the appropriate training and empowerment of key personnel (e.g. the laser champion) is also essential. Execute due diligence in all aspects of the process, and you can expect great results from your laser welding system. ◆

The Greatest Story Never Told: EB Welding on the F-14

Designed almost 40 years ago, the all-electron-beam-welded wing carry-through structure of the F-14 Tomcat *was arguably one of the most sophisticated weldments ever put into production*

BY ROBERT W. MESSLER JR.

Supersonic F-14 Tomcats *in flight.*

In the midst, if not near the peak, of the Cold War in the late 1960s, Michael Pelehach, the senior aircraft designer for Grumman Aerospace Corp., Bethpage, N.Y., conceived an aircraft to offset not only the existing threat posed by the formidable MiG 17s and 19s, but for what he prognosticated would be its logical successors for at least the next two generations of that fighter. Born in the former USSR, Pelehach immigrated with his parents to the United States while he was a pre-teen or teen. As young as he was when he left the USSR, he understood the Soviet thinking and, later, understood their philosophy for air warfare. He became a scholar of their aircraft design. The result was a very advanced fighter generically designated the VFX that became the F-14.

The F-14 *Tomcat*

The F-14 was flown for the first time in prototype form on December 21, 1970, three months after the author joined Grumman as a young materials and processes engineer. The first of 478 F-14A aircraft were delivered to the U.S. Navy in October 1972 for operation as part of the fleet in September 1974. The F-14A was followed by the F-14B, which had a pair of GE-400 turbofans replacing the original P&WA TF30 engines, with de-

ROBERT W. MESSLER JR. (messlr@rpi.edu) *is a professor, Materials Science and Engineering, Rensselaer Polytechnic Institute, Troy, N.Y. Messler worked in the Welding and Metallurgy Group at Grumman Aerospace Corp. when the F-14 entered into production in 1970.*

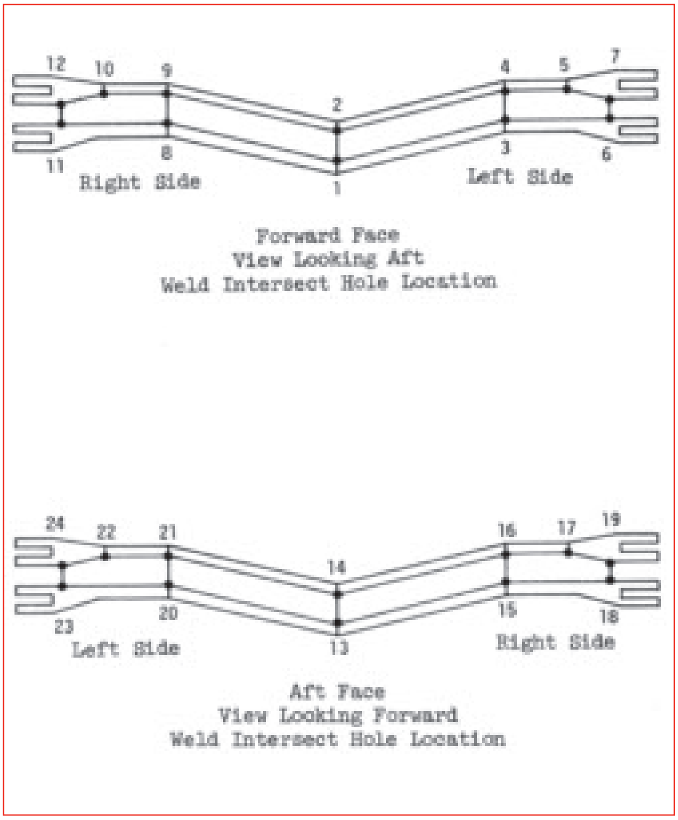

Fig. 1 — Line drawings of the F-14 wing center section. The black dots are the weld intersect hole locations. These holes were bored to remove any trace of possible spiking defects commonly associated with deep partial-penetration EB welds. Each location is where a complete joint penetration weld crosses over an underlying beam or web.

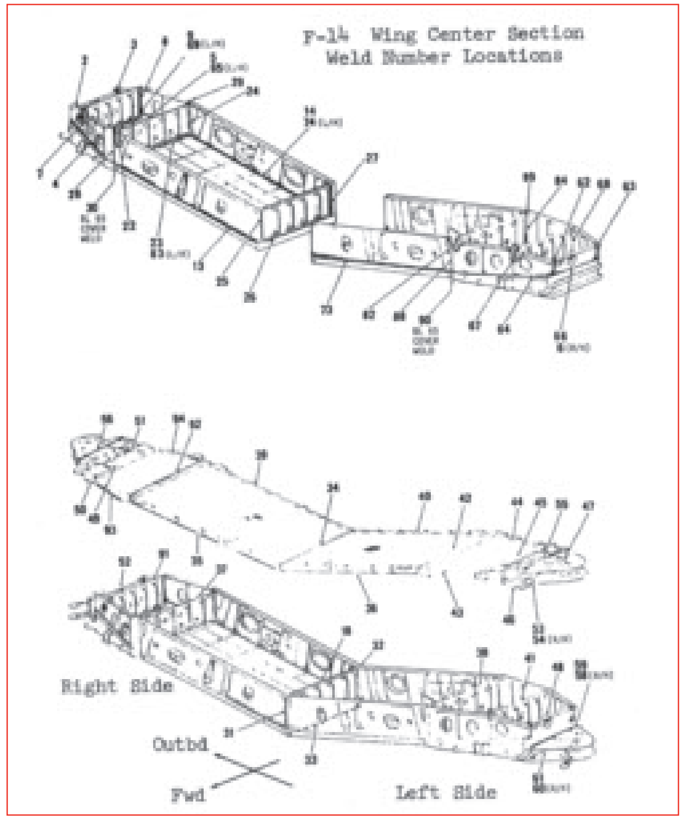

Fig. 2 — Line drawings of the F-14 wing center section, showing the location of all EB welds by the internally used numbering system at Grumman.

ployment in November 1987. A vastly improved model, the F-14D, was produced beginning in 1988. It featured upgrades in radar, avionics, and missile capability. The total production of F-14s exceeded 600. The last aircraft was launched from a carrier in July 2006, and the aircraft was officially retired on September 22, 2006, a service life of just over 35 years. This, in itself, is testimony to just how advanced the aircraft was; being described as "the world's premier air defense fighter" and "one of the most potent interceptors in the world."

Aircraft Capabilities

The F-14 *Tomcat* was a carrier-based, supersonic, twin-engine, twin-tail, variable-geometry wing, two-place fighter designed to attack and destroy enemy aircraft at night and in all weather conditions. Its missions included air defense, intercept, strike, and reconnaissance. It was capable of tracking up to 24 targets simultaneously with its advanced weapons control system and attack six with Phoenix AIM-54A missiles while continuing to scan the airspace. Its armaments also included a mix of other air-intercept missiles, rockets, and bombs, as well as a 20-mm Vulcan MK-61A1 Gatling-type cannon fitted to its left side. Aircraft specifications are shown in Table 1.

Structural Design

The *Tomcat* featured shoulder-mounted wings that were programmed for automatic sweep during flight, with a manual override provided. The wings were attached to a wing pivot carry-through structure (WCS) that crossed the central structure of the aircraft. The carry-through was 22 ft (6.7 m) long, roughly 3 ft (1 m) wide, and about 14–15 in. (0.35–0.4 m) deep. It was constructed from 33 precision-machined titanium alloy parts (forgings and plates) using more than 70 individual electron-beam (EB) welds more than 1800 in. (46 m) in length. It weighed approximately 2200 lb (1000 kg), and was estimated to be about 60% of the weight of a comparable all-high-strength steel structure, and more than 200 lb (about 100 kg) lighter than a comparable Ti alloy structure assembled by bolting. Normal sweep range for the wings was 20 to 68 deg, with a 75-deg "oversweep" position provided for shipboard hangar stowage. Sweep speed was 7.5 deg per second.

Functional Requirements of and Structural Demands on the WCS

If anything was ever the backbone of an aircraft, the wing carry-through structure (WCS) of the F-14 was surely it. Its principal function, of course, was to allow the outer portions of the wings of the aircraft to be swept from a nearly straight-wing (actually, a 20-deg sweep) configuration to a delta-wing (68-deg sweep) configuration. Sweep was enabled by the outer portion of the wing being attached through a pin-and-bearing pivot fitting at each end of the WCS. Aerodynamic and structural demands required that the centerlines of the pivots be precisely located, with a pivot-to-pivot tolerance less than 0.005 in. (0.125 mm) over 22 ft (6.7 m). Beside providing pivots for the wings, the wing carry-though structure, as its name implies, carried wing loading to and through the fuselage.

As if providing the mounting structure for variable-sweep wings for a supersonic fighter was not enough, the WCS also served the following functions:

• It was the point of connection for the forward fuselage (i.e., nose and two-person cockpit), canterlevered from a bulkhead attached to the WCS.

• It carried loads from the main landing gears via a major bulkhead attached to its aft closure beam.

• It was the structure against which the twin engines pushed, through a bulkhead, with combined thrust of 41,800 lb (18,810 kg) for the F14A and 54,000 lb (25,300 kg) for the F-14B and F-14D.

• It carried the shocking loads from arrested landings, as the arresting hook assembly tied into the major bulkhead attached to its aft closure beam.

• It served as a main fuel tank for the aircraft.

Clearly, the wing carry-through structure of the F-14 is a flight-critical structure; the catastrophic failure of which would, absolutely, result in the loss of the aircraft. The F-14 was the first production military airplane (at least for the U.S. Navy, and, possibly, anywhere) to be designed to fracture toughness criteria[1]. From the outset of the design process, certain flight-critical structures (e.g., heavily loaded bulkheads, spars, beams, upper and lower wing covers) would have to possess some minimum ability to tolerate the presence of incipient flaws or defects (e.g., cracks, forging folds or laps, gas pores in castings or fusion welds, etc.). Using the then newly emerging principles of fracture mechanics, the decision was made that any inherent flaws or manufacturing-induced defects smaller than a certain size would be accepted (that is, left in the structure) without necessitating either repair or scrapping of the part. For the WCS, this new criterion was to be applied to a new material for mainstream production aircraft (i.e., Ti alloys) and for welds in the primary structure, when a welded primary structure was virtually unknown in the industry. To say this was a bold approach is an understatement. But, as will be seen, it worked better than could have been expected.

Table 1 — Specifications for the U.S. Navy Grumman F-14 Tomcat

Function	Carrier-based multi-role fighter
Contractor	Grumman Aerospace Corporation
Unit Cost	$38 million
Propulsion	F-14A: Two Pratt & Whitney TF-30P-414A turbofan engines with afterburners; F-14B/F-14D: Two General Electric F-110-GE-400 augmented turbofan engines with afterburners
Thrust	F-14A: 20,900 lb (9405 kg) static thrust per engine; F-14B/F-14D: 27, 000 lb (12,150 kg) per engine
Length	61 ft 9 in. (18.6 m)
Height	16 ft (4.8 m)
Wingspan	64 ft (19 m) unswept; 38 ft. (11.4 m) swept
Maximum Takeoff Weight	72,900 lbs (32,805 kg)
Ceiling	Above 53,000 ft (17,100 m)
Speed	Max Mach Number=1.88 Cruise Mach Number=0.72 Carrier Approach Speed=125 kts.
Mission Radius	500 nm Hi-Med-Hi strike profile 380 nm Hi-Lo-Lo-Hi strike profile
Crew	Two; pilot and radar intercept officer
Armament	Air-to-Air Missiles (up to) 6 AIM-t Sparrows 4 AIM-9 Sidewinders 6 AIM-54 Phoenix Air-to-Ground ordinance MK-82 (500 lb) 4 MK-83 (1000 lb) 4 MK-84 (2000 lb) MK-20 cluster bomb 4 GBU-10- LGB GBU-12 MK-82 LGB 4 GBU-16 MK-83 LGB 4 GBU-24 MK-84 LGB One MK-61A1 Vulcan 20 mm cannon

Basic Geometry of the Wing Carry-through Structure

The wing carry-through structure or wing center section of the F-14 was essentially a monolithic, gull-wing-shaped box, with its dihedral angle at its tip-to-tip midline. The basic shape can easily be seen in the schematics in Figs. 1 and 2. In this view, the outboard platters that contained the pivot fittings that accepted mating pivot fittings located on the inboard ends of the movable wings can be seen to have clevises at their ends. The mating pivot fittings, attached to the upper and lower covers of the wings, fit with precision between these clevises, and were held in place by large precision-fit pins (one for each wing, right and left) — Fig 3.

While not the preferred term to be used outside of Grumman, the wing center section was referred to inside Grumman as simply "the wing box." The basis for (and appropriateness of) this simpler name is obvious from the isometric views shown in Fig. 2. The structure is a box, consisting of forward and aft closure beams, upper and lower covers, and end closures just inboard of the pivot platters. Also visible are some additional webs or ribs running fore and aft; one essentially at the centerline, matching ones at each end of the dihedral section, and another matching set just outboard of these and inboard of the closures at the pivot platters.

Also visible in the schematics of the open box are some other important features of the design. The pockets on the insides of the lower and upper covers provided needed structural strength and, particularly, stiffness, at minimum weight. The numerous openings were to allow accessibility to the inside of the finished structure (which was, at that point, a closed box structure); i.e., hand-holes covered with fastened cover plates. The various lugs on the forward and aft closure beams allowed attachment of other structures (e.g., bulkheads, landing gear linkages, etc.).

The starting product forms for all parts comprising the wing center section were

1. With the possible exception of pressure vessels, the idea that defects or flaws below a certain size may be tolerable below some level of stress intensity and, hence, need not be repaired if they occur, was just emerging within the structural design community.

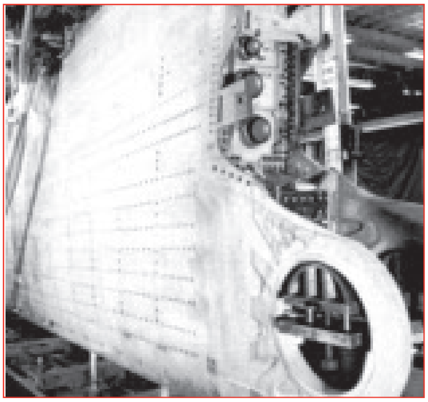

Fig. 3 — Assembled right wing showing the upper and lower forged and machined pivot fittings.

Table 2 — Comparison of Key Properties for Ti-6Al-4V and HSLA Steel

	Ti-6-4	HSLA
Density, g/cm^3 (lb/in.^{3})	4.43 (0.160)	7.85 (0.283)
Modulus of Elasticity, GPa (lb/in.^{2} × 10^6)	114 (16.5)	207 (30)
Yield Strength, MPa (lb/in.^{2} × 10^3)		
Annealed	472 (68.5)	830 (121)
ST + Aged	1103 (160)	—
Q&T	—	1620 (235)
Tensile Strength, MPa (ksi)		
Annealed	745 (108)	900 (130)
ST + Aged	1172 (170)	—
Q&T	1760 (255)	—
Specific Tensile Strength (TS/Density)[(a)]	173.26	180.89 (206.37)
Specific Modulus (E/Density)[(b)]	26.51	26.36
K_{Ic}, MPa(m)$^{1/2}$(ksi (in.)$^{1/2}$)		
Equiaxed, TS=910 MPa	44–66 (40–60)	—
Tempered@260°C, TS=1640 MPa	—	50.0 (45.8)
Tempered@425°C, TS=1420 MPa	—	87.4 (80.0)

a Pure ratio, metric units only, for Ti-6-4 ann. vs. HSLA, tempered at 425°C (260°C).
b Pure ratio, metric units only.

Note: The fracture toughness of the fusion zone of EB welds, while extremely difficult to test, was measured at 55–64 ksi-in.$^{1/2}$ (49.5–57.6 MPam$^{1/2}$). Source: Robert W. Messler Jr., 1981. Electron-beam Weldability of advanced titanium alloys. *Welding Journal* 60(5): 79-s to 84s.

either rolled plate (e.g., inboard upper and lower covers comprising the dihedral portion of the box) or forgings (e.g., outboard upper and lower covers, forward and aft closure beams, webs, and pivot platters). These wrought product forms provided maximum fracture toughness. Extensive CNC milling was used to create details, achieve required precision, and minimize weight in the built-up structure. Some chemical milling was also used for some parts of the WCS and was used extensively for the much thinner upper and lower covers of the wings to remove unneeded material and unwanted weight.

Section thicknesses of precision machined components to be joined ranged from approximately 0.5 in. (12.7 mm) for some web or rib-to-fore or aft closure beams to just over 2 in. (50 mm) for lower (tension) cover-to-cover welds.

Key to the success of the F-14 WCS was the exclusive use of electron beam (EB) welding to assemble the machined details into a monolithic box.

To Weld or Not to Weld?

Other aircraft, military and commercial, had relied on wing carry-through structures prior to the F-14. What made the wing carry-through structure of the F-14 unique were several things; two quite obvious, and one only apparent to the designers. First, the F-14's WCS was constructed entirely of Ti-6Al-4V, used in the annealed condition. This was the first time this interesting metal was used in mainstream aircraft production[2]. What was specifically attractive about Ti alloys, in general, and this alloy, in particular, is its high strength and low density, and, therefore, its especially attractive strength-to-weight ratio compared to steel. Ti-6-4 also competes very well with HSLA steels in the areas of specific modulus, which is important for structural stiffness. Table 2 gives comparisons of some of these key properties.

The second, and especially unique, feature of the F-14's WCS was that welding, rather than bolting, was employed to create a weight- and structurally efficient built-up monolithic structure. While the opportunity for weight savings was apparent and attractive[3], welding had never been used before in a primary, flight-critical structure, especially as critical as a wing carry-through structure. The concerns, of course, were several, but principally included 1) degradation of base metal properties in the fusion zone and the heat-affected zone, 2) distortion and residual stresses in what had to be a high-tolerance structure, and of course, 3) risk (if not high probability) of weld defects (e.g., cracks, pores, inclusions). For the fatigue-critical structures found in aircraft, any of these would be cause for concern, but in combination (i.e., degraded strength in cast structures plus residual stresses plus the near certainty of some defects) the aversion to welding was not surprising.

The less obvious first was that of designing the WCS (and much of the other major structure) of the F-14 to fracture toughness criteria, that is, accounting for the presence of preexisting defects, as opposed to assuming the structure is flawless. Under fracture toughness criteria, flaws below a certain size are acceptable since they will not go unstable (that is, propagate at the speed of sound in the material) until the stress intensity exceeds a certain critical level which, in turn, depends on the inherent resistance of the material to crack propagation. The critical level of stress intensity for any material is given by its value of K_{Ic}.

Of course, the true meaning of employing fracture toughness criteria was profound. It allowed engineers responsible for manufacturing to admit to engineers responsible for design that there was the possibility (if not the certainty) that some (if not most) fusion welds will contain defects (of some severity). This was, truly, a bold admission. In the past, designers shied away from fusion welding in fatigue- and fracture-critical structures because they had had — or were acutely aware of — bad experiences in the past with welds failing due to the presence of unexpected and unaccounted for defects. The risk, of course, was that actually admitting that welds could contain defects (which everyone knew anyway) might not put the designer's mind at ease. It might convince them they were right about welding all along, but for the F-14, the decision to assemble the fatigue- and fracture-critical wing carry-through structure using welding worked.

2. While the general aircraft design and manufacturing community was unaware of it, Ti and Ti alloys were being used by Lockheed on the highly secret SR-71 Blackbird *spy plane.*

3. A projected weight savings of 200+ lb (about 100 kg) in a 2200-lb (1000 kg) structure using welding instead of bolting was significant at near 10%.

The Reasons for Choosing EB Welding

The decision was made to assemble the F-14s WCS using electron beam (EB) welding, exclusively. The selection of EB welding was based on several inherent advantages of the process. These included the following:

1) Being a high-energy-density process that operates in a keyhole mode, EB welding is capable of making single-pass welds in Ti-6-4 to thicknesses greater than 2 in. (50 mm) at relatively high speeds (12–50 + in./min [5–20 + m/s] for 2 in. or 50 mm/s for 0.5 in. [12.5 mm] thicknesses) with a sufficiently powerful beam. Single vs. multipass welding minimized welding time. The process also minimized the amount of heat needed to cause melting and unwanted heat effects.

2) As a keyhole process, EB welding produces fusion welds with especially high depth-to-width ratios, which results in less shrinkage due to the volume decrease associated with solidification of metals like Ti. Less differential contraction in the surrounding heat-affected zone allows greater dimensional precision.

3) High-energy-density processes require less total heat input to cause melting and result in narrower heat-affected zones than arc welding processes. The less extensive the heat-affected zone of a fusion weld, the less extensive are the adverse effects of heat on the microstructure and properties of the base metal. Also, EB welds cool more rapidly, causing less degradation in the heat-affected zone.

4) Electron beam welding is carried out in the highly protective and clean environment provided by high vacuum. The high vacuum shields the highly reactive Ti from the detrimental effects of oxygen, nitrogen, and hydrogen [water vapor] found in air.

5) Electron beam welding is carried out in a highly controlled, semiclean-room environment, using computer-control and highly skilled operators. The result is exceptional quality.

So, in short, EB welding promised deep-penetration, narrow, single-pass welds, at high speeds, with greater dimensional precision, and less distortion, less property disruption, and lower incidence of defects than any other welding alternative. While good for many metals and alloys, Ti alloys proved to be particularly amenable to the process.

The Challenges of EB Welding for Large-Structure Production

Despite the many abilities of EB welding, the process has its challenges and shortcomings. Most obvious among these is the need for welding to be done in a high vacuum (10^{-3} to 10^{-5} atmospheres, or more, depending on the reactivity of the metal being welded). Always a challenge, welding at 10^{-5} atmospheres as was necessary for the all-Ti-alloy WCS was a particular challenge, made even greater by the large size of the structure to be welded. Two special 10 ft W × 11 ft H × 13 ft L (roughly, 3 ×3.4 × 4 m) steel chambers were designed and constructed by Chicago Bridge & Iron. These each had a large, full-width/full-height sliding door at one end, with a system of precision rails outside the chambers on the shop floor and inside the chamber. A movable section of rail was provided to allow loaded welding fixtures to be rolled into and out of the chambers.

Having a chamber big enough to contain the WCS and to tolerate the required vacuum was one thing, but pumping such a large-volume chamber to 10^{-5} atmospheres pressure quickly (to facilitate production), was another. Large mechanical "roughing" pumps were used to bring the chambers quickly to about 10^{-2} to 10^{-3} atmospheres. Large diffusion pumps were then used to bring the pressure down to the required/preferred 10^{-5} atmosphere range. Total pump-down time was about 25–30 min.

Maintaining a constant, temperature-humidity controlled, semiclean-room environment for the EB welding area for the WCS and wing covers was also necessary because fusion welding must always be done on parts made as clean as possible, but also because of the particularly high reactivity of Ti and its alloys. No food, no drinks, and no smoking were the rule in this area, and everyone entering the area had to have their shoes automatically brushed clean of any debris picked up in the surrounding shops where aircraft parts were being fabricated and assembled. Anyone working on parts ready for welding after prior cleaning (in various degreasing and acid and alkaline baths) had to wear clean linen gloves. No tools entered the area without being cleaned.

Finally, besides the huge capital investment in vacuum chambers and pumping equipment, there was the huge investment in EB welding guns (Sciaky 52 kV/1000 mA/52 kVA guns), high-voltage, highly stabilized electronic supplies, and in CNC systems to allow fully automated welding. And, of course, there was the need for highly skilled operators, always-available support engineers, and special, dedicated inspection facilities and inspectors. To allow fracture toughness criteria to work, it was necessary to know precisely whether, how many, what type, and where any weld defects had been introduced during welding. Hence, every weld was 100% visually inspected, 100% dimensionally inspected, 100% fluorescent penetrant inspected, 100% radiographed, and 100% immersion-ultrasonic inspected, and records (as maps) of everything were maintained for every production WCS, by aircraft number.

Fig. 4 — An open WCS before the upper covers have been weld attached.

Building the WCS

The success of the F-14 was dependent on the quality of the design and fabrication of its all-titanium wing carry-through structure, and the fabrication of the wing carry-through structure was only possible using electron beam welding. No other joining process could have provided the combination of low weight, high geometric and structural integrity, and production economy of deep-penetration, single-pass EB welding. But, to successfully EB weld the WCS required extraordinarily creative engineering, manufacturing, and quality assurance. Following are the highlights of what made production of nearly 700 wing carry-through structures possible.

Building from the Middle Outward

To achieve the required tight dimensional tolerances of the WCS, most particularly, the pivot-to-pivot separation being within ±0.005 in. (±0.125 mm) over 22 ft (6.7 m), the assembly was built by EB welding together precision-machined parts; 33 of them, using 77 complete joint penetration, single-pass welds. The WCS was built as an open box first (Fig. 4), and then, after the entire unit was completed pivot platter to pivot platter, the top covers and pivot platters were welded into place, also from the center outward. This approach allowed dimensional variations to be corrected at each stage of assembly. Once the centermost left and right portions of the open box (consisting of fore and aft closure beams EB-welded to the lower covers and the centerline web or rib welded to one end of one of these subassemblies) were EB-welded together, again using complete joint penetration welds approximately 2.15 in. (54.6 mm) thick and only about 0.180 in. (0.82 mm) at the crown and 0.100 in. (0.25 mm) at the root. While shrinkage was minimal with such narrow welds (and uniform, because the welds were parallel-sided as opposed to tapered, like most fusion welds), the ends of the two joined open center portions were machined to the precise dimension required at that butt line. The outboard left and right open sections, less the actual pivot platters, were then EB welded to the center portion of the box. Once again, the free ends to which the pivot platters were to be welded were machined back to the correct dimension for that butt line. The pivot platters were then welded on and the pivot holes were finally bored precisely where they belonged.

The combination of employing a process that caused minimal shrinkage and bringing the subsequent prewelded joint to a required dimension and tolerance by machining allowed the stringent tolerances to be achieved.

Positioning and Design of Weld Joints

As anyone knows who uses welding to assemble critical structures, welds need to be both properly positioned within the structure (e.g., in thicker, lower-stress section, at the neutral axis for any bending, etc.) and properly designed or configured, both to optimize structural performance and facilitate welding and postweld inspection. For the F-14's WCS, the following approaches or techniques were used:

- All welds were positioned and designed to allow complete joint penetration in tight-fitting (precision machined), straight or square butt joint configurations. This was done to avoid defects, known as "spikes," typically associated with the roots of partial penetration welds made in a keyhole mode and to allow thorough x-ray of the final weld.
- To avoid what are known as start and stop defects, which occur for most fusion welding processes, but can be particularly severe for high-energy-density processes operating in the keyhole mode, either integral or tack-welded start and stop tabs were employed. These were removed following welding, with the defects they contained, by machining.
- To allow complete joint penetration, some welds were offset (for example, for a cover-to-cover weld over a web or rib) or the weld was made at an angle off-90 deg.
- To prevent the excess energy that exits from the backside of an EB weld, sacrificial beam-stop blocks made from Ti-6-4 were employed for all complete joint penetration welds.
- Any region of partial penetration (for example, where a complete joint penetration cover-to-cover weld crossed an underlying web/rib or closure beam) was drilled to remove any spiking defects that may have occurred, and was then plugged with an interference-fit Multiphase 35™ headed pin. These pins produced a compressive residual stress that improved resistance to fatigue in these areas. Pins were not installed until all stress relief heat treatment was completed.
- All welds were placed in an area with a raised land approximately 0.100 in. (0.25 mm) high at both the weld crown and weld root surfaces in order to make the cross-section containing the weld greater and, thereby, the working stress lower.

> Employing a process that caused minimal shrinkage and bringing the subsequent prewelded joint to a required dimension and tolerance by machining allowed the stringent tolerances to be achieved.

Assuring Structural Performance

Proper design, including the placement and configuration of weld joints, is critical to assuring proper structural performance, but so too are some of the finer details of manufacturing called for by the designers. The following extra details were employed for the F-14's WCS:

- All weld crown- and root-beads were machined flush to provide consistent fatigue behavior. Normally, the slight variation of joint thickness and, especially, surface contour of well-made fusion welds is acceptable. But, for the fatigue-critical WCS, a decision was made (based on tests) that even the smooth crown and root beads of all EB welds should be machined smooth.
- The WCS was subjected to stress relief heat treatment at several intermediate stages of assembly, with light acid cleaning (in mixed hydrochloric/hydrofluoric acid) to remove any trace of alpha case.
- All weld areas (including the surrounding raised land and its radii) were shot peened to induce a compressive residual stress to improve resistance to fatigue. Obviously, this had to be done after all heat treatment for stress relief had been completed, so that the peening-induced desirable residual stresses were not removed.

Assuring Weld Quality

At Grumman, it was recognized that quality began with design and carried through manufacturing with a combination of stringent process control and inspection. To assure the EB welding of the WCS was done properly, the following were used:

- To preclude cross-contamination of the Ti-6Al-4V, all welding fixtures were fabricated entirely from Ti-6Al-4V. This proved necessary because of cross-contamination from occasional back-spatter from tooling or stop-bars, from errant beams, and from simple scuffing.
- To assure that the deep, narrow EB welds were properly aligned with the joint faying surface, witness lines were used. These consisted of a series of fine, parallel lines scribed into the surface of the metal on each side of the prewelded joint (before the parts were fixtured for welding) every 0.015 in. (0.38 mm) to a distance of about 0.15 in. (3.8 mm). By counting the number of lines remaining visible on each side of the finished weld, at crown and root, it could be determined whether the weld was suitably aligned to the original joint interface (i.e., if there were equal or nearly equal numbers of lines left), and the crown and root were wide enough.
- To assure there were no defects open to the surface, ripe for degrading fatigue resistance, the entire box, with emphasis on the welds, was fluorescent penetrant inspected.
- To assure welds contained no defects (cracks, porosity, voids, missed seams, remnants of spikes), all welds were 100% inspected using x-radiography with a resolution of 1% of the transmission thickness. For intersecting welds, where holes had been bored, film was inserted into tubes inserted into these holes and x-rays were taken.
- To assure that welds contained no defects oriented unfavorably for detection by x-rays, all welds, at various stages of the build-up process, were 100% inspected using immersion ultrasonics.

Welded subassemblies and, eventually, the entire WCS, were immersed in a tank of water and all welds were scanned using 20–30-kHz transducers operating in the pulse-echo mode. Both printed C-scan and dynamic oscilloscope A-scan assessments against previously developed synthesized defects were conducted by specially trained and certified inspectors. The system was tuned to a sensitivity sufficient to detect a $\frac{1}{64}$-in.-(0.4 mm-) diameter flat-bottomed hole at various depths.

Decisions on whether a particular defect had to be repaired or not was made based on drawings of critical areas of the WCS (e.g., corners and other points where several welds intersected with one another), which were zoned with allowable defect sizes. Questionable areas were reinspected in an attempt to refine information on defect size, type, and location. Complete records, in the form of x-ray and U/S maps, were maintained for each WCS by F-14 aircraft number.

Better-than-Expected Structural Integrity

For a military airplane to be accepted by the purchasing service for deployment, it must demonstrate structural soundness and mission suitability. These demonstrations are done by the contractor in sequential tests using different aircraft.

First, a preproduction aircraft is subjected to static tests to demonstrate that expected service static loads can be carried. For aircraft intended for carrier landings, the same airplane is then subjected to drop tests, in which aircraft carrying full fuel, simulated stowed weapon, and simulated crew weights, are literally dropped onto the test hangar's concrete floor from progressively greater heights to produce progressively higher descent rates.

Next, another, usually the second, preproduction aircraft is subjected to expected fatigue loads for various portions of the aircraft's design mission. Even though prototype aircraft were likely flight-tested by the contractor's test pilots, further flight testing is conducted on one or more of the first production aircraft, which have had any design changes indicated necessary from static and fatigue testing incorporated.

Finally, for Navy aircraft intended for carrier operation, an early production aircraft, often one of the flight-test aircraft, is subjected to what are known as carrier suitability trials. In these, the aircraft is evaluated for its ability to make arrested landings on a runway bearing an imprint of an aircraft carrier deck and an actual arresting system, and supported by all of the electronics used to guide the aircraft in for a landing. Additional tests assess suitability for catapult launches.

For the F-14, an accident occurred with one of the flight test aircraft late in 1970 or early in 1971. During flight tests in a restricted area over the Atlantic Ocean about a 100–200 nautical miles southeast of the east end of Long Island (where Grumman's final assembly plant for the F-14 was located, and from where flight testing was conducted), the pilot and his copilot encountered sloppiness in the control of movable surfaces (e.g., flaps, ailerons, rudder, etc.) that rapidly grew progressively worse. It soon became apparent to engineers monitoring the flight test that the aircraft was becoming so uncontrollable and unstable that it needed to be ditched in the restricted zone to allow the U.S. Navy (as opposed to ever-watchful Soviet trawlers) to recover the highly secret aircraft. Despite this decision from the ground, the pilots were determined to bring the airplane home, and they nearly made it. However, as the aircraft lined up on Grumman's extra-long runway, the plane began to pitch up and down violently. Just as the plane cleared the fence surrounding Grumman's property, the aircraft pitched down, not to be recovered. Since the plane was well into its approach for a landing, the distance to the ground was short. The pilot ordered his copilot and friend to eject. Less than five seconds later, the aircraft plunged into the ground in a huge fireball.

Despite forward movement that caused copilot and pilot to follow the aircraft's forward trajectory and nearly land in the fireball, both survived unscathed. The aircraft, which crashed into a heavily wooded area, disintegrated into pieces, but one large structure remained intact — the wing carry-through structure.

The crashed WCS was subjected to dimensional and nondestructive inspection identical to what had occurred during its production. Unbelievably, all of the fixturepoints on the crashed WCS mated with those on the fixture used to check wing attachment. Complete radiographic and immersion ultrasonic inspection (under the engineering supervision of the author) revealed no defects and none left in the structure based on fracture toughness zoning of the welds had grown. The fracture mechanics worked beyond anyone's hope. This unfortunate event added immeasurably to the designers — and the welding engineers — confidence in Ti alloys, EB welding, and fracture-critical design based on fracture toughness.

Epilogue

Production of the F-14 air superiority fighter ran for almost 20 years, from 1970, with almost 700 aircraft built and delivered. No problems ever emerged related to the wing carry-through structure. The risks had been worth it, and the tremendous engineering and manufacturing effort had been worth it, too.♦

Acknowledgments

This article is dedicated to a few manufacturing engineers without whom the F-14 WCS could have never been built. They are Frank Drumm, Alan Lofsten, Dietrich Helms, and Ken Payne. They did what may never be done again. The author is grateful for every moment spent with each of these dedicated and capable Grumman engineers.

Advanced Laser Technology Applied to Cladding and Buildup

Fig. 1 — Laser cladding with coaxial powder supply.

Precision repairs and rapid design changes of molds, tools, and high-value components are possible with direct metal deposition using modern laser technology

BY STEFFEN NOWOTNY, SIEGFRIED SCHAREK, AND ANDREAS SCHMIDT

Repair and rapid geometrical modifications of high-value tools and components are demanding challenges of modern manufacturing technology. Advanced laser cladding techniques with fiber lasers offer outstanding possibilities for applications in aircraft maintenance as well as mold and die industry. The reason the interest in this technology is increasing is its features. High-power fiber lasers open a completely new dimension in material deposition. The beam quality is extremely high, and this results in both small laser focus diameters (10–100 μm) and very long focal lengths. In addition, the current system technology, laser optics, powder feeders and nozzles, as well as CAD/CAM software, permit an easy and efficient integration of the laser process into manufacturing systems.

Process Characteristics

Figure 1 illustrates the laser cladding process. The laser beam generates a localized melting bath on the workpiece surface. The filler material is fed as powder or wire and is heated when moved through the laser beam. However, it only melts once it is in the melting bath. The formation of a metallurgical bond requires a slight melting of the base metal, which happens through thermal conduction. Thermal conduction into the cold substrate facilitates rapid solidification of the molten filler material, which results in the formation of the deposited material. The width of these tracks can typically be varied between 0.2 and 6 mm. The height depends on the application and is between 0.1 and 2 mm. Tracks can overlap and thus

STEFFEN NOWOTNY (Steffen.Nowotny@iws.fraunhofer.de), *SIEGFRIED SCHAREK, and ANDREAS SCHMIDT are with Fraunhofer Institute for Material and Beam Technology, Dresden, Germany.*

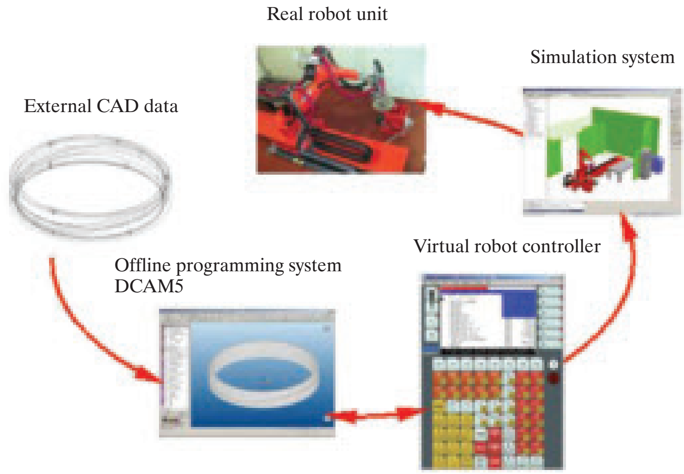

Fig. 2 — Process chain of offline programming using DCAM5.

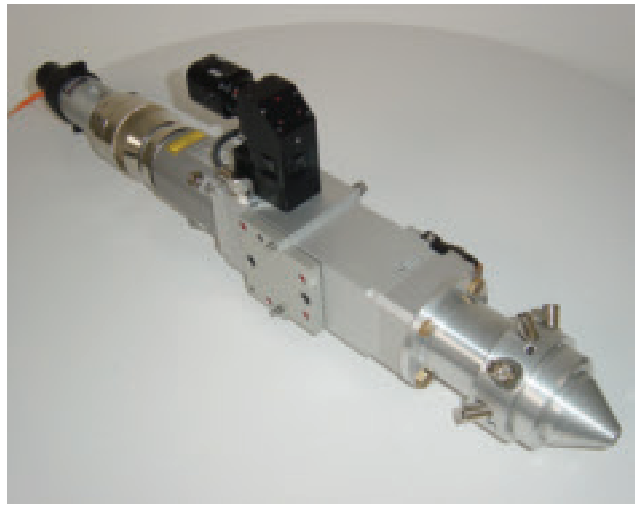

Fig. 3 — A cladding unit for use with fiber lasers, consisting of a COAX nozzle, the adapter/adjustment module, and the laser optic.

coat entire areas. Multiple layers can be deposited to form three-dimensional structures. The characteristic deposition rate is 0.1 to 1.5 kg/h. A higher deposition rate leads to a reduced precision of the depositions.

As beam sources, currently high-power diode lasers, traditional Nd:YAG slab lasers, and the new Yb:YAG fiber lasers are in use in the industry. The typical power range lies between 1 and 6 kW. Lasers with higher output powers are available, but for the most part not cost-effective for cladding applications.

The fiber laser, a special type of the solid-state laser, represents a new generation of high-power lasers for materials processing. The Yb-doped core of a YAG glass fiber is the active medium in this laser. The beam quality is increased about four times compared to conventional Nd:YAG slab lasers. This results in an extremely improved ability to focus the laser beam, which can be as small as 100 to 10 μm at lengthy working distances. This way, the user has a wider window of process options: long and slight cladding optics and powder nozzles for a better powder efficiency, better accessibility of complex welding positions, and better 3-D operation capability. Compared to the traditional Nd:YAG slab laser, the fiber laser is more compact, smaller, the efficiency is much higher (wall plug efficiency >30% (Ref. 1), compared to 5–15%), and the investment costs are less by a factor of 2 to 2.5.

For applications that require less accuracy, the high-power diode laser is a cost-effective alternative. This type of laser is available in the power range of up to 6 kW. Compared to other beam sources, it has the highest available power efficiency of 35–50%. The equipment costs are comparatively low. Since diode lasers are very compact, they can be directly integrated into a machine tool or robot system without the need to transport the laser light via fibers. The low beam quality of this laser type limits the minimum dimension of the laser focus. Thus, the diode lasers are not suitable for high-precision claddings and microprocessing.

System Technology

Offline Programming Software

Laser beam cladding in repair and free-forming mostly implies demanding 3-D problems. The basis of a typical laser working cell is either a 5-axis CNC machine or a robot system, whose working space and geometrical performance are adequate to the particular workpiece. An extremely important precondition for a successful operation is the quick and appropriate preparation of the laser cladding process. The related procedure includes the modeling of the workpiece geometry, programming of the machines as well as the setup of an optimized build-up strategy. The strategy determines the shape, accuracy, and mechanical properties of the generated structures. Additionally, it influences considerably the effectiveness of the whole process chain.

For this purpose, the software system DCAM5 has been developed. It is suitable for the deposition of single tracks, layers, and three-dimensional structures onto flat or contorted surfaces. The CAM software package includes tools for the modeling of 3-D CAD data; support for the definition of an optimum buildup strategy, which includes laser power, welding speed, laser spot dimension, powder feed rate, placement of the weld beads, special solutions for fine walls, and sharp edges; simulation of the machine movement and material build-up; and offline programming.

Especially for the use with robots, the DCAM offline programming software is an efficient alternative to the conventional "teach-in" programming. Figure 2 illustrates the integrated process chain for the programming of a robot system. In a first step, external CAD data are imported into the CAM system. In interaction between the DCAM software and a virtual robot controller the optimized paths and the corresponding process parameters are generated. Hereon the process runs virtually in a simulation. It tests the path on collisions or other trouble. If potential collisions are identified, it is possible to change the location or inclination of the workpiece or the entire laser path. Also, the process parameters can be changed at this point. Finally, a special postprocessor generates the program for the real robot system.

The use of this programming system reduces significantly the time for the preparation of the process. Furthermore, it helps to use the machine optimally, and to fully develop the property profile of the laser generated metal structure.

Laser Cladding Head

As filler materials for laser cladding applications, both powder and wire are of importance. Because of the large number of commercially available metal alloys and hard metals as well as the flexible shape and dimensions of the material flow, powder dominates the technology. To generate an extra stable and direction-independent powder stream, the coaxial nozzle is the most common solution.

The modular nozzle system COAX exhibits the principle of coaxial powder sup-

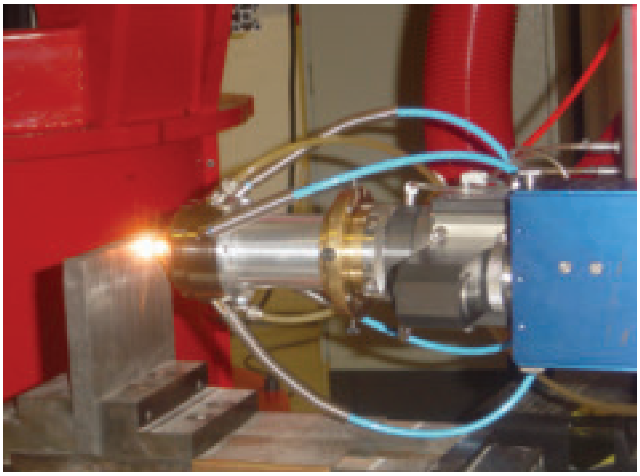

Fig. 4 — Build-up welding in the vertical position.

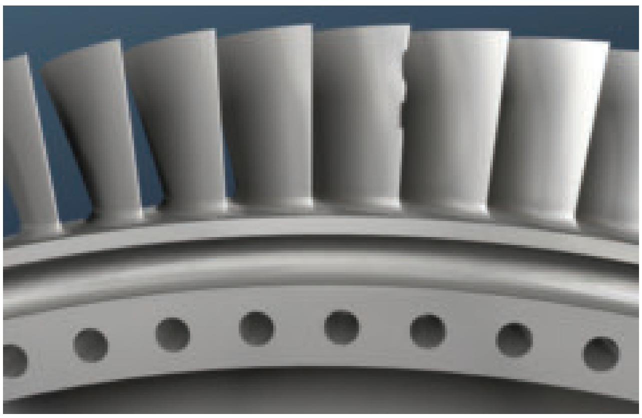

Fig. 6 — Section of a damaged aircraft rotor.

Fig. 5 — Robot system for laser beam cladding and hardening of tools.

ply, and it meets the requirements of industrial laser users. The current design of these nozzles consists of three modules: powder supply and distribution, nozzle tip unit, and adapter/adjustment unit. These modules are available in a large number of different shapes, sizes, and materials, and they are compatible with each other. Thus, a flexible construction kit permits the quick composition of a cladding head, which is precisely adapted to the requirements of the particular application. Figure 3 shows an example of a complete cladding unit for use with fiber lasers. It consists of the standard laser focusing optics, optional sensors for process monitoring, an xyz-adjustment system, and the coaxial nozzle itself.

For a homogeneous distribution of the powder around the laser beam, up to four powder components are blown into a small expansion chamber using a carrier gas such as argon or nitrogen. A powder gas stream is formed in this chamber, which subsequently passes through specially shaped channels. This way a quasi laminar flow, parallel to the axis of the laser beam, is generated. Finally, the ring-shaped slit of the nozzle tip focuses the powder stream onto the laser spot on the workpiece surface.

The minimum diameter of the powder focus is about 1 mm. This guarantees a powder efficiency of 60–90% if the width of a single track is not less than 1.5 mm. Using metal powders with a grain size of 20–90 μm, typical feeding rates lie between 2 and 50 g/min. An additional gas flow partially protects the metal melt from oxidation. Inner and outer parts of the nozzle are intensively water cooled, so uninterrupted operating times of many hours are possible. The weight of the lightest nozzle of aluminum is 290 g compared to 1500 g of the larger and extra robust bronze nozzles. All the media necessary for the cladding process (powder, gases, water) are supplied to the nozzle body via quick-snap connections.

Because of the homogenous particle distribution, the powder supply is independent from the welding direction. So nearly any desired welding contour can be realized. In addition, nozzle inclinations do not influence the powder stream. Even 3-D claddings with a moving nozzle are possible. A related application for the repair of gas turbine components is shown in Fig. 4.

System Integration

It is getting more and more popular to use robot systems coupled with high-power diode or fiber lasers. Such systems are flexible and inexpensive, and the accuracy of the common robot is sufficient for the characteristic laser track formation. Figure 5 shows a robot unit equipped with a 3-kW diode laser, coaxial cladding head, and standard powder feeder as a representative example. This system is in use for laser cladding and hardening for the repair and surface treatment of metal-forming tools and molds (Ref. 2).

On the other hand, the integration of the laser cladding technology into standard machine tools is gaining attention. So a number of laser integrated 3- and 5-axis milling machines are in use in the mold and die industry. There, the direct 3-D material deposition is efficiently combined with the finish machining using the same CNC data.

Other Applications

Figure 6 shows a section of a damaged integral rotor of an aircraft engine. These rotors are made of titanium alloys and get locally damaged over larger areas of the blades. Repair is very challenging since the aerodynamic profile has to be precisely regenerated, and the dynamic mechanical strength has to be completely equal to the new part. The solution is to perform the laser buildup welding under an inert gas atmosphere in a closed CAD/CAM process chain (Ref. 3).

Additionally, laser beam cladding is used for surface protection of hot work tools or lightweight car motors. For these purposes, the spectra of filler materials ranges from Cu-based bearing metals and Co and Ni hard alloys up to carbide hard metals.

Conclusions

The current state of user-friendly and industrial-proven laser technology successfully supports the industrial applications of laser cladding and buildup. Since all the necessary system components are commercially available, laser beam build-up welding has been established in the industry as a high-precision manufacturing technique. The repair of damaged components and tools is currently the most important application. The primary goal is to restore the original shape and properties of the workpiece. The laser also offers the additional possibility to influence structure and properties of the deposited materials.

Current R&D activities are focused on developing increased process know-how using the new generation of fiber lasers, the use of new materials for surface applications, process simulations, and the integration into modern manufacturing procedures.◆

Acknowledgments

The authors would like to acknowledge the support of the companies MTU Aero Engines, Germany, and Härterei Gerster AG, Switzerland.

References

1. Gapontsev, V. 2006. Industrial high power fiber laser systems. *Proceedings of the 2nd International Workshop on Fiber Lasers*, Dresden, Germany.

2. Stiles, E., and Hensel, E. 2006. Combination machine for laser hardening and cladding. *Laser Applications International*, February/March, pp. 13–15.

3. Richter, K.-H., Orban, S., and Nowotny, S. 2004. Laser cladding of the titanium alloy Ti6242 to restore damaged blades. *Proceedings of the 23rd International Congress on Applications of Lasers and Electro-Optics,* ICALEO 2004, San Francisco, Calif.

Improving Laser Welding Efficiency

BY NICK LONGFIELD, TOM LIESHOUT, IMMY DE WIT, TONY VAN DER VELDT, AND WIM STAM

Twin spot laser welding has increased the welding machine's tolerance to entry coil and shear cut quality, resulting in improved machine efficiency and production line throughput

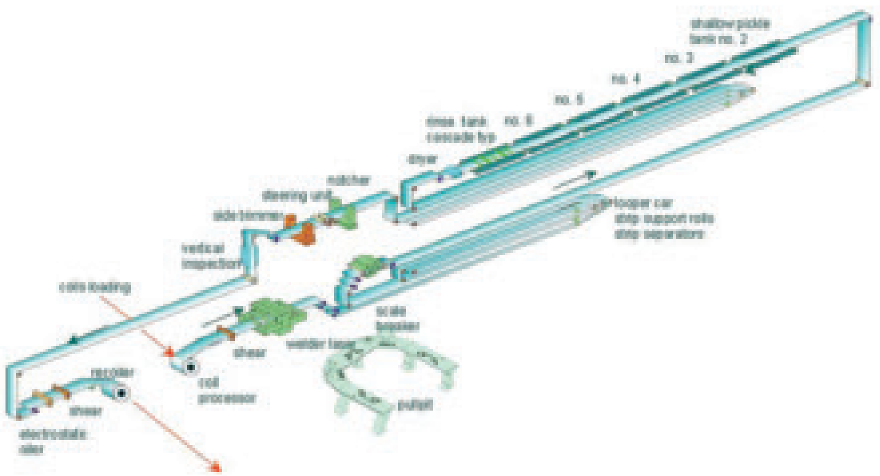

Fig. 1 — Schematic layout of the continuous pickling line.

The Corus continuous pickle line (Fig. 1) located in IJmuiden, North Holland, uses an 8-kW CO_2 laser beam welding machine built by Miebach for coil joining (Fig. 2). The laser welding machine joins the tail of the lead coil to the head of the entry coil, therefore creating a continuous, high-throughput pickling process.

The laser beam welding process produces welds that are of high strength, high aspect ratio, and have a very small heat-affected zone. This is achieved as a direct consequence of the laser's inherent ability to be focused to a very small spot. The small focus spot size of approximately 0.4 mm is ideal for producing welds at high speeds with minimal distortion; however, the laser welding process has limitations in weld quality when considering poor sheared edge quality and poor entry strip shape. If a weld of insufficient quality is sent through the line, the weld may break, creating an entire line stop until the strip is rethreaded and pulled through. Weld breaks, therefore, have a severe impact on the tonnage output of the line and can also lead to damage in associated line components.

The laser welding coil joining machine in the Netherlands has previously run with a first time right welding efficiency of approximately 75 to 85% and has suffered weld breaks, which result in line downtime and a loss in coil production.

The first time right welding efficiency, weld quality, and hence number of weld breaks is influenced by the magnitude of horizontal and vertical misalignment, the strip shape, and sheared edge quality.

An improvement program was initiated at the Corus pickle line during 2005, part of which was the assessment of twin spot laser welding at Corus Research, Development & Technology.

Laser weld quality can be improved by a number of methods; the simplest and one of the most effective for reducing the susceptibility to misalignment issues is twin spot welding (Ref. 1), whereby the raw beam is focused into two spots instead of one. This is achieved by replacing the plain mirror before the focusing optic with a twin spot mirror. Different configurations of twin spots are available — Fig. 3.

Corus research and development engineers performed an investigation to evaluate the twin spot process for increasing the tolerance to fitup and sheared edge quality with respect to installing and commissioning at the Corus pickle line.

Experimental R&D

Initially, the effect of vertical and horizontal strip misalignment (refer to Fig. 4) was characterized at the Corus RD&T laboratory in IJmuiden on a 6-kW Trumpf CO_2 laser and Trumpf TLC flying optics gantry using single spot optics with a focal length of 200 mm. It was found that the vertical and horizontal misalignments had a fundamental effect on the mechanical property of the resulting welds, whereby misalignments created undercut and stress concentrators, reducing the tensile energy before failure occurred. As can be seen from Fig. 4, a horizontal misalignment ([HMA] a gap between the strip) produces a weld that is characterized by undercut on the top and bottom surfaces of the weld. This undercut is detrimental to the tensile strength, whereby the energy required to fracture the weld is halved when compared to a weld produced in the same material with zero gap.

NICK LONGFIELD (Nick.Longfield@corusgroup.com) *is researcher, joining technology, and TONY VAN DER VELDT is knowledge group leader, joining technology, with Corus IJmuiden. TOM LIESHOUT is maintenance manager and WIM STAM is continuous improvement engineer with Corus IJmuiden Beitsbaan. IMMY DE WIT is research assistant, joining technology, with Corus IJmuiden RD&T.*

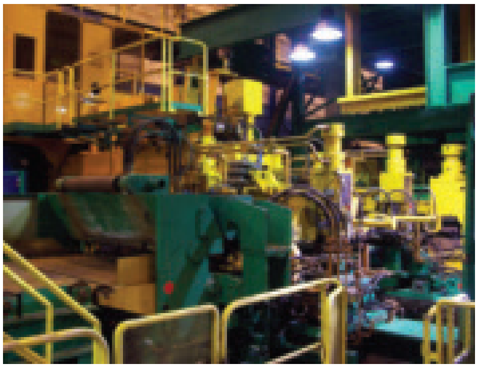

Fig. 2 — The coil joiner installed on the Corus Beitsbaan.

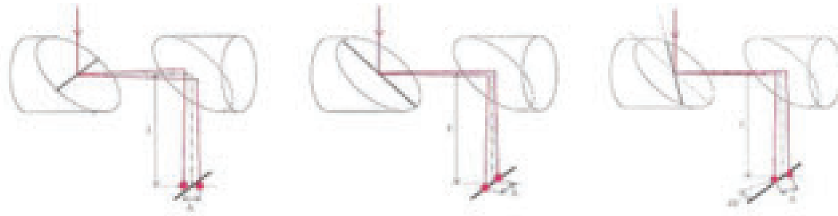

Fig. 3 — Typical versions of twin spot mirrors. Left — Splitting along the plane of deflection; middle — splitting across the plane of deflection; and right — splitting in an angle of 45 deg relative to the plane of deflection. (Reproduced courtesy of Kugler Precision GmbH.)

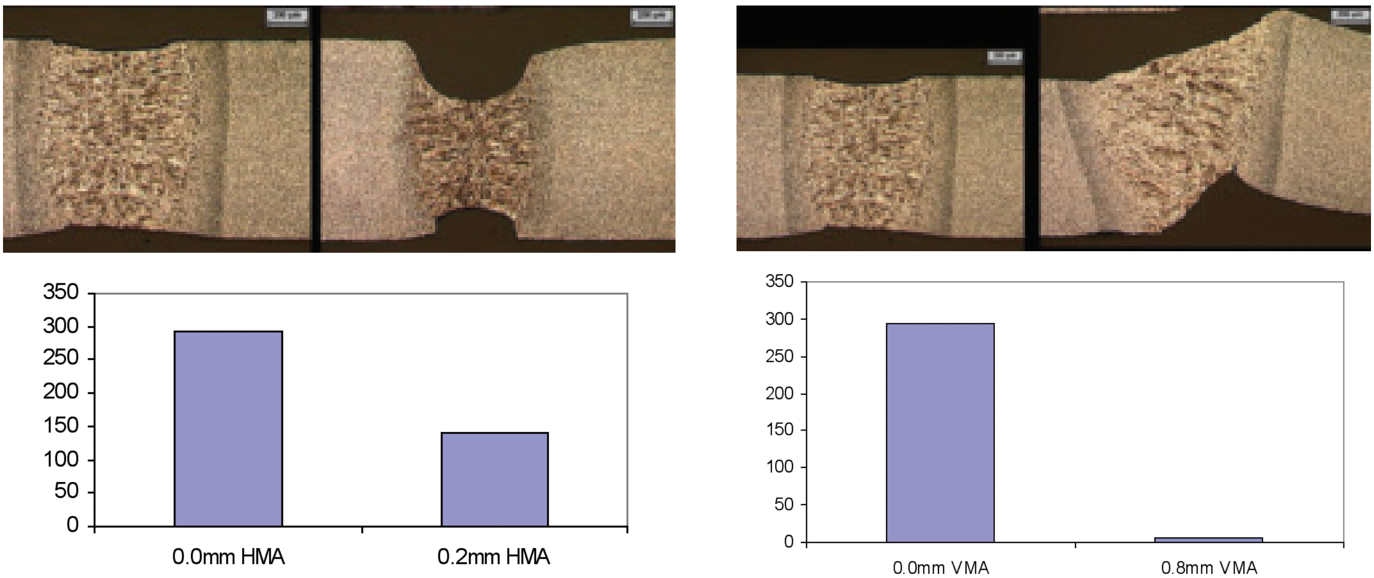

Fig. 4 — The effect of horizontal misalignment (HMA) and vertical misalignment (VMA) on the tensile strength of 2.5-mm C-Mn steel.

Vertical misalignment (VMA) was found to be substantially more detrimental to the strength required to fracture the weld. Indeed, the introduction of a vertical misalignment of only 0.8 mm in 2.5-mm-thick strip reduced the load-carrying ability by 97% (Ref. 2). The more severe effect of vertical misalignment on the tensile strength is realized on account of the stress concentrations at the weld toe that are enhanced by the rollover effect resulting from the sheared edge.

Twin spot optics were then purchased from Kugler Precision GmbH for the RD&T Trumpf TLC welding head. Beam monitoring equipment manufactured by Primes GmbH was used to characterize the focused laser beam. The single spot and 0.7-mm twin spot power intensity profiles are reproduced in Fig. 5.

Single spot and twin spot laser welds were produced at 6-kW laser power to assess the weld quality produced from each optic under a variety of vertical and horizontal misalignments and strip thickness. Vertical misalignment was introduced by placing aluminum shims under one of the plates to be welded and horizontal misalignment was introduced by trapping aluminum shims in between the strips to be welded.

The single and twin spot laser welding processes were then completely characterized for twin spot optics with 0.4-, 0.7-, and 1.0-mm spot separation on 1.0-, 1.5-, 2.0-, and 2.5-mm hot rolled 'black' steel.

It was found that the twin spot welding process appeared to be more stable than the single spot process in terms of plasma plume fluctuations and the generation of spatter. The twin spot welding process was also shown to greatly influence the weld bead geometry, whereby an effective increase in focus spot diameter generated a wider weld, i.e., a weld with lower aspect ratio. When considering an ideal fitup, it was shown that there was no marked difference in the mechanical properties of the welds produced with single and twin spot optics, i.e., tensile failure occurred in the base metal.

The magnitude of generated defects from the vertical and horizontal misalignments were, however, found to be minimized by the twin spot process as more of the base metal was melted to form the joint. In general, horizontal and vertical misalignments can be increased by up to approximately 100% and 40%, respectively, by the implementation of twin spot laser welding without detrimental effects. However, the benefits in terms of tolerance to fitup and sheared quality are a function of the twin spot separation, whereby a higher spot separation gives a lower aspect ratio weld with more ability to 'soak up' undercut and stress concentration defects.

Nevertheless, the benefits of twin spot welding are not without their disadvantage, namely a reduction in welding speed. It was found that the higher the spot separation, the higher the reduction in welding speed required to maintain complete joint penetration. The relationship between spot separation and welding speed is detailed further in Fig. 6. The reduction in welding speed was, however, deemed as an accept-

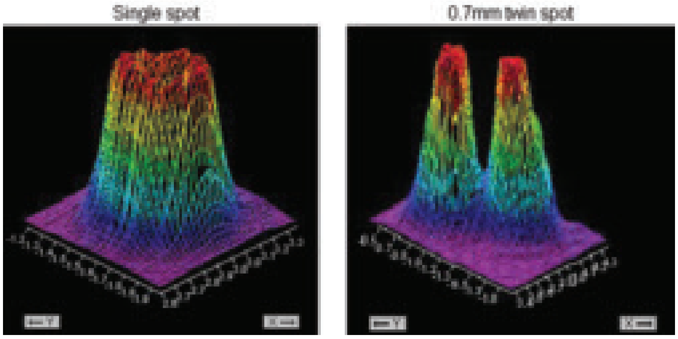

Fig. 5 — Focused beam power density profiles of single spot and 0.7 mm spot separation twin spot.

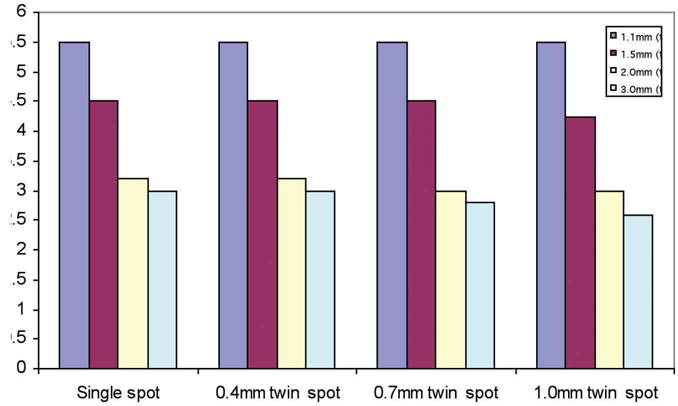

Fig. 6 — The effect of twin spot separation on the welding speed of 1.1-, 1.5-, 2.0-, and 2.5-mm-thick 'black' steel strip.

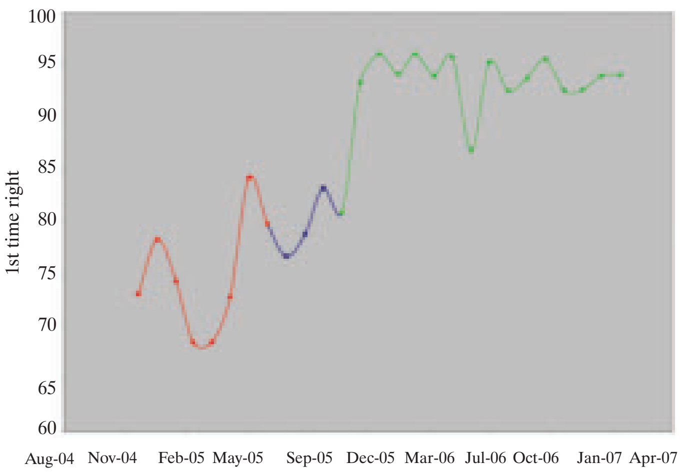

Fig. 7 — First time right welding efficiency of the coil joiner illustrating the decreased reject rate from installing twin spot laser welding.

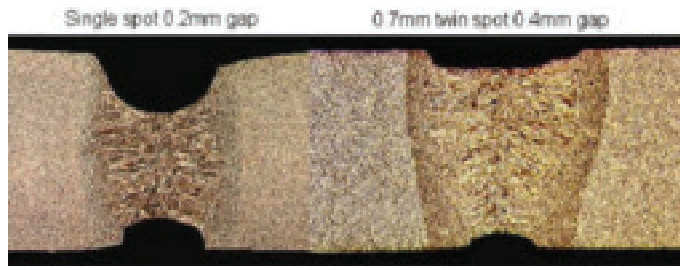

Fig. 8 — Transverse sections of a single spot laser weld with a 0.2-mm horizontal gap (left) and a 0.7-mm twin spot laser weld with a 0.4-mm horizontal gap (right) produced on the Miebach during online trials.

able disadvantage when compared to the benefits of greater tolerance to vertical and horizontal misalignments, and the twin spot process was installed at the pickle line in September 2005.*

Installation and Results

Initially, a small spot separation of 0.4 mm was installed at the pickle line to prove the process in production; installation took approximately 1 hour. Online testing prior to production showed that the 0.4-mm spot separation twin spot required no changes in the standard (single spot) weld parameters (welding speed, laser power, and focus height) to achieve complete joint penetration for all strip thickness tested. The coil joiner ran in full production for four weeks with no strip breaks; however, the first time right welding efficiency was not significantly improved over the single spot process. It was therefore decided to replace the twin spot mirror with a higher spot separation of 0.7 mm. The higher spot separation mirror required modifications to the welding parameters on account of the power density of the focus region being effectively reduced beyond the welding envelope required for complete joint penetration at the original programmed power and speed. Once the correct parameters were identified, the first time right welding efficiency increased to 95% (Fig. 7), although at the expense of a 20% reduction in welding speed. Nevertheless, a 20% reduction in welding speed accounts for, on average, a 5 second increase in welding time, in comparison to several minutes to complete a single reweld.

The other major benefit accrued to the installation of twin spot at the Beitsbaan is the life of the shear cassette. Typically, at 10,000 shear cuts, the weld quality would diminish, resulting in a low first time right efficiency. The application of twin spot has seen the life of the shear cassette double.

Transverse sections of single and twin spot welds taken from the Beitsbaan are detailed in Fig. 8. As can be clearly seen, the weld produced with twin spot illustrates substantially less undercut than the single spot weld, even with twice the root opening of 0.4 mm.

*The twin spot application to continuous coil joining lines is patent pending.

Summary and Conclusions

A research and development program of experimental work on single and twin spot laser welding has shown that a substantial increase in process tolerance, weld quality, and mechanical strength can be achieved with twin spot laser welding when considering vertical and horizontal misalignment and hence bad strip shape and poor sheared edge quality. The development program led to the installation of twin spot laser welding on the Corus IJmuiden Beitsbaan. The twin spot process has been in production since September 2005, and has generated substantially higher first time right welding efficiency (lower scrap rate) and increased shear cassette life, albeit at a lower welding speed.◆

Acknowledgments

The authors would like to acknowledge the kind assistance of Gabe van der Zwaag for metallurgical preparations and Joerg Kugler for designing and manufacturing the twin spot optics.

References

1. Longfield, N. P., and Wit, I. de. 'Beitsbaan 22 Miebach laser welder – initial twin spot laser welding trials at IJTC.' Corus RD&T, April 13, 2005, Reference Source Number 113942.

2. Xie, J. 'Dual beam laser welding.' 80th Annual AWS Convention, April 11–15, 1999, St. Louis, Mo.

Avoiding Defects in Stainless Steel Welds

Here's help in understanding the discontinuities and defects that are unique to stainless steels and higher alloys

BY RICHARD D. CAMPBELL

Stainless steels are selected primarily because of their corrosion resistance, with the mechanical properties (strength, hardness, ductility) being of secondary importance. Stainless steels contain greater than 10.5 to 12 wt-% chromium, which provides a passive chromium oxide layer that forms on the surfaces when exposed to air or other oxidizing environments. As such, it is important when welding stainless steels that the weld metal be protected from sources of contamination or oxidation. Cleanliness is essential in welding stainless steels.

Types of Stainless Steels

There are five basic types of stainless steels:

- Austenitic (200 and 300 Series)
- Ferritic (some of the 400 Series)
- Martensitic (balance of the 400 Series)
- Duplex
- Precipitation hardening

The chemical compositions of some typical stainless steels are provided in Table 1. The first three types are classified according to the metallurgical structure they develop at room temperature. The majority of stainless steels are the austenitic 300 series, which contain chromium and nickel along with other alloying elements. These are nonmagnetic, have good toughness and ductility at elevated and low temperatures, and have the best general corrosion resistance of all stainless steels.

The ferritic stainless steels are ferromagnetic and have better resistance to stress-corrosion cracking, pitting, and crevice corrosion than the austenitics.

The martensitics contain higher levels of carbon, which gives them very high strength.

The duplex stainless steels contain two metallurgical phases at room temperature (austenite and ferrite), and thus they have some of the best properties of each.

The precipitation-hardening stainless steels have other elements added (such as titanium) to form precipitates during a postweld heat treatment. These alloys can develop extremely high strengths.

General Welding Discontinuities and Defects

Welding on stainless steels can produce the typical weld discontinuities or defects, including the following:

- Cracks
- Incomplete fusion
- Incomplete joint penetration
- Overlap
- Porosity
- Slag inclusions
- Tungsten inclusions
- Unacceptable weld profiles
- Undercut
- Underfill

Discontinuities can be caused by the following:

- Welding process
- Poor weld joint design
- Improper welding technique or application
- Base metal or filler metal

These discontinuities can occur in the

- Weld metal
- Heat-affected zone (HAZ)
- Base metal

Specific Discontinuities and Defects in Stainless Steel Welds

Certain discontinuities and defects are unique to welds in stainless steels and higher alloys. Following are several specific welding-related discontinuities in stainless steels.

General Corrosion Issues

Above all else, stainless steels are selected for their corrosion resistance. As such, anything during welding that affects their corrosion resistance can be considered a welding discontinuity.

General Corrosion. The 10.5–12% minimum chromium content helps resist general corrosion over the entire surface of the metal. Rusting of stainless steels cannot occur if the metal is clean and free from contamination with iron.

Rusting. Many stainless steel systems display rust on them. Piping systems often have streaks of rust on them where water stained with rust from carbon steel pipes

---

RICHARD D. CAMPBELL (rdcampbe@bechtel.com), *PhD, PE, is a welding manager, Bechtel National, Inc. This article is taken, in part, from AWS's The Professional's Advisor on Welding of Stainless Steels, which Campbell compiled. Information is also taken from a two-day seminar Campbell presented at the 2006 FABTECH International & AWS Welding Show titled "Welding of Stainless Steels — Basics to Avoiding Defects."*

Fig. 1 — Rust on stainless steel welds.

Fig. 2 — Discoloration on 316L.

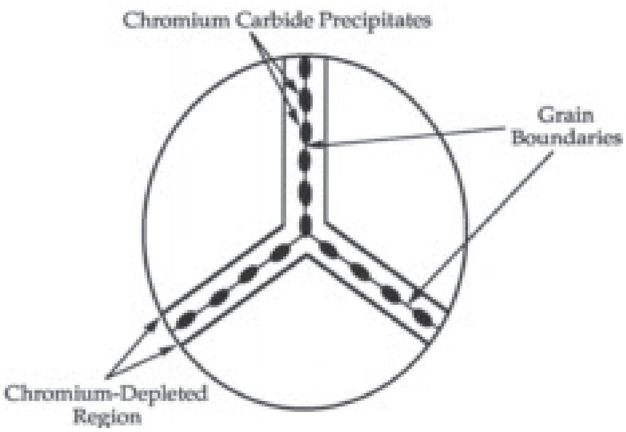

Fig. 3 — Chromium carbide precipitation.

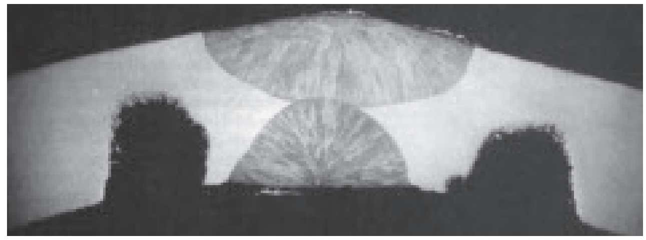

Fig. 4 — Intergranular corrosion in 304.

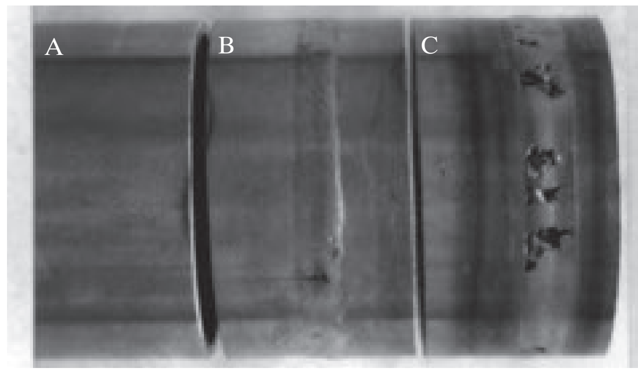

Fig. 5 — 6% Mo samples after accelerated corrosion test. A — Unwelded tube sample; B — weld with ERNiCrMo-10 filler metal; C — autogenous weld.

or structural members above them has flowed onto them, especially when located outdoors. Rust spots or stains on stainless steel pressure vessels are typically caused from contact with carbon steel, where some of the steel has become embedded into the surface of the stainless steel. These are environmental issues in service, not caused by welding.

In many cases, however, welds or HAZs on stainless steels exhibit rust or other contaminants caused by welding or improper preparation. It is important that the stainless steel surfaces do not become contaminated during weld preparation or welding. Avoid the following:

• Contact with carbon steel during preparation (e.g., welding on a carbon steel tabletop, use of tools not dedicated for use on stainless steels, use of carbon steel wire brushes or stainless steel brushes previously used on carbon steel).

• Improper or inadequate gas shielding of the weld face (top side) and weld root (underbead). This can cause excessive discoloration, which is a form of contamination with oxygen, carbon, etc., and can reduce the general corrosion resistance.

• Using improper welding processes, such as oxyfuel welding.

Figure 1 illustrates several stainless steel welds on nozzles on a tank with rusting caused by contamination with "free iron" during preparation. Any rust in a stainless steel weld or HAZ should be mechanically removed and the area chemically treated with a passivation treatment to ensure that all rust has been removed.

Weld Contamination/Discoloration. Stainless steel welds can become discolored on the weld face (top) or weld root (underbead) if not properly shielded or purged with inert gas or flux during welding. Stainless steel pipe, tube, and vessels are normally purged on the inside with an inert shielding gas such as argon or helium. There are also fluxes developed for stainless steels that are applied to the backside of the joint before welding, which help protect the backside of the weld from oxidation and contamination. However, these fluxes do not protect the weld underbead as well as inert gases, and should not be used in critical or high-purity applications.

Discoloration is simply varying compositions and thicknesses of oxides (or other contaminants) on the stainless steel surfaces. Depending upon the application, different levels of discoloration or oxidation may be acceptable. AWS D18.2, *Guide to Weld Discoloration Levels on Inside of Austenitic Stainless Steel Tube* [taken from AWS D18.1, *Specification for Welding of Austenitic Stainless Steel Tube and Pipe Systems in Sanitary (Hygienic) Applications*] shows examples of discoloration. Figure 2, taken from AWS D18.2, shows ten weld underbeads produced on 316L tubing using different amounts of oxygen in the argon purging gas. Weld number 1 was made with 0.0010% oxygen, weld 4 with 0.0100% oxygen, and weld 7 with 0.1000% oxygen. These show the tremendous impact of oxygen on causing discoloration. It is important to note that typical welding-grade argon is 99.985% pure, meaning that 0.0150% is other than argon. If all of the contaminants were oxygen, this would be represented by a weld between numbers 4 and 5.

This color chart is used by several industries to identify acceptable weld discoloration levels, as follows:

• In the semiconductor industry, the weld and HAZ shall have no color on them

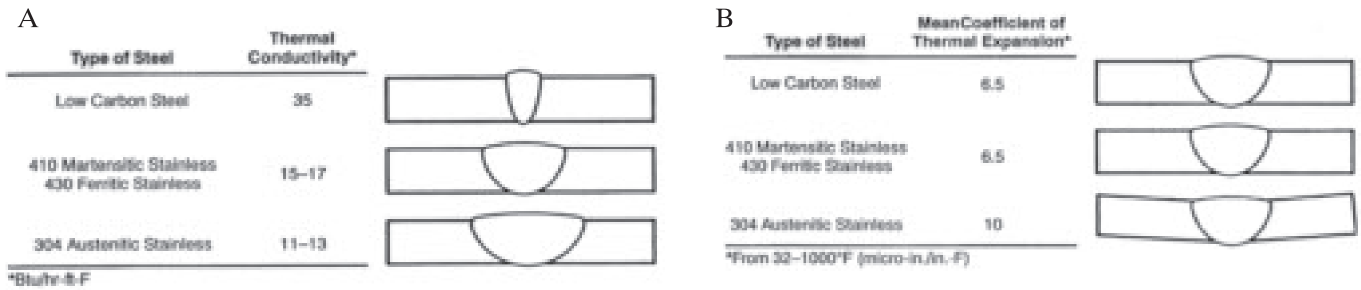

Fig. 6 — A — Thermal conductivities; B — coefficients of thermal expansion.

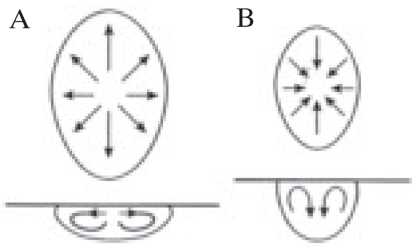

Fig. 7 — Weld pool fluid flow. A — Low sulfur; B — high sulfur.

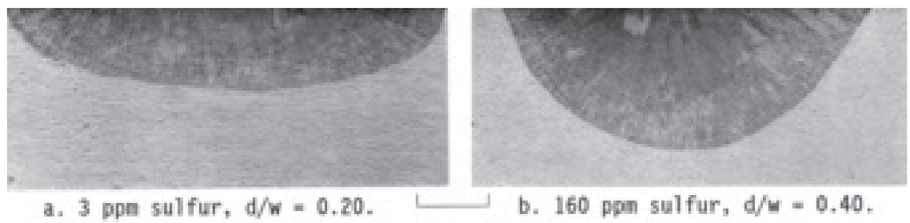

Fig. 8 — Weld cross sections in 304 made with same GTA welding parameters.

at all (number 1 or better).

- In the biotechnology and pharmaceutical industries, the ASME (American Society of Mechanical Engineers) *Bioprocessing Equipment Standard* requires no discoloration on the weld surface, and only a light blue or light straw color on the HAZ, such as HAZ numbers 1 through 3 on the color chart (for surfaces that are in contact with the drug product).
- In the food, dairy, and beverage industries, AWS D18.1 requires no discoloration darker than the straw or blue of weld number 4.
- In other industries, even darker discoloration levels may be acceptable.

Sugaring (a black oxidation with white "crystals" of oxide frequently present) is the extreme condition of weld oxidation/contamination, and is typically unacceptable for all stainless steel applications.

All forms of discoloration or contamination leave a surface that is less corrosion resistant than the stainless steel. Depending upon the conditions, this can lead to corrosion of the stainless steel. Proper mechanical or chemical cleaning followed by a passivation treatment are necessary to restore corrosion resistance (simple "passivation" will not remove these regions). The best option is to keep the stainless steel welds free from discoloration during welding.

Sensitization (Intergranular Corrosion) of Stainless Steels

Sensitization is a problem that can occur mainly in austenitic and ferritic stainless steels, when chromium carbides (or nitrides) precipitate at grain boundaries — Fig. 3. In the austenitic stainless steels, these chromium carbides form when the stainless steel is exposed to temperatures in the range of 800° to 1500°F (427° to 816°C). Because the chromium has diffused to the carbides, there is a region surrounding each carbide where the chromium content is significantly reduced. When exposed to a corrosive environment, intergranular corrosion will likely occur at the grain boundaries, because of the chromium-depleted areas.

The greater the carbon content, the more extensive the sensitization. 304 and 316 stainless steels contain a maximum of 0.08% carbon. Figure 4 shows intergranular corrosion in the HAZs of a longitudinal seam weld in 304 stainless steel pipe.

Sensitization is a defect only if the stainless steel is exposed to the proper corrosive environment, such as an acid; however, some sensitized stainless steels have "rusted" or oxidized when simply exposed to air. Bands of "rust" in the HAZs of pipe welds are a prime example of this.

A weld on stainless steel will most often produce sensitization in the HAZ, because this region is within the sensitization temperature range during heating, welding, and cooling. Welds that are sensitized and exposed to a corrosive environment will often show "wagon wheel tracks" or parallel lines of corrosion along the HAZ on either side of the weld.

Typically, the weld metal of a single-pass weld does not get sensitized, because the material exceeds the temperature range for sensitization, and cools through this temperature range rapidly enough that chromium carbides do not have time to form. Sensitization rarely occurs in single-pass welds or in the HAZs on thin stainless steels, because these regions do not remain in the sensitization temperature range long enough.

Multipass welds on stainless steel, especially on thicker material, can produce sensitization in the HAZ as well as in the first, and subsequent, weld passes. The heat from the second and subsequent weld passes sensitizes the root pass. In the same manner, the second weld pass is sensitized by the third pass, etc.

Sensitization thus can occur during

- Heat treatment
- Multipass welding
- Service at elevated temperatures

Therefore, avoiding exposure to these temperatures is important.

Detection of Sensitization. Since sensitization becomes a defect only after the material has been exposed to a corrosive or oxidizing environment, it cannot be detected by normal visual or other nondestructive examination methods immediately following welding. Any specifications that call for a visual examination to verify that there is no sensitization are meaningless. Metallographic analysis on a sample is the only accurate method to detect sensitization, and unfortunately, this is a destructive test.

Methods to Avoid Sensitization. There are several practical ways to avoid sensitization or to reduce the negative consequences/effects of sensitization.

1. **Solution Anneal and Water Quench.** If austenitic stainless steels have already been sensitized, annealing at 1900°–2050°F (1038°–1121°C) causes the chromium carbides to dissolve and allows the chromium to diffuse back to the depleted regions. Water quenching (rapid cooling) is important to avoid reformation of the chromium carbides through the sensitization temperature range. Note that quenching is not the issue it is with high-strength low-alloy steels, because the austenitic stainless steels will not transform to martensite during rapid cooling.

However, annealing often is not a practical solution. Full annealing of a structure is often impractical. Annealing of stainless steels, especially the austenitic stainless steels, produces significant distortion. Finally, localized heat treatment will not work. While this treatment can remove sensitization in the heated region, it can also produce sensitization on each side of the heated area, which will be exposed to the sensitization temperature range.

2. **Use of Stabilized Stainless Steels.** 321, 347, 348, and 444 stainless steels contain "stabilizing" elements such as titanium, niobium, tantalum, and cobalt. These elements are intentionally added because they form carbides of these elements (e.g., titanium carbides) and these are more stable than chromium carbides. Since chromium carbides do not form, there is no depletion of chromium and thus no sensitization. These stabilized stainless steels were developed to avoid sensitization. (Note that the carbon content of 321, 347, and 348 is the same as the 0.08% maximum as 304, and these are stabilized versions of 304.)

It is important to note that the amount of the stabilizing elements is critical. For example, the amount of titanium needed in 321 is at least five times the carbon content. If the titanium content is less than this, some chromium carbides could still form, thus producing sensitization.

To avoid sensitization with stabilized stainless steels, it is important to select stabilized grades of filler metal to match the stabilized grades of base metal (e.g., use ER321 filler metal for 321 base metal).

3. **Use of Low-Carbon Stainless Steels.** Numerous grades of stainless steel have been developed with lower carbon contents. 304L and 316L contain a maximum carbon content of 0.03 wt-% compared with 304 and 316, which have a maximum carbon content of 0.08 wt-%. For 304 with 0.08% carbon, sensitization can occur in less than 1 min. For 304L with 0.03% carbon, it would take several hours at the appropriate temperature to produce sensitization due to the extremely low carbon content of the stainless steel.

These low-carbon stainless steels were specifically developed to avoid sensitization (the 'L' designation in 304L denotes low carbon content). There is simply not enough carbon to allow the chromium carbides to form.

To avoid sensitization with the low-carbon stainless steels, it is important to use low-carbon grades of filler metal to match the low-carbon content of the base metal (e.g., use ER308L filler metal with 304L base metal). (Note: while the low-carbon stainless steel filler metals such as ER308L can be used on moderate or high-carbon-content base metals such as 304, the weld metal will have a lower strength than that of the base metal because of the lower carbon content.)

4. **Avoid Contact with Carbon.** Proper cleaning and surface preparation are very important to avoid introducing carbon into the stainless steel. Avoid contamination of the stainless steel weld joint from exposure to carbon steel, tools that have contacted carbon steel, or other sources of carbon, such as grease, oil, paint, graphite, etc.

Fig. 9 — Irregular weld penetration in 304L.

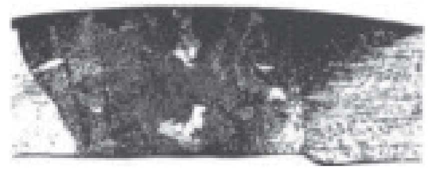

Fig. 10 — Shifted weld in orbital tube weld on 316L.

Crevice and Pitting Corrosion

Both crevice and pitting corrosion are localized forms of corrosion that can occur in stainless steel welds. Crevice corrosion typically occurs where a crevice has been created that can concentrate the corroding environment. To reduce crevice corrosion, avoid unacceptable weld profiles that create crevices, such as the following:

- Incomplete fusion
- Incomplete joint penetration
- Porosity
- Weld spatter
- Arc strikes
- Rough weld ripples

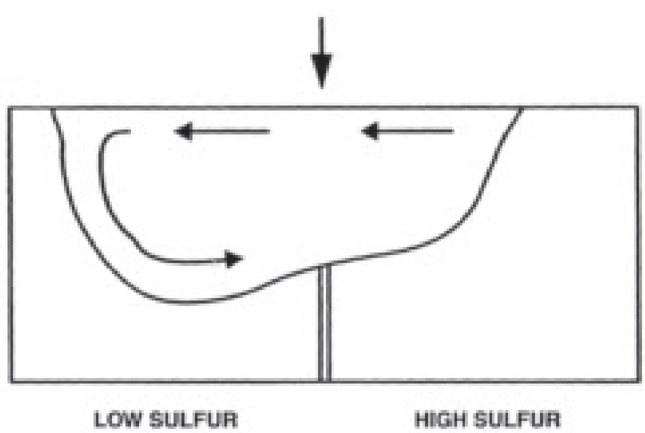

Fig. 11 — Schematic of fluid flow.

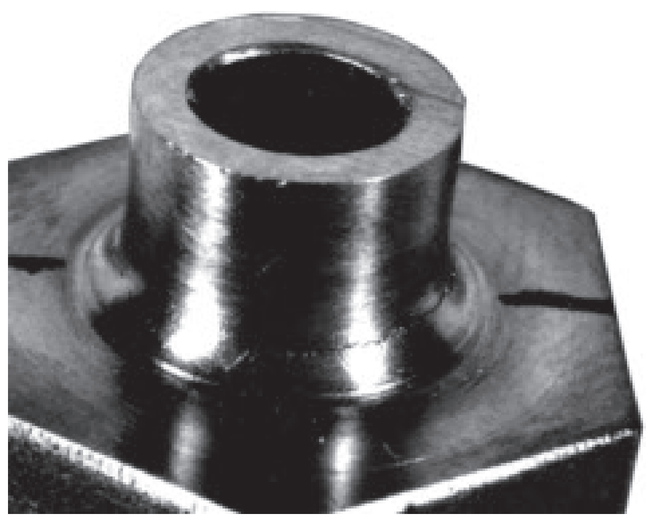

Fig. 12 — Centerline hot crack in 304L weld.

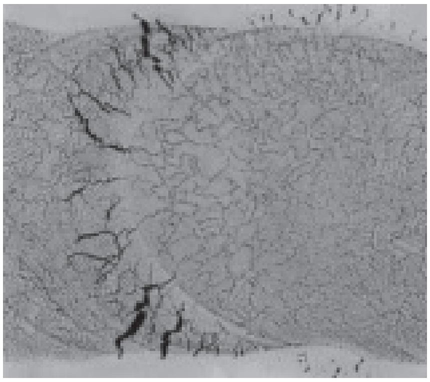

Fig. 13 — Hot cracks in 444 ferritic stainless steel weld.

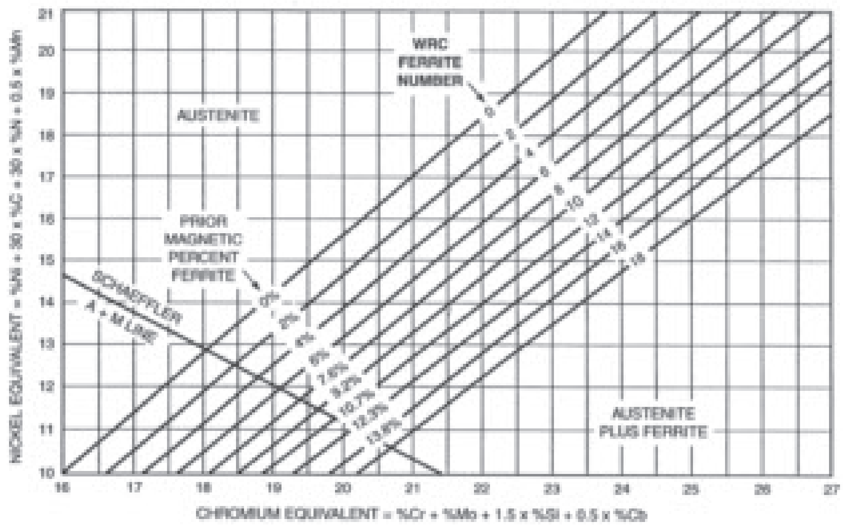

Fig. 14 — DeLong diagram.

• Overlap

Pitting corrosion typically occurs because of a local segregation of corrosion-resistant elements in the material. The pitting and crevice corrosion resistance of stainless steels, especially to chloride environments, is improved dramatically by the addition of molybdenum and nickel.

316L is a modification of 304L with 2–3% Mo added (and slightly lower chromium but higher nickel contents). 317L has more molybdenum (3–4%), 904L even more (4–5%), and the 6% Mo alloys (UNS N03867 or AL-6XN) have 6–7% Mo. All of these were designed to provide increased pitting corrosion resistance to chloride environments.

Most stainless steels are welded with "matching" filler metals. 304L is welded with E308L or ER308L (308L was designed as the filler metal for 304L, with slightly elevated chromium and nickel compositions to account for loss of some of these elements through vaporization in the arc). 316L is welded with E316L or ER316L, which contain 2–3% Mo.

During welding of some higher-alloy materials, segregation of certain chemical elements occurs. In the 6% Mo alloy, there can be significant segregation of molybdenum in the weld metal, such that some areas are highly concentrated in this element while other areas have concentrations similar to the 2–3% Mo present in 316L.

To accommodate for this segregation, overmatching filler metals are recommended, such as ERNiCrMo-3 (UNS N06625 or Alloy 625), ERNiCrMo-10 (UNS N06022 or Alloy C22), or ERNiCrMo-4 (UNS N10276 or Alloy C276). These filler metals contain nominally 9%, 13%, and 16% molybdenum, respectively. When welded with these higher-molybdenum-bearing filler metals, the nominal composition of the weld metal is raised, and the segregated regions are higher in molybdenum.

Figure 5 shows three samples of a 6% Mo alloy after being exposed to an elevated temperature, accelerated-time chloride corrosion test. Figure 5A is an unwelded sample, Fig. 5B was welded with ERNiCrMo-10 filler metal, and Fig. 5C is an autogenously welded sample (no filler metal added). Significantly more pitting

Table 1 — Chemical Compositions of Some Typical Stainless Steels

Composition (wt-%). Single values are maximum unless indicated.

Type	C	Cr	Ni	Mo	P	S	Other
Austenitic Stainless Steels							
303	0.15	17.0–19.0	8.0–10.0	0	0.20	0.15 min	
304	0.08	18.0–20.0	8.0–10.5	0	0.045	0.03	
304L	0.03	18.0–20.0	8.0–12.0	0	0.045	0.03	
321	0.08	17.0–19.0	9.0–12.0	0	0.045	0.03	5 × %C = Ti min
347	0.08	17.0–19.0	9.0–13.0	0	0.045	0.03	* (see below)
348	0.08	17.0–19.0	9.0–13.0	0	0.045	0.03	0.20 Co; 0.10 Ta plus*
316	0.08	16.0–18.0	10.0–14.0	2.0–3.0	0.045	0.03	
316L	0.03	16.0–18.0	10.0–14.0	2.0–3.0	0.045	0.03	
317L	0.03	18.0–20.0	11.0–15.0	3.0–4.0	0.045	0.03	
6Mo	0.03	20.0–22.0	23.5–25.5	6.0–7.0	0.040	0.030	
Ferritic Stainless Steels							
409	0.08	10.5–11.75	0	0	0.045	0.045	6 × %C = Ti min
444	0.025	17.5–19.5	1.00	1.75–2.5	0.04	0.03	Nb + Ta
Martensitic Stainless Steels							
410	0.15	11.5–13.0	0	0	0.04	0.03	
440A	0.060–0.075	16.0–18.0	0	0	0.04	0.03	

*10 × %C = (Nb+Ta) min

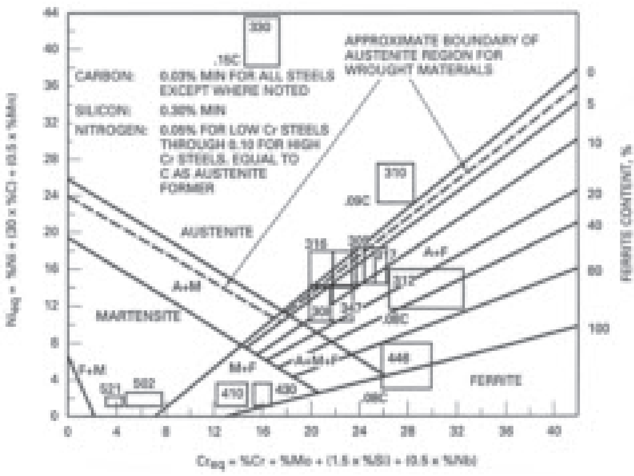

Fig. 15 — Schaeffler diagram.

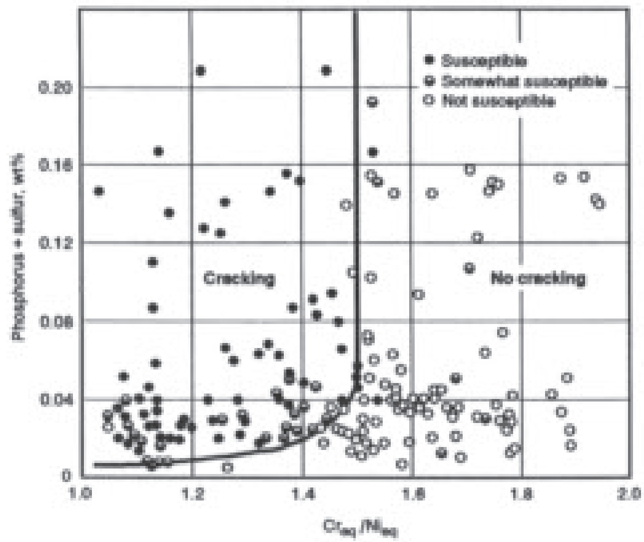

Fig. 16 — Suutala diagram.

corrosion has occurred in the autogenously welded sample than in the base metal or the sample welded with ERNiCrMo-10. This is true for several other stainless steel alloys, and it is imperative to follow the base metal manufacturer's recommendations on filler metals.

Other Forms of Corrosion

Stress Corrosion Cracking can occur in highly stressed austenitic stainless steels (base metals or welds) when exposed to chlorides or fluorides.

Galvanic Corrosion can occur when two base metals are welded together that have different corrosion-resistant properties (one is more anodic than the other on an electromotive series). This can also occur when a filler metal with more anodic or cathodic properties is used to weld a stainless steel.

Distortion, Thermal Conductivity, Thermal Expansion

One of the main discontinuities or defects in welding of austenitic stainless steels is distortion or shrinkage. Two major physical properties of austenitic stainless steels dramatically affect distortion and shrinkage — thermal conductivity and thermal coefficient of expansion. Figure 6A and B illustrates the effects of these properties on fusion welding (arc or beam welding).

Thermal Conductivity. Austenitic stainless steels have a thermal conductivity only approximately 33% of the value of low-carbon steels — Fig. 6A. Therefore, if they are welded with the same arc welding parameters, as shown in Fig. 6A, significantly less heat will be conducted away from the weld. This produces a much larger weld bead on austenitic stainless steels than on low-carbon steels, for the same welding heat input. The martensitic and ferritic stainless steels have thermal conductivities approximately 50% lower than low-carbon steels, but not as low as the austenitics. The weld beads made on these alloys produce a larger weld bead than on carbon steel, but smaller than on the austenitic stainless steels.

To produce a similar size weld bead on each material, a lower heat input (e.g., lower welding current, faster travel speed) would be used on the martensitic and ferritic stainless steels than on the carbon steels. The austenitics would require an even lower heat input.

Thermal Expansion. There are also differences in the coefficients of thermal expansion of austenitic stainless steels compared with carbon steels. This property determines how much a metal will expand when heated and shrink when cooled. During welding, thermal expansion produces distortion. The higher the coefficient, the more expansion and contraction, and the greater the amount of distortion.

As shown in Fig. 6B, austenitic stainless steels have a coefficient of thermal expansion approximately 150% that of carbon steels, while those of martensitic and ferritic stainless steels are similar to the carbon steels. If the welding parameters are changed for the austenitic stainless steels to provide the same weld shape as in the carbon steels (and the martensitic and ferritic stainless steels), the distortion will be significantly greater with austenitic stainless steels.

Figure 6A and B illustrates that fusion welding parameters for austenitic stainless steels need to be significantly different from those for carbon steels. Recommended arc welding parameters for the austenitic stainless steels are cooler (e.g., lower current, faster travel speed) than those for carbon steels. This is due to the lower heat input required (from the low thermal conductivity), as well as to reduce the distortion (because of the higher thermal expansion).

Tables of recommended welding parameters for "stainless steels" always refer to the austenitic stainless steels, because of the drastic differences in the thermal properties. Parameters for the ferritic and martensitic stainless steels would be about midway between those for the carbon steels and for the austenitic stainless steels.

Weld Penetration

Weld penetration variations, especially in arc welds, can be caused by many factors. Normal methods to overcome incomplete joint penetration problems include

- Decreasing travel speed.
- Increasing welding current.
- Changing joint design (such as decreasing weld root face or land thickness).

In stainless steels, however, weld penetration is often dramatically affected by the chemical composition of the weld (from the base metals and the filler metal). The main element that causes this variable weld penetration is sulfur, and to a lesser extent, oxygen and certain other elements.

Figure 7 illustrates weld pools in low- and high-sulfur 304 stainless steel. With low levels of sulfur present (<0.003%), the liquid weld pool flows outward, producing shallow weld penetration — Fig. 7A. When the sulfur content is higher (>0.005%), the weld pool flows inward, producing deep, narrow weld penetration — Fig. 7B. This phenomenon is called surface tension fluid flow, and it is produced because sulfur is a surface-active element that segregates to the surface of the weld pool, causing a change in the surface tension and the resultant inward fluid flow. Figure 8 shows gas tungsten arc bead-on-plate welds on two heats of 304, one with low sulfur (0.0003%, Fig. 8A) and the other with a high sulfur content (0.016%, Fig. 8B). The weld on the high-sulfur material is significantly deeper and narrower.

This problem can sometimes be overcome by the methods presented at the beginning of this section. However, each of those options simply increases the existing driving force. Therefore, if the weld pool is wide and shallow, increasing the welding current will make the weld pool deeper, but also wider at a faster rate than it becomes deeper.

Increasing the sulfur content of the base metal or filler metal may be the only acceptable option for avoiding incomplete penetration. This is the reason that some stainless steel specifications presently require sulfur contents of 0.005–0.017% sulfur (e.g., ASTM A270 for 316L tubing and the *ASME Bioprocessing Equipment Standard* for 316L stainless steel fittings made from tubing). The minimum of 0.005% sulfur prevents the shallow penetration problem.

This penetration problem can be further aggravated when a low-sulfur stainless steel is welded to a high-sulfur stainless steel — Fig. 9. The weld pool can be shifted off-center, causing a missed joint, as shown in Fig. 10 for an autogenous orbital tube gas tungsten arc weld made on 316L stainless steel tubing. The weld pool is shifted toward the low-sulfur component, as illustrated schematically in Fig. 11. The high-sulfur side flows toward the hot center of the weld pool (under the arc), which is to the left. The low-sulfur side has fluid flow toward the cooler outer regions of the weld pool, which is to the left. The combination of these fluid flows produces a shift to the low-sulfur side.

If the sulfur compositions of the two base metals are known, the welding electrode can be offset toward the high-sulfur component prior to welding, which should shift the weld pool back and allow the weld to consume the joint. The difference in the minimum and maximum composition limits of 0.005–0.017% are controlled to reduce the amount of this shift between the components.

This type of weld penetration variation hardly ever occurs in carbon and alloy steels because they have sulfur levels that are above the ranges that produce shallow penetration. By comparison, stainless steels are significantly "cleaner," with lower levels of sulfur.

Hot Cracking

Welding of stainless steels often results in hot cracks in the weld metal or in the HAZ. Typical examples of hot cracks include centerline cracks (Fig. 12), which often occur with fast travel speeds, and crater cracks, which occur when the crater of the weld is not filled properly. Hot cracks occur while the weld is still hot, before it has cooled to room temperature. Other names or forms of hot cracks include

- Microfissures
- HAZ cracks
- Reheat cracks (cracks in previous weld beads caused by subsequent weld passes)
- Solidification cracks

Hot cracking is caused by the following:

- Tensile stress (such as external restraint or residual stress)
- Crack-susceptible microstructure (especially austenite compared with ferrite)
- Contaminants (especially sulfur, phosphorus, titanium, and niobium).

Hot cracking can occur in any of the stainless steels. The free-machining stainless steels that contain high levels of sulfur and phosphorus to improve machinability (such as 303) are especially susceptible. Some of the stabilized grades that contain titanium or niobium (321, 347, 444) are also susceptible (Fig. 13), in addition to the precipitation-hardening grades (such as 17-4PH, which contains copper).

Welding conditions can also affect hot cracking. The following methods are suggested for reducing hot cracking:

- Use stringer beads
- Reduce travel speed
- Use high-ferrite base metal and / or filler metal
- Use materials with low levels of contaminants
- Fill all craters
- Reduce tensile stress (e.g., stress relieve, change joint design)
- Avoid long arc lengths (which can introduce more nitrogen from the atmosphere into the arc. Nitrogen increases the austenite content.)

The grades most susceptible to hot cracking are the austenitic stainless steels, because compared with ferrite, austenite is the more susceptible microstructure. At elevated temperatures, contaminants (such as sulfur) are more readily dissolved in ferrite than in austenite. Therefore, it is desirable to have a small amount of ferrite (primary delta ferrite) present in an austenitic stainless steel weld, because this will reduce the contaminants present during solidification.

Several diagrams and equations have been developed to predict the amount of ferrite present in austenitic stainless steel welds, depending on the base metal and filler metal compositions. The DeLong diagram (Fig. 14) shows the microstructures that would be present in a gas tungsten arc or gas metal arc stainless steel weld, based on the chemical composition of the weld metal.

This diagram uses two equations: the chromium equivalent and the nickel equivalent. Certain elements tend to behave like chromium to produce ferrite, while other elements tend to form austenite, similar to nickel. Using the chemical analyses of the two base metals and the filler metal, the chromium and nickel equivalents are calculated, and the point on the diagram where they intersect provides the predicted ferrite number (FN). Typically, a ferrite number exceeding 3 will produce a weld that should not be subject to hot cracking.

Certain instruments are available that can measure the ferrite number (or the percent ferrite, another indicator). These instruments measure the magnetic field produced by the ferromagnetic ferrite within the nonmagnetic austenite. AWS A4.2M:2006 (ISO 8249: 2000 MOD), *Standard Procedures for Calibrating Magnetic Instruments to Measure the Delta Ferrite Content of Austenitic and Duplex Ferritic-Austenitic Stainless Steel Weld Metal*, describes some of these instruments and the techniques to calibrate them.

The Schaeffler diagram (Fig. 15) has also been developed to predict the ferrite content. The chromium and nickel equivalent equations are slightly different from those shown on the DeLong diagram, since they do not include the strong effect of nitrogen. The Schaeffler diagram plots typical composition ranges for various stainless steel filler metals. 310 stainless steel filler metal has such a high nickel content that it produces no ferrite in the weld. 316 stainless steel produces some ferrite, and 308 even more. 312 has the highest ferrite content of the austenitic filler metals, and produces the least amount of hot cracking. This diagram also plots some of the ferritic and martensitic stainless steels.

Another method to predict hot cracking is the Suutala diagram (Fig. 16), which plots the phosphorus plus sulfur composition vs. a Cr_{eq}/Ni_{eq} ratio. If the Cr_{eq}/Ni_{eq} ratio is greater than 1.5 for GTA welds on 304 stainless steel, then hot cracking is not likely to occur.

Cold Cracking

Cold cracking is another form of cracking, but it is not a problem in the austenitic stainless steels. This occurs after the weld has solidified and cooled to room temperature, and can occur hours or even days after the weld has been completed. Various terms for this include

- Cold cracking
- Hydrogen cracking
- Delayed cracking

This type of cracking occurs only in martensitic stainless steels, in some ferritic stainless steels that form martensite, in certain martensitic precipitation-hardening stainless steels, as well as in dissimilar metal welds between austenitic stainless steels and carbon or alloy steels.

Cold cracking is caused by

- Tensile stress
- Crack-susceptible microstructure (martensite)
- Hydrogen

Although martensite is a very strong and hard microstructure, it has very low ductility and toughness, and therefore can easily cause cracking. The greater the carbon content, the harder and less ductile the martensite. If hydrogen is present, it can diffuse through the metal (even at room temperature), accumulate at the martensite, and increase pressure until more cracking occurs.

Martensitic and Ferritic Stainless Steels. Methods to avoid cold cracking include the following:

- Preheat. This is the best solution. Preheating slows down the cooling rate, so less martensite forms. It also drives off moisture and hydrogen. Some of the martensitic stainless steels are preheated at 300°F (149°C) (whereas austenitic stainless steels, which produce no martensite, are hardly ever preheated).
- Postweld heat treat. A postweld heat treatment tempers the martensite and makes it more ductile (although this is not as effective as preheating in preventing the problem). Some martensitic stainless steels are postweld heat treated at 1400°–1475°F (760°–800°C)
- Reduce the stress.

Dissimilar Metal Welding. Typically, when two different base metals are welded together, the filler metal selected is that for the "higher" alloy of the two — typically to provide the corrosion properties of the higher alloy. There are cases, however, where this does not work. An example is welding 304 stainless steel to carbon steel. The 304 is welded with a 308 filler metal (e.g., ER308) while the carbon steel is typically welded with a 70,000 lb/in.^{2} tensile strength filler metal (e.g., ER70S-2 for GMAW). If ER308 was used, it would produce a weld metal with a composition somewhere between the compositions of the 304 base metal, the carbon steel base metal, and the ER308 filler. While this would provide sufficient corrosion resistance and no hot cracking, there will be a tremendous susceptibility for cold cracking because the high carbon content in the carbon steel will produce significant amounts of martensite in the weld. Suggested filler metals for these base metals include 309 and 310. Both of these contain higher nickel compositions (and higher Ni_{eq}, as seen in Fig. 15) than 308 filler metal. The nickel reduces the martensite formation and cold cracking susceptibility.

Summary

Stainless steels can be readily welded, provided necessary precautions are taken. One of the most essential considerations is to maintain cleanliness of the stainless steel during preparation and welding.◆

American Welding Society

Friends and Colleagues:

I want to encourage you to submit nomination packages for those individuals whom you feel have a history of accomplishments and contributions to our profession consistent with the standards set by the existing Fellows. In particular, I would make a special request that you look to the most senior members of your Section or District in considering members for nomination. In many cases, the colleagues and peers of these individuals who are the most familiar with their contributions, and who would normally nominate the candidate, are no longer with us. I want to be sure that we take the extra effort required to make sure that those truly worthy are not overlooked because no obvious individual was available to start the nomination process.

For specifics on the nomination requirements, please contact Wendy Sue Reeve at AWS headquarters in Miami, or simply follow the instructions on the Fellows nomination form in this issue of the *Welding Journal*. Please remember, we all benefit in the honoring of those who have made major contributions to our chosen profession and livelihood. The deadline for submission is July 1, 2007. The Committee looks forward to receiving numerous Fellow nominations for 2008 consideration.

Sincerely,

Nancy C. Cole
Chair, AWS Fellows Selection Committee

AlcoTec Offers Training and Certification in Aluminum Welding

AlcoTec, a subsidiary of ESAB Welding and Cutting Products, is the technology leader in the manufacture of aluminum welding, brazing, and metallizing wire. As a result, AlcoTec employees are uniquely qualified to offer training, certification, and consultation in aluminum welding.

AlcoTec's welding school incorporates theory and a hands-on approach to welding aluminum alloys, as well as one-on-one discussions with staff. Topics include general characteristics of aluminum, metal preparation, welding procedures, and inspection. AlcoTec also offers welder performance qualification and welding procedure qualification.

Training is provided at AlcoTec's facility in Traverse City, Michigan; customized training can be developed to meet your needs. For more information, contact AlcoTec toll free at 1-800-228-0750 or online at www.alcotec.com.

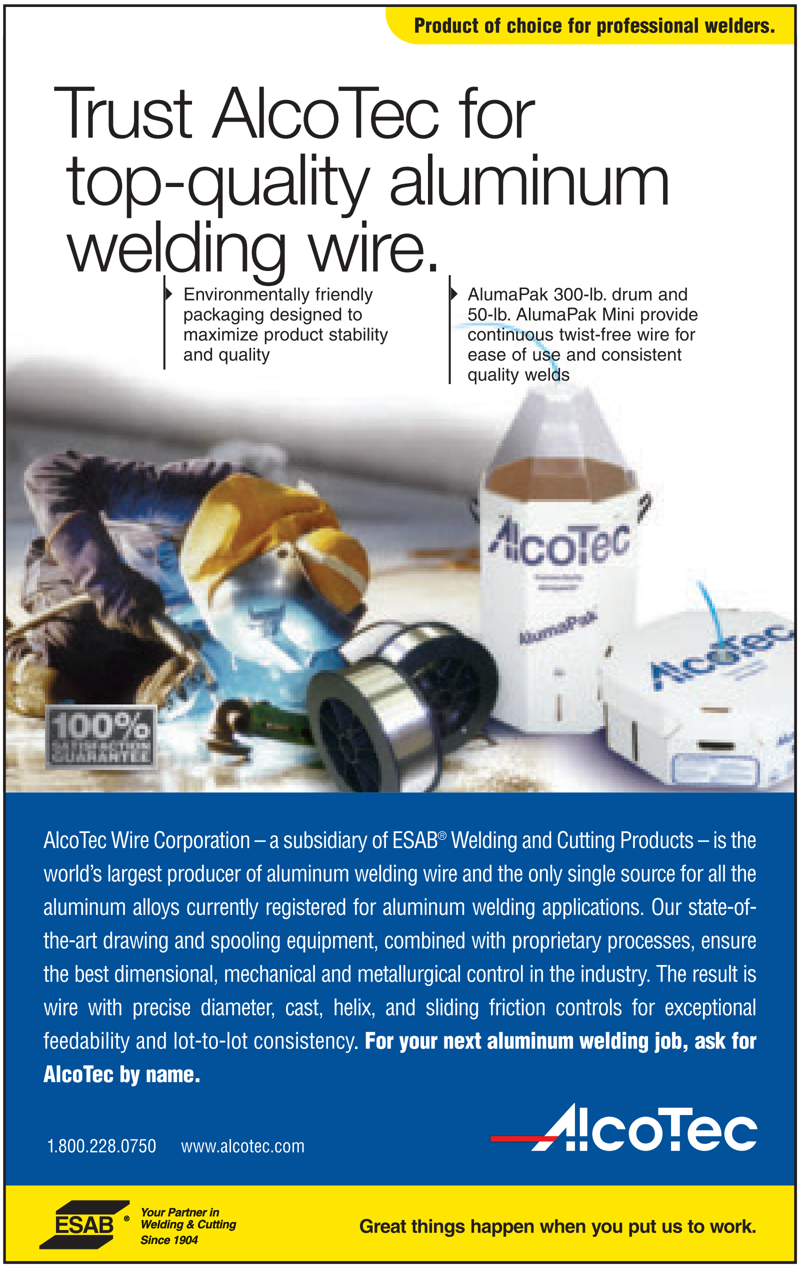

Circle No. 31 on Reader Info-Card

Convenient Package Sizes Speed Production in Aluminum Welding

AlcoTec quality aluminum welding wire is offered in convenient packages designed to provide continuous twist-free wire in high volume for production applications. Twist-free wire delivery ensures ease of use and consistent quality welds. The packaging also maximizes product stability and protects product quality from the time the wire leaves the factory until it is put to use. The wire is easily installed, and when empty, the environmentally friendly packaging is fully recyclable.

Most popular alloys and diameters are available in the AlumaPak 300-lb. drum for high production applications or the convenient 50-lb. AlumaPak Mini for medium-to-high volume users. For more information, contact AlcoTec toll free at 1-800-228-0750 or online at www.alcotec.com.

ESAB Backs Products With 100% Satisfaction Guarantee

ESAB Welding and Cutting Products has been a leader in the welding and cutting industry for more than 100 years and is one of the world's largest manufacturers of welding and cutting equipment and welding filler metals. To demonstrate the confidence ESAB has in its welding and cutting products, the company backs these products with an exclusive 100% Satisfaction Guarantee. Service and support starts from the moment the order is confirmed, with an expanded service organization to ensure that customers are completely satisfied with their ESAB product. Spare and consumable parts are manfactured according to ESAB's quality plan. Product and process training for end users is offered as part of a total ESAB package. The 100% Satisfaction Guarantee is evidence of ESAB's commitment to total customer satisfaction and support. Talk to your local ESAB representative or call 800-ESAB-123 for more information.

Joining Dissimilar Metals
Orlando, Florida
May 22, 23

The joining of dissimilar metals is one of those topics that some people would like to see "swept under the rug." Nevertheless, it's a situation that results in more questions than answers in a typical day. It's a topic that's not even mentioned in the codes; however, help is on the way. This conference will combine the latest innovations in the appropriate welding processes and in welding metallurgy. The keynoter will be Dr. Thomas Eagar of MIT, who knows a lot about this problem and will share that information with you.

Explosion of New Processes
San Diego, California
August 14, 15

There was a time years ago when new welding processes were being introduced in fairly rapid succession. Industry then went into a long stretch during which hardly anything new was being introduced. The tide has since turned. We are now entering into another period of new welding technology. Some of the new processes include higher-powered ultrasonic welding, the various types of friction stir welding, the fiber laser, additive manufacture, hybrid welding, laser stir welding, and gas metal "buried" arc welding. These processes will bring new life to the industry.

Weld Cracking VI
Las Vegas, Nevada
October 16, 17

The popular Weld Cracking Conference continues to attact large audiences wherever it is held. In this conference, leading experts will describe the various problems that trigger cracking in weldments and also the steps that can be taken to prevent the problems from occurring in the first place. This conference is not just confined to steels. Attention will also be paid to the stainless steels, aluminum, and titanium. There will be a great amount of useful information for everybody.

5th Charting the Course in Welding U.S. Shipyards Conference
Newport News, Virginia
October 18, 19

Welding is the most vital and fundamental manufacturing process in the construction of ships and metal hull boats. Given welding's critical importance, the Shipbuilding Conference endeavors to provide up-to-date information on new and emerging technologies being developed for shipbuilding applications. The conference serves as a forum for communicating the focus and progress of these new, innovative developments, as well as their potential value and impact to the shipbuilding community.

Friction Stir Welding Conference
Chicago, Illinois
FABTECH International & AWS Welding Show
November 12

The big three of friction welding — conventional friction welding, linear friction welding, and friction stir welding — will all be included in a full-day conference on Monday, November 12, at the FABTECH International & AWS Welding Show in Chicago. Among the presentations will be talks on such topics as direct drive vs. inertia friction welding, the friction welding of automotive pistons, the linear friction welding of blades onto discs in aircraft engines, the marriage of robotics and friction stir welding, and the ability of any process within this family to weld just about any metal or alloy or even plastic. Also, experts will be on hand to discuss the ability to use any of these processes to weld dissimilar metals on the fly.

Hot Wire Welding and Cladding Conference
Chicago, Illinois
FABTECH International & AWS Welding Show
November 13

There is a great deal of interest lately regarding hot wire welding and cladding. Although invented many years ago, this technology never really saw the light of day until recently. One version or other is already being used by participants in the oil and gas industry, by the U.S. Navy, and by builders of aircraft engines. Hot wire welding and cladding will be the subjects of a one-day conference at the FABTECH International & AWS Welding Show in Chicago. Presentations on both the hot wire GTA and plasma processes will be on the agenda. One topic that will be addressed will be the popular use of hot wire GTA cladding of tube and piping for the offshore oil and gas industries. In another, hot wire GTA "narrow groove" welding will be shown to perform well on titanium. The overall advantages are increased deposition rates and faster travel speeds.

For more information, please contact the AWS Conferences and Seminars Business Unit at (800) 443-9353, ext. 223. You can also visit the Conference Department at *www.aws.org* for upcoming conferences and registration information.

Conference on Weld Cracking
Las Vegas • Imperial Palace Hotel & Casino
October 16-17, 2007

Weld cracking is everybody's problem and there is more than one way to tackle it. The popular AWS-sponsored Weld Cracking Conference will move to Las Vegas this fall. Now known as Weld Cracking VI, this conference will differ from previous weld cracking conferences, with **greater emphasis on the role of the heat-affected zone** in such problems. Many solutions will be presented.

Circle No. 14 on Reader Info-Card

Conference price is $550 for AWS members, $680 for nonmembers. To register or to receive a descriptive brochure, call (800) 443-9353 ext. 224, (outside North America, call 305-443-9353), or visit www.aws.org/conferences

American Welding Society

Founded in 1919 to advance the science, technology and application of welding and allied joining and cutting processes, including brazing, soldering and thermal spraying.

NJC Hosts Friction Stir Welding Technology Workshop for Defense Applications

The Navy Joining Center (NJC) was host to the third in a series of Friction Stir Welding Technology Workshops, held Feb. 21, 22, in Columbus, Ohio.

The workshop was jointly organized by the NJC and the Navy Metalworking Center. The workshop updated industry and the Department of Defense (DOD) organizations on state-of–the-art advances in friction stir welding (FSW) technology, with a focus on DOD applications using the FSW process.

Keynote speakers from the Navy, Army, and Air Force provided workshop attendees with their individual perspectives on the value and development efforts needed to support the wider application of friction stir welding in current and future weapons systems programs.

Speakers from industry and academia presented diverse applications for the friction stir welding process including joining steel, aluminum, stainless steel, and titanium alloys. The applications ranged from the manufacturing of armored vehicles and ship structures to aircraft and space launch vehicles.

Friction stir welding permits the DOD to meet its requirements for improved survivability, improved structural performance, enhancing capability, and affordability. The aerospace industry has been a pioneer in the application of FSW technology in the United States. Friction stir welding processing is presently used in noncritical aircraft structures.

The Air Force keynote speaker addressed the challenges in employing FSW for "critical aircraft structure." Barriers and possible solutions were identified for technology transition opportunities in FSW processing of critical structures.

The Navy keynote speaker highlighted manufacturing technologies as being essential to achieving the Littoral Combat Ship (LCS) program's strategy to reduce acquisition costs. With the planned 55 ship LCS class being a key part of the 313 ship Navy strategy, friction stir welding of aluminum panel structures is playing a key role in reducing LCS costs.

The Navy's challenge to industry is to develop low-cost friction stir welding processing for stiffened aluminum panels. A project has been initiated by the Navy ManTech Program to develop a portable system that is tailored to the needs of LCS and mid-tier shipyards.

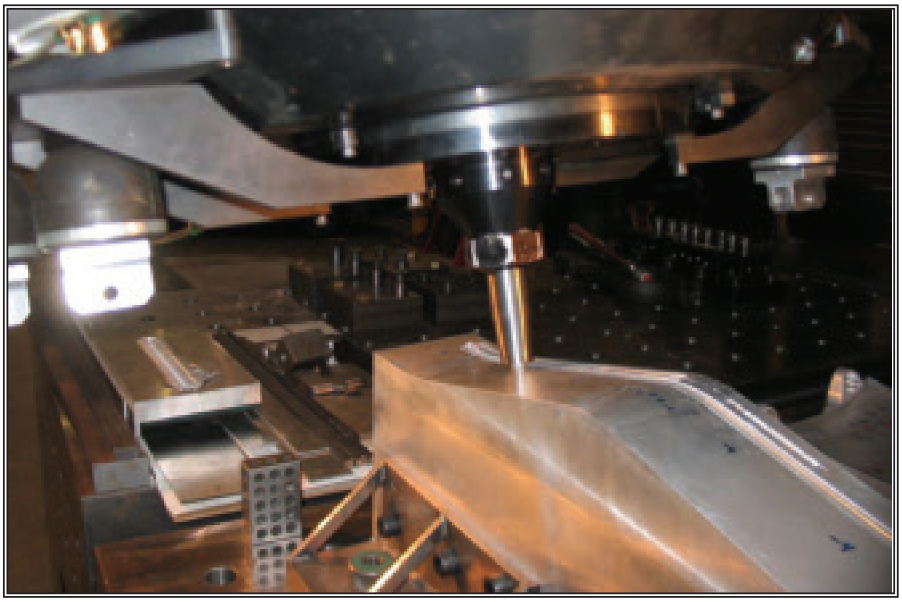

Fig. 1 — Friction stir welding was demonstrated to excel at joining materials with complex shapes during the recent Navy Joining Center-sponsored workshop held in Columbus, Ohio.

Presentations of Army programs showed how Army facilities are collaborating with industry to overcome technology barriers for rapid transition of new capabilities to the soldiers. Weld manufacturing technologies are being developed for the next-generation of ground combat vehicles — Future Combat System. These vehicles must be lightweight and capable of transport by C-130 aircraft, while being fully combat capable. Manufacture of the FCS will push the state of the art for material joining. Friction stir welding is one process that is being developed to join similar and dissimilar aluminum alloys for improved weld properties and reduced distortion. The Army has a vision to migrate FSW to depot facilities for other combat vehicles to increase knowledge and acceptance of the process within the Army community.

Workshop speakers from industry and academia presented their respective activities in friction stir process development for joining and material modification, process modeling, material characterization, pin/tool designs, and process qualification requirements for both present and future applications. Demonstrations of FSW were given during the workshop showing present development at EWI. One such demonstration showed 3-D FSW processing for complex shapes — Fig. 1. Also demonstrated were advanced eddy current and ultrasonic nondestructive evaluation techniques for inspection of FSW weldments.

The workshop clearly showed that friction stir welding is not a novel laboratory process but is being employed by many Department of Defense contractors. Friction stir welding can now be found in a variety of platforms supporting ground, sea, air, and outer space applications. Friction stir welding permits the Navy and other DOD services to meet performance requirements for improved survivability, improved structural performance, and affordability.

For more information contact Larry Brown at (614) 688-5080 or e-mail at *larry_brown@ewi.org.*

njc
Operated by
EWI
The Navy Joining Center
1250 Arthur E. Adams Dr.
Columbus, OH 43221
Phone: (614) 688-5010
FAX: (614) 688-5001
e-mail: *NJC@ewi.org*
www: *http://www.ewi.org*
Contact: Larry Brown


Your Job.
Your Show.
Circle No. 11 on Reader Info-Card
New day. New challenge. No matter what part of operations you're responsible for, you need the best there is. That's why you and your team need to be at the 2007 FABTECH International & AWS Welding Show. It's the way to go to—
• See metal fabricating machinery in action.
• Compare new products and technology.
• Talk face-to-face with suppliers.
• Evaluate new materials and consumables.
• Learn best practices from the pros.
Register today for YOUR SHOW at
www.aws.org/show
FABTECH INTERNATIONAL & AWS WELDING SHOW
North America's Largest Metal Forming, Fabricating & Welding Event
November 11–14, 2007
McCormick Place • Chicago, IL USA
COSPONSORED BY
AWS
FMA
SME

Dimensional Discrepancies in Weldments

Production of satisfactory weldments depends on maintaining specified dimensions, whether these pertain to the size and shape of welds or the finished dimensions of the assembly. Requirements of this nature are found in the drawings and specifications. Departures from the requirements in any respect should be regarded as dimensional discrepancies which, unless a waiver is obtained, must be corrected before acceptance of the weldment. They can be largely avoided if proper controls are exercised when the base metals are cut to size.

Distortion involves the buckling of sheets or plates parallel or transverse to the weld axis. It can generally be controlled by using the proper welding processes, welding sequences, preheat, or by aligning the workpieces in suitable fixtures prior to welding. The types of distortion are shown in Figure 1. Transverse shrinkage of the weld is distortion perpendicular to the axis of the welding — Fig. 1A. Angular distortion in a butt joint (Fig. 1B) results from the rotation of the base metal about the longitudinal axis of the weld. Longitudinal shrinkage (Fig. 1C) is distortion parallel to the weld axis. Angular distortion in a fillet weld, which occurs as a result of the rotation of one member about the longitudinal axis of the weld is shown in Fig. 1D. Figure 1E and F show the pulling effect of the weld above and below the neutral axis, respectively.

Incorrect joint preparation. Established welding practices require proper dimensions for each type of joint geometry consistent with the base metal composition and thickness, and the requirements of the welding process. Departure from the required joint geometry increases the probability of weld discontinuities. Joint preparation should meet the requirements of the shop drawings and be within the specified limits.

Weld joint mismatch is another common discontinuity. In plate, mismatch involves offset or misalignment in a direction perpendicular to the plate surface and weld axis. In pipe, offset or mismatch occurs in the radial direction at a butt joint or T-joint. Excessive mismatch results from improper fitup, fixturing, tack welding, or a combination of these factors. This term is often used to denote the amount of offset or mismatch across a butt joint between members of equal thickness. Many codes and specifications limit the amount of allowable offset because mismatch can result in stress raisers at the toe and the root of the weld.

Incorrect weld size. With respect to fillet welds, the required weld size should be specified on the detailed drawings. Oversized fillet welds are not harmful provided they do not interfere with subsequent assembly. They are not economical, however, and can cause excess distortion.

Groove weld size is dependent on its joint penetration, which is defined as the depth of the joint preparation plus root penetration. Incorrect weld sizes include undersized, oversized, and underfilled welds. Adding one or more weld passes can correct undersized fillet welds. Performing additional passes can repair underfilled groove welds.

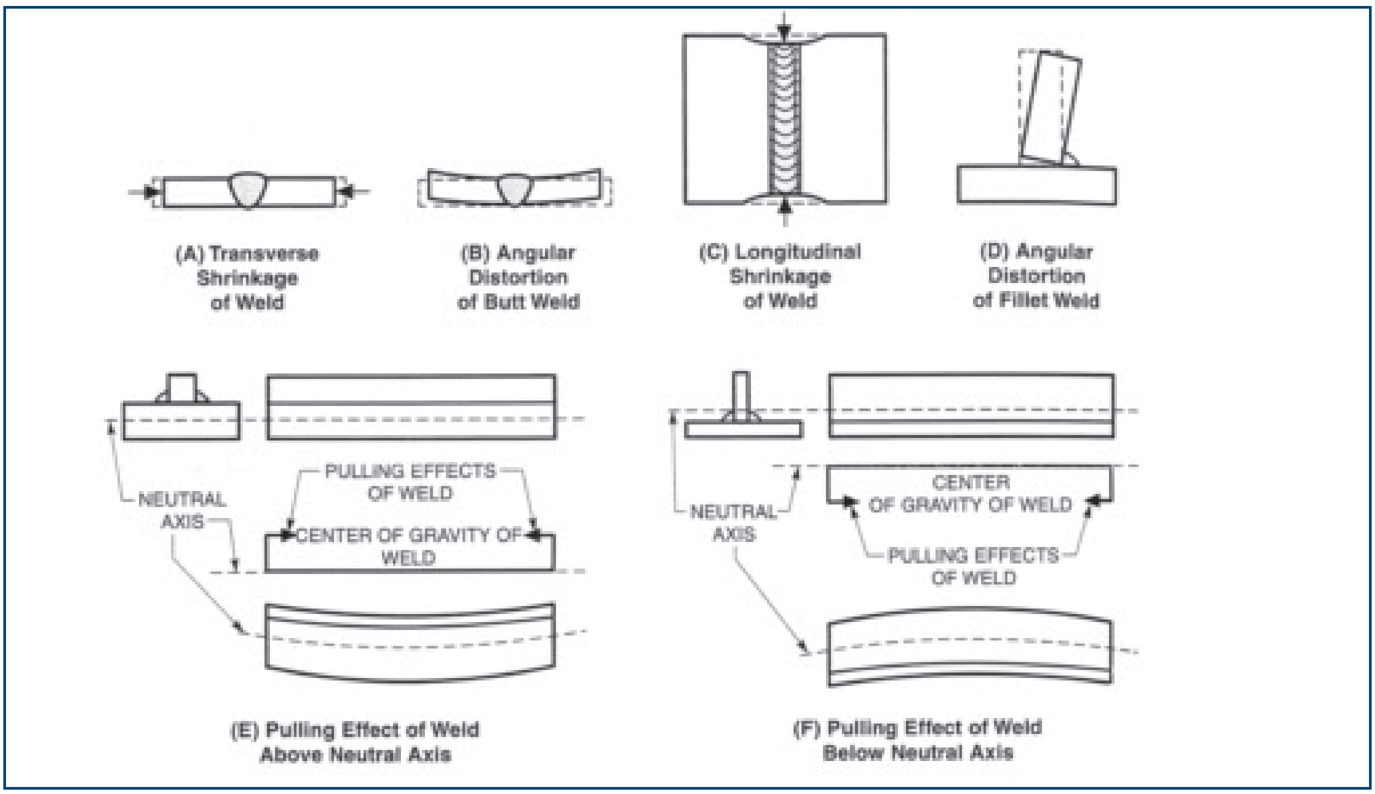

Fig. 1 — Types of distortion.

Excerpted from the *Welding Handbook,* Vol. 1, ninth edition.

NOTE: A DIAMOND (♦) DENOTES AN AWS-SPONSORED EVENT.

62nd STLE Annual Meeting. May 6–10, Marriott Hotel (downtown), Philadelphia, Pa. Contact: Society of Tribologists and Lubrication Engineers, (847) 825-5536, ext. 201; *www.stle.org.*

Materials Joining: Building for the Manufacturing Future. May 8, 9, Greater Columbus Convention Center, Columbus, Ohio. Contact: Edison Welding Institute, *www.ewi.org/conference07.*

Int'l Welding and Joining Conf. — Korea 2007. May 10–12, COEX Convention Center, Seoul, Korea. Visit *www.iwjc2007.org.*

PowderMet 2007, Int'l Conf. on Powder Metallurgy & Particulate Materials. May 13–16, Denver, Colo. Visit *www.mpif.org.*

***Marine Log Tugs & Barges* 2007 Conf. & Expo.** May 15, 16, Stamford Marriott, Stamford, Conn. Details vessel design, construction, and regulation. Visit *www.marinelog.com.*

Automotive Industry Advancements with NDT Conf. May 16, 17, Doubletree Hotel, Dearborn, Mich. Contact: American Society for Nondestructive Testing, (800) 222-2768; *www.asnt.org.*

XXXVIII Int'l Steelmaking Seminar. May 20–23, Belo Horizonte, Minas Gerais, Brazil. Sponsored by Associação Brasileira de Metalurgia e Materials. Simultaneous translations in English and Portuguese. Visit *www.abmbrasil.com.br/seminarios.*

♦ Joining Dissimilar Metals Conf. May 22, 23, Orlando, Fla. Talks will detail latest innovations and appropriate welding processes and metallurgy. Keynote speaker will be Dr. Thomas Eagar. Contact: AWS Conferences and Seminars Business Unit, (800) 443-9353, ext. 223; *www.aws.org/conferences.*

♦ National Robotics Arc Welding Conf. May 22, 23, Milwaukee, Wis. Sponsored by the AWS Milwaukee Section and the AWS D16 Committee for Robotic and Automatic Welding. Includes a tour of the John Deere plant in Horicon, Wis. For complete information, to register, or exhibit, visit *www.aws.org/sections/milwaukee*.

Tube Russia 2007. May 28–31, ZAO Expocenter, Moscow, Russia. Tube manufacture, raw materials, and measuring and control technology. Contact Messe Düsseldorf North America, (312) 781-5180; *www.mdna.com.*

Int'l Robots & Vision Show, 38th Int'l Symposium on Robots, and Sensors Expo. June 12–14, Donald E. Stephens Convention Center, Rosemont, Ill. Visit *www.robots-vision-show.info.*

Duplex 2007, Int'l Conf. and Expo. June 18–20, Grado and Aquileia, Italy. English is the official language. Sponsored by the Italian Metallurgical Assn. Visit *www.aimnet.it/duplex2007.htm.*

♦ 8th Int'l Conf. on Brazing, High-Temperature Brazing, and Diffusion Bonding (LÖT 2007). June 19–21, Aachen, Germany. Sponsors include American Welding Society and ASM Int'l. Contact: DVS (German Welding Society), *tagungen@dvs-hg.de; www.dvs-ev/loet2007.*

♦ **12th Beijing Essen Welding & Cutting Fair.** June 19–22, Shanghai New Int'l Expo Center, Shanghai, China. Sponsored by AWS. Visit *http://essen.cmes.org.*

ASTM 15th Int'l Symposium on Zirconium in the Nuclear Industry. June 24–28, Sunriver Resort, Sunriver, Ore. Visit *www.astm.org/MEETINGS/COMMIT/b10symp0607.html.*

SkillsUSA 43rd National Leadership and Skills Conf. and Skills USA Championships. June 25–29. Kansas City, Mo. Contact The Office of Communications and Government Relations, (703) 737-0607; *tholdsworth@skillsusa.org.*

♦ **Explosion of New Processes Conf.** Aug. 14, 15, San Diego, Calif. To include higher-powered ultrasonic welding, laser and various types of friction stir welding, fiber laser, additive manufacture, hybrid welding, and GMA "buried" arc welding. Contact: AWS Conferences and Seminars Business Unit, (800) 443-9353, ext. 223; *www.aws.org/conferences.*

Metariciclo 2007: Second Run; Int'l Exhibition on Technologies for the Recovery and Recycling of Ferrous and Nonferrous Metals. Sept. 13–15, Garda Exhibition Center, Montichiari, Brescia, Italy. Contact: *www.metalririclo.com.*

EMO Hannover — World of Machine Tools and Metalworking. Sept. 17–22, Hannover Fairgrounds, Hannover, Germany. Visit *www.hf-usa.com/emo.*

24th Annual ASM Heat Treating Society Conf. and Exposition. Sept. 17–19, Cobo Hall, Detroit, Mich. Visit *www.asminternational.org/heattreat.*

Circle No. 51 on Reader Info-Card

***Marine Log* Global Greenship Conf. & Expo.** Sept. 20, 21, Washington Marriott, Washington, D.C. Will focus on cost-effective solutions for meeting pollution-prevention regulations. Visit *www.marinelog.com.*

SOUTH-TEC and SME Motorsports. Oct. 2–4, Charlotte Convention Center, Charlotte, N.C. Cosponsored by Society of Mfg. Engineers, Assn. for Mfg. Technology, and American Machine Tool Distributors' Assn. Visit *www.sme.org, www.amtonline.org,* or *www.amtda.org.*

3rd Annual Careers in Construction Week. Oct. 15–19, Gainesville, Fla. Contact: National Center for Construction, Education, and Research, *www.nccer.org.*

Southeast Asia Wire and Tube Trade Fairs. Oct. 16–18, Bangkok, Thailand. Contact: Messe Düsseldorf North America, *info@mdna.com; www.mdna.com.*

♦**Weld Cracking VI Conf.** Oct. 16, 17, Imperial Palace Hotel, Las Vegas, Nev. To include conditions that trigger cracking in weldments and steps to prevent cracking in steel, stainless steels, aluminum, and titanium. Contact: AWS Conferences and Seminars Business Unit, (800) 443-9353, ext. 223; *www.aws.org/conferences.*

ICALEO® 2007 Conf. Oct. 29–Nov. 1, Hilton Hotel, Walt Disney World Resort, Orlando, Fla. Contact: Laser Institute of America, Conference Dept., *conferences@laserinstitute.org*.

Kiev Industrial Week 2007. Oct. 31–Nov. 2, National Complex Expocenter of Ukraine, Kiev, Ukraine. Contact *www.weldexpo.com.ua.*

Circle No. 28 on Reader Info-Card

Circle No. 16 on Reader Info-Card

16th Steelmaking Conf. and 6th Ironmaking Conf. Nov. 6–8, Metropolitano Convention Center, Rosario, Argentina. *www.siderurgia.org.ar.*

♦**FABTECH International & AWS Welding Show.** Nov. 11–14, McCormick Place, Chicago, Ill. This show is the largest event in North America dedicated to showcasing a full spectrum of metal forming, fabricating, tube and pipe, and welding equipment and technology. Contact: American Welding Society, (800/305) 443-9353, ext. 462; *www.aws.org.*

♦**Friction Welding.** Nov. 12, 13, Chicago, Ill., during the FABTECH Int'l & AWS Welding Show. Will include numerous short presentations on linear friction, friction stir, and conventional friction welding. Contact: AWS Conferences and Seminars Business Unit, (800) 443-9353, ext. 223; *www.aws.org/conferences.*

PICALO 2008. April 16–18, Capital Hotel, Beijing, China. Third Pacific Int'l Conf. on Applications of Lasers and Optics. For information, visit *www.laserinstitute.org/conferences.*

Educational Opportunities

Aluminum Brazing Course. June 12, 13, Hartford, Conn. Details furnace, torch, induction, and dip brazing. Contact: Kay & Associates, *www.kaybrazing.com;* (860) 651-5595.

Rimrock-Wolf Robotics Workshop. June 14, 15, Fort Collins, Colo. Presented by Ed Craig. Visit *www.weldreality.com.*

AISC Building Standard and Bridge Criteria Course. June 19–21, Chicago, Ill. Atema, Inc. Contact: *atemasolutions.com.*

Circle No. 54 on Reader Info-Card

ASME Section IX Seminars. Oct. 23–25, Houston, Tex.; Dec. 3–5, Atlanta, Ga.; April 8–10, 2008, Las Vegas, Nev. Contact: ASME Continuing Education Institute, (800) 843-2763; *www.asme.org/education.*

Automotive Body in White Training for Skilled Trades and Engineers. Orion, Mich. A 5-day course covers operations, troubleshooting, error recovery programs, and safety procedures for automotive lines and integrated cells. Contact: Applied Mfg. Technologies, Inc., (248) 409-2000; *www.appliedmfg.com.*

Boiler and Pressure Vessel Inspectors Training Courses and Seminars. Columbus, Ohio. Contact: Richard McGuire, (614) 888-8320; *rmcguire@nationalboard.org*; *www.nationalboard.org*.

Certified Laser Safety Officer® Exams. June 8, Baltimore, Md.; Sept. 21, San Francisco, Calif.; Nov. 2, Orlando, Fla. Contact: Board of Laser Safety®, *www.lasersafety.org.*

Continuing Education for Welding Inspectors and CWIs. Nov. 27–30, Chicago, Ill. Atema, Inc. Contact: *atemasolutions.com.*

CWI/CWE Course and Exam. This 10-day program prepares students for the AWS CWI/CWE exam. Contact: Hobart Institute of Welding Technology, (800) 332-9448; *www.welding.org*.

CWI Preparation. Courses on ultrasonic, eddy current, radiography, dye penetrant, magnetic particle, and visual at Levels 1–3. Meet SNT-TC-1A and NAS-410 requirements. Contact: T.E.S.T. NDT, Inc., (714) 255-1500; *ndtguru@aol.com*; *www.testndt.com.*

CWI Preparatory and Visual Weld Inspection Courses. Classes presented in Pascagoula, Miss., Houston, Tex., and Houma and Sulphur, La. Contact: Real Educational Services, Inc., (800) 489-2890; *info@realeducational.com*.


WELDING Journal
Laser-Hybrid Welding Aids Automaker
Robots Build Complex Assemblies
Brazing & Soldering Conference Preview
Joining Coated Sheet Metals
Gas Welding and Cutting During the War
By H. SIDNEY SMITH
American Welding Society
THE STRENGTH OF WELDING
The Complete
WELDING Journal
Collection
1930-39
Journal
of the
American Welding Society
October, 1929
"Heliarc" Welding in Production
by T. E. Piper
HISTORICAL SUMMARY
GENERAL PRODUCTION APPLICATIONS
Need to weld a complex elliptical joint stimulates the evolution of an advanced designed computer-controlled welding machine in a uniquely miniaturized configuration for
Automatic Welding of LOX Tunnels on the Saturn V Booster
Introduction

BY HOWARD M. WOODWARD

District 10 Tackles the Shortage of Skilled Welders

District 10 has taken the first steps toward improving welder education in the area with the establishment of a District Advisory Council to mentor the existing advisory groups in local high school and vocational schools.

The six-hour kickoff event was held March 14 at the Sheet Metal Workers Local 33 in Parma, Ohio, hosted by **Richard Harris,** District 10 director, and **Dennis Klingman,** AWS Education Committee chairman and manager of technical training at The Lincoln Electric Co.

In addition to Klingman and Harris, the members of the new District Advisory Council include **Larry Klemens,** principal, Mercer County Career Center; **Huck Hughes,** instructor, Columbiana County Career & Technology Center (CCCTC); **Rob Davis,** owner, General Welding Supply, Erie, Pa.; **Dave Hughes,** president, Specialty Fab, Inc., Youngstown, Ohio; and **John Nesta,** training coordinator, Sheet Metal Workers Local 33. The Council intends to stay in close contact with the advisory committees at local schools to help generate new welding programs that connect with the needs of local businesses and unions, to combat the welder shortages, increase recruitment levels, and reinforce welding standards and certifications in the region.

In Harris's opening remarks, he said AWS is attempting to coalesce the energy, time, and talents of the resources from various public and private sectors in order to establish and maintain effective working relationships among all of them. The concept is to establish a representative panel from these groups to participate on an advisory council that will steer these groups in the same direction at the same time.

AWS Vice President **Victor Matthews,** Lincoln Electric, acknowledged the presence at the meeting of the Ohio and Pennsylvania education officials, welding instructors, and the company representatives who will employ the welding graduates from local schools.

Others who made presentations included **James Gronski,** Pennsylvania Department of Education; **Glenn Smith,** Ohio Department of Education; **Huck Hughes, Dave Hughes**; **John Nesta, Larry Klemens, Terry Urbanek,** United Association of Journeymen and Apprentices of the Plumbing and Pipe Fitting Industry of the United States and Canada; **Marty Siddall,** Lincoln Electric; **Stan Roberts,** a student at CCCTC; **Art Baughman,** welding instructor, Canton local schools; and **Sam Gentry,** executive director, AWS Foundation.

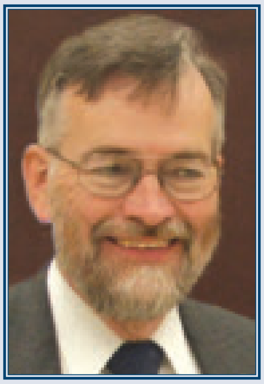

James Gronski, Pennsylvania Dept. of Education, supports the initiative.

Harris is confident this District 10 initiative will become a model for other AWS Districts to follow. ♦

AWS Participates in Asian Pacific IIW Congress

The 5th Asian Pacific IIW International Congress, held in Sydney, Australia, March 7–9, attracted 185 delegates from 14 countries. Presented were about 120 papers on the four subject streams: Structures/Pipelines, Pressure Equipment, Nondestructive Testing, and Welding Process/Corrosion.

The event was hosted by the Welding Technology Institute of Australia and the Australian Institute for Non-Destructive Testing. The Congress sponsors included Santos, Australian Dept. of Defense, The Lincoln Electric Co., Alcan, and the Government of Queensland, Australia.

Present were **H. Glenn Ziegenfuss,** executive director, Standards Engineering Society (USA); **Daniel Beaufils,** IIW chief executive; **Chris Smallbone,** IIW president (2005–2008); and **Jeff Weber,** AWS associate executive director and publisher emeritus of the *Welding Journal.* ♦

Shown at the IIW Congress are (from left) H. Glenn Ziegenfuss, Daniel Beaufils, Chris Smallbone, and Jeff Weber.

Tech Topics

Amendment A1 to QC1:2006 Incorporated into QC1:2007

The content of Amendment A1 to AWS QC1:2006, *Standard for AWS Certification of Welding Inspectors,* published on page 70 of the April 2007 *Welding Journal,* has been incorporated into the new AWS QC1:2007 edition verbatim, except for the revision to the Statement on Use which was corrected to read, "An endorsement to a certification adds to a certification by indicating demonstration of ability in a particular skill area that may not be sufficiently broad or unique to support a separate and distinct certification designation. An endorsement is not an indication of approval by AWS or an assurance of future performance."

QC1:2007 may be downloaded free of charge from *www.aws.org/certification.* ♦

Technical Inquiries

A5.1-91, Specification for Carbon Steel Electrodes for Shielded Metal Arc Welding

The response to the following technical inquiry has been approved by the A5A Subcommittee on Carbon and Low-Alloy Steel Electrodes and Rods for Shielded Metal Arc and Oxyfuel Gas Welding, and the A5 Committee on Filler Metals and Allied Materials.

Inquiry (paraphrased by A5A chair)**: In Figure 2 (Groove Weld Test Assembly for Mechanical Properties and Soundness. Except for E6022 and E7018M Electrodes) of ANSI/AWS A5.1-91 (identical to SFA-5.1 of ASME 2004 Section II, Part (C)), Note 9 (not Note 8) states that "In addition to the stops and starts at the ends, each pass shall contain a stop and start in between the ends." Can this note be interpreted to mean that during the groove assembly welding, no grinding or filing shall be permitted, and weld cleaning shall be limited to slag chipping, brushing, and needle scaling?**

Response: No. Fig. 3 (Fillet Weld Test Assembly), Note 8, of ANSI/AWS A5.1-91, states that "weld cleaning shall be limited to slag chipping, brushing, and needle scaling. Grinding or filing of the weld face is prohibited." The requirements for the Fillet Weld Test Assembly in Fig. 3 do not apply to the Groove Weld Test Assembly in Fig. 2.

D1.3, Structural Welding Code — Sheet Steel

Subject: Low-hydrogen electrode requirements for sheet to plate (> ¼ in.) welds
Code Edition: D1.3-98
Code Provision: Sections 1.4.4.2 and 1.4.2
AWS Log: D1.3-98-I06

Inquiry: Does Clause 1.4.4.2 require the use of low-hydrogen electrodes on sheet steel welded to primary structural members that are thicker than ¼ in. (6.4 mm)?

Response: No. ♦

ERRATA D1.1

AWS D1.1/D1.1M:2006,
Structural Welding Code — Steel

Page 19: Section 2.24.1.4 — incorrect reference — correct reference from "Note 4" to "Note d".

Page 68: Table 3.2 — new materials (ASTM A 1018 HSLAS and HSLAS-F, Grades 60 and 70, Class 2) were not added to Table 3.2, Category C — add new materials (ASTM A 1018 HSLAS and HSLAS-F, Grades 60 and 70, Class 2) to Table 3.2, Category C.

Page 68: Table 3.2, Note 1 — incorrect reference — correct reference from "3.5.3" to "3.5.2".

Page 73: Notes for Figures 3.3 and 3.4 — incorrect reference in Note i — Correct reference in Note i from "Note 6" to "Note f".

Page 126: Section 4.12.4.1(1) — incorrect metric equivalent for outside diameter — correct "10 mm" to "100 mm".

Pages 145–149: Tables 4.10 and 4.11 — incorrect references — correct all references to Figures 4.28–4.36 by increasing each by one, for example, Figure 4.28 correct to Figure 4.29.

Page 147: Table 4.11 — incorrect reference — top row, change "Nominal Wall or Plate Thickness[c]" to "Nominal Wall or Plate Thickness[d]".

Page 147: Table 4.11 — incorrect reference, two places — top row and middle of table, change "Dihedral Angles Qualified[g]" to "Dihedral Angles Qualified[h]".

Page 151: Table 4.14 — incorrect metric value — third row, seventh column — change "15 [00]" to "15 [20]".

Page 237: Figure 6.1 — note 3 reference to page 225 is incorrect — correct reference to page 236.

Page 240: Figure 6.4 — note 3 reference to page 225 is incorrect — correct reference to page 236.

Page 241: Figure 6.5 — note 3 reference to page 225 is incorrect — correct reference to page 236.

Page 242: Figure 6.6 — note 3 reference to page 225 is incorrect — correct reference to page 236.

ERRATA A5.23

AWS A5.23/A5.23M:1997, ***Specification for Low-Alloy Steel Electrodes and Fluxes for Submerged Arc Welding***

Page 12 — Figure 3A, Groove Weld Test Assembly, Detail (D) BUTTERED GROOVE: Change root opening callout "Z" to "R" at one place only.

ERRATA C3.2

AWS C3.2M/C3.2:2001, ***Standard Method for Evaluating the Strength of Brazed Joints***

Page 10, 4.7.1, Equation (4): Replace "shear" with "tensile".

New Standards Project

Development work has begun on the following revised standard. Affected individuals are invited to contribute to its development. For information, contact Staff Engineer **Annette Alonso,** ext. 299. Participation on AWS technical committees is open to all persons.

C4.3/C4.3M:200X, *Recommended Practices for Safe Oxyfuel Gas Heating Torch Operation.* The newly revised manual for oxyfuel gas heating torch operation includes the latest procedures to be used in conjunction with oxyfuel gas heating equipment. The manual also includes the latest safety requirements. Complete lists of equipment are available from individual manufacturers. Stakeholders: This document will be used by oxyfuel gas heating torch operators, users of oxyfuel gas welding systems: steel mills, fabrication, tool shops, and construction personnel.

Standards for Public Review

AWS was approved as an accredited standards-preparing organization by the American National Standards Institute (ANSI) in 1979. AWS rules, as approved by ANSI, require that all standards be open to public review for comment during the approval process. The following standards have been submitted for public review. Draft copies may be obtained from **R. O'Neill,** ext. 451, *roneill@aws.org.*

A5.17/A5.17M-97 (R200X), *Specification for Carbon Steel Electrodes and Fluxes for Submerged Arc Welding.* Reaffirmed — $25.00. 4/16/07.

A5.23/A5.23M:1997, *Specification for Low-Alloy Steel Electrodes and Fluxes for Submerged Arc Welding.* Revised — $46. 5/7/07.

C4.3/C4.3M:200X, *Recommended Practices for Safe Oxyfuel Gas Heating Torch Operation.* Revised — $25. 4/23/07.

D14.5/D14.5M:200X, *Specification for Welding of Presses and Press Components.* Revised — $91. 4/23/07.

D18.1/D18.1M:200X, *Specification for Welding of Tube and Pipe Systems in Sanitary (Hygienic) Applications.* Revised — $25. 5/15/07.

Standards Approved by ANSI

A10.1M:2007, *Specification for Calibration and Performance Testing of Secondary Current Sensing Coils and Weld Current Monitors used in Single-Phase AC Resistance Welding.* Approved: 3/5/07.

D17.2/D17.2M:2007, *Specification for Resistance Welding for Aerospace Applications.* Approved: 1/4/07.

A5.3/A5.3M:1999 (R2007), *Specification for Aluminum and Aluminum-Alloy Electrodes for Shielded Metal Arc Welding.* Reaffirmed: 1/22/07.

Technical Committee Meetings

May 2, SH1 Subcommittee on Fumes and Gases. Columbus, Ohio. Contact: S. Hedrick, ext. 305.

May 9, B2F Subcommittee on Plastic Welding Qualifications. Dallas, Tex. Contact: S. Hedrick, ext. 305.

May 9, G1A Subcommittee on Hot Gas Welding and Extrusion Welding. Dallas, Tex. Contact: S. Hedrick, ext. 305.

May 21–23, D16 Committee on Robotic and Automatic Welding. Milwaukee, Wis. Contact: J. Gayler, ext. 472.

June 13, Safety and Health Committee. Columbus, Ohio. Contact: S. Hedrick, ext. 305. ♦

Image of Welding Awards Announcement

Now is the time to nominate an individual or organization for one of the Image of Welding Awards to be presented at a special ceremony in Chicago, Ill., Nov. 12, during the FABTECH International & AWS Welding Show.

The awards will be presented in seven categories: 1) Individual; 2) AWS Section; 3) Large Business (200+ employees); 4) Small Business; 5) Welding Products Distributor; 6) Educator; and 7) Educational Facility.

The awards recognize individuals and organizations that have shown exemplary dedication to promoting the image of welding in their communities.

Jim Horvath, chairman of the AWS Image of Welding Subcommittee, said, "Raising public awareness about welding is vital to creating a positive image for the industry. Every year," he added, "welding professionals triumph in inspiring young adults to join the field." Horvath noted, "Many people are still unaware of the critical role welding plays in our society and the excellent career opportunities available. Honoring those who are driving real improvements for this industry encourages others to get involved."

Nominations will be judged by the Welding Equipment Manufacturers Committee (WEMCO), an AWS standing committee. The committee's members include executives from welding industry suppliers who work to promote the welding equipment market. Enhancing the image of welding as a critical industry is among the committee's priority programs.

To nominate an individual, a Section, or an organization for one of these awards, just send a written explanation of the nominee's qualifications, along with your name, phone number, e-mail and mailing addresses, to **Adrienne Zalkind,** *azalkind@aws.org;* or mail to Image of Welding Awards, 550 NW LeJeune Rd., Miami, FL 33126. The deadline for submitting nominations is Aug. 15. ♦

Robotic Arc Welding Awards Notice

Nominations are solicited for the 2008 Robotic and Automatic Arc Welding Award. The nomination packet should include a summary statement of the candidate's accomplishments, interests, educational background, professional experience, publications, honors, and awards.

December 31 is the deadline for submitting nominations. Send the nomination package to Wendy Sue Reeve, awards coordinator, 550 NW LeJeune Rd., Miami, FL 33126. For more information, contact Reeve at *wreeve@aws.org,* or call (800/305) 443-9353, ext. 293.

In 2004, the AWS D16 Robotic and Automatic Arc Welding Committee, with the approval of the AWS Board of Directors, established the Robotic and Automatic Arc Welding Award. The award was created to recognize individuals for their significant achievements in the area of robotic arc welding. This work can include the introduction of new technologies, establishment of the proper infrastructure (training, service, etc.) to enable success, and any other activity having significantly improved the state of a company and/or industry. The Award, funded by private contributions, is presented annually at the AWS Awards/AWS Foundation Recognition Ceremony and Luncheon, held in conjunction with the FABTECH International & AWS Welding Show. ♦

Prof. Koichi Masubuchi Award Nominees Sought

December 1 is the deadline for submitting nominations for the 2008 Prof. Koichi Masubuchi Award, sponsored by the Dept. of Ocean Engineering at Massachusetts Institute of Technology. It is presented each year to one person who has made significant contributions to the advancement of materials joining through research and development.

The candidate must be 40 years old or younger, may live anywhere in the world, and need not be an AWS member. The nomination should be prepared by someone familiar with the research background of the candidate, and include a résumé listing background, experience, publications, honors, awards, plus at least three letters of recommendation from researchers.

This award was established to recognize Prof. Koichi Masubuchi for his numerous contributions to the advancement of the science and technology of welding, especially in the fields of fabricating marine and outer space structures.

Submit nominations to Prof. **John DuPont** at *jnd1@lehigh.edu.* ♦

New AWS Supporters

New Sustaining Companies

BALDOR
2660 Hwy 9 E., Clio, SC 29525
www.dodge-pt.com
Representative: **Guy S. Mulee**

The Clio plant is a leading manufacturer of CEMA and engineered pulleys for the mining industry, and is part of the Dodge Power Transmission Components Group. The plant is the only pulley manufacturer that is ISO 9001 certified with welders and welding processes qualified to ASME Section IX, AWS D1.1, and AWS B2.1. The plant manufactures pulleys from under 200 lb up to 20 tons, motor mounts, and take-up frames.

Keville Enterprises, Inc.
363 Dorchester Ave.
South Boston, MA 02127
www.keville.com
Representative: **Geoffrey Durant**

Keville Enterprises is a full-service construction management and inspection firm with offices in Massachusetts, Connecticut, Maryland, Virginia, Florida, and Texas. It provides quality assurance and quality control welding inspection services for clients in both public and private sectors. The company employs 18 CWIs and two CWEs with multiple certifications from ASNT, NACE, and ICC, and was the recipient of the 2006 Image of Welding Award in the small business category.

Senco Construction, Inc.
1408 S. Eaton St., PO Box 651
Robinson, IL 62454
Representative: **Steven E. Neely**

SENCO Construction, Inc., offers a broad line of services for new construction and plant maintenance fields, including site work, concrete installation, structural steel erection, mechanical installation, and nondestructive testing. A large inventory of heavy construction equipment is available for bare rentals. SENCO is a VPP star OSHA contractor.

Tri-County Technical College
Welding Dept.
7900 Hwy. 76
Pendleton, SC 29670
www.tctc.edu
Representative: **Paul R. Phelps**

The Welding Department at Tri-County Technical College has trained welders for industry since 1965. The college offers an associate's degree and shorter certificate programs. The staff includes two AWS CWI/CWEs who provide welder certification testing, as well as customized company training.

Vanguard Machinery Int'l, LLC
14309 Sommermeyer St.
Houston, TX 77041
www.vanguardmachinery.com
Representative: **Jean Harris Jr.**

Vanguard Machinery is a new company with a proud heritage and sterling reputation. The company sells and services new high-quality welding, cutting, and positioning equipment for a wide variety of applications. The products are in stock and available for immediate delivery at competitive prices.

New Affiliate Companies

Alliance Services Corp.
23 Van Siclen Ave.
Floral Park, NY 11001

Arco Iron Works, Inc.
9151 Hampton Overlook
Capitol Heights, MD 20743

Campbell Steel Co.
2200 Congaree Dr., Cayce, SC 29033

Clay's Welding Co., Inc.
10541 Bristersburg Rd.
Catlett, VA 20119

Duluth Decal
5739 Rose Rd., Duluth, MN 55811

Galamba Metals Group, LLC
3005 Manchester Traffic Way
Kansas City, MO 64129

Gouldey Welding & Fabrication, Inc.
84 Allentown Rd.
Souderton, PA 18964

Iron Cross Fabrication & Design
17413 FM 2920, Ste. G
Tomball, TX 77377

Metallic Bellows (India) Pvt. Ltd.
3/136 East Coast Rd.
Vettuvankeni Village Injambakkam
Chennai- 41600 041, India

Productos del Aire de Guatemala, S.A.
41 Calle 6-27 Zona 8
01008 Guatemala

Progressive Construction Systems
246 N. 300 E.
Providence, UT 84332

Stallone Testing Labs, Inc.
4465 Bronx Blvd.
Bronx, NY 10470

WAB Fabricating Co.
7835 Broadway
Cleveland, OH 44105

Membership Counts

Member Grades	As of 4/1/07
Sustaining	457
Supporting	280
Educational	419
Affiliate	397
Welding distributor	46
Total corporate members	**1,599**
Individual members	45,882
Student + transitional members	5,084
Total members	**50,966**

New Supporting Company

Watson Bowman Acme
95 Pineview Dr.
Amherst, NY 14228

New Educational Institutions

College of DuPage Welding Technology
425 Fawell Blvd.
Glen Ellyn, IL 60137

Dawson Community College
Welding Technology
300 College Dr., Box 421
Glendive, MT 59330

Pipefitters Training Center
9876 Hickman Mills Dr.
Kansas City, MO 64137

Polaris Career Center
7285 Old Oak Blvd.
Middleburg Heights, OH 44130

Give Us Your Opinion to Help Shape New AWS Products and Services

The AWS Product Development Committee is conducting a survey to evaluate ideas for new AWS products. Your input is a crucial part of developing new products and services that meet the needs of the welding industry. To complete this brief survey, visit *www.aws.org/education/pdc07-survey.html.* Thank you in advance for participating in this important effort.

Harvey Castner, Chair
AWS Product Development Committee

SECTION NEWS

DISTRICT 1

Director: Russ Norris
Phone: (603) 433-0855

BOSTON & CENTRAL MASS./ RHODE ISLAND

MARCH 6
Activity: This was a joint meeting of the Boston and the Central Massachusetts/ Rhode Island Sections. The members toured Simonds International in Fitchburg, Mass., to study the manufacture of industrial bandsaw blades, power tool accessory blades, files, welding magnets, and magnetic tools. **Jim Kelly,** plant manager, and **Anthony Maietta,** manufacturing engineer, conducted the tour. Simonds is the oldest cutting tool manufacturer in North America, currently celebrating its 175th anniversary.

BOSTON

MARCH 10
Activity: A team of Section members conducted the testing of 38 candidates for certifications as AWS Certified Welding Inspector, Educator, or Engineer, at Four Points by Sheraton in Boston, Mass. The team included Section Chairman **Tom Ferri, Jim Shore, Teila Norris,** and **Russ Norris,** District 1 director.

CONNECTICUT

FEBRUARY 20
Activity: The Section members toured the Wheelabrator Lisbon, Inc., facility in Lisbon, Conn. **Scott Waddleton,** operations manager, presented a talk and conducted the tour. The company is a division of Waste Management, an operation that burns trash to generate electricity.

Scott Waddleton conducted the Connecticut Section members on a tour of Wheelabrator Lisbon in February.

MAINE

FEBRUARY 22
Speaker: **Fran Piccirillo,** account manager
Affiliation: Advantage Gases & Tools, Lewistown, Maine
Topic: Maine SkillsUSA test materials procurement
Activity: **Mike Gendron** explained the changes to this year's SkillsUSA test. **Dave Watson** of The Lincoln Electric Co. vol-

Jim Kelly (left) and Anthony Maietta (center) are shown with Tom Ferri, Boston Section chair, during the joint Boston and Central Massachusetts/Rhode Island Sections' tour of Simonds International.

West and Roberts Tapped for Student Member Awards

Tom West and **Stan Roberts** have been selected to receive the AWS Student Chapter Member Award.

Tom West, a member of the AWS Whitmer Career and Technology Center Student Chapter, Toledo, Ohio, served the past two years as Student Chapter chairman, working with Chapter Advisor **Craig Donnell.** After graduating with a 4.0 grade point average in welding, he was accepted into the Welding Technologies program at Ferris State University. Recently, he won the local SkillsUSA welding competition at Whitmer, then went on to compete in the Regional Welding Competition where he was awarded the silver medal, qualifying him to compete in the state competition.

Stan Roberts is currently publicity chairman for the AWS Columbiana County Career and Technical Center Student Chapter, Lisbon, Ohio. Last year, he served the Chapter as vice chairman and worked with Chapter Advisor **Huck Hughes.** He is a member of the Honor Society and was the only student chosen to speak at the District 10 Advisory Committee Conference held March 14, 2007.

The AWS Board of Directors established the Student Chapter Member Award to recognize members whose Student Chapter activities have produced outstanding school, community, or industry achievements.

This award provides an opportunity for Student Chapter advisors, Section officers, and District directors to recognize outstanding students affiliated with Student Chapters, as well as to enhance the image of welding in their communities.

Complete information and nomination form can be downloaded from *www.aws.org/w/s/membership/stchawards.html,* or call the AWS Membership Dept. at (800) 443-9353, ext. 260. ♦

Shown at the Maine Section program are (from left) speaker Fran Piccirillo, Mike Gendron, Chairman Scott Lee, District 1 Director Russ Norris, Jeff Fields, Bob Bernier, and Dave Watson.

Shown at the joint Lancaster, York Central Pa., and ASNT program are (from left) Ed Macejak (ASNT), AWS President Gerald Uttrachi, Dave Herr, York Central Pa. vice chair, and John Ament, Lancaster Section chair.

York County Student Chapter members pose with AWS President Gerald Uttrachi (second from left) and Alan Badeaux (far right), District 3 director.

unteered four Power MIG 255C welding machines for the event. On hand was **Jeff Fields,** Maine Skills cochair. The program was held at Village Café in Portland, Maine.

DISTRICT 2

Director: Kenneth R. Stockton
Phone: (732) 787-0805

PHILADELPHIA

February 24

Activity: For more than 30 years, the Section has hosted an annual welding competition. This year, the event was held at the Pennsauken Campus of Camden County Technical Schools with 25 contestants working through a written test followed by three projects involving welding steel and aluminum plates. For the past six years the Section contest has been held at a different school in the district. The event furthers the Section's efforts to promote the Image of Welding by involving local newspapers and representatives from schools, industry, unions, and welding equipment vendors. Judged by CWIs, including **Pat Thomashesky,** a past Section chair, the winners received more than $2500 in donated prizes. The top three winners were **Edward Schoal** and **David Thornton** (Gloucester County Institute of Technology), and **Michael Cogdill** (Salem County Vocational Technical School). On hand for the event were teachers **Dan Roskiewich** and **Robert Sandelier.**

DISTRICT 3

Director: Alan J. Badeaux Sr.
Phone: (301) 753-1759

CUMBERLAND VALLEY

February 15

Speaker: **Brian Bain,** welding engineer and a past Section chairman

Topic: The Alaska Pipeline

Activity: District 3 Director **Alan Badeaux** met with the Section board members to discuss plans for funding a welding class for disadvantaged youth. The class will be taught by past chairman **Dave Nicholas** who is a CWI and a CWE.

LANCASTER & YORK CENTRAL PA.

February 21

Speaker: **Gerald D. Uttrachi,** AWS president

Affiliation: WA Technology, LLC, president

Topic: Welding race cars

Activity: This was a joint meeting of the Lancaster and York Central Pennsylvania

Sections, and the Susquehanna Valley Chapter of ASNT. The program was held at Four Points Sheraton in York, Pa.

York County Student Chapter

MARCH 8
Speaker: **Gerald D. Uttrachi,** AWS president
Affiliation: WA Technology, LLC, president
Topic: Careers in welding
Activity: Uttrachi toured the York County School of Technology then addressed the members of the Student Chapter. Attending the program were District 3 Director **Alan Badeaux; Claudia Bottenfield,** York Central Pa. chair; and **Brian Yarrison,** Student Chapter advisor, York County School of Technology.

DISTRICT 4

Director: Roy C. Lanier
Phone: (252) 321-4285

SOUTHWEST VIRGINIA

NOVEMBER 16
Activity: The Section members toured Altec Industries, Inc., in Daleville, Va. The facility manufactures bucket trucks and lifting equipment used in the communications, service, construction, and electric power industries.

JANUARY 16
Activity: The Southwest Virginia Section members toured the Norfolk Southern Railroad Shop in Roanoke, Va. The spokesman and guide for the tour was **R. J. (Red) Lehman.**

DISTRICT 5

Director: Leonard P. Connor
Phone: (954) 981-3977

PALM BEACH

FEBRUARY 21
Speaker: **Rich DePue**
Affiliation: IWELD International
Topic: Welding inspection and failure analysis
Activity: The program was held at Palm Beach Community College in West Palm Beach, Fla.

SOUTH CAROLINA

FEBRUARY 15
Speaker: **Dave Lackey,** welding engineering consultant
Affiliation: The Lincoln Electric Co., ret.
Topic: The AWS CWI and CWE programs and the changes planned for CWI certifications

Southwest Virginia Section members pose during their tour of Altec Industries in November.

Southwest Virginia Section Chair Ted Alberts (left) is shown with (from left) Treasurer David Cash, speaker R. J. (Red) Lehman, and Secretary Bill Rhodes.

Shown at the South Carolina Section program are (from left) Chair Gale Mole, speaker Dave Lackey, and Richard Temple of National Welders.

Activity: This South Carolina Section program was held in North Charleston, S.C.

DISTRICT 6

Director: Neal A. Chapman
Phone: (315) 349-6960

OLEAN-BRADFORD

FEBRUARY 15
Activity: The Section members visited Jamestown Community College in Jamestown, N.Y., to tour its welding school facilities. **Brent Harkness,** welding instructor, reviewed the college's programs and guided the tour. Guests included **Kraig Okerland,** GTS account

Rich DePue (left) accepts a speaker gift from Frank Rose, Palm Beach Section chairman, at the February program.

Shown at the Olean-Bradford tour are (from left) Kraig Okerland, Brent Harkness, Tom Pecoraro, Ken Shaffer, and Bob Lindberg.

Shown are some of the students at the Dayton Section program held at Hobart Institute of Welding Technology.

Trenton Doane (back row, center) led the Holston Valley Section members on a tour of Hapco Aluminum Pole Products.

Judy Schneider discussed her research work on friction stir welding for the Northeast Mississippi Section members.

Greg Dobson discussed robotic welding in shipyards for the New Orleans Section.

Speaker and HIWT instructor Chuck Ford congratulates Sarah Albers for winning the grand raffle prize at the Dayton Section's students' night program.

manager, welding student **Tom Pecoraro, Ken Shaffer,** welding instructor at North Central Industrial Technical Education Center, and **Bob Lindberg.**

DISTRICT 7

Director: Don Howard
Phone: (814) 269-2895

DAYTON

MARCH 13

Speaker: **Chuck Ford,** technical instructor

Affiliation: Hobart Institute of Welding Technology (HIWT)
Topic: The AWS Certified Welding Inspector program
Activity: The Dayton Section held its annual students' night program for 100 attendees, including students, parents, instructors, and Section members. Section Chair **Chris Anderson** served as emcee and focused his comments on the student memberships and scholarships offered by the American Welding Society. The meeting was held at and hosted by Hobart Institute of Welding Technology, Troy, Ohio. **Sarah Albers,** a welding student at Tri-Star Career Compact, Celina, Ohio, won the grand prize of a Hobart Handler 125EZ welding package.

DISTRICT 8

Director: Wallace E. Honey
Phone: (256) 332-3366

HOLSTON VALLEY

FEBRUARY 15
Activity: The Section members toured Hapco Aluminum Pole Products, in Abingdon, Va., to study the manufacture of aluminum and steel light poles. **Trenton Doane,** second-shift supervisor, conducted the program. Highlights included viewing the "spinning" of the aluminum tubing to produce the tapered poles, plasma arc cutting of parts, and various gas metal arc welding operations.

NORTHEAST MISSISSIPPI

FEBRUARY 15
Speaker: **Judy Schneider,** assoc. professor of mechanical engineering
Affiliation: Mississippi State University
Topic: Friction stir welding
Activity: The meeting was held at Mississippi State University.

WESTERN CAROLINA

Calendar
Saturday, May 19, 12:30 p.m.
Scholarship Golf Tournament
Saluda Valley Country Club
Contact **Duke Moses**
duke.moses@bmwmc.com
(864) 989-6791

DISTRICT 9

Director: George D. Fairbanks
Phone: (225) 673-6600

MOBILE

MARCH 6
Activity: The Section members toured the IPSCO Steelworks in Mobile, Ala. The facility produces about 200 tons of liquid steel/h, using 100% recycled scrap metal. Assisting with the tour were **Steve McNair, Richard Gravely, George (Chip) Byrd, Bill Smith, Tim Strickland, Marc Richardson, Kaye Terry, Charlie Jordan, Jon Howley,** and **Shawn Crites.**

Mobile Section Chair Eleanor Ezell is shown with (seated, from left) Steve McNair, Richard Gravely, George (Chip) Byrd, and (standing, from left) Bill Smith, Tim Strickland, Marc Richardson, Kaye Terry, Charlie Jordan, Jon Howley, and Shawn Crites.

NEW ORLEANS

FEBRUARY 13
Speaker: **Greg Dobson**
Affiliation: Robotic Welding, Northrop Grumman Ship Systems
Topic: Robotic welding in shipyards
Activity: Following the talk, the Section members took a guided bus tour of the shipyard and studied welding demonstrations in the facility's welding school.

New Orleans Section members study a welding operation in the welding school at Northrop Grumman Ship Systems.

DISTRICT 10

Director: Richard A. Harris
Phone: (440) 338-5921

CLEVELAND

MARCH 13
Speaker: **Mike Kaplan,** attorney
Affiliation: Kaplan & Associates
Topic: Protecting your company against lawsuits
Activity: The Section appointed **David Verhas** *(dvhas@yahoo.com)* to the newly created position of Section webmaster. Following the talk, Kaplan answered questions about workman's comp, liability, insurance, and product failures issues.

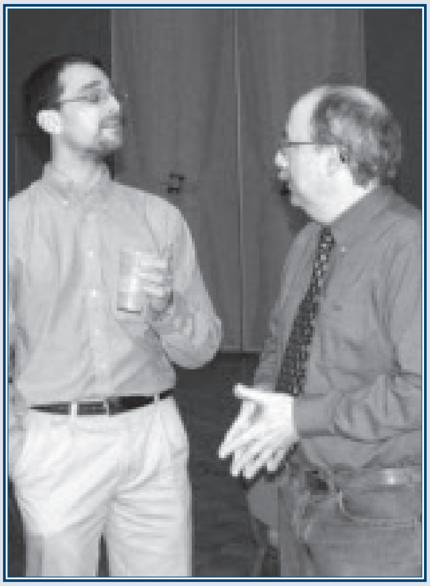

Speaker Mike Kaplan (right) chats with Todd Morris of Williams Welding Alloys at the Cleveland Section program.

DRAKE WELL

MARCH 13

Shown at the Drake Well Section program are (from left) Secretary Charles Mundt, Treasurer Ward Kiser, speaker Marty Siddall, Chair Mike Owens, and Vice Chair Jason Fry.

Shown at the Northwest Pennsylvania Section program are (from left) Chairman Steve DeHart, speaker Tim Rosiek, and Delayne Jacobs.

Students pose with Congressman Tim Ryan at the Mahoning Valley Section program.

Tim Hurley (left) receives a speaker plaque from Mike Karagoulis, Detroit Section technical program chair.

Shown at the Mahoning Valley Section program are (from left) ASM Chair Rich Polencik, Ohio Congressman Tim Ryan, and Chuck Moore, Section chair.

Speaker: **Marty Siddall,** technical sales representative and automation specialist
Affiliation: The Lincoln Electric Co.
Topic: Robotic welding and automation
Activity: Introduced were the Drake Well Section's officers: Chairman **Mike Owens,** Vice Chair **Jason Fry,** Secretary **Charles Mundt,** and Treasurer **Ward Kiser.** The meeting was held at The Mill Restaurant and Lounge in Titusville, Pa.

MAHONING VALLEY

February 22
Speaker: **Tim Ryan,** Ohio District 17 congressman
Topic: Congressional update
Activity: This was a joint meeting with members of the Warren, Ohio, chapter of ASM International. The program was held at 422 Cafe in Warren.

NW PENNSYLVANIA

February 20
Speaker: **Tim Rosiek,** environmental engineer
Affiliation: The Lincoln Electric Co.
Topic: Welding fumes and regulatory changes
Activity: The meeting was held at Tristate Business Institute. Sixty-five people attended this meeting, including Chairman **Steve DeHart,** president of Welders Supply Co., and **Delayne Jacobs,** director of Tristate Welding School.

DISTRICT 11

Director: Eftihios Siradakis
Phone: (989) 894-4101

DETROIT

March 8
Speaker: **Tim Hurley,** district sales manager
Affiliation: The Lincoln Electric Co.
Topic: Advances in GMA welding process and their applications for advanced high-strength steels
Activity: This Old Timers' Night program was held at the Ukrainian Cultural Center in Detroit, Mich. Four members were cited for their service to the Society: **Tony Metzger** (50 years), **Ray Roberts** (30 years), and **Robert Wolfcale** and **Doug Juhl**, 25 years each.

NORTHWEST OHIO

February 26
Speakers: **Dick West** and **Larry Blake,**

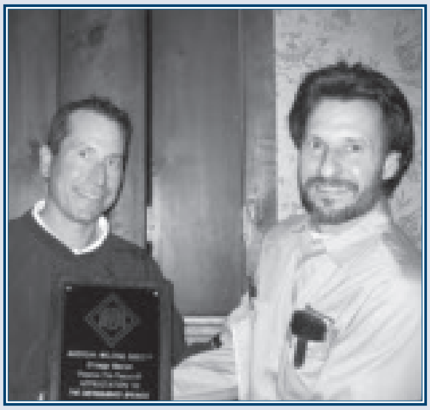

Ed Libby (left) accepts an appreciation plaque from Craig Tichlar, Chicago Section vice chair and secretary.

Section chair and vice chair, respectively
Topic: Using the touch start gas tungsten arc welding process
Activity: The presentations discussed the process, what equipment is required, and how to set it up. Following the talks, the process was demonstrated, and the Section members tried welding with and without filler metal using the process.

DISTRICT 12

Director: Sean P. Moran
Phone: (920) 954-3828

FOX VALLEY & LAKESHORE

MARCH 8
Speakers: **Sam Gentry,** AWS Foundation, executive director; and **Dale Dulberger,** WisPASS, project director, Milwaukee Area Technical College
Topic: Forum to supply a continuous quality welding workforce
Activity: This joint meeting of the Fox Valley and Lakeshore Sections began with a tour of the Miller Electric Mfg. Co.'s manufacturing facility in Appleton, Wis., to study the manufacture of welding power supplies. **Ben Mueller,** Lakeshore Section, was presented the AWS District Educator Award by **Sean Moran,** District 12 director. The business meeting was held at Barlow Planetarium at the University of Wisconsin.

RACINE-KENOSHA

FEBRUARY 15
Activity: The Section members toured the Bucyrus Erie, Inc., facility in South Milwaukee, Wis. Guests on the tour were members of the Gateway Technical College welding students.

The Detroit Section honored its Old Timers (from left) Robert Wolfcale, Doug Juhl, Tony Metzger, and Chairman Ray Roberts.

Racine-Kenosha Section members and Gateway Technical College welding students are shown during their tour of Bucyrus Erie, Inc.

CHICAGO

FEBRUARY 28
Activity: The Section members toured Oakley Steel Products Co. in Bellwood, Ill., a fabrication shop that custom bends, rolls, forms, and shapes steel products for original equipment manufacturers. **Ed Libby** conducted the tour. The dinner and meeting were held following the tour.

MARCH 14
Speaker: **John C. Bruskotter,** AWS vice president
Affiliation: Bruskotter Consulting Services
Topic: Development and installation of an offshore oil- and gas-production platform from inception through startup
Activity: This past chairmen's night program was held at Ray Harrington Catering in Chicago, Ill.

Sean Moran (left), District 12 director, presents Ben Mueller the District Educator Award at the Fox Valley and Lakeshore Sections' program in March.

DISTRICT 13

Director: W. Richard Polanin
Phone: (309) 694-5404

DISTRICT 14

Director: Tully C. Parker
Phone: (618) 667-7744

Shown at the Saskatoon Section seminar are (from left) Huawei Guo, treasurer; Ike Oguocha, membership chair; Larry Postnikoff, program chair; and Gus Marisca, chairman.

Shown at the North Texas program are (from left) past AWS President Ernest Levert, Vice Chair Robert Tessier, AWS President Gerald Uttrachi, and Chairman Howie Sifford.

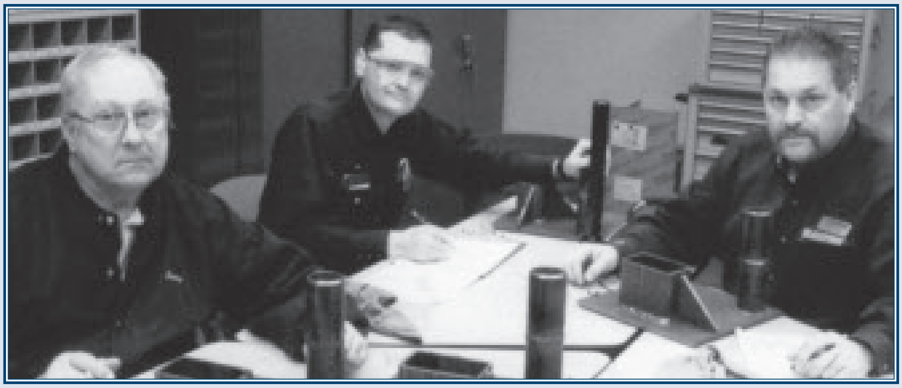

Judges for the Tulsa Area SkillsUSA welding contest are (from left) Jerry Knapp, Tim Cruse, and Jerry Allen.

INDIANA

February 17
Activity: The Section hosted the Indiana SkillsUSA, Indianapolis Regional Welding Contest. Chair **Gary Dugger** and Vice Chair **Bennie Flynn** served as cochairs of the event and as judges. Also serving as judges were **Tony Brosio, Gary Tucker,** and **Rick Eckstein.** The event included 21 participants from six high school welding programs. The qualifiers for the state contest were **Eric Young, Kyle Gibson,** and **Jayson McGee** from New Castle Career Programs, and **Jesse Rickman** from Whitewater Technical Career Center.

February 21
Speaker: **Richard L. Holdren,** vice president
Affiliation: Applications Technologies Co.
Topic: Conflicts between weld quality and welding inspection

District 17 Director Oren Reich (left) presents the District Meritorious Award to Jerry Knapp at the Tulsa Section program.

Activity: This Indiana Section program was held in Indianapolis, Ind.

DISTRICT 15

Director: Mace V. Harris
Phone: (952) 925-1222

SASKATOON

February 26
Activity: **Hanan Farhat,** a master's student at the University of Saskatchewan, conducted a seminar for 63 attendees. Farhat's topic was the effect of submerged arc welding speed on the weld quality and mechanical properties of X80 pipeline steels using multiple wires. The event was held at the University of Saskatchewan in Saskatoon, Saskatchewan, Canada.

DISTRICT 16

Director: David Landon
Phone: (641) 621-7476

CENTRAL IOWA

March 13
Activity: The Section toured the State Steel warehouse. **Ron Bingham,** outside sales, conducted the program.

DISTRICT 17

Director: Oren P. Reich
Phone: (254) 867-2203

CENTRAL ARKANSAS

January 25
Speaker: **Bob Hlass**
Affiliation: The Lincoln Electric Co.
Topic: Classification of electrodes
Activity: The meeting was held at Hot Springs Rehabilitation Center in Hot Springs, Ark.

March 1
Speaker: **Aaron Campbell**

Affiliation: Welsco
Topic: Air filters and compliance with OSHA regulations
Activity: This Central Arkansas Section program was held at National Park Community College In Hot Springs, Ark.

NORTH TEXAS

FEBRUARY 20
Speaker: **Gerald D. Uttrachi,** AWS president
Affiliation: WA Technology, LLC, president
Topic: Welding race cars and hot rods
Activity: The program was held at Spring Creek Barbeque in Irving, Tex. In attendance was **Ernest Levert,** past AWS president.

TULSA

FEBRUARY 10
Activity: The Section hosted its annual Ladies Night Out program featuring a Bingo party at Freddie's Steak House in Sapulpa, Okla. **Jerry Knapp** received the District 17 Meritorious Award. Introduced were the judges for the Tulsa Area SkillsUSA welding contest: **Jerry Knapp, Tim Cruse,** and **Jerry Allen.**

DISTRICT 18

Director: John L. Mendoza
Phone: (210) 353-3679

EL PASO

FEBRUARY 21
Speaker: **Gerald D. Uttrachi,** AWS president
Affiliation: WA Technology, LLC, president
Topic: Gas savings in GMA welding
Activity: The program was held at Carnitas Mexican Restaurant in El Paso, Tex. District 18 Director **John Mendoza** attended the program.

HOUSTON

FEBRUARY 21
Activity: The Section hosted its Ask the Experts program featuring welding and metallurgy experts **Dean Hannam** with Cameron, **Michael Hayes** with Acute Technological Services, **John Lee** with Chicago Bridge and Iron, and **Ron Richter** with Houston Metallurgical Laboratory. The panel answered questions posed by the attendees. Special guests at the program were 22 welding students, who received prizes provided by several local welding supply companies. The program was held at Brady's Landing in Houston, Tex.

El Paso Section members posed for a group shot in February. From left are Bob Fisher, Mike Jordan, Joe Angelo, George Medina, Jeremy Nunn, Bobby Brito, Guadalupe de la Cruz, Chairman David Twitty, Lawrence Romero, AWS President Gerald Uttrachi, Tim Jackson, District 18 Director John Mendoza, Lee Lowers, Thomas Evans, and Cruz Anthony Sanchez.

Shown at the El Paso Section meeting are (from left) Secretary Joseph Angelo, Chair David Twitty, AWS President Gerald Uttrachi, Treasurer Guadalupe de la Cruz, and Vice Chair George Medina.

Shown at the Houston Section's Ask the Experts program are (from left) John Lee, Dean Hannam, Chair Dennis Eck, Michael Hayes, and Ron Richter.

Spokane Section Treasurer Rich Irving presents Deb Cox with a door prize at the Ladies' Night program in February.

Sabine Section Chair Glynn Savage (left) presents a speaker plaque to Mitch Woods.

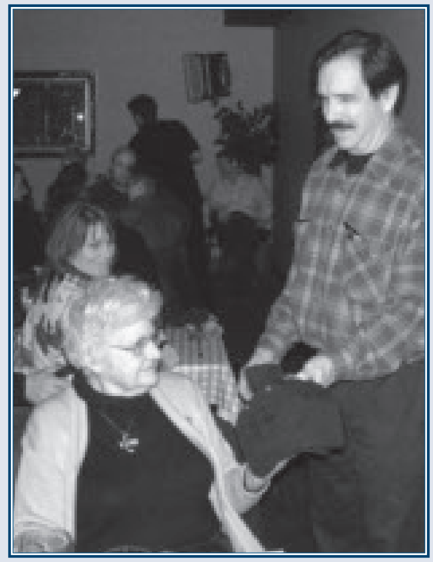

Art Sabiston, Spokane Section chair, presents a gift to speaker Sister Paula Turnball at the annual Ladies' Night program.

Eddie Hooks (right) accepts a speaker's plaque from Robert Medina, San Antonio Section chairman, in March.

Ray Hegwer (left) receives a speaker appreciation plaque from Bexar Schenk at the San Antonio Section meeting in February.

Glynn Savage (left), Sabine Section Chair, presents the past chairman certificate to Grady Hatton.

Albuquerque Section Vice Chair Tom Lienert (left) is shown with Associate Dean Dusty Heritage and welding instructor Brandon Whatley at the December 7 program held in Roswell, N.Mex.

SABINE

FEBRUARY 27
Speaker: **Mitch Woods,** sheriff
Affiliation: Jefferson County, Tex.
Topic: Local Homeland Security changes that will impact local industry
Activity: The members took nominations for officers and directors for the upcoming year. Chair **Glynn Savage** presented the past chairman certificate to **Grady Hatton.**

SAN ANTONIO

FEBRUARY 13
Speaker: **Ray Hegwer,** regional manager
Affiliation: Metabo International
Topic: Abrasive wheel technology
Activity: The meeting was held at Spaghetti Warehouse in San Antonio, Tex.

MARCH 13
Speaker: **Eddie H. Hooks Jr.,** CEO
Affiliation: On & Offshore Inspection
Topic: Quality control in pipeline inspection
Activity: This San Antonio Section program was held at La Posada Del Rey Restaurant in San Antonio, Tex.

DISTRICT 19

Director: Neil Shannon
Phone: (503) 201-5142

SPOKANE

FEBRUARY 21
Speaker: Sister **Paula Turnball**
Affiliation: Convent of the Holy Names
Topic: Artistic applications for welding
Activity: This annual Ladies' Night program was held at Luigi's Italian Restaurant in Spokane, Wash.

DISTRICT 20

Director: William A. Komlos
Phone: (801) 560-2353

ALBUQUERQUE

DECEMBER 7
Speaker: **Thomas J. Lienert**
Affiliation: Los Alamos National Laboratory, and Section vice chair
Topic: Welding of aluminum alloys
Activity: This meeting was held at East-

ern New Mexico University in Roswell, N.Mex. **Brandon Whatley,** a welding instructor at the university, received the Section Educator Award. **Dusty Heritage,** associate dean for career and technical education, received a Section appreciation award. Presentations were also made by the owners of local machine and fabrication shops, including **Duane Green** of The Machine Ship, Inc., and **Robert Flowers** of RDF Enterprises.

COLORADO

March 8
Speaker: **David Fullen,** district manager
Affiliation: The Lincoln Electric Co.
Topic: OSHA guidelines for exposure to hexavalent chromium
Activity: The program was held at the Lincoln Electric district office in Denver, Colo.

Dave Fullen explained the OSHA Cr(VI) guidelines for the Colorado Section.

SOUTHERN COLORADO

February 21
Activity: The Section members participated in the Airgas Orange County Chopper Road Show and 25th Anniversary Open House. Demonstrations were presented by Lincoln Electric, Tweco/Victor Equipment, and Ansell Gloves. The event was held at Airgas Intermountain, Inc., in Denver, Colo. Presenters included **Myron Delgado** from Lincoln, **Carol Salamon** with Airgas Intermountain, and **Don Gatewood** representing Tweco/Victor Equipment.

Jean (left) and Pat Mulville are shown at the Southern Colorado Section program.

Shown at the Southern Colorado program are (from left) Myron Delgado, Carol Salamon, and Don Gatewood.

DISTRICT 21

Director: Jack D. Compton
Phone: (661) 362-3218

LONG BEACH/ ORANGE COUNTY

February 22
Speaker: **David Randal**
Affiliation: Randal Welding
Topic: Case hardening
Activity: The meeting was held in the welding laboratory at Orange Coast College.

Shown at the Long Beach/Orange County Section program are (from left) William Galvery Jr., speaker David Randal, and Richard Hutchinson, treasurer.

DISTRICT 22

Director: Dale Flood
Phone: (916) 933-5844

SACRAMENTO

February 21
Speakers: **Silvio Modena,** district manager, and **Chuck Crete,** owner/manager
Affiliations: Miller Electric Co. and MJB Welding Supply, respectively
Topic: Advanced gas metal arc welding
Activity: The speakers followed their lectures with a workshop held for the 55 attendees at Butte Community College in Paradise, Calif. The attendees had the opportunity to work with the Miller Axcess™ 300 and aluminum GMA welding equipment. In attendance were District 22 Director **Dale Flood,** and past chairs **Rob Purvis** and **Kerry Shatell.**

Shown at the Sacramento Section program are (from left) past Chairs Rob Purvis and Kerry Shatell, District 22 Director Dale Flood, and Chairman Mike Rabo.

SAN FRANCISCO

March 7
Speaker: **Dave Buttress**
Affiliation: Digital Welding Systems, Inc.
Topic: Orbital welding
Activity: The meeting was held at Pyramid Alehouse in Berkeley, Calif.

Shown at the San Francisco Section program are (from left) Vice Chair Tom Smeltzer, Chair Richard Hashimoto, and speaker Dave Buttress.

SIERRA NEVADA

March 10
Activity: The Section hosted its SkillsUSA and Sierra Nevada Section-sponsored welding competition for 35 contenders at the Western Nevada Community College campus in Carson City. The judges and facilitators included **Jesse Mandoki,** Basalite Concrete Products; **Curtis Smith,** A-L Sierra Welding Products, Inc.; **Victor Garcia,** Chromalloy; **Randy Naylor,** event coordinator; welding instructor **Edward Martin; Brett Wernett,** a welder with Paramount Iron; and **Richard Sheridan** with Risk Services-Nevada, Inc.

Member-Get-A-Member Campaign

Listed are the members participating in the 2006–2007 Campaign for the period June 1, 2006, through May 31, 2007. See page 101 for rules and the prize list. Call the Membership Dept. (800/305) 443-9353, ext. 480, for information about your status as a member proposer. Listings are for March 16, 2007.

Winners Circle

AWS Members who have sponsored 20 or more new members, per year, since 6/1/1999. The superscript denotes the number of times Winners Circle status has been earned if more than once.

J. Compton, San Fernando Valley[6]
E. Ezell, Mobile[4]
J. Merzthal, Peru[2]
G. Taylor, Pascagoula[2]
B. Mikeska, Houston
R. Peaslee, Detroit
W. Shreve, Fox Valley
M. Karagoulis, Detroit
S. McGill, NE Tennessee
T. Weaver, Johnstown/Altoona
G. Woomer, Johnstown/Altoona
R. Wray, Nebraska
M. Haggard, Inland Empire

Note: The superscript indicates the number of times an Individual Member has achieved Winner's Circle status. Status awards will be determined at the close of each membership campaign year.

President's Guild

AWS Members sponsoring 20 or more new Individual Members between June 1, 2006, and May 31, 2007.

L. Taylor, Pascagoula — 67
J. Compton, San Fernando Valley — 28

President's Roundtable

AWS Members sponsoring 9–19 new Individual Members between June 1, 2006, and May 31, 2007.

M. Palko, Detroit — 16
W. Shreve, Fox Valley — 15
C. Daon, Israel — 11
E. Ezell, Mobile — 11
R. Myers, L.A./Inland Empire — 10
R. Ellenbecker, Fox Valley — 9
A. Hoover, Northwestern Pa. — 9
L. Mathieu, International — 9
G. Mulee, Charlotte — 9

President's Club

AWS Members sponsoring 3–8 new Individual Members between June 1, 2006, and May 31, 2007.

D. Eck, Houston — 8
G. Fudala, Philadelphia — 8
R. Wilsdorf, Tulsa — 7
J. Bruskotter, New Orleans — 5
G. Taylor, Pascagoula — 5
B. Converse, Detroit — 4
T. Ferri, Boston — 4
H. Jackson, L.A./Inland Empire — 4
J. Leen, Chicago — 4
K. Smythia, Kansas City — 4
P. Zammit, Spokane — 4
S. Chuk, International — 3
J. Goldsberry Jr., SE Nebraska — 3
G. Lau, Cumberland Valley — 3
P. Phelps, Western Carolina — 3
T. White, Pittsburgh — 3

President's Honor Roll

AWS Members sponsoring 1 or 2 new Individual Members between June 1, 2006, and May 31, 2007. Only those sponsoring 2 AWS Individual Members are listed.

C. Amick, Columbia — 2
A. Badeaux, Washington, D.C. — 2
G. Beer, Northern New York — 2
W. Cash, Fresno — 2
G. Cottrell, South Florida — 2
G. Cunningham, North Texas — 2
J. Dolan, New Jersey — 2
D. Gillies, Green & White Mts. — 2
R. Gollihue, Tri-State — 2
S. Harris, Triangle — 2
D. Herr, York-Central Pa. — 2
D. Irvin, Mid-Ohio Valley — 2
J. Jones, Maine — 2
G. Koza, Houston — 2
M. Lamarre, Palm Beach — 2
E. Lamont, Detroit — 2
D. Lawrence, Peoria — 2
J. Little, British Columbia — 2
D. Malkiewicz, Niagara Frontier — 2
P. Newhouse, British Columbia — 2
R. Pierce, Mobile — 2
M. Rieb, Inland Empire — 2
D. Shackelford, L.A/Inland Empire — 2
L. Weathers, Tulsa — 2
E. White, Southwest Virginia — 2
D. Wright, Kansas City — 2
R. Wright, San Antonio — 2

Student Member Sponsors

AWS Members sponsoring 3 or more new AWS Student Members between June 1, 2006, and May 31, 2007.

C. Daily, Puget Sound — 196
D. Williams, North Texas — 63
A. Demarco, New Orleans — 45
H. Hughes, Mahoning Valley — 44
G. Euliano, Northwestern Pa. — 43
H. Jackson, L.A./Inland Empire — 43
S. Burdge, Stark Central — 34
S. Siviski, Maine — 30
B. Yarrison, York-Central Pa. — 30
J. Ciaramitaro, N. Central Florida — 27
B. Suckow, Northern Plains — 26
A. Zinn, Eastern Iowa — 24
T. Kienbaum, Colorado — 22
A. Reis, Pittsburgh — 22
M. Anderson, Indiana — 21
T. Geisler, Pittsburgh — 21
D. Ketler, Willamette Valley — 20
B. Lavallee, Northern New York — 19
G. Smith, Lehigh Valley — 18
M. Arand, Louisville — 17
H. Browne, New Jersey — 17
R. Boyer, Nevada — 17
M. Pointer, Sierra Nevada — 17
W. Harris, Pascagoula — 16
R. Robles, Corpus Christi — 16
C. Donnell, Northwest Ohio — 15
B. Butela, Pittsburgh — 14
D. Kowalski, Pittsburgh — 14
S. Robeson, Cumberland Valley — 14
D. Zabel, Southeast Nebraska — 14
A. Badeaux, Washington D.C. — 13
J. Daugherty, Louisville — 13
L. Collins, Puget Sound — 11
M. Koehler, Milwaukee — 11
G. Kirk, Pittsburgh — 10
G. Koza Jr., Houston — 10
S. Luis Jr., Calif. Central Coast — 10
J. Smith Jr., Mobile — 10
J. Cox, Northern Plains — 9
L. Davis, New Orleans — 8
A. Mattox, Lexington — 8
G. Putnam, Green & White Mts. — 8
J. Compton, San Fernando Valley — 7
D. Newman, Ozark — 7
J. Robillard, Columbus — 7
C. Schiner, Wyoming — 7
W. Younkins, Mid-Ohio Valley — 7
D. Combs, Santa Clara Valley — 6
G. Gammill, Northeast Mississippi — 6
R. Grays, Kern — 6
R. Hutchison, Long Beach/Or Cty. — 6
C. Kipp, Lehigh Valley — 6
G. Saari, Inland Empire — 6
J. Angelo, El Paso — 5
T. Buchanan, Mid-Ohio Valley — 5
J. Carney, Western Michigan — 5
C. Chancy, Long Beach/Or Cty. — 5
A. Kitchens, Olympic — 5
J. Boyer, Lancaster — 4
A. Dropik, Northern Plains — 4
J. Morash, Boston — 4
C. Neichol, Houston — 4
M. Rahn, Iowa — 4
R. Richwine, Indiana — 4
J. Swoyer, Lehigh Valley — 4
J. Swoyer, Lehigh Valley — 4
D. Wright, Kansas City — 4
C. Yaeger, NE Carolina — 4
T. Zablocki, Pittsburgh — 4
C. Bridwell, Ozark — 3
S. Click, Lexington — 3
J. Crosby, Atlanta — 3
T. Garcia, New Orleans — 3
F. Gorglione, Connecticut — 3
L. Gross, Milwaukee — 3
L. Ibarra, San Francisco — 3
W. Menegus, Lehigh Valley — 3
S. Miner, San Francisco — 3
T. Moore, New Orleans — 3
D. Robinson, Sacramento — 3
R. Rowe, Kansas City — 3
R. Stein,Baltimore — 3
T. Strickland, Arizona — 3
M. Vann, South Carolina — 3
R. Vann, South Carolina — 3♦

Guide to AWS Services

550 NW LeJeune Rd., Miami, FL 33126
www.aws.org; phone (800/305) 443-9353; FAX (305) 443-7559
(Phone extensions are shown in parentheses.)

AWS PRESIDENT

Gerald D. Uttrachi
guttrachi@aol.com
WA Technology, LLC
4313 Byrnes Blvd., Florence, SC 29506

ADMINISTRATION

Executive Director
Ray W. Shook.. *rshook@aws.org* . . . .(210)

CFO/Deputy Executive Director
Frank R. Tarafa.. *tarafa@aws.org* . . . .(252)

Deputy Executive Director
Cassie R. Burrell.. *cburrell@aws.org* . . . .(253)

Associate Executive Director
Jeff Weber.. *jweber@aws.org* . . . .(246)

Executive Assistant for Board Services
Gricelda Manalich.. *gricelda@aws.org* . .(294)

Administrative Services

Managing Director
Jim Lankford.. *jiml@aws.org* . . . .(214)

IT Network Director
Armando Campana..*acampana@aws.org* .(296)

Director
Hidail Nunez..*hidail@aws.org* . . . .(287)

Human Resources

Director, Compensation and Benefits
Luisa Hernandez.. *luisa@aws.org* . . . . . .(266)

Manager, Human Resources
Dora Shade.. *dshade@aws.org* . . . .(235)

INT'L INSTITUTE of WELDING

Senior Coordinator
Sissibeth Lopez . . *sissi@aws.org* . . . . . .(319)
Provides liaison services with other national and international professional societies and standards organizations.

GOVERNMENT LIAISON SERVICES

Hugh K. Webster. . . . . *hwebster@wc-b.com*
Webster, Chamberlain & Bean, Washington, DC
(202) 466-2976; FAX (202) 835-0243
Identifies funding sources for welding education, research, and development. Monitors legislative and regulatory issues of importance to the industry.

Brazing and Soldering Manufacturers' Committee

Jeff Weber.. *jweber@aws.org* . . . .(246)

RWMA — Resistance Welding Manufacturing Alliance

Manager
Susan Hopkins.. *susan@aws.org* . . . .(295)

WEMCO — Welding Equipment Manufacturers Committee

Manager
Natalie Tapley.. *tapley@aws.org* . . . .(444)

CONVENTION and EXPOSITIONS

Associate Executive Director
Jeff Weber.. *jweber@aws.org* . . . .(246)

Corporate Director, Exhibition Sales
Joe Krall.. *krall@aws.org* . . . .(297)
Organizes the annual AWS Welding Show and Convention, regulates space assignments, registration items, and other Expo activities.

PUBLICATION SERVICES

Department Information . . . .(275)

Managing Director
Andrew Cullison.. *cullison@aws.org* . . . .(249)

Welding Journal
Publisher/Editor
Andrew Cullison.. *cullison@aws.org* . . . .(249)

National Sales Director
Rob Saltzstein.. *salty@aws.org* . . . .(243)

Society and Section News Editor
Howard Woodward..*woodward@aws.org* (244)

Welding Handbook
Welding Handbook Editor
Annette O'Brien.. *aobrien@aws.org* . . . .(303)

Publishes the Society's monthly magazine, *Welding Journal*, which provides information on the state of the welding industry, its technology, and Society activities. Publishes *Inspection Trends*, the *Welding Handbook,* and books on general welding subjects.

MARKETING COMMUNICATIONS

Director
Ross Hancock.. *rhancock@aws.org* . . . .(226)

Assistant Director
Adrienne Zalkind.. *azalkind@aws.org* . . .(416)

MEMBER SERVICES

Department Information . . . .(480)

Deputy Executive Director
Cassie R. Burrell.. *cburrell@aws.org* . . . .(253)

Director
Rhenda A. Mayo... *rhenda@aws.org* . . . .(260)
Serves as a liaison between Section members and AWS headquarters. Informs members about AWS benefits and activities.

EDUCATION SERVICES

Managing Director
Dennis Marks.. *dmarks@aws.org* . . . .(237)

Director, Education Services Administration and Convention Operations
John Ospina.. *jospina@aws.org* . . . .(462)

Director, Education Product Development
Christopher Pollock.. *cpollock@aws.org* (219)

Tracks effectiveness of programs and develops new products and services. Coordinates in-plant seminars and workshops. Administers the S.E.N.S.E. program. Assists Government Liaison Committee with advocacy efforts. Works with Education Committees to disseminate information on careers, national education and training trends, and schools that offer welding training, certificates, or degrees.

Also responsible for conferences, exhibitions, and seminars on topics ranging from the basics to the leading edge of technology. Organizes CWI, SCWI, and 9-year renewal certification-driven seminars.

AWS AWARDS, FELLOWS, COUNSELORS

Senior Manager
Wendy S. Reeve.. *wreeve@aws.org* . . . . .(293)
Coordinates AWS awards and AWS Fellow and Counselor nominees.

CERTIFICATION OPERATIONS

Department Information . . . .(273)

Managing Director
Peter Howe.. *phowe@aws.org* . . . .(309)

Director, Operations
Terry Perez.. *tperez@aws.org* . . . .(470)

Director, Int'l Business Accreditation and Welder Certification
Walter Herrera.. *walter@aws.org* . . . .(475)
Provides information on personnel certification and accreditation services.

TECHNICAL SERVICES

Department Information . . . .(340)

Managing Director
Andrew R. Davis.. *adavis@aws.org* . . . . .(466)
Int'l Standards Activities, American Council of the Int'l Institute of Welding (IIW)

Director, National Standards Activities
John L. Gayler.. *gayler@aws.org* . . . .(472)
Structural Welding, Machinery and Equipment Welding, Robotic and Automatic Welding, Computerization of Welding Information

Manager, Safety and Health
Stephen P. Hedrick.. *steveh@aws.org* . .(305)
Metric Practice, Personnel and Facilities Qualification, Safety and Health, Joining of Plastics and Composites

Technical Publications
AWS publishes about 200 documents widely used throughout the welding industry.
Senior Manager
Rosalinda O'Neill.. *roneill@aws.org* . . . .(451)

Staff Engineers/Standards Program Managers
Annette Alonso.. *aalonso@aws.org* . . . . .(299)
Welding in Sanitary Applications, Automotive Welding, Resistance Welding, High-Energy Beam Welding, Aircraft and Aerospace, Oxyfuel Gas Welding and Cutting

Stephen Borrero.. *sborrero@aws.org* . . . .(334)
Welding Iron Castings, Joining of Metals and Alloys, Brazing and Soldering, Brazing Filler Metals and Fluxes, Brazing Handbook, Soldering Handbook

Rakesh Gupta.. *gupta@aws.org* . . . .(301)
Filler Metals and Allied Materials, Int'l Filler Metals, Instrumentation for Welding, UNS Numbers Assignment

Brian McGrath . *bmcgrath@aws.org* . . . .(311)
Methods of Inspection, Mechanical Testing of Welds, Thermal Spray, Arc Welding and Cutting, Welding in Marine Construction, Piping and Tubing, Titanium and Zirconium Filler Metals, Filler Metals for Naval Vessels

Selvis Morales.....*smorales@aws.org* . . .(313)
Welding Qualification, Friction Welding, Railroad Welding, Definitions and Symbols

Note: *Official interpretations of AWS standards may be obtained only by sending a request in writing to the Managing Director, Technical Services. Oral opinions on AWS standards may be rendered. However, such opinions represent only the personal opinions of the particular individuals giving them. These individuals do not speak on behalf of AWS, nor do these oral opinions constitute official or unofficial opinions or interpretations of AWS. In addition, oral opinions are informal and should not be used as a substitute for an official interpretation.*

Nominees for National Office

Only Sustaining Members, Members, Honorary Members, Life Members, or Retired Members who have been members for a period of at least three years shall be eligible for election as a director or national officer.

It is the duty of the National Nominating Committee to nominate candidates for national office. The committee shall hold an open meeting, preferably at the Annual Meeting, at which members may appear to present and discuss the eligibility of all candidates.

To be considered a candidate for the positions of president, vice president, treasurer, or director-at-large, the following qualifications and conditions apply:

President: To be eligible to hold the office of president, an individual must have served as a vice president for at least one year.

Vice President: To be eligible to hold the office of vice president, an individual must have served at least one year as a director, other than executive director and secretary.

Treasurer: To be eligible to hold the office of treasurer, an individual must be a member of the Society, other than a Student Member, must be frequently available to the national office, and should be of executive status in business or industry with experience in financial affairs.

Director-at-Large: To be eligible for election as a director-at-large, an individual shall previously have held office as chairman of a Section; as chairman or vice chairman of a standing, technical, or special committee of the Society; or as District director.

Interested persons should submit a letter stating which office they seek, including a statement of qualifications, their willingness and ability to serve if nominated and elected, and a biographical sketch.

E-mail the letter to Gricelda Manalich, *gricelda@aws.org,* c/o Damian J. Kotecki, chair, National Nominating Committee.

The next meeting of the National Nominating Committee is scheduled for November 2007. The terms of office for candidates nominated at this meeting will commence January 1, 2009.

Honorary Meritorious Awards

The Honorary-Meritorious Awards Committee makes recommendations for the nominees presented for Honorary Membership, National Meritorious Certificate, William Irrgang Memorial, and the George E. Willis Awards. These awards are presented during the FABTECH International & AWS Welding Show held each fall. The deadline for submissions is December 31 prior to the year of awards presentations. Send candidate materials to Wendy Sue Reeve (*wreeve@aws.org),* secretary, Honorary-Meritorious Awards Committee, 550 NW LeJeune Rd., Miami, FL 33126. Descriptions of the awards follow.

National Meritorious Certificate Award: This award is given in recognition of the candidate's counsel, loyalty, and devotion to the affairs of the Society, assistance in promoting cordial relations with industry and other organizations, and for the contribution of time and effort on behalf of the Society.

William Irrgang Memorial Award: This award is administered by the American Welding Society and sponsored by The Lincoln Electric Co. to honor the late William Irrgang. It is awarded each year to the individual who has done the most over the past five-years to enhance the American Welding Society's goal of advancing the science and technology of welding.

George E. Willis Award: This award is administered by the American Welding Society and sponsored by The Lincoln Electric Co. to honor George E. Willis. It is awarded each year to an individual for promoting the advancement of welding internationally by fostering cooperative participation in areas such as technology transfer, standards rationalization, and promotion of industrial goodwill.

International Meritorious Certificate Award: This award is given in recognition of the recipient's significant contributions to the worldwide welding industry. This award reflects "Service to the International Welding Community" in the broadest terms. The awardee is not required to be a member of the American Welding Society. Multiple awards can be given per year as the situation dictates. The award consists of a certificate to be presented at the awards luncheon or at another time as appropriate in conjunction with the AWS president's travel itinerary, and, if appropriate, a one-year membership in the American Welding Society.

Honorary Membership Award: An Honorary Member shall be a person of acknowledged eminence in the welding profession, or who is accredited with exceptional accomplishments in the development of the welding art, upon whom the American Welding Society sees fit to confer an honorary distinction. An Honorary Member shall have full rights of membership.

AWS Publications Sales

Purchase AWS Standards, books, and other publications from
World Engineering Xchange (WEX), Ltd.
Toll-free (888) 935-3464 (U.S., Canada)
(305) 824-1177; FAX (305) 826-6195
www.awspubs.com

Welding Journal Reprints

Copies of *Welding Journal* articles may be purchased from Ruben Lara.
Call toll-free
(800/305) 443-9353, ext. 288; *rlara@aws.org*

Custom reprints of *Welding Journal* articles, in quantities of 100 or more, may be purchased from
FosteReprints
Toll-free (866) 879-9144, ext. 121
sales@fostereprints.com

AWS Foundation, Inc.

The AWS Foundation is a not-for-profit corporation established to provide support for educational and scientific endeavors of the American Welding Society. Information on gift-giving programs is available upon request.

550 NW LeJeune Rd., Miami, FL 33126
(305) 445-6628; (800) 443-9353, ext. 293
e-mail: *vpinsky@aws.org*
general information:
(800) 443-9353, ext. 689

AWS Mission Statement

The mission of the American Welding Society is to advance the science, technology, and application of welding and allied processes, including joining, brazing, soldering, cutting, and thermal spraying.

It is the intent of the American Welding Society to build AWS to the highest quality standards possible. The Society welcomes your suggestions. Please contact any staff member or AWS President Gerald D. Uttrachi, as listed on the previous page.

New UltraCore™ Wire Catalog Released

The 24-page, well-illustrated *UltraCore™ Wire Product Catalog,* Bulletin C3.12, begins with a detailed selection guide — matching shielding gases, AWS class, diffusible hydrogen levels, and arc performance with the corresponding UltraCore™ wire. Also presented is a detailed discussion about each of the line's offerings, further describing the information provided in the selection guide plus each wire's mechanical properties, deposit composition, and typical operating procedures. Included is a question-and-answer section on understanding flux cored wire classifications and their applications, as well as a chart on agency approvals (such

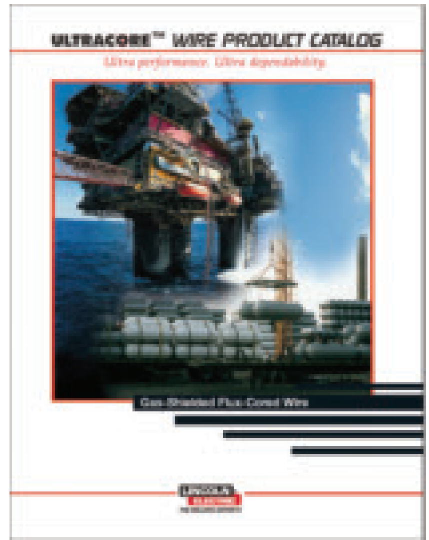

as AWS), and a chart comparing the line with other wires on the market. Call (216) 481-8100 to order a copy of the guide, or visit *www.lincolnelectric.com* to download the document in PDF.

Kwik-Lok™ Pins Featured in Catalog

The *Jergens® Kwik-Lok™ Pins Catalog* is a complete sourcing guide for a variety of applications in manufacturing, aviation, military, general industrial, medical equipment, recreation, and marine industries. New products displayed for the first time in this catalog include lifting pins and lanyards. The products are shown in full color, with specifications stated in both U.S. Customary and metric units. It includes two pages of specifications and material specifications, applications, and complete ordering information for both standard and Mil-Spec.

Jergens, Inc. 114

Jergens Way, 15700 S. Waterloo Rd., Cleveland, OH 44110-3898

Steels Highlighted in Publications Brochure

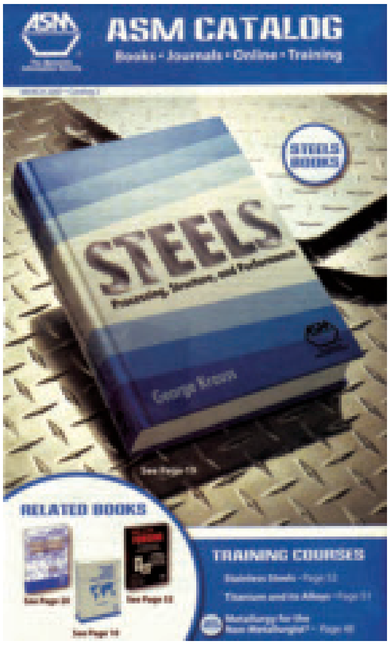

The 70-page, March 2007 *ASM Catalog* features books on steels, cold and hot forging, powder metallurgy, stainless steels, and training courses on welding, metallurgy, failure analysis, and heat treating. Listed too are the complete *ASM Handbooks* and an exhaustive selection of literature on virtually every aspect of metals, metallurgy, processes, and research topics.

ASM International 115

9639 Kinsman Rd., Materials Park, OH 44073-0002

Text Aims to Make Welding Easier for Beginners

Welding Essentials, Second Edition, by William L. Galvery Jr. and Frank B. Marlow, is described as a concise yet thorough introduction to welding that makes it easier for beginners to learn while serving as a handy reference for professionals. The 480-page, 7- x 10-in. book employs a question-and-answer format organized to make topics easy to find and understand. Included are how to recognize safety hazards and solutions to common problems encountered with each welding process. Provided is a valuable reference that explains step-by-step setup and shutdown procedures, along with explanations for the need for equipment grounding and ground-fault indicators. Other subjects include determining welding tip sizes, discussions on carbon arc cutting, and using plasma arc and laser beam. All of the major industrial processes are discussed including thermal cutting, brazing, soldering, controlling distortion, welding symbols, inspection, friction stir welding, etc. This second edition, available from Industrial Press for $37.50, includes new and improved drawings throughout. Visit *www.industrialpress.com/en/BookDetails/tabid/54/CatalogItemID/394/Default.aspx* for complete information or to order.

Guide Offers Tips for Welding Cast Iron

A Guide to Welding Cast Iron Successfully explains basic metallurgy, welding processes, and welding techniques for repairing a wide range of cast iron parts and equipment. The text includes procedures with photos and sketches. It is intended as a reference book for use in maintenance, automobile, diesel engine, and machine shops. The book is $21.45, postpaid. Order from Stone Alloys, PO Box 134, Jar-

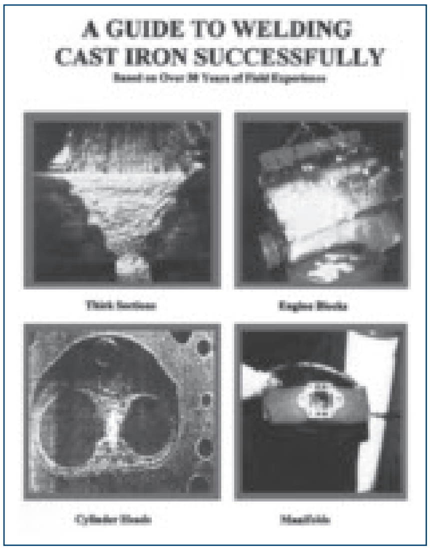

rettsville, MD 21084; for more information, e-mail *stonealloys@clearviewcatv.net.*

Data Sheet Details New Cryogenic Cylinder

An illustrated technical data sheet details the 265-HP cryogenic cylinder for gas and liquid withdrawal. Specified are the unit's extended product holding time and high-pressure performance, combined with very high gas withdrawal rates. Described are the unit's dent-resistant outer shell, heavy-duty casters, all stainless steel construction, and easy-to-read magnetic contents gauge. The cylinder is designed to hold O_2, N_2, Ar, CO_2, and N_2O.

Cyl-Tec, Inc. **116**

553 N. North Ct., Ste. 110, Palatine, IL 60067

Robots and Software Pictured for Easy Selection

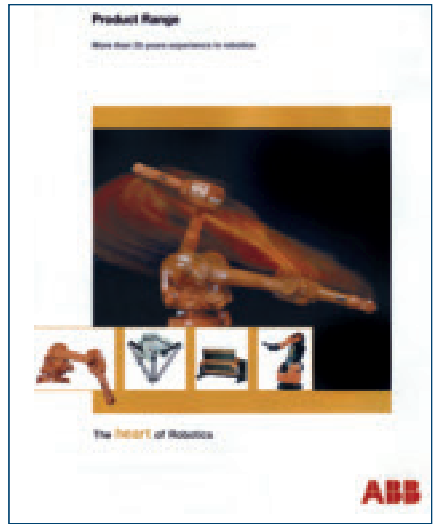

A 12-page, full-color brochure illustrates and details the ABB Robotics lines of robots, positioners, arc and spot welding and painting equipment, plus application software for painting, arc welding, plastics, packaging, and spot welding. Applications are shown for each configuration, including welding, assembly, cleaning, spraying, deburring, machine tending, material handling, picking, packing, and palletizing.

Integrated Robotics 117
40 Old Dover Rd., Newington, NH 03801

CD Catalog Displays Dust Collection Equipment

The company's 348-page catalog, detailing its complete lines of general dust-collection equipment, is offered on a CD. Shown are baghouse and cartridge dust collectors with in-depth information on various applications, product literature, technical data, application guidelines, drawings, and case studies.

Scientific Dust Collectors 118
4101 W. 126 St., Alsip, IL 60803

Handbook of Manufacturing Processes Published

The 864-page, *Handbook of Manufacturing Processes: How Products, Components, and Materials Are Made,* by James G. Bralla, includes more than 600 line drawings and photographs. It is described as an ambitious in-depth compilation of the workings of more than 1500 manufacturing processes in the metalworking, chemicals, textiles, plastics, ceramics, electronics, wood, and food industries. It also details how more than 600 products, components, and materials are made. The book is directed to process engineers, factory managers, supervisors, and others who need to know how products are made, including persons without technical training in the manufacturing field. The text reflects the contributions from an editorial board of 24 experts. Some of the topics in Section 1 are casting, metal forming, machining, finishing, assembly, joining, fusion, heat treating, and advanced manufacturing methods. Section 2 addresses how products, components, and materials are made, and an extensive index. The list price of the text is $115. Order from Industrial Press Inc., 989 Avenue of the Americas, New York, NY 10018; (212) 889-6330; *www.industrialpress.com.*

Welding Wires Catalog Updated

Hobart Brothers' updated Tri-Mark catalog provides the features and benefits for all of the company's flux cored, metal cored, and self-shielded wires. Other catalog features include technical specifications, performance properties, and packing options for each product. The 44-page catalog features charts for filler metal requirements set forth by the American Welding Society, American Bureau of Shipping, Canadian Welding Bureau, and QPL military specifications. Tables are provided to help estimate filler metal consumption based on the joint configura-

— continued on page 112

KUKA Robotics Names President

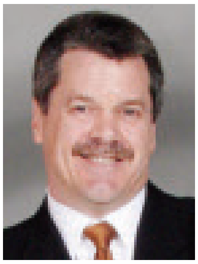

Stuart Shepherd

KUKA Robotics Corp., Clinton Township, Mich., has appointed **Stuart Shepherd** president. Prior to joining the company, Shepherd was founder and president of Shepherd Solutions, a business development and management consulting firm that focused on robotic automation.

Industrial Scientific Fills Three Management Posts

Industrial Scientific Corp., Pittsburgh, Pa., a supplier of gas monitoring instruments, systems, and related products, has promoted **Martin Lutzen** to manager, sales and marketing, for Industrial Scientific Corp. Asia Pacific (ISCAP). **Michael Sullivan** has been promoted to regional sales manager, Australia and New Zealand, for ISCAP; and **Stephen Chen** has been promoted to engineering manager for ISCAP. Lutzen, Sullivan, and Chen previously held sales and engineering positions with the company.

District Manager Appointed at VP Buildings

Greg Limpert

VP Buildings, Memphis, Tenn., a supplier of preengineered metal building systems, has appointed **Greg Limpert** to serve as district manager for portions of New York and Pennsylvania. Previously, Limpert was director of business development at Hayner Hoyt Corp., in Syracuse, N.Y.

Hobart Institute Builds Teaching Staff

Hobart Institute of Welding Technology (HIWT), Troy, Ohio, recently added

Russ Shurtz

Richard Smith

Russ Shurtz and **Richard Smith** to its teaching staff. Shurtz, a graduate of HIWT and Arizona State University, has five years of experience in welding and inspection of cryogenic tanks and boiler pressure vessels. Smith, formerly a welder and hull maintenance technician in the U.S. Navy, is a graduate of the HIWT structural and pipe welding program.

Kaliburn Announces Personnel Changes

Kaliburn, Charleston, S.C., a manufacturer of plasma arc cutting systems, has named **Brian E. O'Hara** vice president of sales and marketing, and hired **Allan H.**

Brian O'Hara

Allan H. Holst

Holst to fill the newly created position of business development director. O'Hara, with the company for four years, previously served as national sales manager. Holst has worked for nearly 30 years in the plasma and CNC cutting machine industry, serving in various sales and product management capacities.

In the April 2007 Welding Journal*, the following item from Ivy Tech Community College, was featured in the Welding School Profile section on page 53. The telephone number was listed incorrectly. This is the correct version.*

Ivy Tech Community College
Founded 1963

The Welding Training Program at Ivy Tech Community College offers a technical certificate, and associate of applied science degrees in Manufacturing and Industrial Technology with a concentration in Welding. Skills taught at our facility could lead to AWS and ASME certification. Ivy Tech Community College, Lafayette is an AWS educational institution member and have AWS certified welding inspectors and certified welding educators on staff. Our welding program has sustained a steady enrollment of over one-hundred students each semester for the past several years.

3101 South Creasy Lane
Lafayette, IN 47905
(765) 269-5149
Dennis A. Nance,
Email: dnance@ivytech.edu

NEW PRODUCTS

— *continued from page 25*

and cut resistance that is necessary while performing hazardous work. The glove is dry cleanable or machine washable with minimal shrinkage.

North Safety Products **109**
2000 Plainfield Pike, Cranston, RI 02921

Mounted Points Reach Deep into Channels

Rex-Cut® mounted points feature multiple layers of nonwoven cotton fiber and aluminum oxide or silicon carbide abrasives that are pressed and bonded into a variety of industry standard shapes and sizes. Useful for mold and die repair and maintenance, they are capable of reaching deep into channels and provide smooth, controlled operation, with virtually no vibration. The points are offered in very-fine to coarse grain sizes and two bonds — MTX where more metal removal is required and GFX for light metal removal, cleaning, and polishing. They can deburr, grind, and finish without changing the part geometry.

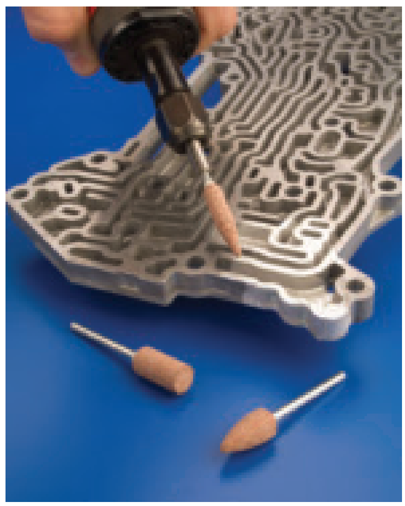

Also, they are suitable for use on aluminum, mild steel, stainless steel, titanium, and other exotic and highly alloyed parts.

Rex-Cut Products, Inc. **110**
960 Airport Rd./PO Box 2109, Fall River, MA 02722

Magnetic Particle Spray System Equipped with Casters

The Magnetic Particle Spray System works when inspecting large parts where users need a portable spray system that holds a larger volume of magnetic particle bath. The 30-gal pot comes equipped with a 15-ft recirculation hose attached to a fan pattern spray gun. The portable unit is also equipped with casters for added mobility. Depending on the process, the system can handle water or oil-based solution. The

continuously agitated bath keeps the particles suspended and uniform through the tank, hose, and spray gun.

Magnaflux **111**
3624 W. Lake Ave., Glenview, IL 60026

Super Duplex Stainless Steel Handles Chloride Environments

RA2507 plate products and welding consumables are available from the company. RA2507 is a super duplex stainless steel with 25% chromium, 7% nickel, and 4% molybdenum. It possesses a minimum yield strength of 80,000 lb/in.^{2} and is approved for ASME pressure vessel use. In addition, it is highly resistant to chloride environments and is suitable for seawater applications.

Rolled Alloys **112**
125 W. Sterns Rd., Temperance, MI 48182

— *continued on page 113*

— continued from page 109

tions. To obtain a copy, call (937) 332-4000, or to download, visit *www.hobart-brothers.com.*

Environmental Systems Guide Updated

The *Environmental Product Selection Guide,* Bulletin MC05-183, is designed for companies looking to purchase their first fume-extraction system or who are in the market to upgrade or enhance their current systems. The pictorial guide serves as a starting point to aid in the decision-making process. Displayed are six low-vacuum mobile and stationary units with nonfiltration, disposable filter and self-cleaning filter options, as well as the flexible extraction arms and fans available for these products. The next level highlights the company's five high-vacuum portable and stationary units with various filter options, and accessories, including extraction nozzles and fume guns. Also illustrated is a typical low-vacuum central system, a high-vacuum central system, and a robotic cell with fume extraction. Call (216) 481-8100 to order a copy of the guide, or visit *www.lincolnelectric.com* to download the brochure in PDF.

Industrial Brushes Pictured in Resource Guide

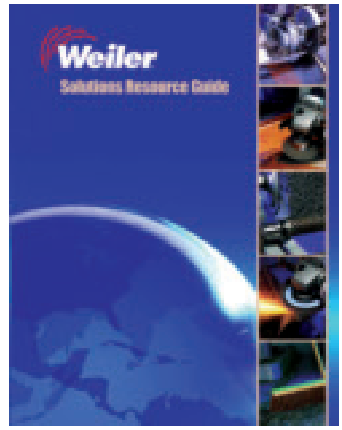

A Solutions Resource Guide presents the company's lines of wire and Nylox® nylon abrasive filament brushes, abrasives, and maintenance products. Illustrated and described are products for deburring, grinding, finishing, and cleaning. Features include color-coded sections for the various product lines, product and application photographs, in-depth technical information, troubleshooting tips, and an easy-reference table of contents with item numbers and alphabetical listings.

Weiler Corp. **119**

One Weiler Dr., Cresco, PA 18326-0149

New Welding Reels Catalog Released

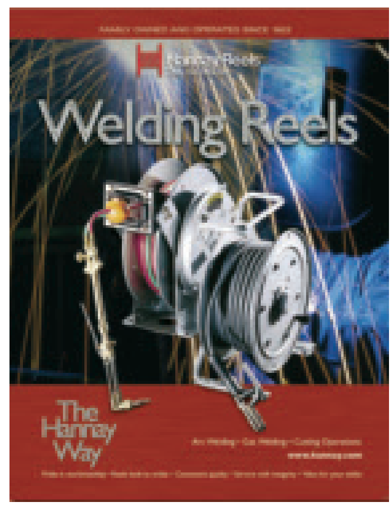

The company recently released its updated catalog featuring its lines of durable hose reels used in arc welding, gas welding, and cutting operations. The reels are described as offering improved efficiency and safety while extending the life of the hoses.

Hannay Reels, Inc. **120**

553 State Rte. 143, Westerlo, NY 12193-0159

Change of Address? Moving?

Make sure delivery of your *Welding Journal* is not interrupted. Contact the Membership Department with your new address information — (800) 443-9353, ext. 217; *smateo@aws.org*.

— continued from page 10

Tulsa Tech Machining Program Earns National Accreditation

Tulsa Technology Center's Machining Technology program at the Broken Arrow Campus, Broken Arrow, Okla., recently earned accreditation by the National Institute for Metalworking Skills (NIMS). The Machining program has been recognized by the organization as one of 125 schools nationwide to be accredited following rigorous examination.

The NIMS establishes national industry skill standards used in metalworking. Tulsa Tech students will be able to take performance examinations following graduation to qualify for NIMS credentials.

Tulsa Tech offers three years of machining coursework from Precision Machining to Advanced CNC Operations and Programming. The center also participates in Craftsmanship, a three-year apprenticeship program in machining and automation and robotics technology.

Industry Notes

- Probe Manufacturing, Inc., Lake Forest, Calif., has received an annual blanket order for building and testing electronics for Miyachi Unitek Corp.'s spot resistance welding machines.
- Rolled Alloys, Temperance, Mich., recently announced the opening of Rolled Alloys (Suzhou) Co. Ltd., including a new warehousing and processing facility in the Suzhou Industrial Park, Jiangsu Province, People's Republic of China. This 30,000-sq-ft facility includes shearing, sawing, and plasma arc cutting capabilities.
- ESAB Welding & Cutting Products recently announced that, after nearly four years of technical discussions, Ingalls Shipyards in Mississippi and Avondale Shipyards in Louisiana have each placed orders with the company for a new panel cutting machine. Both machines will be manufactured in Florence, S.C. Construction is expected to take approximately 18 months.
- Petro Construction Management, Metairie, La., has opened. The company has been serving the oil and gas industry for three years working in the Construction Management Division at Audubon Engineering. Paul C. Hebert and Ken Pierrotti serve as vice presidents of operations, and Donny Faust will serve as vice president of business development.
- Xycom Automation, Saline, Mich., known for supplying industrial PC and flat panel monitor solutions, is adopting Pro-face as its new corporate name.
- Ohio's Lieutenant Governor Lee Fisher recently announced six communities will receive grants totaling more than $1.6 million from the Ohio Small Cities Community Development Block Grant Programs. Among these are an $185,000 Economic Development grant awarded to Vinton County to assist Steelial Welding and Metal Fabrication, Inc., in purchasing a laser cutting machine. The company provides welding and metal fabrication services for the food processing, steel building, mining, and milling industries. The $540,000 project is expected to create 15 jobs in Ohio's Appalachian region.
- Gales Industries, Inc., Bay Shore, N.Y., will acquire all of the outstanding shares of Welding Metallurgy, Inc., a metallurgical engineering and welding services provider and manufacturer based in West Babylon, Long Island, N.Y. As part of the purchase agreement, the company has agreed to pay approximately $6 million in a combination of cash, restricted stock, and debt. The closing of the acquisition is expected to be on or about May 2007.
- Tregaskiss Welding Products of Windsor, Ont., Canada, has again won Canada's 50 Best Managed Companies Program for 2006. Tregaskiss was also a winner in 2005. This national award is sponsored by Deloitte, CIBC Commercial Banking, National Post, and Queen's School of Business.
- F&M Mafco, Inc., Cincinnati, Ohio, a distributor of construction and industrial supplies, has entered into an agreement pursuant to which it will acquire substantially all the assets of Carolina Industrial Tools, Inc., a corporation located in Charlotte, N.C., that is engaged in the business of selling, renting, and servicing tools, equipment, consumables, machinery, and related products. The transaction was expected to close on March 27.
- Miller Electric Mfg. Co.'s online Smart Selector™ at *http://www.millerwelds.com/select* uses a simple, intuitive graphic interface to ease welding product selection. It uses patent-pending software and an interface to make customer recommendations for gas metal arc welding, shielded metal arc welding, gas tungsten arc welding, engine-driven, and plasma cutting products. For those who are unsure which welding process best fits their needs, the Smart Selector explains the benefits, skill level required, and common uses of each.
- DayMark® Safety Systems, Bowling Green, Ohio, a manufacturer and distributor of dissolvable paper products, has acquired Dissolvo® LLC from Gilbreth International. Dissolvo markets a line of dissolvable purge dams for use in gas tungsten arc welding of steel, steel alloy, and aluminum pipes.
- U-Mark, Inc., Belleville, Ill., a manufacturer of industrial markers, has moved into the building formerly occupied by Ideal Stencil, where many of the U-Mark employees once worked. The move would have never seemed possible five years ago when Ideal Stencil, a Belleville, Ill., business founded in 1911, was bought and quickly shut down as a result of a corporate merger. The 18,000-sq-ft building is currently undergoing renovations to accommodate the company's anticipated growth.

NEW PRODUCTS

— continued from page 111

Sander Works in Tight Applications

The air-powered HiVac Dynorbital-Spirit®, available as a 3-in.-diameter random orbital sander, efficiently vacuums through a three-hole sanding pad. Ergonomically designed for comfortable operation, the tool's sanding pad is weight-mated to the tool, ensuring low vibration and smooth finishes. Weighing 1.3 lb, the sander is available in a 3⁄16-in. orbital sanding pattern for generalized sanding, or a tighter, 3⁄32-in. orbital pattern for ultrafine sanding. The product is available in two models — the self-generated vacuum model vacuums directly through the tool's exhaust to an optional portable dust collection system, and the central vacuum model utilizes a 1-in.-diameter vacuum port, which connects to an external vacuum source.

Dynabrade, Inc. **113**
8989 Sheridan Dr., Clarence, NY 14031-1490

CAREER OPPORTUNITIES

MACTEC Engineering & Consulting

CWI/NDT Quality Assurance Steel Inspector

Opportunity to work on New San Francisco – Oakland Bay Suspension Bridge. Inspectors perform QA in fabrication facilities (domestic and international) and at bridge site. Requirements: CWI with multiple NDT Level II's; QC/QA experience; Residence or relocation to California; valid passport & driver's license.

MACTEC

To apply: Fax 858-268-1352 or apply online at www.mactec.com.

Pipe Welder

Toromont Energy Systems needs experienced pipe welders at our Northwest Houston plant.

Candidates must:

Pass GTAW on a 2 inch open butt pipe in 6 G position.

Pass GMAW/FCAW on 2 inch open butt pipe in rollout.

Pass drug screening.

Demonstrate a stable work record.

This is a night shift position, 4:30 p.m. to 2:30 a.m. with extensive overtime (60 + hrs. per week). s

Direct hire. Benefits.

Email resumes to:

US-HR@toromontsystems.com
or fax to 281-345-7434
Attn: Production Manager

Red-D-Arc Welderentals

When you're ready to weld.

North America's leader in the Welder Rental industry is looking for key individuals to join our team:

RED-D-ARC (a division of Airgas) is North America's largest welder rental company. We presently operate a rental fleet of over 30,000 welding machines from over 30 branch locations in North America. Our business includes rentals, leasing and used & new sales of welding equipment and related accessories.

We require highly motivated people with excellent communication skills, superior interpersonal skills, proven customer service aptitude and the ability to work in a fast-paced team environment. Knowledge of welding equipment and processes is an asset.

For a list of open positions and to submit a resume visit our website at www.red-d-arc.com

Don't miss your opportunity to become part of a dynamic team of industry leaders. Red-D-Arc offers competitive wage and benefits package. If you are interested in exploring employment opportunities further, please contact us today! Red-D-Arc is an equal opportunity employer.

Combine your relationship with your existing industrial customers with our line of premium quality welding alloys for maximum profitability.

Success Formula

✔ Vulcan - Premium quality products
- consumable products
- compliments your existing line(s) of industrial products.
- leverage your existing relationship

✔ with your - customers to maximum your profitability.

"Your High Integrity and Our High Quality... An Unstoppable Combination"

✔ Doug Field
Vulcan Systems, Inc.
1-810-730-6052

Quality Systems through Superior Performance

AWS JobFind

Post Jobs. @ Find Jobs.

www.aws.org/jobfind

Job categories for welders, engineers, inspectors, and more than 17 other materials joining industry classifications!

EQUIPMENT FOR SALE OR RENT

TOOLS & SUPPLIES FOR SALE OR RENT

CERTIFICATION & TRAINING

SERVICES

ADVERTISER INDEX

IFC = Inside Front Cover
IBC = Inside Back Cover
OBC = Outside Back Cover
RI = Reader Information Card

CAN WE TALK?

The *Welding Journal* staff encourages an exchange of ideas with you, our readers. If you'd like to ask a question, share an idea or voice an opinion, you can call, write, e-mail or fax. Staff e-mail addresses are listed below, along with a guide to help you interact with the right person.

Publisher/Editor
Andrew Cullison
cullison@aws.org, Extension 249
Article Submissions

Senior Editor
Mary Ruth Johnsen
mjohnsen@aws.org, Extension 238
Feature Articles

Associate Editor
Howard Woodward
woodward@aws.org, Extension 244
Society News
Personnel

Assistant Editor
Kristin Campbell
kcampbell@aws.org, Extension 257
New Products
News of the Industry

Managing Editor
Zaida Chavez
zaida@aws.org, Extension 265
Design and Production

Advertising Sales Director
Rob Saltzstein
salty@aws.org, Extension 243
Advertising Sales

Advertising Sales & Promotion Coordinator
Lea Garrigan Badwy
garrigan@aws.org, Extension 220
Production and Promotion

Advertising Production Manager
Frank Wilson
fwilson@aws.org, Extension 465
Advertising Production

Peer Review Coordinator
Erin Adams
eadams@aws.org, Extension 275
Peer Review of Research Papers

Welding Journal Dept.
550 N.W. LeJeune Rd.
Miami, FL 33126
(800) 443-9353
FAX (305) 443-7404

FABTECH INTERNATIONAL & AWS WELDING SHOW

AN INVITATION TO AUTHORS

to present Brazing and Soldering Abstracts at the AWS 36th International Brazing and Soldering Symposium (IBSS)
November 13-14, 2007 - Chicago, Illinois

Submission Deadline Extended to May 15, 2007

The American Welding Society's C3 Committee on Brazing and Soldering invites you to submit your work for consideration in the Symposium. The program organizers are accepting on a separate piece of paper **500-600-word abstracts** describing original, previously unpublished work. The work may pertain to current research, actual or potential applications, new developments, or outlook into some actual technical areas.

A Symposium Proceedings will be published as a part of the book "AWS Abstracts of Papers" together with other Symposiums and Technical Sessions being held at FABTECH International & AWS Welding Show.

All abstract submissions must be completed by **May 15, 2007**. A final abstract with requested revisions and will be due on **June 15, 2007.**

Before submitting your abstract, we ask that you carefully consider your ability to present your work at the Symposium. Speakers are not required to pay a registration fee for the AWS Professional Program, but are responsible for their travel, housing and any other related expenses.

Return your application and abstract via email to gladys@aws.org or fax it to 305-648-1655 by **May 15th**.

AUTHOR APPLICATION FORM

FOR

36th INTERNATIONAL BRAZING AND SOLDERING SYMPOSIUM

Chicago, Illinois - November 13-14, 2007

Please complete this form legibly. This completed form is to accompany the 500–600 word summary as described on the invitation. Please fax it to 305-648-1655 or via email to gladys@aws.org by ***no later than*** *May 15, 2007.*

Primary Author (full name): ❑ Dr. ❑ Professor ______________________________

Affiliation: ______________________________

Mailing Address: ______________________________

City ____________ State/Province ____________ Zip/Mail Code ____________ Country ____________

E-mail: ______________________________

Coauthor(s) Name: ____________ **Affiliation:** ____________ **Address:** ____________ **City:** ____________ **State/Province:** ____________ **Zip/Mail Code:** ____________ **Country:** ________ **Email:** ________	**Coauthor(s) Name:** ____________ **Affiliation:** ____________ **Address:** ____________ **City:** ____________ **State/Province:** ____________ **Zip/Mail Code:** ____________ **Country:** ________ **Email:** ________
Coauthor(s) Name: ____________ **Affiliation:** ____________ **Address:** ____________ **City:** ____________ **State/Province:** ____________ **Zip/Mail Code:** ____________ **Country:** ________ **Email:** ________	**Coauthor(s) Name:** ____________ **Affiliation:** ____________ **Address:** ____________ **City:** ____________ **State/Province:** ____________ **Zip/Mail Code:** ____________ **Country:** ________ **Email:** ________

PROPOSED TITLE (10 words or less): ______________________________

____

Keywords: Please indicate the top four keywords associated with your research below:

______________________ ______________________

______________________ ______________________

Guidelines for abstract submittal and selection criteria:

Only those abstracts submitted on this form will be considered. Follow the guidelines and word limits indicated. Complete this form and submit it electronically via email to gladys@aws.org or via fax 305-648-1655.

SUBJECT CLASSIFICATIONS:

1. Classify your paper by choosing **one** of the appropriate boxes in each of the following two groups (a) and (b):
   a. ❑ Applied Technology ❑ Education ❑ Research Oriented
   b. ❑ Original Contribution ❑ Progress Report ❑ Review ❑ Tutorial
2. Brazing process (es) used: ______________________________
3. Materials used: ______________________________
4. The main emphasis is more: ❑ process oriented ❑ materials oriented
5. Industries this paper most applies to are: ______________________________
6. Has material in this paper ever been published or presented previously? Yes ❑ No ❑

Below are some of the topical areas covered at IBSS:

__Aircraft and Aerospace
__Automotive and Transportation
__Ceramic / Glass to Metal Joining
__Electronic Packaging / Sensors
__Fuel Cells
__Filler Metal Properties
__Fluxes and Atmospheres
__Furnace / Vacuum Brazing
__Joint Reliability
__Lead Free Solders
__Light Metals
__Materials and Process Design / Control
__Modeling and Process Control
__Power and Electrical Equipment
__Sensors / Micro-Electronics
__Solder Joining Methods
__Special / Advanced Brazing Processes
__Test Methods and Evaluat

WELDING RESEARCH

SUPPLEMENT TO THE *WELDING JOURNAL,* MAY 2007
Sponsored by the American Welding Society and the Welding Research Council

Optimum Evaluation for Electron Beam Weldments of AZ61A-F Extruded Plates

Seventy-seven sets of specimens were joined by changing variables to determine the optimum parameters for welding 11-mm AZ61A alloy

BY CHAO-TING CHI AND CHUEN-GUANG CHAO

ABSTRACT. Recently there has been a renewed interest in magnesium alloys because of their extensive applications in industries, such as computing, communications, consumer electronics, aerospace, and traffic. However, the plastic deformation of these alloys is restricted because HCP magnesium has fewer dislocation slip systems. This limitation can be circumvented by dividing shape-complicated workpieces into several more easily made parts, which are then combined into one. Due to the interaction between material properties and welding conditions, there are various kinds of defects in the welds of magnesium alloys, and these defects cause obvious stress concentrations and serious material damage. This study used a custom-made 11-mm-thick AZ61A extruded plate. By operating and comparing the variable parameters of electron beam welding (EBW), the condition was optimized for ultimate tensile strength (UTS) at 100 mA, 50 kV, 60.6 mm/s, and a focal position at the bottom of the workpiece. Under these conditions, ultimate tensile strengths of 83% and 96%, respectively, were obtained for the base metal in weldments with and without stress concentrators on their surface. For worse conditions such as 100 mA, 45 kV, 86.0 mm/s, and a focal position at the bottom, the UTS of electron beam weldments for AZ61A-F plates was reduced by the three factors of root concavity, heat-affected zone (HAZ), and cavities.

*CHAO-TING CHI (*joseph.mse92g@nctu.edu.tw*) is with Department of Materials Science and Engineering, National Chiao-Tung University, Taiwan, ROC., and the System Manufacturing Center, Chun Shan Institute of Science and Technology, Taipei, Taiwan, ROC. CHUEN-GUANG CHAO (*c_g_chao@hotmail.com*) is with Department of Materials, Science and Engineering, National Chiao-Ting University, Taiwan, ROC.*

Introduction

Of the lightweight metals, magnesium alloys are important structural materials due to their properties of low density and high specific strength. Magnesium alloys are readily available since pure magnesium can be extracted from sea water or reduced from magnesite and dolomite. In addition, the surface treatment of magnesium alloys has been extensively researched and developed using both physical and chemical methods. Therefore, the use of different magnesium alloys has steadily increased, and at this point AZ series magnesium alloys (Al content is below 11.5 wt-%) are the most commonly used. In this series, AZ61 plays a very significant role due to its optimal combination of strength and ductility, which results from being heat treatable as Al content is above 6 wt-% (Ref. 1).

The plastic deformation of AZ61 alloys is restricted because hexagonal close-packed (HCP) magnesium has fewer dislocation slip systems. It cannot be extensively formed, and if fabricated into shape-complicated parts or assemblies, it will fail relatively easily. Although this problem can be solved by using die casting, the average price of each facture will be increased significantly for fractional production because of lower product reliability and more expensive dies. Moreover, die casting is a mass product process with poor mechanical properties in comparison with the extrusion process. In order to reduce the extent of plastic deformation and to raise the mechanical properties, a shape-complicated workpiece can be divided into several simple structural forging parts that are then combined into one. This method will effectively improve problems with forming.

KEYWORDS

Electron Beam Welding
Heat-Affected Zone
Lightweight Metals
Magnesium Alloys
Stress Concentration
Weld Tensile Strength

Particularly in the aerospace and national defense industries, it is important to select a suitable way to join various parts and assemblies. Welding and mechanical fastening are mostly used in these situations. Compared to mechanical fastening, welding usually provides better performance. However, interface junctions are still the major issues since many weld failures result from them. Because high-energy-density beam welding (HBW) has much higher precision, greater depth-to-width ratio of the weld, lower net heat input, narrower HAZ, and finer microstructure as compared with conventional welding (such as GTAW) (Ref. 2), it can be adopted in order to reduce the failure probability of parts and assemblies.

Generally speaking, HBW is very suitable for the welding of magnesium alloys, although it requires the use of a flux or a vacuum environment to protect the molten metal due to the high reactivity of magnesium alloys. Overall, most studies of HBW of magnesium alloys have concentrated on laser welding (Refs. 3–5). Though laser welding is a very convenient process, its maximum depth of complete join penetration (limited by the tolerance of optical device for beam power) is smaller than that of electron beam welding (EBW), and this consideration generally makes EBW the most effective technique for attaching pieces.

Electron beam welding, which achieves the highest precision in position and forms

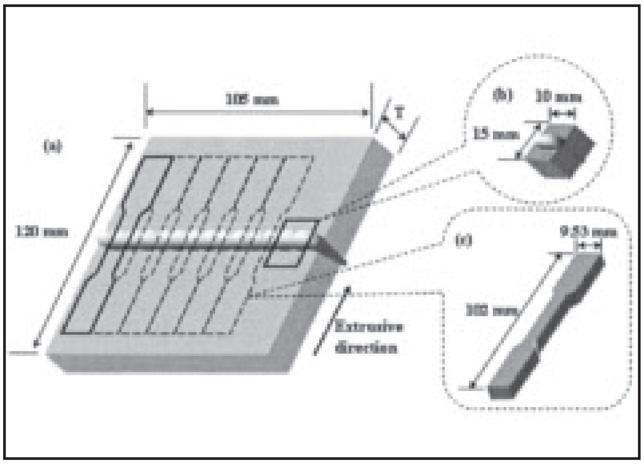

Fig. 1 — Sketch of EB-welded magnesium alloy specimen for different testing purposes.

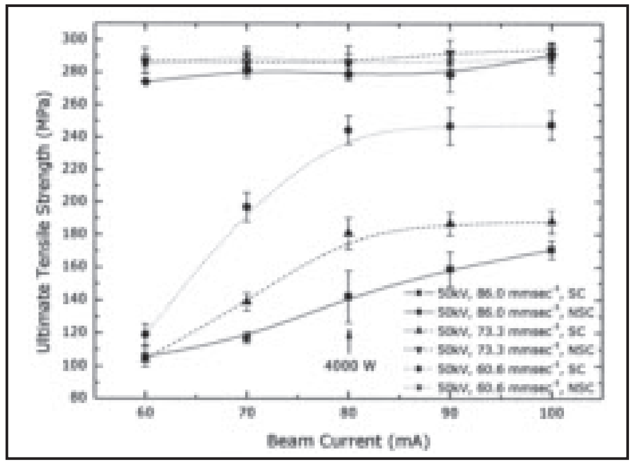

Fig. 2 — Effects of beam current and welding speed on the UTS of AZ61A weldments. Curves are linked by parameters A, E, J, O, and U with individual welding speed. Base metal UTS is 297.4 MPa.

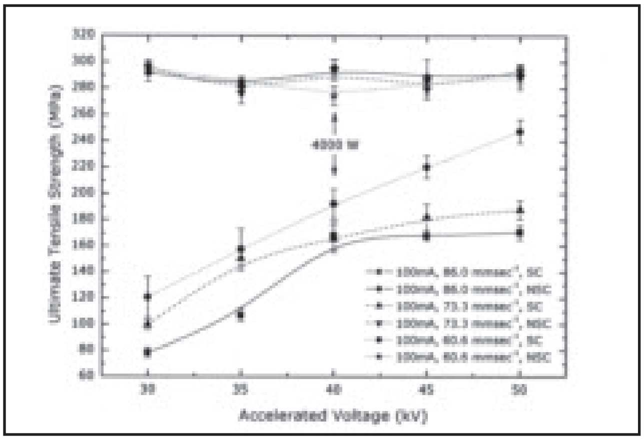

Fig. 3 — Effects of accelerated voltage and welding speed on the UTS of AZ61A weldments. Curves are linked by parameters A, F, K, Q, and W with individual welding speed. Base metal UTS is 297.4 MPa.

the highest depth-to-width ratio of a weld, was developed in 1950s and used in the nuclear industry (Ref. 6). In the early stages of EBW development, since its equipment required high vacuum levels, it was not used extensively because of the high cost and low productivity. From research over the last several decades, low vacuum and nonvacuum systems were developed to greatly reduce the working time (Ref. 7). So far, EBW has been applied to the automobile, aerospace, and national defense industries. Maybe it is possible that EBW of magnesium alloys will become the primary technology of lightweight alloys.

The melted magnesium alloys have higher vapor pressure and better fluidity than the melted aluminum or iron alloys. This reduces the stability of the weld pool surface and its process window (Ref. 9). Furthermore, imperfect parameter condition with asymmetrical Gaussian distribution of input energy (Ref. 10) and additions of unsuitable elements such as excessive Zn (above 1 wt-%) (Ref. 1) caused defects in the fusion zone (FZ) of weldments, which could seriously influence the weld mechanical properties. Presently, there have been only a few studies on EBW of magnesium alloys (Refs. 8, 10–12), which is generally due to the high cost of EBW equipment and magnesium alloys for academic research. Therefore, it is worth examining this subject more closely.

The authors adjusted the variable parameters of EBW including beam current, acceleration voltage, welding speed, and focal position. Accordingly, 77 sets of custom-made specimens of 11-mm-thick AZ61A extruded plate were fabricated and examined in a comparative study.

Experimental Procedure

In this study, the research material used was custom-made AZ61A extruded plate, which had a dimension of 105 × 60 × 12 mm (Ref. 3). The surface, bottom, and side of the AZ61A-F plate were removed to a thickness of 0.5 mm to avoid influence of the oxide layer. After being stored in a vacuum desiccator (10^{-3} torr) for three days, the AZ61A-F plates were welded together with a low-voltage EBW machine for a final dimension of 105 × 120 × 11 mm (Ref. 3) — Fig. 1A. The variable parameters of EBW were arranged and combined in turn according to five fixed power values (3000, 3500, 4000, 4500, and 5000 W) under high vacuum (3 × 10^{-5} torr). The two parameters have three major repeated values (beam current of 100, 125, 150 mA and accelerating voltage of 30, 40, 50 kV) and some minor nonrepeated values in their specific regions (beam current of 60–167 mA and accelerating voltage of 20–50 kV). The conditions of welding speed (60.6, 73.3, and 86.0 mm/s) and the focal position (bottom [0 mm] of the plate) remained the same. Only one parameter was changed at a time in order to study the individual characteristic of these parameters. A weldment with maximum UTS can be selected from them, and then compared with focusing at the surface (+11.0 mm) and middle (+5.5 mm) of the plate. All parameter combinations are indicated in Table 1. Accordingly, 77 sets of specimens (i.e., 3 × 25 + 2 = 77) were fabricated and examined for comparison.

The direction of all welds was perpendicular to that of the extrusion. These weldments were cut into one metallographic sample (Fig. 1B) and six tensile specimens (Fig. 1C). Three of the specimens had a milled finish on the top and bottom surfaces as nonstress concentration (NSC) specimens, while the other three retained the original weld feature as stress concentration (SC) specimens. These specimens, whose detailed dimensions were according to ASTM B557-02 standard specification (Ref. 13), were used for comparing the influence of stress concentration. In particular, the weld should be perpendicular to the longitudinal direction of the standard tensile specimens and located at the center of gauge length to achieve precise measurement of the weld strength. Additionally, after microstructure inspection, the metallographic specimen was divided into two pieces along the central line of the weld

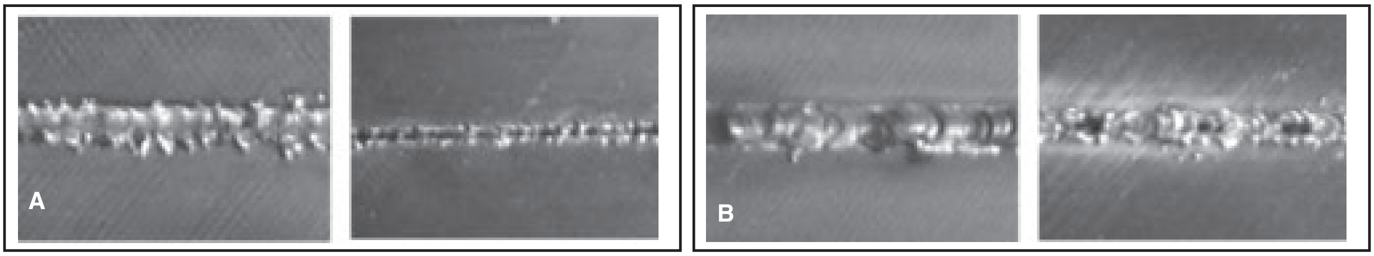

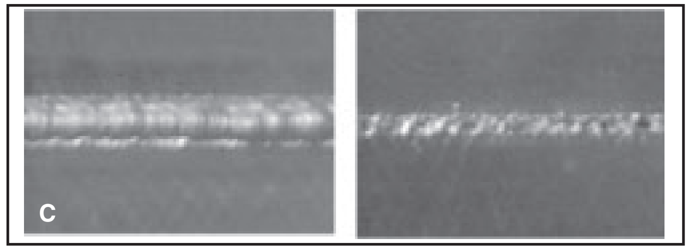

Fig. 4 — Comparison of weld appearance at different focal positions of AZ61A-F plates. Fixed conditions are 100 mA, 50 kV, and 60.6 mm/s. A — Focus at surface; B — Focus at middle; C — Focus at bottom. (crest and root respectively)

cross section. Thus the phase of the transverse plane of the extruded plate could be identified by x-ray diffraction (XRD).

Except for the foregoing inspections, the assessment of postwelding characterization of the workpiece also included chemical composition analysis of the material and distribution of micro-indentation hardness (Vickers, HV) on the transverse plane. The optimum parameters for maximum value of UTS were obtained in accordance with these experimental results.

Results and Discussions

Chemical Composition Analysis

The chemical compositions of AZ61A-F plate were analyzed using inductively coupled plasma-atom emission spectrometer and mass spectrometer (ICP-AES and ICP-MS). As shown in Table 2, all chemical element contents coincide with the ASTM B275-02 standard specification (Ref. 14).

Tensile Test

In this study, the tensile test played the most important role, which used a direct measurement of UTS of the weldment in order to understand the influences of beam current, accelerating voltage, welding speed, and focal position. As shown in Figs. 2 and 3, the UTS of SC samples of AZ61A alloy clearly increases with increasing beam current and accelerating voltage, whereas it decreases with increasing welding speed. When the power is below 4000 W, this will cause incomplete joint penetration and result in occurrence of SC. But if the power is between 4000 and 5000 W, the strength of the samples remained constant over nearly the entire period studied. While the fixed accelerating voltage or beam current is individually changed to another condition (30, 40 kV or 125, 150 mA), they will have the similar trend. However, whether for changing the condition or not, the UTS of NSC samples have no obvious difference and its curves almost keep horizontal. For reasons stated above, there was no other special phase transformation in the weld when different energy was input by EBW.

Figure 4 shows the differences of weld appearance at different focal positions. Because the boiling point (1090°C) and melting point (650°C) of pure magnesium are lower than general engineering materials, while the energy density of EBW is higher than other arc welding, the AZ61A alloy in the weld will exhibit better fluidity during melting. At this time if the focal position of the electron beam is close to the top surface of the workpiece, the weld will produce worse spatter on the surface and lead to more apparent incomplete joint penetration at the root. Since these areas will incur severe stress concentration, UTS values of the samples from top to bottom approach 175.5 MPa (Fig. 4A), 242.8 MPa (Fig. 4B), and 247.5 MPa (Fig. 4C) in that order. This indicates an accurate reflection of actual conditions.

Judging from the above, the control parameters of the maximum value of UTS could be optimized with a beam current of 100 mA, accelerating voltage of 50 kV, welding speed of 60.6 mm/s, and focal position at bottom. The maximum value (247.5 MPa) of UTS for all SC samples

Table 1 — List of 77 sets of Parameters for EBW of AZ61A Extruded Plates

Code	Acceleration Voltage (kV)	Beam Current (mA)	Power (W)
A	50.0	100.0	
B	40.0	125.0	
C	33.3	150.0	5000
D	30.0	167.0	
E	50.0	90.0	
F	45.0	100.0	
G	40.0	113.0	4500
H	36.0	125.0	
I	30.0	150.0	
J	50.0	80.0	
K	40.0	100.0	
L	32.0	125.0	4000
M	30.0	133.0	
N	26.7	150.0	
O	50.0	70.0	
P	40.0	88.0	
Q	35.0	100.0	
R	30.0	117.0	3500
S	28.0	125.0	
T	23.3	150.0	
U	50.0	60.0	
V	40.0	75.0	
W	30.0	100.0	3000
X	24.0	125.0	
Y	20.0	150.0	

NOTE: A weldment with maximum UTS is selected from these coding parameters with 60.6, 73.3, and 86.0 mm/s with focus at bottom, and then it is compared with focusing at surface and middle of the plate.

Table 2 — Chemical Compositions of AZ61A Alloy as Measured by ICP-AES and ICP-MS (wt-%)

Element/ Material	Mg	Al	Zn	Mn	Si	Cu	Fe	P	Pb
AZ61A	93.0585	5.8800	0.7985	0.2205	0.0240	0.0007	0.0030	0.0012	0.0062

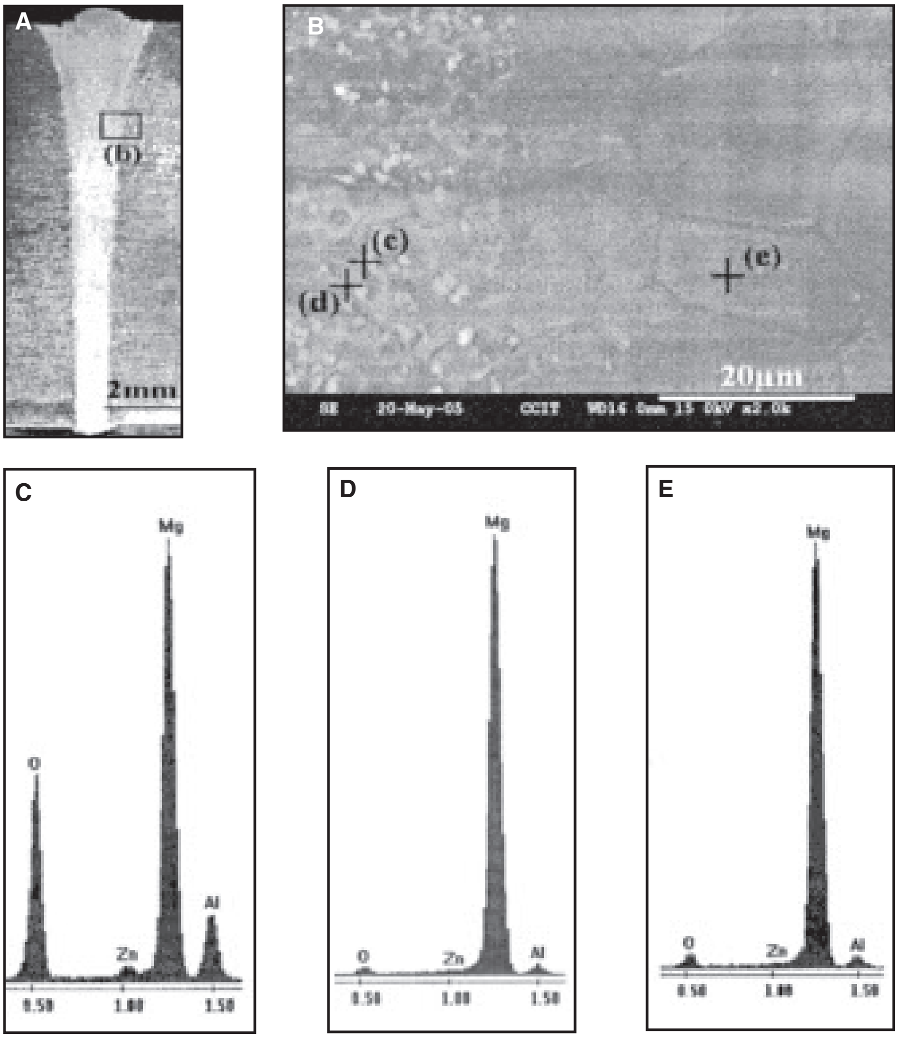

Fig. 5 — Microstructure observation and EDS analysis for the cross section of optimum weld. A — Cross section; B — SEM photograph at the weld boundary; EDS analysis. C — Particle; D — particle vicinity; E — base metal.

for base material, and the average value of UTS (286.0 MPa) for all NSC samples would reach 96% of UTS for the base metal. There was evidence showing that the impingement of SC reached at least 13% of UTS for the base metal. The follow-up experimental results discussed below further explain the remaining 4%. On the contrary, the UTS of the worst weldment reached only 168.1 MPa under the situation of complete joint penetration. Its parameters include a beam current of 100 mA, an accelerating voltage of 45 kV, a welding speed of 86.0 mm/s, and the focal position at the bottom.

Microstructure Observation

Figures 5 and 6 show the microstructures of the optimum and the worst weld cross section, respectively. The mean grain size of the FZ, HAZ, and base metal are 10, 20, and 15 μm, respectively. The small-sized equalaxial grain forms in the FZ (without columnar grain) due to the fast cooling of EBW. On the other hand, the HAZ has the largest grain and it precipitates some submicron-sized crystals in an annealing effect. Many precipitates are observed and concentrated in the FZ — Fig. 5B. Using energy-dispersive spectrometer (EDS) analysis, the chemical compositions of these precipitates (Fig. 5C) with more Al and Zn content than that of the base metal (Fig. 5E) were moved from the vicinity of these precipitates — Fig. 5D. Their Al content levels were 9.43, 4.80, and 5.81 wt-%, respectively; and their Zn content levels were 3.01, 1.57, and 2.37 wt-%, respectively.

The root concavity (Fig. 6A) and cavities (Fig. 6B) became the critical factors for weld fracture, which would cause excessive SC and reduce the UTS value of weldments. Visual inspections reveal that the fracture surfaces of all weldment tensile samples can be divided into two modes: the irregular FZ fracture (48%) and the regular HAZ fracture (52%). In the former mode, cracks running randomly across the middle of the weld are initiated and terminated in an undercut, HAZ, or root concavity. In the latter mode, a break occurs along the weld boundary.

In the Mg-Al binary phase diagram, the maximum solid solubility of aluminum is 11.5 wt-% at 437°C. It decreases to about 2 wt-% at room temperature. After solidification, 6% of Al element can be held in solid solution from 525° to 300°C in AZ61A alloy. $Mg_{17}Al_{12}$ does not precipitate near the grain boundary until the temperature is below 300°C. According to the authors' previous study (Ref. 15), the Vickers hardness of the weld is mainly affected by many brittle precipitates, which vary from scattered particles to dense dendrites as the Al content increases. With regard to the fracture modes of AZ61A alloy, it mainly depends on the distribution (denseness or scattering) of precipitates in FZ.

XRD Analysis

The preferred orientation and specific phase of these samples can be analyzed by XRD. As shown in Fig. 7, there is no formation of other phases in the unwelded or welded samples, and there is very little differences between the optimum and the worst weldments. It is found that the high fraction of $(1\,0\,\bar{1}\,1)$ and $(1\,0\,\bar{1}\,0)$ planes lie on the transverse plane of AZ61A extruded plate before EBW. However, after using EBW, the preferred orientation in FZ will remain only in the $(1\,0\,\bar{1}\,1)$ plane, and the (0 0 0 2) orientation will increase with stepwise diffraction intensity. It follows that the γ phase ($Mg_{17}Al_{12}$) is the sole intermetallic compound whose peak is beside $(1\,0\,\bar{1}\,1)$, and the weldments will not form any other phase transformation that affects its UTS. According to the experimental results of 77 sets of specimens, there were two different kinds of fracture modes in the tensile tests. Some parts broke along the HAZ, while others cracked randomly across the middle of the

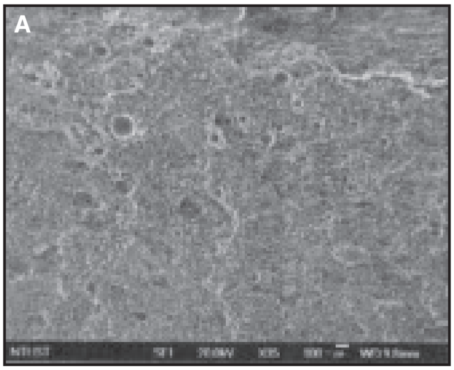

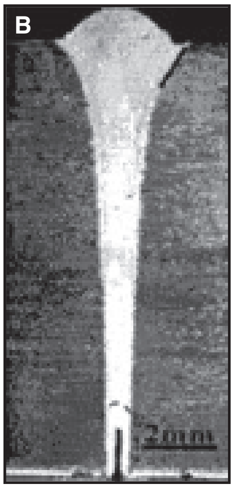

Fig. 6 — Microstructure observation of the worst weld. A — Cross section; B — SEM photograph at the fracture face of the weld.

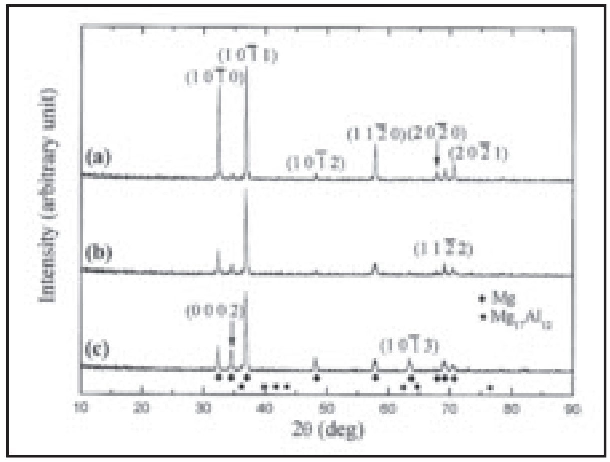

Fig. 7 — Comparison of XRD spectrum for prewelding and postwelding samples of AZ61A-F. A — Prewelding sample; B — optimum weld sample; C — worst weld sample.

weld with initial and terminal positions located in the HAZ or root concavity. This phenomenon clarified that the distribution of γ phase and cavities in the weld would influence the strength of the weldment.

Micro-Indentation Hardness Test

The positions for micro-indentation hardness tests are indicated in Fig. 8A, with the results presented in Fig. 8B. It can be seen that the hardness is high in the center of the upper weld, and decreases toward the bottom of the sample and away from the FZ axis because of the spatial distribution of the brittle γ phases. Moreover, the curve of the optimum sample is more symmetrical than the worst one. This may be because of the softening effect of annealing in the HAZ and the existence of cavities in the weld together caused the larger area of indentation and thus influenced the test value of the micro-indentation hardness. Therefore, there was a sudden dip in the random positions of the HAZ. From this viewpoint, the crack initiation and propagation in AZ61A weldments would also occur in the HAZ. In other words, the HAZ would be the main reason that the UTS reduced at least 4% in the base metal for NSC weldment.

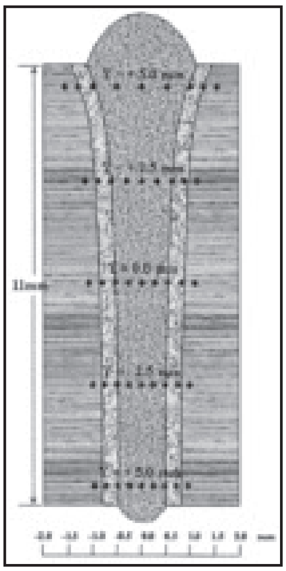

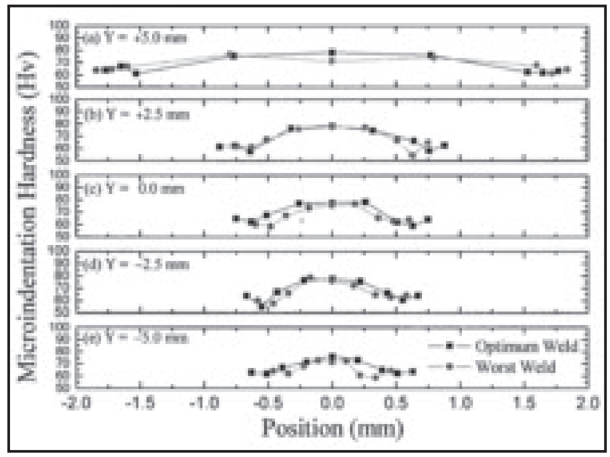

Fig. 8 — Distribution relationship of micro-indentation hardness in cross section of weld. A — Test position of microhardness; B — microhardness distribution of optimum and worst sample.

Conclusions

In this study, the parameters were optimized with a beam current of 100 mA, accelerating voltage of 50 kV, welding speed of 60.6 mm/s, and focal position at the bottom. The maximum value (247.5 MPa) of the UTS for the SC weldment of AZ61A-F and the average value (286.0 MPa) of the UTS for the NSC weldment of AZ61A-F resulted in 83% and 96% of UTS for the base metal, respectively. The harmful influence of SC and HAZ reached at least 13% and 4%, respectively, of the UTS for the base metal.

The power was suitable between 4000 and 5000 W for welding 11-mm-thick AZ61A extruded plates. Under worst conditions, the UTS of EBW on AZ61A extruded plates was reduced by the three factors of root concavity, HAZ, and cavities.

Acknowledgments

The authors heartily acknowledge the support from the National Science Council, ROC., under Project No. NSC 93-2623-7-182-002. The authors also thank C. L. Chang and Z. G. Chang of System Manufacturing Center of Chung-Shan Institute of Science and Technology for technical assistance.

References

1. Avedesian, M. M., and Baker, H. 1999. *Magnesium and Magnesium Alloys.* ASM International, Materials Park, Ohio.

2. Sun, Z., Wei, J., Pan, D. Y., and Tan, Y. K. 2002. Comparative evalution of tungsten inert gas and laser welding of AZ31B magnesium alloy. *Science and Technology of Welding and Joining* 7(6): 343–351.

3. Weisheit, A., Galun, R., and Mordike, B. L. 1998. CO_2 laser beam welding of magnesium-based alloys. *Welding Journal* 77(4): 149–154.

4. Pan, L. K., Wang, C. C., Hsiao, Y. C., and Ho, K. C. 2004. Optimization of Nd: YAG laser welding onto magnesium alloy via taguchi analysis. *Optics & Laser Technology* 37: 33–42.

5. Pan, L. K., Wang, C. C., Shin, Y. C., and Sher, H. F. 2005. Optimizing multiple qualities of Nd: YAG laser welding onto magnesium alloy via grey relational analysis. *Science and Technology of Welding and Joining* 10(4): 1–8.

6. Sun, Z., and Karppi, R. 1996. The application of electron beam welding for the joining of dissimilar metals: An overview. *Journal of Materials Processing Technology* 59: 257–267.

7. Haferkamp, H., Dilthey, U., Träger, G., Burmester, I., and Niemeyer, M. 1998. Beam welding of magnesium alloys. *Magnesium Al-*

loys and Their Application. Eds. B. L. Mordike and K. U. Kainer, pp. 595–600, Werkstoff-Informationsgesellschaft.

8. Dilthey, U., and Weiser, J. 1997. Investigations of EB characteristics and their influences on the weld shape. *Welding in the World* 39(2): 89–98.

9. Su, S. F., Huang, J. C., Lin, H. K., and Ho, N. J. 2002. Electron beam welding behavior in Mg-Al based alloys. *Metallurgical and Materials Transactions* 33A: 1461–1473.

10. Guenther, S., and Armando, J. 2001. Electron beam welding of die cast magnesium. *Advanced Materials & Processes* 159(8): 67–69.

11. Vogelei, C., Dobeneck, D., Decker, I., and Wohlfahrt, H. 2000. Strategies to reduce porosity in electron beam welds of magnesium die-casting alloys. *Magnesium Alloys and their Application*. Ed. K. U. Kainer, pp. 191–199, WILEY-VCH.

12. Draugelates, U., Bouaifi, B., Bartzsch, J., and Ouaissa, B. 1998. Properties of nonvacuum electron beam welds of magnesium alloys. *Magnesium Alloys and their Application*. Eds. B. L. Mordike and K. U. Kainer, pp. 601– 606. Werkstoff-Informationsgesellschaft.

13. American Society for Testing and Materials. 2002. *Standard Test Method of Tension Testing Wrought and Cast Aluminum and Magnesium Alloy Products*. ASTM B557-02.

14. American Society for Testing and Materials. 2002. *Standard Practice for Codification of Certain Nonferrous Metals and Alloys Cast and Wrought*. ASTM B275-02.

15. Chi, C. T., Chao, C. G., Liu, T. F., and Wang, C. C. 2006. A study of weldability and fracture modes in electron beam weldments of AZ series magnesium alloys. *Materials Science and Engineering* 435-436A. 672–680.

The 2007 World Standards Day Paper Competition

The Standards Engineering Society (SES) has established the theme of this year's World Standards Day Paper Competition as "Standards and the Global Village." For many decades, standards have successfully created international consensus on critical issues such as consumer information and protection, the quality and safety of products and services, the environment, health care, security, Internet protocols, and fair trade, among others. The 2007 competition invites papers that show, using specific examples, ways that standards developing organizations have encouraged and created global consensus for the economic and social benefit of the global village.

Paper competition winners will be announced and given their awards at the U.S. celebration of World Standards Day, which will be held this year on October 18, at the Ronald Reagan Building and International Trade Center in Washington, D.C.

Cash prizes are awarded by SES and the World Standards Day Planning Committee for the best three papers submitted. The first place winner will receive a plaque and $2500. second and third place winners will receive $1000 and $500, respectively, along with a certificate. In addition, the winning papers will be published in SES's journal, *Standards Engineering*.

All paper contest submissions must be received with an official entry form by midnight August 31, 2007, by the SES Executive Director, 13340 SW 96th Avenue, Miami, Fla., 33176. For details on the winners' recognition, cash awards, judging, and rules, go to *www.ses-standards.org* and follow the link for 2007 WSD Paper Competition.

CAN WE TALK?

The *Welding Journal* staff encourages an exchange of ideas with you, our readers. If you'd like to ask a question, share an idea or voice an opinion, you can call, write, e-mail or fax. Staff e-mail addresses are listed below, along with a guide to help you interact with the right person.

Publisher/Editor
Andrew Cullison
cullison@aws.org, Extension 249
Article Submissions

Senior Editor
Mary Ruth Johnsen
mjohnsen@aws.org, Extension 238
Feature Articles

Associate Editor
Howard Woodward
woodward@aws.org, Extension 244
Society News
Personnel

Assistant Editor
Kristin Campbell
kcampbell@aws.org, Extension 257
New Products
News of the Industry

Managing Editor
Zaida Chavez
zaida@aws.org, Extension 265
Design and Production

Advertising Sales Director
Rob Saltzstein
salty@aws.org, Extension 243
Advertising Sales

Advertising Sales & Promotion Coordinator
Lea Garrigan Badwy
garrigan@aws.org, Extension 220
Production and Promotion

Advertising Production Manager
Frank Wilson
fwilson@aws.org, Extension 465
Advertising Production

Peer Review Coordinator
Erin Adams
eadams@aws.org, Extension 275
Peer Review of Research Papers

Welding Journal Dept.
550 N.W. LeJeune Rd.
Miami, FL 33126
(800) 443-9353
FAX (305) 443-7404

Application of Magnetic Pulse Welding for Aluminum Alloys and SPCC Steel Sheet Joints

Welding process parameters and characteristics were developed for a variety of similar and dissimilar metals magnetic pulse welds

BY T. AIZAWA, M. KASHANI, AND K. OKAGAWA

ABSTRACT. Magnetic pulse welding (MPW) is a cold process for welding conductive metals to similar or dissimilar materials. Magnetic pulse welding uses magnetic pressure to drive the primary metal against the target metal sweeping away surface contaminants while forcing intimate metal-to-metal contact, thereby producing a solid-state weld. In this paper, the MPW method and its application for several aluminum alloys (A1050, A2017, A3004, A5182, A5052, A6016, and A7075) and joints in steel (SPCC) sheets were investigated, and the welding process parameters and characteristics are reported.

Introduction

One of the most difficult problems in welding is to weld dissimilar metals such as aluminum and steel together. Hybrid structures of aluminum alloy and steel are suggested for reducing the weight of automobiles to improve fuel efficiency and control air pollution. Therefore, the joining of steel and aluminum alloy in different shapes is receiving attention. However, steel and aluminum are not compatible metals as far as fusion welding is concerned. The reason for this is attributed to the large difference between their melting points (660°C for Al and 1497°C for steel), the nearly zero solid solubility of iron in aluminum, and the formation of brittle intermetallic compounds such as Fe_2Al_5 and $FeAl_3$. Further, differences in their thermal properties such as expansion coefficients, conductivities, and specific heats lead to internal stresses after fusion welding. Therefore, fusion welds of steel and aluminum suffer from heavy cracking with brittle failure in service. The material properties of aluminum and steel are summarized in Table 1.

TOMOKATSU AIZAWA and MEHRDAD KASHANI (kashani@asrl.org) *are with Department of Electronic and Information Engineering, and KEIGO OKAGAWA is with Department of Electrical Engineering, Tokyo Metropolitan College of Technology, Shinagawa-Ku, Tokyo, Japan.*

Magnetic pulse welding (MPW) provides an excellent tool for achieving aluminum to steel sheet joints. Magnetic pulse welding is a solid-state joining process of conductive metals. The welding process is heat-free, which can eliminate localized annealing. This paper describes MPW formation in the dissimilar joining of aluminum alloys (A1050, A2017, A3004, A5182, A5052, A6016, and A7075) and steel plate cold rolled commercial grade (SPCC).

A typical MPW system includes a power supply, which contains a bank of capacitors, a fast switching system, and a coil. The parts to be joined are inserted into the coil, the capacitor bank is charged, and the low inductance switch is triggered by a pulse trigger system and the current flows through the coil. When current is applied to the coil, a high-density magnetic flux is created around the coil, and as a result an eddy current is created in the workpieces. The eddy currents oppose the magnetic field in the coil and a repulsive force is created. This force can drive the workpieces together at an extremely high rate of speed and creates an explosive or impact type of weld. For more conductive metals, such as aluminum and copper, less energy is required to achieve a weld. The conventional MPW method with solenoidal coil is used for joining tubular parts and its features are most well known (Refs. 1–3). However, a few papers on MPW of sheet workpieces have been reported.

In a previous paper, we proposed a new one-turn flat coil instead of the solenoidal coil. This coil consisted of upper and lower H-shaped plates, which we call the double layer H-shaped coil. The overlapped sheet workpieces were inserted between these two H-shaped plates. When the high current flows through the coil, it can create the magnetic field to both sides of the overlapped sheet workpieces, and as a result, the sheet metals were welded in the seam state. The magnetic flux produced by this type of coil is shown in Fig. 1A. In this method, the eddy currents that flow in both sheets are considerably different when dissimilar sheet metals like Al/steel sheets are welded. And, also, the thickness of the workpieces was limited by the space between two H-shaped plates. Therefore, for more applications, some contrivance or improvement was needed. These experimental results and welding characteristics for several samples such as Al-Al (Ref. 4), Al-Cu (Ref. 5), Al-Mg, Al-Ti, and Al-Fe (Ref. 6) were reported in previous papers.

In the present experiment, a new coil was designed to improve the welding characteristics of Al alloy and SPCC-steel sheet joints. This new coil is a one-layer E-shaped flat coil that the overlapped sheet workpieces were put on the one side of the coil (Fig. 1B). This type of coil can be designed for applications ranging from short and small to large and long workpieces and also T-shaped joints with higher weld quality.

KEYWORDS

Magnetic Pulse Welding
Seam Welding
Dissimilar Metal
Aluminum Alloys
Steel

Experimental Procedures

MPW Principle

The principle of the magnetic pulse welding method for one Al/Fe sheet sample is shown in Fig. 2. When a high current is applied to the coil, a high magnetic flux density **B** is suddenly generated and penetrates into Al/Fe sheets, then the eddy currents (current density **i**) pass through them to hinder its further penetration. As a result, an electromagnetic force of **i** ×**B** acts mainly on the Al sheet and the Al sheet is accelerated away from the coil and collides rapidly with the steel sheet. At the

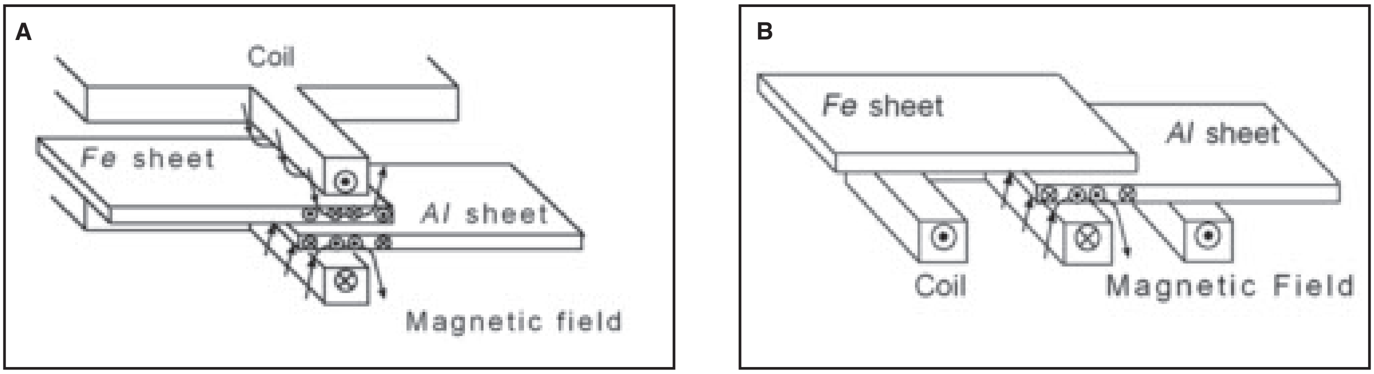

Fig. 1 — MPW coil structure. A — Double-layer, H-shaped flat coil; B — one-layer E-shaped flat coil.

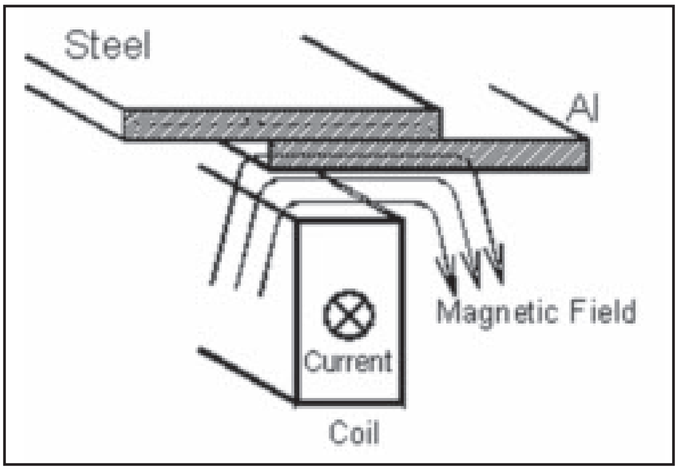

Fig. 2 — Principle of MPW for welding of the Al/steel sheet sample (cross-section view).

moment of collision, the colliding surfaces can be cleared by a large kinetic energy getting before the collision. After the collision, the cleared surfaces are being pressed together by electromagnetic force and a fixture.

The eddy current i and the magnetic pressure p are given as follows:

$$\nabla \times \boldsymbol{i} = -\kappa \left(\frac{\partial \boldsymbol{B}}{\partial t} \right) \quad (1)$$

$$p = \left(B_o^2 - B_i^2 \right) / 2\mu = \left(\frac{B_o^2}{2\mu} \right) \left(1 - e^{-2x/\delta} \right)$$

$$\text{and } \delta = \sqrt{2/\omega\kappa\mu} \quad (2)$$

where κ, μ, τ, B_o, and B_i are the electrical conductivity, magnetic permeability, thickness, and magnetic flux density at lower and upper surfaces of Al sheet, respectively. The depth of skin effect can be obtained by $\delta = \sqrt{2/\omega\kappa\mu}$, where ω is the angular frequency of changing field.

When the eddy current flows through the workpieces, Al sheet is pressed to the Fe sheet by magnetic pressure and is heated by a Joule heating effect ($Q = i^2/\kappa$). Equation 1 shows that more eddy currents are produced at the surface of the metal sheet for materials that have a higher electrical conductivity κ and, as a result, the stronger magnetic pressure *p* and a large amount of Joule heat are generated during the weld process. In addition, from Equation 2 it can be obtained that the magnetic pressure also increases for higher conductive materials.

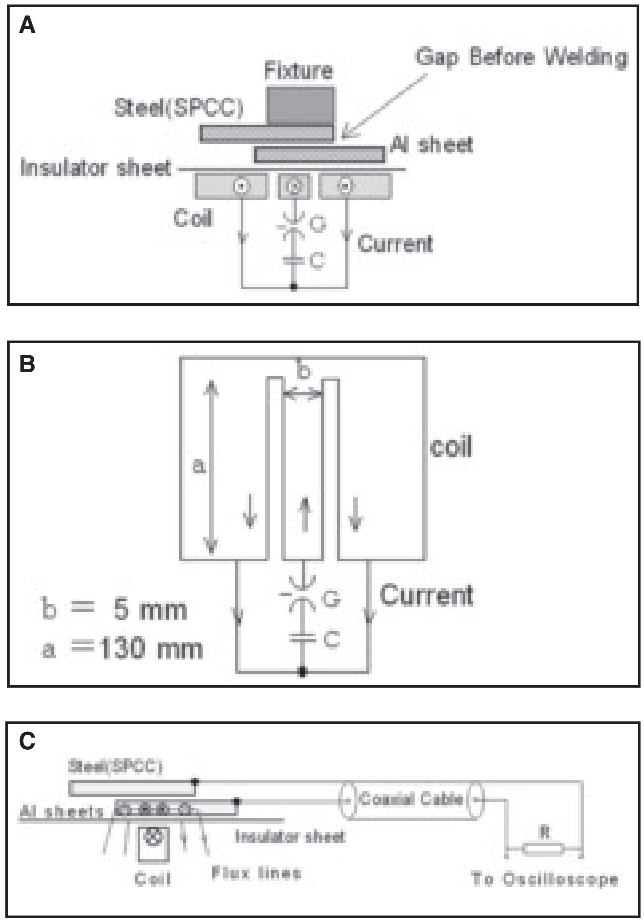

Fig. 3 — General outlines of apparatus. A — Cross-section view of the coil containing lap of Al/steel (SPCC) sheets and discharge circuit; B — plan view of coil with discharge circuit; C — collision speed measurement. C denotes the capacitor bank and G the gap switch.

Table 1 — Aluminum and Steel Properties

	Melting Point °C	Specific Heat J/kg.°C	Density kg/m³	Thermal Conductivity J/m³.°C.s	Electrical Resistivity μΩ.cm
Aluminum	660	900	2700	220	2.65
Steel	1497	460	7870	73	13.30
Al/Steel Ratio	0.44	1.96	0.34	0.33	0.20

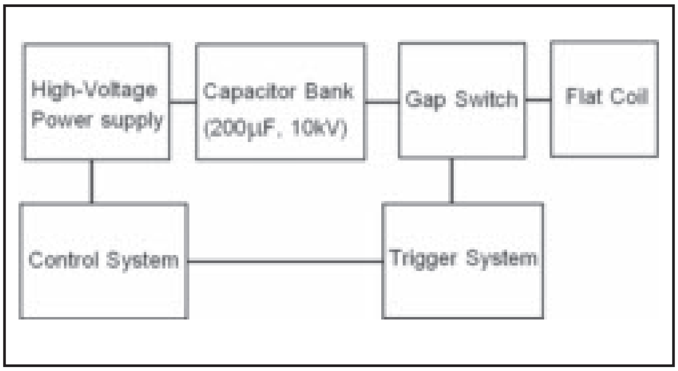

Fig. 4 — The block diagram of the discharge system.

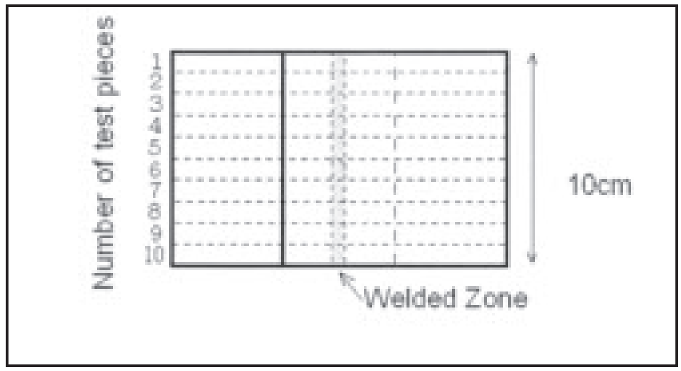

Fig. 5 — Divided region of the welded sample for shearing tensile test, optical micrograph, and SEM image observations.

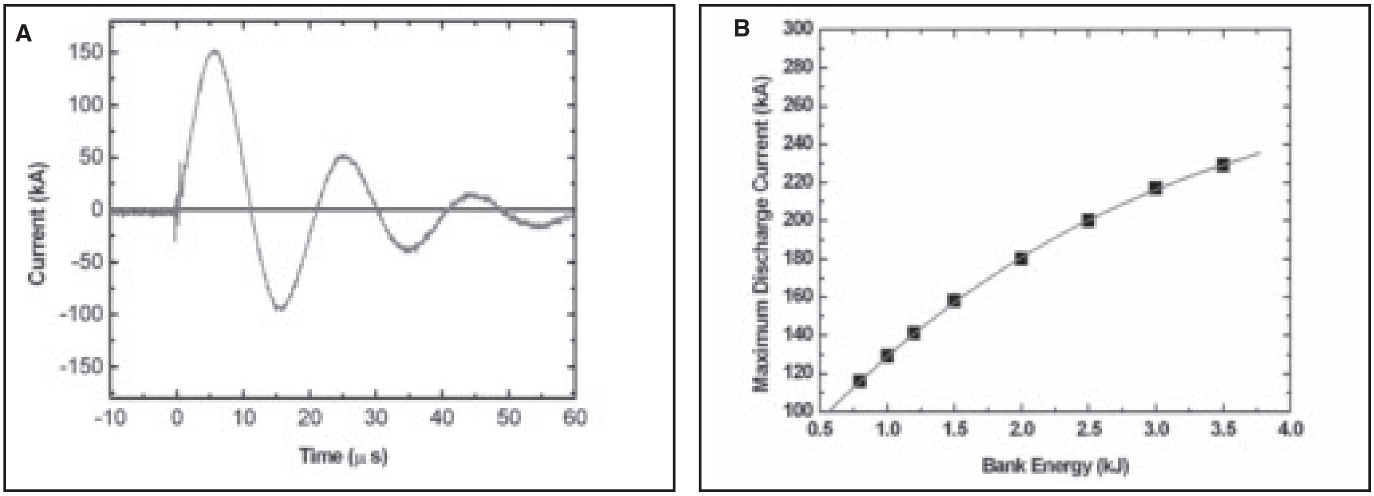

Fig. 6 — A — Typical current signal at 1.4-kJ discharge (200 μF/3.8 kV); B — bank energy vs. maximum discharge current.

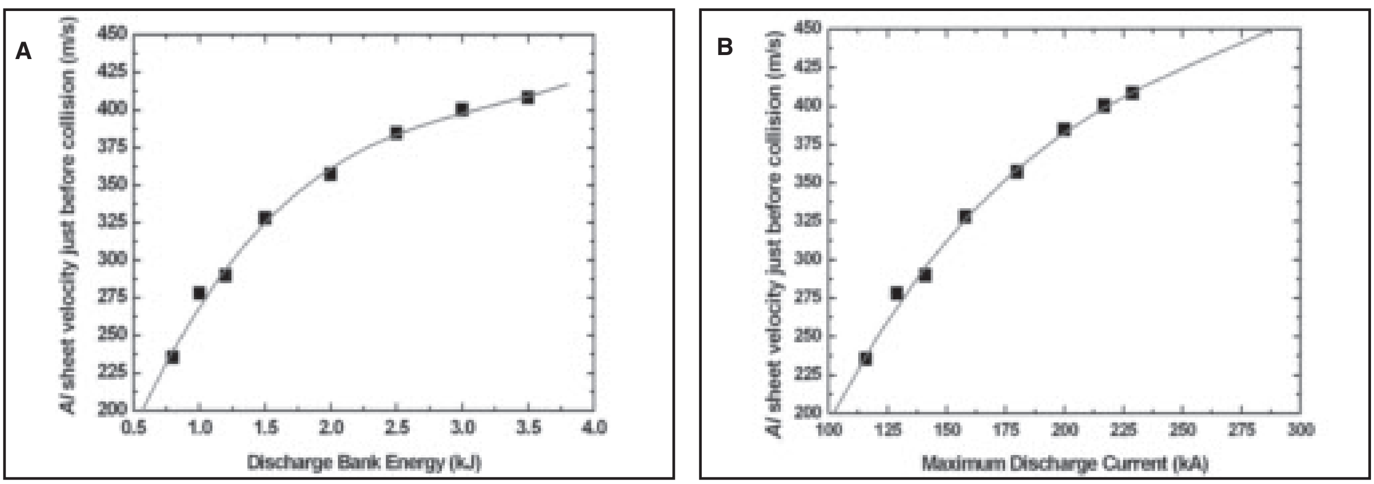

Fig. 7 — The speed of the Al sheet just before collision vs. the following: A — Discharge bank energy; B — maximum discharge current.

Experimental Apparatus

Figure 3 shows the general outlines of the magnetic pulse welding apparatus, which consists of a capacitor bank (C) and a spark gap switch (G) with a one-layer, E-shaped flat coil. It was attempted to make a low-inductance discharge circuit that can generate a high-density magnetic flux around the coil area.

The capacitor bank that drives the discharge system of the MPW device consists of two capacitors of 100 μF/10 kV in parallel. The inductance of the bank capacitor is 0.02 μH, and it is connected to the gap switch and one-turn coil by a low-inductance transmission line. The circuit is designed to keep the inductance as low as possible to carry out fast welding. The flat, E-shaped, one-turn coil was made of a Cr-Cu alloy. The coil thickness is 2 mm and the inductance of the coil is 0.04 μH. The block diagram of the discharge system is shown in Fig. 4. When the gap switch is

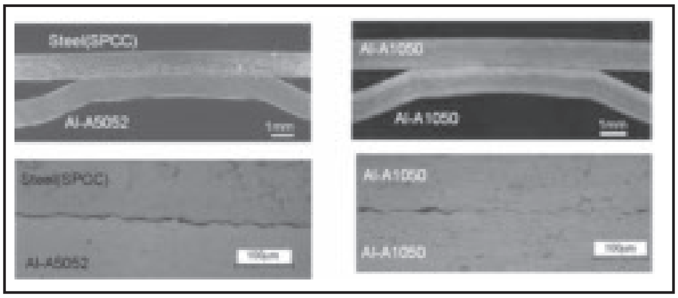

Fig. 8 — Typical microstructure of joined interface zone for A1050/A1050 and A5052/SPCC.

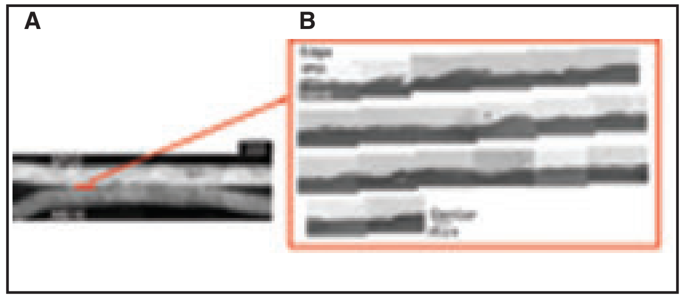

Fig. 9 — A — Cross-section image of welded sample (the red zone is the observation area by SEM); B — SEM image of joined interface for A6016/SPCC sample.

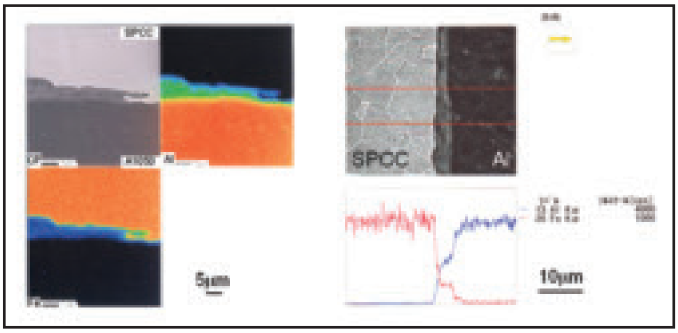

Fig. 10 — EPMA result for Fe and Al distribution across the SPCC/A1050 interface layer.

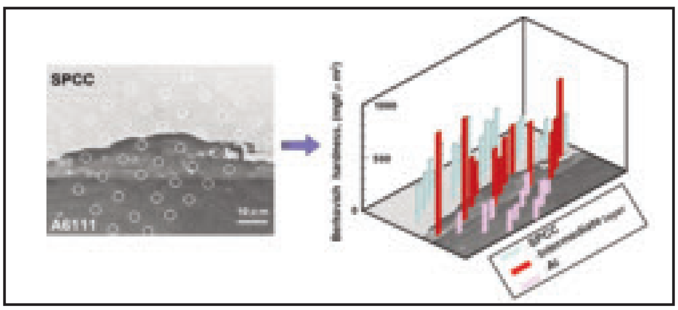

Fig. 12 — Typical microstructure of the interface layer of the A6111/SPCC sample, including Berkovich hardness indentation across the interface.

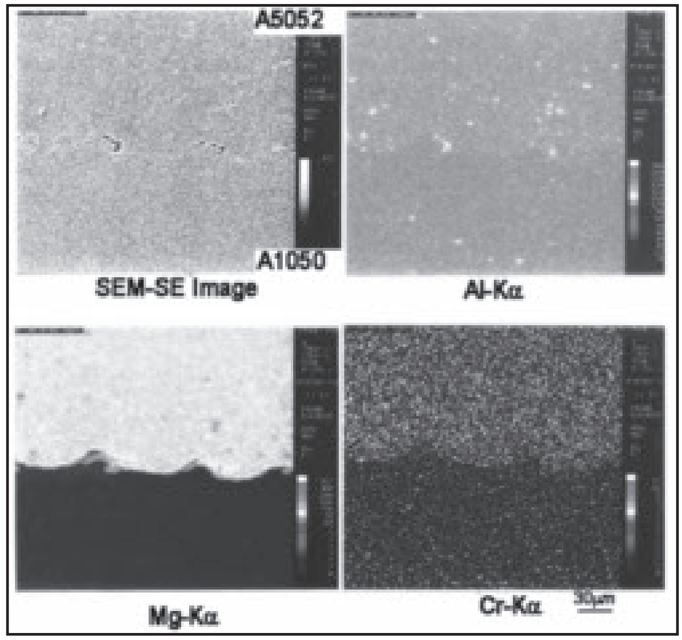

Fig. 11 — SEM-SE image and EPMA result for Al, Mg, and Cr distribution for A1050/A5052 sample.

Table 2 — The Aluminum Alloy and SPCC Steel Characteristics

Sample Specification	A1050	A2017	A3004	A5182	A5052	A6016	A7075	SPCC
Conductivity [IACS•]	61	49	41	33	35	53	45	13
Tensile Strength [MPa]	165	187	255	360	290	212	292	350

closed, an impulse discharge current from the capacitor bank (C) passes through the coil and the MPW process begins.

Aluminum alloy (A1050, A2017, A3004, A5182, A5052, A6016, and A7075) and steel (SPCC) sheets were prepared to carry out the weld process. The characteristic parameters of the aluminum alloys and SPCC steel that were used in the experiments are shown in Table 2.

The size of all samples was 100 mm long and 100 mm wide with a thickness of 1.0 mm. The contact surface between two samples was polished and cleaned with abrasives and methanol. The 0.1~0.3-mm-thick insulating sheets were loaded between the coil surface and the overlapped ends of the workpiece sheet. It was ascertained that the welding characteristics could be improved by fixing the initial root opening (0.5~1 mm) between two metal sheets. The optimization of root opening distance is described in the section titiled "collision speed measurement."

It should be noted here that the more conductive metal works as a base metal (Al sheet is the base metal for the Al/SPCC workpieces), and the main eddy current appears in the base metal. The coil is clamped with the fixture during the welding operation. After welding, the welded sample was divided into ten pieces for tensile shearing strength tests and optical micrograph and scanning electron microscope (SEM) image observations — Fig. 5.

Experimental Results and Discussion

Discharge Current and Flux Density

A typical current waveform is shown in

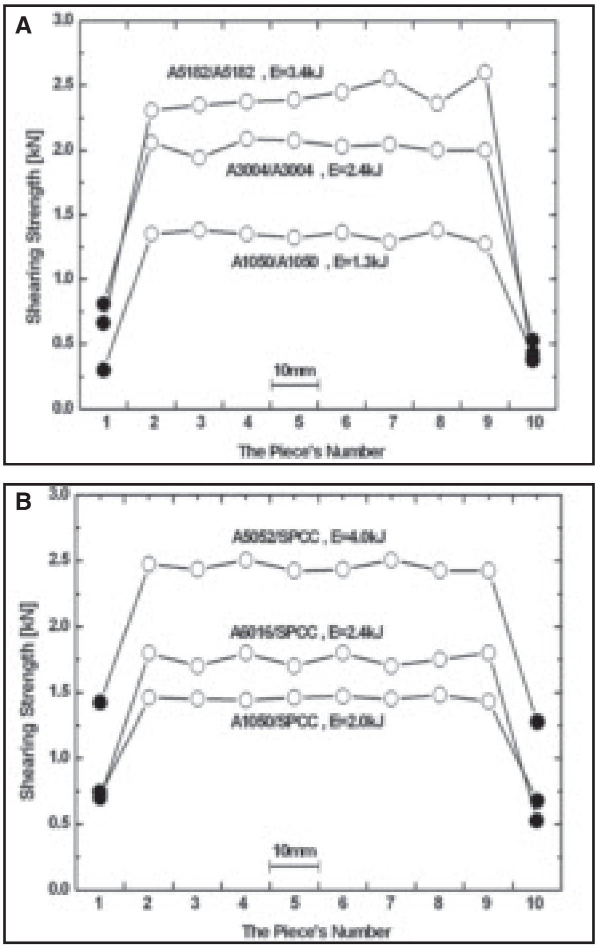

Fig. 13 — Distribution of tensile shear strength for ten divided pieces of the welded samples. A — A1050/A1050, A3004/A3004, and A5182/A5182 sheets; B — A1050/SPCC, A5052/SPCC, and A6016/SPCC sheets: ❍ The rupture of base metal, ● the rupture of the welded area.

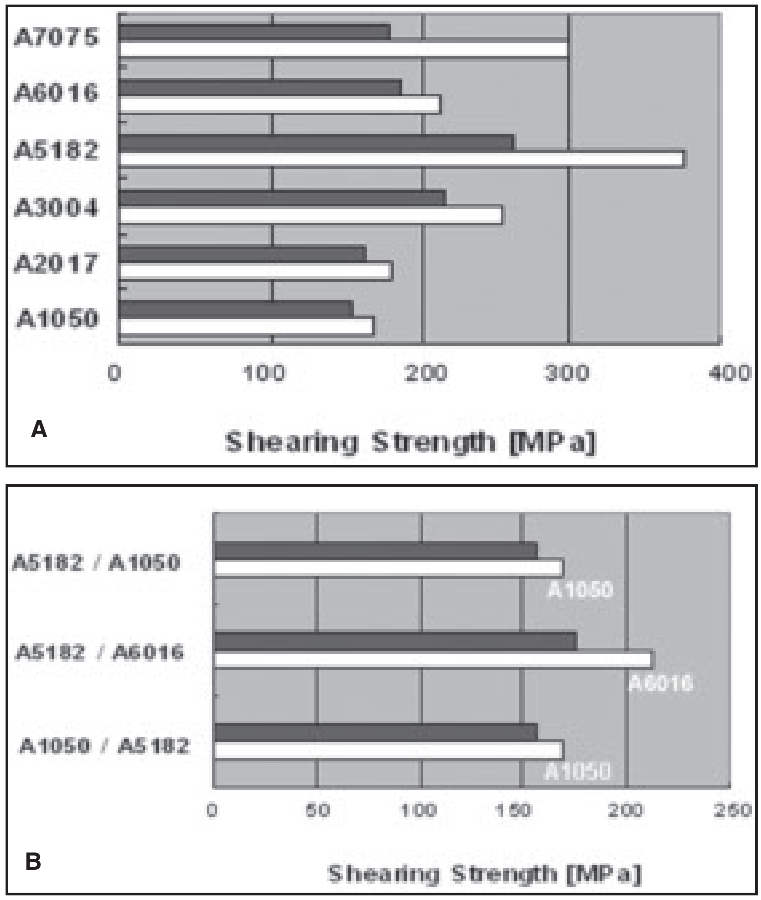

Fig. 15 — Comparison of the maximum tensile shear strength for the following: A — The same aluminum alloy combinations; B — different aluminum alloy combinations: ■ The maximum tensile shearing strength of welded sample. ❑ The maximum tensile shearing strength of the base alloy without weld.

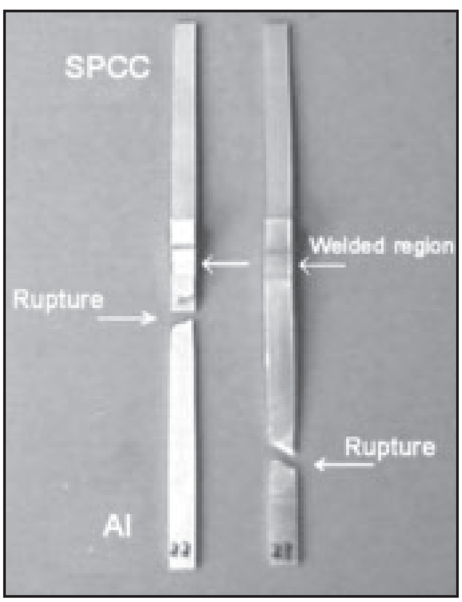

Fig. 14 — Typical rupture of Al alloy in the tensile shear strength test of SPCC/Al joints.

Fig. 6A. This current signal was obtained at 1.4-kJ discharge (200 μF/3.8 kV) by using a magnetic probe. The current signal shows that a damping and oscillating current flows through a one-turn coil for the duration of about 50 μs and the oscillating period is about 22 μs. The maximum current was measured at about 150 kA at 1.4 kJ bank energy discharge. The relation between the bank energy and discharge current in our system is shown in Fig. 6B.

If the discharge current flows uniformly on the surfaces of the middle portions of the coil, then the depth of skin effect ($\delta=\sqrt{2/\omega\kappa\mu}$) was calculated at 0.38 mm for Al sheet, and under this condition, the maximum magnetic flux density is estimated at about 20T, while the maximum magnetic pressure is calculated at about 150 MPa from Equation 2.

Collision Speed Measurement

In order to measure the collision speed of the aluminum sheet just before welding, a simple circuit was prepared to measure the time of travel of the base metal in the root opening that existed between the two workpieces before welding. The circuit consists of a coaxial cable and matching resistance — Fig. 3C (Ref. 7).

When the impulse discharge current passes through the coil, a voltage is induced on the two workpieces by magnetic coupling between the coil and these workpieces. Just after the collision, the voltage appears at input terminals of the measuring circuit and that voltage signal can be detected by a digital oscilloscope. If we assume that the sheet movement is like a uniform acceleration motion, the collision speed just before welding can be estimated by using the time of travel and root opening distance. The collision speed has a relation with the bank energy and the discharge current and the maximum collision speed can be obtained at the first maximum in the current signal. Therefore, by inserting the appropriate root opening between sample sheets, the collision time can be nearly the same as quarter period of the current signal at the first maximum current peak. The optimum root opening has a relation with the capacitor bank energy and the discharge system inductance. However, our experimental result shows that a 0.5~1 mm root opening between sheets is necessary for achieving high weld quality in the aluminum alloy and steel sheet joint. Figure 7 shows the Al sheet speed just before collision vs. the maximum current and bank energy.

Microstructure of Joined Interface

The width of the weld zone was nearly equal to the middle part of the coil (b = 5 mm). The welded sheets were divided into ten 10-mm-wide test pieces as shown in Fig. 5, and one longitudinal side of the division of No. 5 was polished for observing the joined interface. Several welded combinations of Axxxx/Axxxx and Axxxx/ SPCC steels were tested. For the similar workpieces, the joined interface was not very clear. However, in the aluminum alloy and SPCC steel combination after etching and polishing, the interface layer were clearly seen against the base metals. Typical macrostructure of the joined interface zone for A1050/A1050 and A5052/SPCC are shown in Fig. 8. As a result of magnetic pulse welding, a nonuniform wavy interface is visible for all welded samples. The wavy interface zones were formed with amplitudes as high as 20 μm and widths of 100 μm. Figure 9 also shows the macrostructure of the joined interface zone for an A6016/SPCC combination.

The SEM image of A6016/SPCC also shows that the wavy morphology weld-interface was formed in the interface layer without any significant heat-affected zone (HAZ).

Electron Probe Microanalysis (EPMA)

The result of an EPMA test for SPCC/A1050 combination is illustrated in Fig. 10. A single step decrease was observed in the EPMA profile for all combinations (Al/SPCC) across the interface. The EPMA result shows that the 5-μm-wide transition layer is formed in the welding interface.

Figure 11 shows the secondary electron images obtained by scanning electron microscopy (SEM-SE) and also EPMA of Al, Mg, and Cr in the A1050/A5052 interface layer. The EPMA result for Mg clearly shows that a wavy bond interface was formed in the welded zone.

Microhardness Profile

To obtain the nano-hardness profile of the interface layer, the Berkovich indenter was used. Figure 12 shows the interface microstructure along with traces of the Berkovich nano-hardness indentations for the A6111/SPCC sample. The hardness measurement across the interface layer clearly shows that the hardness of the intermediate layer is higher than the aluminum base metal in all points. The reason for this higher hardness at the intermediate results from intense plastic deformation due to a high-velocity collision or to a fine-grain microstructure that was formed by rapid solidification of the welded interface.

Tensile Shear Test

Welded samples were investigated on a standard tensile shear testing machine at a test rate of 10 mm/min. Tensile shear tests were made for each ten divided pieces to determine the maximum shear tensile strength. The test results for Al/SPCC and aluminum alloy combination are shown in Fig. 13, where a mark (❍) indicates the rupture of based metal and (●) a rupture of the welded area. Based on the shear strength test results, the tensile shear of divisions No. 1 and No. 10 were less than the others. However, in other divisions the failures always occurred in the weaker metal and outside of the welded area. Figure 14 shows the typical rupture of based metal for SPCC/Al joints.

The comparison of the maximum tensile shear strength for the same aluminum alloy combinations and different aluminum alloy combinations are shown in Fig. 15. The results of division No. 5 in Fig. 5 was used for this consideration.

The comparison of the maximum tensile shear for the same alloy combination (Fig. 15A) shows that except for A5182/A5182 and A7075/A7075 joints, the maximum tensile shearing for all other cases is nearly the same as the tensile shear strength of base metal without a weld and for different alloy combinations (Fig. 15B), the maximum tensile shear strength of the welded sample is also the same as a weaker base metal value. It can be pointed out that the sheet metals retain their original properties without the heat-affected zone problems during the weld process, and the welded zone is stronger than the weaker base metals so failure always occurred outside of the welded zone for these combinations. These results would be expected for a solid-state joining process.

Conclusions

We can determine the solid-state weld quality achievable for most aluminum alloys and SPCC steel combinations using the MPW method. Our experimental results show that the weld joint is always stronger than the weaker metal and in all tested combination a discontinuous or continuous pocket-type, wavy transition layer was formed without any significant heat-affected zone. The capability of our MPW method has also been successfully examined for several other types of metal joints, such as T-joints, circular joints, and long sheet samples (up to 500 mm).

Acknowledgments

The authors wish to express thanks to Professor K. Ikeuchi of Osaka University and Dr. M. Kumagai of Sumitomo Light Metal Industries Ltd. for fruitful and useful discussions. The authors also would like to thank Professor S. Kumai of Tokyo Institute of Technology for the observation of the joined interface and Mr. M. Matsuda of Chuo Seisakusho Ltd. for useful help about the EPMA test.

References

1. Brower, D. F. 1969. *Metals Handbook* 4 Forming. Metals Park, Ohio: ASM International, p. 256.
2. Shribman, V., Stern, A., Livshitz, Y., and Gafri, O. 2002. Magnetic pulse welding produces high-strength aluminum welds. *Welding Journal* 81(4): 33.
3. Masumoto, I., Tamaki, K., and Kojima, M. 1980. *Journal of the Japan Welding Society* 1(49): 29.
4. Aizawa, T., Okagawa, K., Yoshizawa, M., and Henmi, N. 2001. *Proc. of 4th Int. Symposium on Impact Engineering*, Kumamoto, Japan, p. 827.
5. Aizawa, T., and Yoshizawa, M. 2001. *Proc. of 7th Int. Symposium of Japan Welding Society*, Kobe, Japan, p. 295.
6. Aizawa, T., and Kashani, M. 2004. *Proc. of IIW International Conference on Technical Trends and Future Prospective of Welding Technology for Transportation, Land, Sea, Air and Space*, Osaka, Japan.
7. Okagawa, K., and Aizawa, T. 2004. *Proc. of International Conference on New Frontiers of Process Science and Engineering in Advanced Material*, Kyoto, Japan, p. 501.

Weldability Evaluation of Supermartensitic Stainless Pipe Steels

A look at the as-welded mechanical properties of supermartensitic pipe steel welded joints, their susceptibility to hydrogen-induced stress corrosion, and the influence of short postweld heat treatment

BY J. E. RAMIREZ

ABSTRACT. Significant interest exists in the use of supermartensitic materials for oilfield applications. However, the hardness for both the weld deposit and the heat-affected zone (HAZ) of different material combinations may exceed the NACE requirement of 23 HRC (253 HV). Therefore, further studies to quantify the mechanical properties of welded joints and variables controlling the sulfide stress cracking (SSC) resistance in the as-welded condition remain necessary both for economical fabrication and to ensure reliable service operation. In this program, the as-welded mechanical properties of three different supermartensitic pipe steels were compared using different welding consumables and welding procedures. The susceptibility to hydrogen-induced stress corrosion cracking of selected weldments under slightly sour conditions and under cathodic protection was evaluated. Additionally, the influence of short postweld heat treatment (PWHT) on the HAZ mechanical properties and on the microstructure of three supermartensitic stainless pipe steels was studied. The results show that the filler metal and welding procedure combination affect the matching characteristics of the welded joint and their toughness and ductility properties. Additionally, supermartensitic steel welded joints with a maximum hardness ranging from 282 to 313 HV_1 and under an applied stress level equal to the measured yield strength of the base material did not crack under slightly sour conditions. The result also showed that a short PWHT is effective in reducing the microhardness of the HAZ to levels very close to the hardness of the base metal in the as-received condition. It is assumed that the main mechanism responsible for the changes of hardness with PWHT is the amount of reverted and stable austenite.

Introduction

Gradual depletion of easily obtainable hydrocarbons has accelerated the production of oil and gas from deep hot wells. With the development of deep wells containing CO_2 and H_2S, many users began using corrosion-resistant alloys (CRAs). A variety of CRA materials are now commercially available in a range of tubular sizes. However, for reasons of cost, martensitic-type stainless steels are primarily used.

Supermartensitic stainless steels have been developed with higher resistance than conventional martensitic 13Cr to general and localized corrosion in CO_2 environments at elevated temperatures (Ref. 1). They are also sulfide stress cracking (SSC) resistant in environments containing a small amount of H_2S (Refs. 1, 2–6). In a typical supermartensitic stainless steel, the C content is reduced to below 0.03 mass percent in order to suppress the reduction of Cr concentration in the matrix due to Cr carbide precipitation, about 5.5 mass percent Ni content is added to obtain the martensite single phase, and 2 mass percent Mo content is added to improve SSC and localized corrosion resistance (Ref. 4). There are also supermartensitic steels that contain around 4% Ni and 1% Mo. Thus, supermartensitic steels can play an intermediate role between conventional martensitic 13Cr and duplex stainless steels regarding both the corrosion resistance and the material cost.

In general, supermartensitic stainless steels have good weldability. At carbon levels below 0.04% the hardness in the as-welded heat-affected zone (HAZ) of martensitic 13Cr base materials does not exceed 350 HV 10, which is considered to be the threshold of cold cracking. Therefore, a decrease in C content up to 0.03% is effective to improve the resistance to cold cracking or hydrogen assisted cracking of the HAZ. Additionally, at this low carbon content, the microstructure changes from ferrite + martensite to simple martensite with the addition of Ni from 0 to 3%. Therefore, the high nickel content help limit the ferrite content or to completely avoid its occurrence in the HAZ and in the base material, which is the primary reason for any inadequate toughness or limited toughness in the HAZ of martensitic 13Cr steels.

The maximum hardness limit to avoid the potential for sulfide stress cracking in standard martensitic 13Cr steels, as well as for newer supermartensitic stainless steel, in CO_2/H_2S environments is 23 HRC per the NACE MR0175. However, reliable attainment of NACE MR0175 limits can be extremely difficult, particularly in weld metals (Ref. 7). Therefore, a postweld heat treatment (PWHT) operation probably cannot be avoided.

However, the PWHT is more complicated with supermartensitic steels. The presence of nickel depresses the A_{c1} temperature, so that tempering is necessarily carried out at fairly low temperatures, 600°–620°C. Tempering reactions therefore tend to be sluggish while, even with such a low temperature, the A_{c1} may be exceeded, leading to partial reformation of austenite during heat treatment and formation of virgin martensite on cool out. Maximum softening can normally be achieved using two stage heat treatment with a first intermediate cycle typically at 650–690°C and subsequent heat treatment at 600–620°C.

Therefore, it is desirable to obtain an estimate of the A_{c1} temperature to set PWHT conditions for different supermartensitic alloys. A fine balance must be struck between achieving a temperature high enough to give tempering, and low enough to restrict austenite formation, which will revert to virgin martensite on cooling. Some researchers (Ref. 8) pointed out that discernible hardening after a heat treatment occurs only when the A_{c1} is exceeded by a temperature interval sufficient to induce approximately 20% austenite. Unfortunately, a reliable

KEYWORDS

Supermartensitic Pipe Steels
Heat-Affected Zone (HAZ)
Sulfide Stress Cracking (SSC)
Postweld Heat Treatment (PWHT)
Welded Joints

J. E. RAMIREZ (jose_ramirez@ewi.org) *is with the Edison Welding Institute, Columbus, Ohio.*

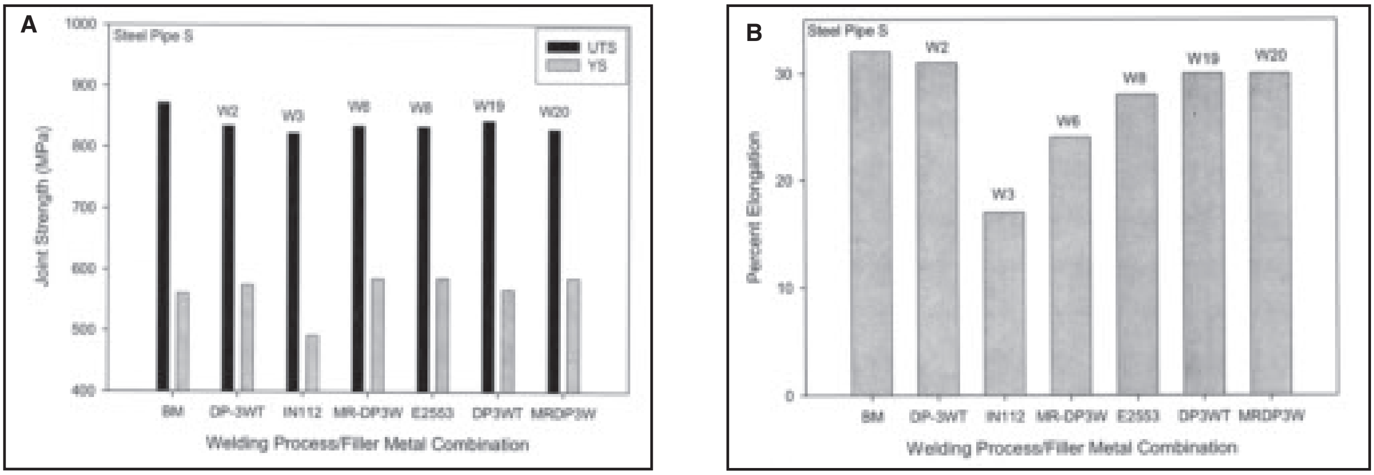

Fig. 1 — Tensile properties of supermartensitic steel pipe S welded joints. A — UTS and yield strength, and B — percent elongation.

Table 1 — Supermartensitic Pipe Steels, Welding Process, and Filler Metals

	S	K	N
Pipe inside diameter	228.6 mm (nominal)	5.2 in. (measured)	9.75 in. (measured)
Pipe wall thickness	12.3 mm (nominal)	0.3 in. (measured)	0.50 in. (measured)
	Pipe chemistry, wt-%		
	Reported	Analyzed	Analyzed
Carbon	0.007	0.031	0.013
Manganese	0.45	0.39	0.45
Phosphorus	0.018	0.012	0.017
Sulfur	0.0007	0.002	0.002
Silicon	0.31	0.16	0.16
Chromium	12.1	12.89	11.19
Nickel	6.2	3.96	6.24
Molybdenum	2.53	1.01	2.58
Titanium	0.07	Not measured	0.015
Copper	Not reported	Not measured	0.57
Nitrogen	0.004	Not measured	Not measured
Welding Process		Filler Metals	
SMAW	E2553, ENiCrMo-3 (IN112)	E2209, ENiCrMo-3 (IN112)	E2209, ENiCrMo-3 (IN112)
GMAW	MR-DP3W	—	—
GTAW	DP-3WT	—	—

relationship between composition and A_{c1} does not seem to have been produced for these alloys. Thus, further study of the transformation behavior of commercial supermartensitic steels in terms of both the A_{c1} and Ms/Mf temperatures, and of the tendency for supermartensitic steels to undergo reaustenization during tempering heat-treatment cycles is necessary.

On the other hand, in most situations, the sour environment will be present only on one side of the steel. In consequence, there will be a gradient of hydrogen concentration through the thickness, from high at the face in contact with the sour environment to very much lower at the free surface. The risk of cracking will therefore diminish through the thickness, so that higher hardnesses may be safely permitted on the outside of the pipe or pressure vessel. The relaxation possible has not been fully defined, but, for wall thicknesses above some 10 mm, an external hardness of say 300 HV should be acceptable (Ref. 7).

Therefore, widespread application of supermartensitic steels depends upon solving the challenge of girth welding them in an economical way. At the same time, it should be recognized that blanket impositions of hardness or other limits can restrict welding procedures and increase fabrication costs. Further studies to quantify the mechanical properties of welded joints in the as-welded condition and variables controlling the SSC resistance remain necessary both for economical fabrication and to ensure reliable service operation. Short PWHT cycles are desirable for productivity reasons. However, recognizing the diffusional reactions involved in tempering, the effect of short PWHT on partial reaustenitization, degree of softening, and the influence on toughness need to be evaluated for different supermartensitic steels.

In this study, the as-welded mechanical properties of three different supermartensitic pipe steels with a specified minimum yield strength of 80 ksi were compared using different welding consumables and welding procedures. The susceptibility to hydrogen-induced stress corrosion cracking of selected weldments under slightly sour conditions and under cathodic protection was evaluated. Additionally, the influence of short PWHT on mechanical properties and microstructure of Gleeble simulated HAZ of the three supermartensitic stainless pipe steels was also studied.

Experimental Procedures

Materials and Consumables: The general dimensions and chemical compositions of the three supermartensitic pipe steels, and the welding process/filler metal combinations that were used in this study are listed in Table 1. The three different pipe steels were identified as S, N, and K, respectively. In general, the supermartensitic steels S and N are of the type 13Cr-5Ni-2Mo and the steel K is of type 13Cr-4Ni-1Mo. Additionally, these three steels present some differences in the carbon content as indicated in Table 1. The filler metals DP-3WT and MR-DP3W (metal cored), and the covered electrode E2553 are designated as superduplex. The covered electrodes E2209 and ENiCrMo-3 (IN112) are duplex and nickel-based electrodes, respectively.

Welding: Welded sections of the three supermartensitic steel pipes were produced with the welding process and consumables combinations described in Table 2. Each section had a gas tungsten arc welding (GTAW) root pass made with DP-3WT wire. The rest of each joint was com-

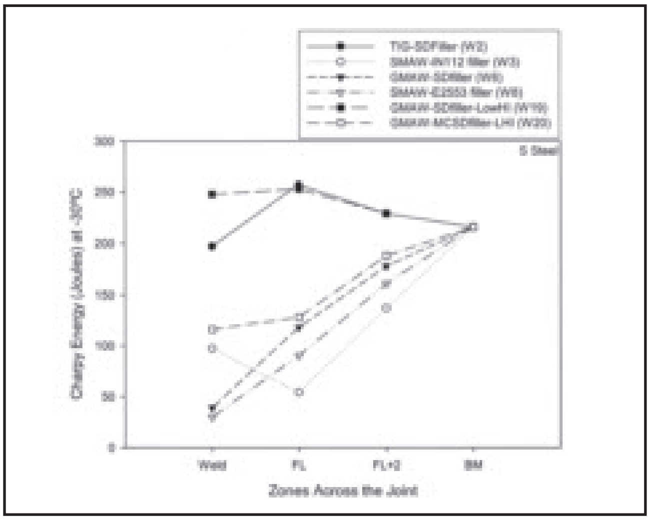

Fig. 2 — Charpy impact energy across welded joints of supermartensitic steel S as a function of welding process – filler metal combination.

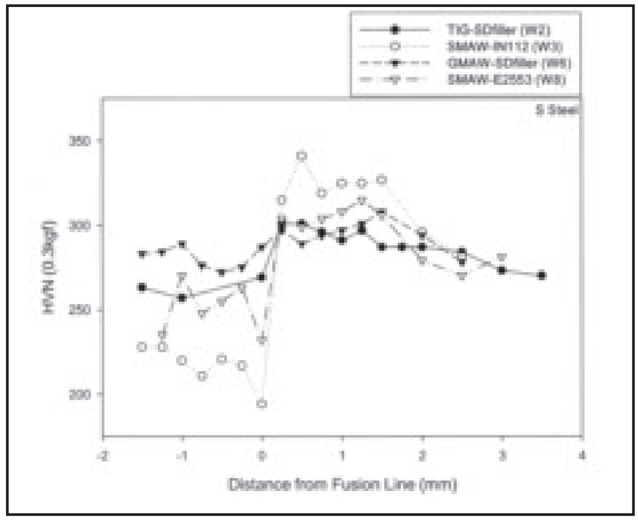

Fig. 3 — Microhardness profile near the cap of welded joints made with supermartensitic steel S.

pleted using GTAW, shielded metal arc welding (SMAW), or manual or mechanized gas metal arc welding (GMAW) process. No preheat was used and 150°C (300°F) maximum interpass temperature was maintained.

Mechanical Testing: The mechanical properties of the welded joints were characterized by using tensile and bend tests at room temperature. Charpy V-notch impact energy was determined at –30°C for the weld metal, fusion line, fusion line + 2 mm, and base metal locations. The weld metal, fusion line, and fusion line + 2 mm Charpy samples were taken near the 3, 6, and 12 o'clock positions of the weld. The weld metal, fusion line, and fusion line + 2 mm indicate the position of the middle of the sample relative to the welded joint.

Microstructural Characterization: Microhardness profiles were determined across some of the welded joints near the cap region. Additionally, the HAZ hardness of the joints W19 and W20 were determined at different through thickness locations. The microstructure of the fusion zone and HAZ of different welded joints were characterized using light microscopy after proper sample preparation.

Corrosion Testing: Selected supermartensitic welded joints and base metals were tested to evaluate their susceptibility to hydrogen-induced corrosion cracking under cathodic protection (CP) and under slightly sour (H_2S) service conditions. Table 3 shows a summary of the specimen identification, base material, loading method, specimen side in tension, and the type of corrosion tests that were carried out. The test conditions under CP and slightly sour environment are reported in Table 4. After testing specimens were cut, mounted, and polished. Visual inspection with a magnification of up to 1000× was performed on all tested specimens to observe any cracks.

Influence of Short PWHT on Gleeble Simulated HAZ: The transformation temperatures, A_{C1} and martensite start formation, for each one of the steels were determined by dilatometric analysis. Heat-affected zone weld simulations were performed with a peak temperature of roughly 1350°C and a cooling rate between 800° and 500°C of 40°C/s simulating normal GMAW heat inputs. A PWHT was performed in a Gleeble machine, at temperatures equal to A_{c1}, A_{c1} + 40°C, and A_{c1} – 40°C, for 5 and 10 min. The resulting HAZ mechanical properties (hardness and impact Charpy V-notch energy) and microstructure of three supermartensitic stainless pipe steels were evaluated.

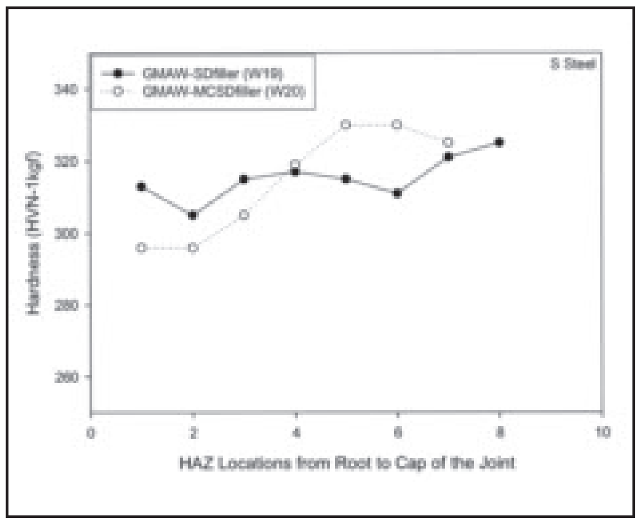

Fig. 4 — Microhardness of HAZs at different through-thickness locations of welded joints made with supermartensitic steel S.

Results and Discussions

Tensile Properties: The observed tensile properties of the supermartensitic welded joints are listed in Table 5 and some of the results are shown in Fig. 1. The welded joint made with ENiCrMo-3 (IN112) or duplex filler metal failed in the weld metal. Welded joints made with superduplex filler metal failed in the base metal. The yield strength of all the joints welded with either duplex or superduplex filler metal was higher than 550 MPa (80 ksi). The percent elongation measured in the tensile test samples of the supermartensitic steel welded joints ranged from about 6 to 33.

Normally, oil and gas companies require a yield strength overmatching in the weld metal of circumferential joints in comparison with the pipe material. Therefore, Ni-base electrodes (ENiCrMo-3) are not recommended to join X80 grade supermartensitic steel pipes due to the resulting undermatching condition of the weld metal. The duplex and superduplex consumables provided an increasing degree of overmatching in the weld metal of X80 supermartensitic steel pipe joints.

The range of 6 to 33% elongation observed in the supermartensitic steel joints is influenced by the welding consumable, matching characteristics of the joints, and

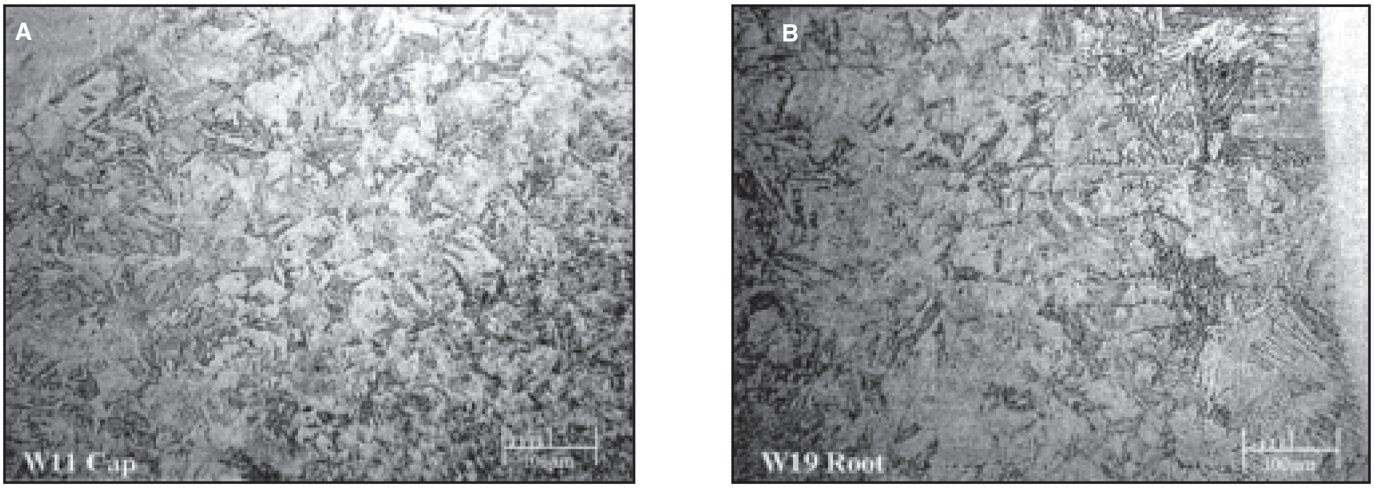

Fig. 5 — Microstructures observed in the intermixing zone of the weld metals and in the HAZs of the supermartensitic steels. A — Cap; B — root.

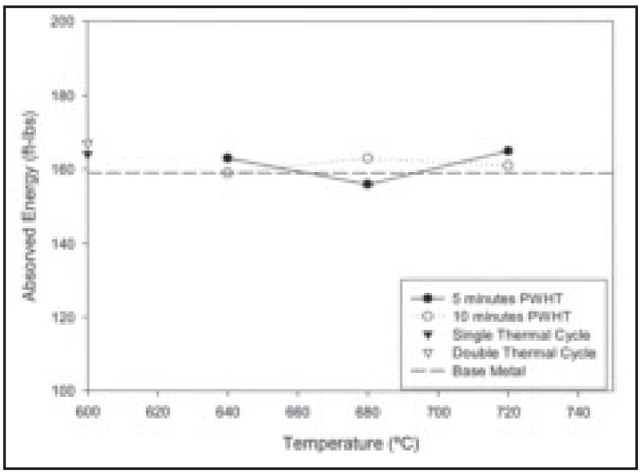

Fig. 6 — Charpy V-notch absorbed energy at –30°C in simulated HAZ from supermartensitic pipe steel S as a function of thermal experience.

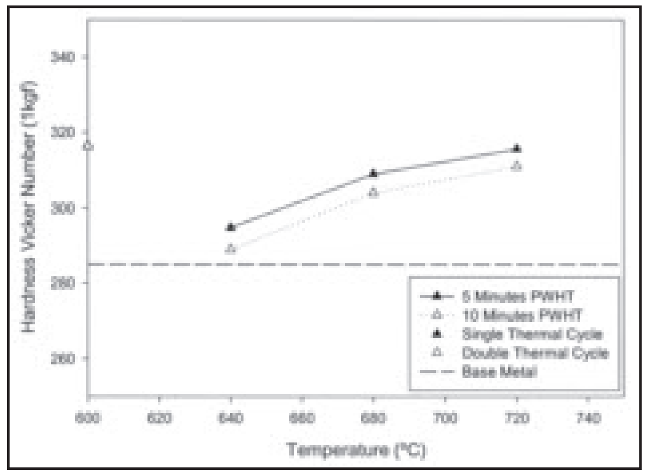

Fig. 7 — Hardness of simulated HAZ from pipe steel S as a function of thermal experience.

welding procedure used. Joints made with duplex and superduplex consumables using SMAW, GMAW, and GTAW processes show an elongation between 20 to 33%. The lower levels of ductility (14–15% elongation) measured in the joints made with the nickel-base electrode (ENiCrMo-3) may be explained by the concentration of plastic deformation in the weld during the tensile test as a result of the undermatching characteristics of the weld metal. Most of the plastic deformation is localized in the weld metal instead than in the complete gauge length. However, the lowest level of ductility (6% elongation) in the welded joints was observed in a K steel joint made with the nickel-base electrode without heat input control using a weave technique. The further decrease in ductility may have resulted from the formation of niobium nitride due to migration of nitrogen from the base metal into the niobium-rich weld metal. K steel has the highest reported level of nitrogen out of the three supermartensitic steels used in this study as shown in Table 1.

Impact Absorbed Energy: It was observed, in general, that the absorbed energy in the welded joints at –30°C decreased from the base metal to the fusion line and to the weld metal. The average impact energy of the supermartensitic steel pipes was about 200 joules. The decrease in impact energy in the fusion line and HAZ of the supermartensitic welded joints as compared to the base metals is considered to be a result of the microstructural variation present near the fusion lines in these dissimilar metal joints. The microstructural variation is a result of the inevitable compositional gradient across the fusion boundary of these welding joints with nonmatching consumables. Additionally, the untempered condition of the martensite and the present of strings of ferrite in the HAZ, as discussed in the following section, may have also affected the absorbed impact energy.

The impact energy of the weld metal depends on the welding procedures and filler metals used for welding the pipe joints. Increasing average weld metal impact energies in the range between 30 to 248 joules are achieved with the SMAW, GMAW, GMAW with heat input control, and GTAW process, respectively. Decreasing impact energies are obtained in nickel-base, duplex, and superduplex weld metals deposited without heat input control. The minimum impact energy of the welded joints ranged from 25 to 181 joules. The Charpy V-notch impact testing

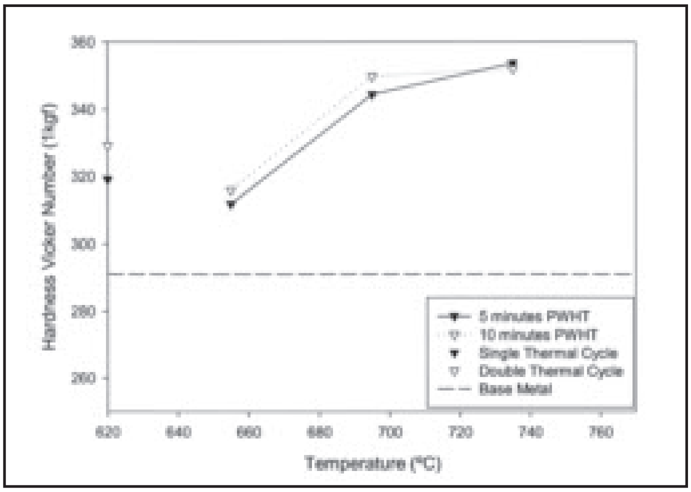

Fig. 8 — Hardness of simulated HAZ from pipe steel N as a function of thermal experience.

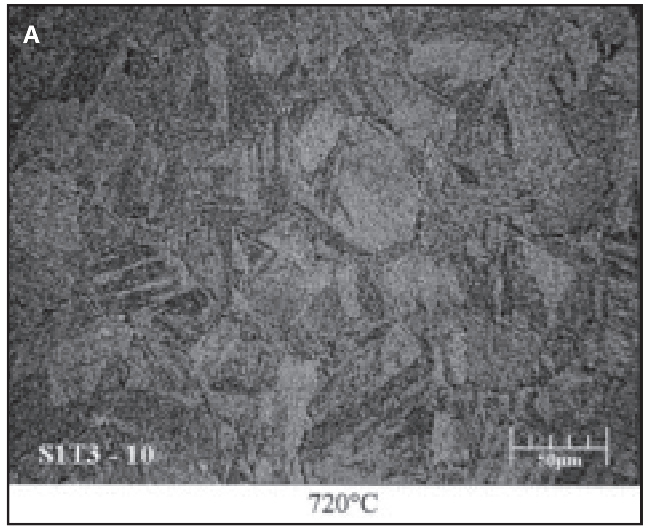

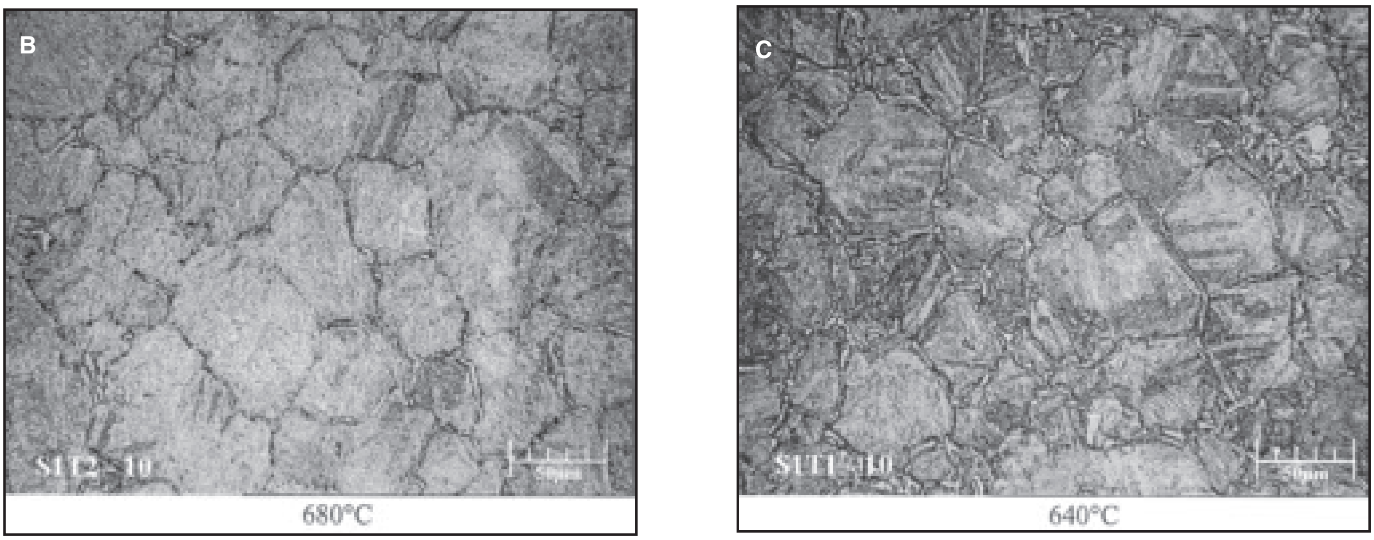

Fig. 9 — Fraction of retained austenite at room temperature in a simulated HAZ from pipe steel S after PWHT for 10 min at different temperatures. A — 720°C; B — 680°C; C — 640°C.

results of supermartensitic pipe steel S is shown in Fig. 2.

The increasing weld metal impact energies achieved with the SMAW, GMAW using a weave technique, GMAW with heat input control, and GTAW process can be explained based on two main factors. First, a higher level of inclusions in the weld metal is expected in joints made with a flux-shielded process such as SMAW as compared to joints made with gas-shielded processes such as GMAW and GTAW. The higher the level of inclusions in the weld metal, the lower the expected impact absorbed energy. Second, duplex and superduplex weld metals are very susceptible to the formation of intermetallic compounds that affect the impact absorbed-energy of the weld metal. A high heat input or weave technique decreases the cooling rate and, therefore, increases the susceptibility to the formation of intermetallic compounds. This results in decreasing impact energies in welds made with nickel-base (ENiCrMo-3), duplex, and superduplex consumables and deposited without heat input control. Therefore, the weld metals with the best impact absorbed energies are obtained with gas-shielded processes such as GMAW and GTAW, and with control of heat input to avoid the formation of intermetallic compounds in the duplex and superduplex microstructures.

However, most of the welding process-filler metal combinations used to weld the different supermartensitic steel pipes are expected to provide average impact energies in the welded joints above the minimum absorbed energy of 27 to 40 joules at –30°C required for different industrial applications.

Microstructural Characterization: The maximum hardness of the HAZ corresponding to different base metal/filler metal/welding process combinations is listed in Table 6. The maximum hardness of the HAZs near to the cap region range from 301 to 341, 346 to 362, and 378 to 391 HV_1 in the supermartensitic steels S, N, and K, respectively. The hardness of the three supermartensitic steels ranges from 281 to 301 HV_1 and is included in Table 6 as a reference. Figure 3 shows the microhardness profiles across different welded joints corresponding to different filler metal/welding process combinations used to weld supermartensitic pipe steel S. Figure 4 shows the hardness of the HAZs in different through-thickness locations of

Table 2 — Characteristics of Different Welded Pipe Sections

Weld ID	Base Metal	Welding Process	Filler Metal [a]	Shielding Gas
W1	S	Manual GTAW	1.2-mm DP-3WT	Argon
W2		Manual GTAW	1.2-mm DP-3WT	Argon
W3		SMAW	3/32-in. ENiCrMo-3	None
W4		SMAW	3/32-in. ENiCrMo-3	None
W5		SMAW	3/32-in. ENiCrMo-3	None
W6		GMAW	1.2-mm MR-DP3W	Argon
W7		GMAW	1.2-mm MR-DP3W	Argon
W8		SMAW	3/32-in. E2553	None
W9		SMAW	3/32-in. E2553	None
W19		Mech. GMAW	1.2-mm DP-3WT	80%Ar-20%N_2
W20		Mech. GMAW	1.2-mm MR-DP3W	Argon
W10	N	SMAW	3/32-in. ENiCrMo-3	None
W11		SMAW	3/32-in. E2209	None
W12		SMAW	None (only root pass)	None
W13	K	SMAW	3/32-in. ENiCrMo-3	None
W14		SMAW	3/32-in. ENiCrMo-3	None
W15		SMAW	3/32-in. ENiCrMo-3	None
W16		SMAW	3/32-in. E2209	None
W17		SMAW	3/32-in. E2209	None

(a) One to three root passes were deposited in each weld with GTAW using 1.2-mm DP-3WT wire.

two welded joints. The hardness of the HAZ shows an increasing trend from the root to the cap region of the joint.

The microstructure of the weld metals ranges from fully austenitic in welds made with the Ni-base (ENiCrMo-3) electrode to a ferritic-austenitic duplex microstructure with different levels of ferrite and austenite in welds made with the duplex and superduplex filler metals. The microstructure observed in the HAZ of the supermartensitic steel pipes corresponds to untempered martensite as shown in Fig. 5. Figure 5B shows some strings of retained ferrite observed in the coarse-grained HAZ of the supermartensitic steel S. In the intermixing zone of the weld metal near to the fusion line, a variety of microstructures were present.

The increasing maximum hardness

Table 3 — Summary of Cathodic Protection and Slightly Sour Condition Testing

Sample	Material	Maximum Hardness, HV_1	Loading Method	Side in Tension	Test
W2	S	301	4-point Bend	Cap	CP
W19	S	320	4-point Bend	Cap	CP
W20	S	320	4-point Bend	Cap	CP
W8	S	315	4-point Bend	Cap	CP
W11	N	346	4-point Bend	Cap	CP
W17	K	378	4-point Bend	Cap	CP
W2	S	301	4-point Bend	Root	H_2S
W19	S	313	4-point Bend	Root	H_2S
W20	S	296	4-point Bend	Root	H_2S
W2	S	301	3-point Bend	Root	H_2S
W19	S	313	3-point Bend	Root	H_2S
W20	S	296	3-point Bend	Root	H_2S
Base Metal	S	282	3-point Bend	Base metal	H_2S

Table 4 — Test Conditions under CP and Slightly Sour Environments

Parameter	Test		
	Cathodic Protection	Slightly Sour Environment	
		Procedure A	Procedure B
Solution	NACE-seawater	NACE-seawater	5%NaCl + Water + Buffer solution[a]
pH	8.2	3.5–4.0	3.0–3.5
CO_2 Pressure	None	3 MPa (435 lb/in.^{2})	3 MPa (435 lb/in.^{2})
H_2S Pressure	None	0.001 MPa (0.15 lb/in.^{2})	0.001 MPa (0.15 lb/in.^{2})
Polarization (SCE)	–800 mV	Free corrosion potential	Free corrosion potential
Applied Stress	100% yield strength of base metal	100% yield strength of base metal	100% yield strength of base metal
Loading Mode	Four-point bending	Four-point bending	Three-point bending
Specimen Geometry (in.)	Flat-bar specimens 5.5 × 0.675 × 0.275	Flat-bar specimens 5.5 × 0.675 × 0.275	Flat-bar specimens 1.7 × 0.675 × 0.125
Temperature, °C	25 ± 2	25 ± 2	25 ± 2
Exposure Time	30 days	30 days	30 days

(a) Solution containing CH_3COONa-CH_3COOH to control pH.

ranges of 301 to 341, 346 to 362, and 378 to 391 HV_1 observed in the HAZs near to the cap in the supermartensitic steel S, N, and K welded joints are in agreement with the expected trend in untempered martensite microstructures with increasing levels of carbon. The carbon content in the steel controls the hardness level in the untempered martensitic microstructure. As reported in Table 1, the carbon content in S, N, and K steels is 0.007, 0.013, and 0.031, respectively. The tempering effect of subsequent passes induces some softening of the HAZ in the root and results in the increasing hardness levels observed in the through-thickness microhardness profile from the root to the cap zone in the welded joints.

The hardness for the welding deposits and the HAZ of all the material-welding process-welding consumables combinations tested in this program exceeds the NACE requirements of 23 HRC (253 HV). Additionally, the hardness of the as-received supermartensitic steel pipes ranges from 282 to 301 HV_1, therefore, is also above the maximum hardness limitations established by NACE.

However, there are several issues that need to be addressed regarding the maximum hardness of 23 HRC allowed by NACE for use of supermartensitic steels in sour service. First, it has been indicated that the ASTM E140 and BS 860: Rockwell-Vickers correlations are not applicable to 13Cr-4Ni steels (Ref. 8), and if the Hays-Patrick relationship is accepted, the NACE limit of 23 HRC can be taken as equivalent to 275 H_V instead of 253 (Ref. 8). Second, in most situations the sour environment will be present only on one side of the steel. Consequently, there will be a gradient of hydrogen concentration through the thickness, from high at the face in contact with the sour environment to very much lower at the free surface. The risk of cracking will therefore diminish through the thickness, so that higher hardness may be safely permitted on the outside of the pipe. The amount of hardness relaxation in supermartensitic steels has not been fully defined. For example, in C-Mn steels with a wall thickness above 10 mm, an external hardness maximum has been relaxed from 248 to 300 HV (Ref. 7). Additionally, the softening of the HAZ in the root region of the welded joint induced by the tempering effect of subsequent passes will reduce the susceptibility to SSC in supermartensitic steel welded joints. Third, there is a need to document maximum hardness levels in supermartensitic steel for sour service, as the existing criteria are lower than the hardness of the pipe materials as delivered.

Hydrogen-Induced Corrosion Cracking under CP or Slightly Sour Conditions: Table 7 lists a summary of the results of the testing under CP and under slightly sour conditions. Even though the applied stresses used in this experimental work were equal to the measured yield strength of the base metals, and the maximum hardness of different specimens tested under cathodic protection (–800 mV SCE) or under slightly sour conditions (0.001 MPa, 0.15 lb/in.^{2} P_{H2S}) ranges from 301 to 378, and from 282 to 313 HV_1, respectively, cracking was not observed.

These results indicate that under the testing conditions used, the tested supermartensitic steels are not susceptible to cracking under either proper CP or under slightly sour conditions at hardness level above the 23 HRC (253 HV) limit established by NACE.

The observed resistance to SSC in slightly sour conditions of the tested supermartensitic steels in spite of the high level of hardness may be explained based on the good corrosion resistance of these materials that results in low corrosion rates. The SSC behavior of typical martensitic stainless steel has been explained based on the decrease of the hydrogen diffusion coefficient with an increase in content of alloying elements. Since hydrogen content in steel is proportional to the inverse of the hydrogen diffusion coeffi-

Table 5 — Tensile Test Results

Sample ID Area	Tensile Strength MPa (ksi)	Yield Strength MPa (ksi)	Elongation (%)	Reduction in Area (%)	Fracture
Steel Pipe S					
BM-T1	872 (126.5)	565 (82.0)	31.7	72.1	—
BM-T2	871 (126.3)	557 (80.8)	31.6	72.2	—
W2-T1	834 (121.0)	565 (81.9)	31.1	71.6	Base
W2-T2	836 (121.3)	586 (85.0)	30.5	71.0	Base
W3-T1	834 (120.9)	488 (70.8)	14.9	28.5	Weld
W3-T2	812 (117.7)	496 (71.9)	18.4	32.6	Weld/HAZ
W6-T1	842 (122.1)	579 (84.0)	25.8	71.4	Base
W6-T2	829 (120.2)	592 (85.9)	21.2	74.3	Base
W8-T1	841 (121.9)	586 (85.0)	27.8	66.7	Base
W8-T2	827 (120.0)	587 (85.2)	28.6	72.6	Base
W19-T1	838 (121.5)	564 (81.8)	29.4	70.3	Base
W19-T2	848 (123.0)	570 (82.7)	31.5	70.2	Base
W20-T1	834 (121.0)	574 (83.2)	32.3	67.1	Base
W20-T2	823 (119.4)	598 (86.7)	27.5	72.4	Base
Steel Pipe N					
BM-T1	866 (125.6)	652 (94.5)	19.9	59.6	—
BM-T2	866 (125.6)	675 (97.9)	23.4	63.2	—
W10-T1	834 (121.0)	491 (71.2)	13.8	34.0	Weld
W10-T2	821 (119.0)	523 (75.8)	14.5	56.7	Weld
W11-T1	839 (121.7)	604 (87.6)	20.0	43.8	Weld
W11-T2	838 (121.5)	579 (84.0)	20.2	42.6	Weld
Steel Pipe K					
BM-T1	849 (123.2)	698 (101.2)	23.9	70.7	—
BM-T2	847 (122.9)	703 (101.9)	23.7	69.5	—
W14-T1	754 (109.4)	537 (77.9)	5.7	23.0	Weld
W14-T2	777 (112.7)	561 (81.4)	6.4	21.3	Weld
W16-T1	824 (119.5)	623 (90.3)	18.8	72.5	Weld
W16-T2	845 (122.6)	627 (91.0)	21.3	71.9	Weld

Table 6 — Maximum HAZ Hardness Near the Cap Region of the Welded Joints

Base Metal	Welding Process-Filler Metal	Maximum HAZ Hardness, HV_1
S	Base Metal	282
	GTAW-SD filler	301
	SMAW-ENiCrMo-3	341
	SMAW-E2553	315
	GMAW-SD filler	308
N	Base Metal	301
	SMAW-ENiCrMo-3	362
	SMAW-E2209	346
K	Base Metal	282
	SMAW-ENiCrMo-3	391
	SMAW-E2209	378

Table 7 — Summary of Test Results (Cracking) for Corrosion Testing under CP and Sour Conditions

Specimen	Steel	Test	Hardness, HV_1	Results
W2	S	CP-Cap tension	301	No cracking
W19	S	CP-Cap tension	320	No cracking
W20	S	CP-Cap tension	320	No cracking
W8	S	CP-Cap tension	315	No cracking
W11	N	CP-Cap tension	346	No cracking
W17	K	CP-Cap tension	378	No cracking
W2	S	H_2S-Root Tension-Procedure A	282–301	No cracking
W19	S	H_2S-Root Tension-Procedure A	313	No cracking
W20	S	H_2S-Root Tension-Procedure A	296	No cracking
W2	S	H_2S-Root Tension-Procedure B	282–301	No cracking
W19	S	H_2S-Root Tension-Procedure B	313	No cracking
W20	S	H_2S-Root Tension-Procedure B	296	No cracking
Base metal	S	H_2S-BM Tension-Procedure B	282	No cracking

Table 8 — Transformation Temperatures of Supermartensitic Pipe Steels S, N, and K

Pipe Steel	A_{c1} (°C)	A_{c1}(a)	A_{c3} (°C)	Ms (°C)
S	680	630	780	201
N	695	602	765	224
K	745	680	820	277

(a) Determined based on chemical composition.
A_{c1} (°C) = 850 – 1500 (C + N) – 50Ni – 25Mn + 25Si + 25Mo + 20 (Cr–10) (Ref. 9)

cient, the hydrogen content in high-chromium steel may become quite large. As result, the high-Cr steel may have a high susceptibility to hydrogen embrittlement due to the smaller hydrogen diffusion coefficient. Therefore, the best way to control the susceptibility to hydrogen embrittlement of high-Cr steels is by decreasing the hydrogen permeation rates. The low corrosion rate of supermartensitic steel decreases the amount of hydrogen generated on the surface, which may result in lower hydrogen permeation rates in the steel a better SCC resistance.

Materials may also be susceptible to hydrogen embrittlement caused by cathodic protection dependent on the environmental conditions. The lower limit of the cathodic protection is in principle limited by the hydrogen equilibrium potential. The hydrogen evolution potential is a function of the pH and is equal to (–0.24–0.059 pH) V_{SCE}. For a pH of 8.2, the hydrogen evolution potential is equal to –0.72 V_{SCE}. Therefore, the potential of –0.8 V_{SCE} impressed on the sample during the CP testing was more negative than the hydrogen evolution potential and demonstrates the hydrogen-induced cracking resistance observed in the tested supermartensitic steels.

Therefore, supermartensitic 13Cr steel can be perfectly protected against corrosion without any risk of hydrogen embrittlement when the cathodic protection is properly controlled between the protection potential and the hydrogen evolution potential. In practice, the production of hydrogen is expected to be very limited at a potential slightly lower than the hydrogen equilibrium potential and, in the absence of H_2S, potentials 100 mV lower than the hydrogen equilibrium potential may be acceptable in practice.

Influence of Short PWHT on Gleeble Simulated HAZ: The transformation temperatures of pipe steels S, N, and K, as determined by dilatometer analysis, are shown in Table 8. Additionally, the temperature at which the austenite starts to form during heating, A_{c1}, was determined based on chemical composition, and it is also included in Table 8 as a comparison. The A_{c1} temperature, based on chemical composition, was determined using an equation that was developed empirically from data for 13Cr steels with carbon content below about 0.05 wt-% (Ref. 9). The difference between the transformation temperatures of the different supermartensitic pipe steels can be explained based on the effect of the alloying elements, especially Ni, on the stability of austenite.

The impact Charpy V-notch toughness of the HAZs of pipes S and N in every thermal condition, single-/double-thermal cycle, and tempered at temperatures equal to A_{c1}, A_{c1} + 40°C, and A_{c1} – 40°C, for 5 and 10 min, were equal, or higher than the toughness of the base metal in the as-received conditions. The results of the Charpy V-notch tests for the HAZ of supermartensitic pipe steel S is shown in Fig. 6. On the other hand, the toughness of the simulated HAZ of pipe steel K after a single- and double-thermal cycle, and after PWHT at 785°C was lower than the base metal in the as-received condition. However, metallographic evaluation of samples from the simulated HAZ of pipe K material indicated a nonuniform microstructure as the result of a nonuniform thermal experience across the section of the sample. This may have resulted from an improper contact between the samples and the grips in the Gleeble machine. Due to the size of the pipe, specimens from pipe steel K were subsize. Therefore, the results obtained from the evaluation of the simulated HAZ from pipe steel K are considered to be invalid, and no further analysis was attempted from the samples prepared from pipe steel K.

The microhardness of the simulated HAZs of supermartensitic pipe steels S and N after different welding thermal cycles and PWH treatments are listed in Table 9. Figures 7 and 8 show how the average microhardness of the simulated HAZs of pipe steels S and N changed with thermal cycles and with temperature and holding time during tempering. The microhardness of the HAZs from pipe S increases from 285 to 316 HVN (1 kgf) after a single- or double-thermal cycle. Tempering at 720°C does not affect the hardness of the HAZ. However, as the tempering temperature decreases from 720° to 640°C, the microhardness decreases. A microhardness of 289 HVN is obtained in the HAZ after a PWHT at 640°C for 10 min — Fig. 7. This result shows that a short PWHT is effective to reduce the microhardness of the HAZ to levels very close to the hardness of the base metal in the as-received condition. As shown in Fig. 8, single- and double-thermal cycles increase the hardness of the HAZ of pipe steel N from 291 to 320 and 330 HVN, respectively. Postweld heat treatment of the HAZ at 735° and 695°C for 5 and 10 min further increases the hardness to about 350 HVN. However, PWHT at 655°C for 5 and 10 min softens the HAZ to a level of about 314 HVN.

A fully martensitic microstructure was observed in the simulated HAZ of both pipes steel S and N after a single-thermal cycle. The main characteristic observed in pipe steel S was the increase of retained austenite, at the grain boundaries, as the tempering temperature was decreased from 720° to 640°C as shown in Fig. 9. The fraction of retained austenite in the grain boundaries increases with holding time during PWHT. On the other hand, etching

Table 9 — Results of Hardness Measurements [HVN (1 kgf)] in Simulated HAZ from Pipe Steels S and N after Different Thermal Cycles and PWHT

Specimen	HVN (1 kgf)	Average HVN	Specimen	HVN (1 kgf)	Average HVN
Base Metal		285	Base Metal		291
S1	318	316.5	N1	318	319.2
	319.5			315	
	315.5			318	
	313			326	
S2	315.5	316.3	N2	326	329.2
	321			329	
	314.5			326	
	317.5			338	
	313			327	
S1T3-5	314	315.6	N1T3-5	350	353.7
	311			356	
	319.5			354	
	318			355	
S1T3-10	319	311	N1T3-10	335	352
	309.5			340	
	316.5			357	
	299.5			357	
				355	
				351	
S1T2-5	305	309	N1T2-5	345	344.4
	303			346	
	306			345	
	316			314	
	315			340	
				346	
S1T2-10	300	304	N1T2-10	350	349.8
	310.5			354	
	298.5			350	
	307			345	
S1T1-5	302	294.8	N1T1-5	306	311.8
	293			314	
	291			318	
	293			309	
S1T1-10	279	289	N1T1-10	309	316
	295			316	
	291			318	
	291			321	

of pipe steel N only revealed very small amounts of retained austenite at the grain boundaries when PWH treated at 695°C.

The increasing fraction of austenite observed in pipe steel S as the PWHT temperature is decreased from 720° to 640°C is the result of the reversion and stability of austenite as a function of time and temperature. At PWHT temperature, reformation of austenite is promoted. Since the reaction is diffusion controlled, the austenite formed after PWHT will differ compositionally from austenite retained after the welding operation. In the latter case, the martensitic matrix and residual austenite will be of identical composition, whereas the reverted austenite formed during heat treatment will be enriched in Ni, C, and N. The degree of enrichment determines the stability of the austenite formed during the PWHT operation. If the A_{c1} is exceeded only slightly, by say 40°C, then the enriched austenite formed will be stable on cooling to room temperature. At temperatures further above the A_{c1} point, the equilibrium austenite content is greatly increased, the relative enrichment is reduced, and on cooling to room-temperature transformation to virgin martensite will occur, thus decreasing the amount of austenite retained at room temperature.

Based on the microstructural analysis and as expected, the A_{c1} determined by dilatometry is higher than the equilibrium-transformation temperature. The heating rate affects the transformation temperature determined by dilatometry; the higher the heating rate, the higher the transformation temperature. According to the microstructural analysis, the equilibrium-transformation temperature for pipe steel S is below 640°C.

To some degree, the effect of PWHT depends on the M_f of the alloy. If this is low, substantial austenite will be retained at room temperature after PWHT simply because the material remains above the M_f point. However, PWHT may induce sufficient carbide precipitation to deplete the matrix of C and raise the Ms. The austenite is destabilized and will transform to virgin martensite on cooling from the PWHT temperature; the reaction sequence depends on the C content of the steel, and the effect will be of less significance with very-low-C alloys. The resulting higher Ms temperature of pipe steel N may be responsible for the absence of any major fraction of austenite at room temperature.

An important additional consideration is the effect of retained austenite on the corrosion performance of supermartensitic stainless steel pipe. It has been observed that there is no harmful influence of retained austenite on the corrosion resistance of supermartensitic steels (Ref. 10). Additionally, a higher content of retained austenite reduces the diffusible hydrogen and the SSC susceptibility of the steel. Due to the high solubility of hydrogen in austenite, austenite act as a hydrogen trap and reduces the effective diffusion coefficient of hydrogen.

The changes in the mechanical properties on tempering can now be discussed on the basis of the microstructural changes. It is assumed that three mechanisms are responsible for the changes of hardness with PWHT, i.e., reversion of austenite, reduction in dislocation density, and precipitation. In pipe steel S, the hardness decreases with a decrease in PWHT temperature from 720° to 640°C and an increase in holding time from 5 to 10 min due to the increase in the fraction of stable austenite. Additionally, a reduction in dislocation density and decrease of C level in the untransformed martensite may also influence the hardness level. On the other hand, the hardness of pipe steel N increases with PWHT at the two highest temperatures, 735° and 695°C. Higher levels of C and lower levels of Ti in pipe steel N as compared to pipe steel S may increase the susceptibility to secondary hardening during PWHT due to the formation of carbides based on V, Cr, or Mo. Additionally, the formation of Cu precipitates may also play a factor in the increase of hardness during PWHT at the two highest temperatures. Softening of the HAZ of pipe steel N during PWHT at 655°C may result from a reduction dislocation density and from the fact that some C has been taken out of solid solution and has formed some carbides.

Conclusions

The following conclusions can be drawn from this work:

- Nickel-base ENiCrMo-3 electrodes are not recommended to join X80 grade supermartensitic steel pipes due to the resulting undermatching condition of the weld metal and the low levels of ductility (6 to 15% elongation) of the welded joints.

- Duplex and superduplex consumables provided an increasing degree of overmatching in the weld metal of X80 supermartensitic steel pipe joints resulting in a yield strength of the joint above 550 MPa (80 ksi) and an elongation between 20 to 33% when using SMAW, GMAW, and GTAW processes.

- All of the welding process-filler metal combinations used to weld the different supermartensitic steel pipes provided averaged impact energies in the welded joints above the minimum absorbed energy of 27 to 40 joules at –30°C required for different industrial applications.

- The maximum hardness observed in the HAZ near to the cap in the S, N, and K supermartensitic steel welded joints ranges from 301 to 341, 346 to 362, and 378 to 391 HV_1, respectively. The hardness of the weld metal and HAZ resulting from all the material-welding process-welding consumables combinations exceeds the NACE requirements of 23 HRC (253 HV).

- The tested supermartensitic steels are not susceptible to cracking under either CP or slightly sour conditions at hardness levels above the 23 HRC (253 HV) limit established by NACE, under the testing conditions used including an applied stress level equal to the measured yield strength of the base material.

- The transformation temperature at which the austenite starts to form during heating, A_{c1}, of pipes steels S, N, and K, as determined by dilatometric analysis, are 680, 695, and 745°C, respectively. The martensitic start temperatures, Ms, are 201°, 224°, and 277°C for pipes S, N, and K steel, respectively. According to the microstructural analysis, the equilibrium-transformation temperature, A_{c1}, for pipe steel S is below 640°C.

- The fraction of retained austenite in the simulated HAZ in pipe steel S at room temperature increases as the tempering temperature was decreased from 720° to 640°C and increases with hold time during PWHT.

- A microhardness of 289 HVN is obtained in the HAZ of supermartensitic pipe steel S after a PWHT at 640°C for 10 min. This result shows that short PWHT are effective for reducing the microhardness of the HAZ to levels very close to the hardness of the base metal in the as-received condition.

- The toughness of the simulated HAZ of pipe steels S and N in every thermal condition, single-/double-thermal cycle, and after PWHT is equal to or higher than the toughness of the base metal in the as-received conditions. In general, the change in toughness reflected the change in hardness; i.e., a reduction in hardness was accompanied by an increase in toughness.

References

1. Duisberg, J., Niederhoff, K. A., and Popperling, R. K. 1996. 13%Cr steels for flowline and pipeline applications. *Stainless Steel World* 8(6): 29–33.
2. Biagiotti, Jr., S. F., and Reichman, J. S. 1995. Justifying the use of 13Cr for corrosive CO_2 operations. Corrosion/95, Paper 81, NACE International, Houston, Tex.
3. Ueda, M., Amaya, H., Kondo, K., Ogawa, K., and Mori, T. 1996. Corrosion resistance of weldable super 13%Cr stainless steel in H_2S containing CO_2 environments. Corrosion/96, Paper 58, NACE International, Houston, Tex.
4. Amaya, H., Kondo, K., and Hirata, H. 1998. Effect of chromium and molybdenum on corrosion resistance of super 13Cr martensitic stainless steel in CO_2 environment. Corrosion/98, Paper 113, NACE International, Houston, Tex.
5. Miyata, Y., Kimura, M., Toyooka, T., and Murase, F. Weldable martensitic stainless steel seamless pipe for linepipe application. Kawasaki report: 59–71.
6. Asahi, H., Hara, T., and Sugiyama, M. 1996. Corrosion performance of modified 13Cr OCTG. Corrosion/96, Paper 61, NACE International, Houston, Tex.
7. Pargeter, R. J., and Gooch, T. G. 1994. Welding for sour service. Update on sour service: materials, maintenance and inspection in the oil and gas industry. Conference, London: 17 pp.
8. Gooch, T. G. 1995. Heat treatment of welded 13%Cr-4%Ni martensitic stainless steel for sour service. *Welding Journal* 74(7): 213-s to 223-s.
9. Gooch, G. T., Woollin, P., and Haynes, A. G. 1999. Welding metallurgy of low carbon 13% chromium martensitic steels. *Proceedings of Supermartensitic Stainless Steels '99 Congress*, 188–195. Belgium.
10. Kimura, M., Miyata, Y., and Kitahaba, Y. 2001. Effect of retained austenite on corrosion performance for modified 13% Cr steel pipe. *Corrosion* 57(5): 433–439.

Prediction of Element Transfer in Submerged Arc Welding

Several studies were conducted to better understand the chemical behavior of fluxes in order to control weld metal chemistry

BY P. KANJILAL, T. K. PAL, AND S. K. MAJUMDAR

ABSTRACT. The transfer of elements across the molten weld pool has been predicted by developing quadratic models in terms of flux ingredients with the application of statistical experiments for mixture design. Bead-on-plate weld deposits were made at fixed welding parameters using submerged arc welding fluxes prepared as per extreme vertices algorithm of mixture experiments in a CaO-MgO-CaF_2-Al_2O_3 flux system. The results show that some of the individual flux ingredients and their binary mixtures have a predominant effect on weld metal transfer of oxygen, manganese, silicon, and carbon contents.

The analysis of experimental data also indicates that transfer of oxygen is affected by several properties of flux ingredients such as oxygen potential, thermodynamic stability, and viscosity. In the element transfer of silicon, both thermochemical and electrochemical reaction mechanisms operate simultaneously. Transfer of manganese is principally related to the weld metal oxygen contents as well as electrochemical reaction in the molten weld pool. The transfer of carbon was generally governed by the oxidation reaction. Iso-response contour plots were also developed to quantify the transfer of elements against different flux compositions.

Introduction

Submerged arc fluxes play a very complex role during the welding process. Besides protecting the weld pool and influencing the bead geometry, fluxes also melt in a specific temperature range, refine the weld metal, as well as take part in slag-metal reaction (Refs. 1–4) before finally being removed as slag. Several studies were carried out to understand the chemical behavior of fluxes in order to control the weld metal chemistry (Refs. 4–13). Furthermore, physical properties such as viscosity, fluidity, etc. have also been reported to have pronounced effects on weld metal chemistry (Refs. 14–16). Significant interaction effect of the flux ingredients on weld metal chemistry has also been reported by previous investigators (Ref. 10).

It is well established that sumerged arc welding (SAW) fluxes consisting of easily reduced oxides are the main source of weld metal oxygen. The behavior of flux has been characterized in terms of basicity index, which, however, could be considered only as a rough guide for an engineer (Ref. 1), as it fails to address the fundamental question of transfer of oxygen from flux to weld, as well as the extent of slag metal reaction in the molten weld pool (Refs. 10, 11, 13, 17, 18). Later, oxygen potential, representing the driving force for oxygen transfer from flux to weld metal was observed to facilitate better prediction of flux behavior (Ref. 5). Again, the stability of flux ingredients based on free energy of formation has been shown to be altered in the presence of welding plasma (Refs. 6, 14). Detailed studies have revealed that along with thermochemical reactions of flux, electrochemical reactions also have a significant effect on weld metal chemistry (Refs. 17, 19–22). Therefore, final weld metal chemistry is based on the integration of all possible mechanisms operating within the molten weld pool.

KEYWORDS

Submerged Arc Welding
Mixture Design Experiment
Extreme Vertices Algorithm
Element Transfer
Flux Ingredients
Binary Synergism
Binary Antagonism
Oxidation Loss
Electrochemical Reaction

In general, the final weld metal composition for a particular element is made up of contributions from the filler metal, flux, and base metal. The nominal composition of each weld is calculated considering just the dilution effect (Refs. 3, 23–25). The extent of loss or gain of a specific element is evaluated by a quantity called "delta," which is the difference between the analytical and nominal composition (Refs. 23, 25). These quantities are an indication of the influence of flux on the element transfer behavior during the SAW process (Refs. 2, 3). Therefore, in order to obtain the desired weld metal composition, it is very necessary to understand and control the flux ingredients governing the weld metal delta quantities.

In this paper, an attempt has been made to find out the quantitative effects of individual flux ingredients and their interactions on the weld metal transfer of elements in terms of delta quantities, with the application of statistical experiments for mixture design, in particular, "extreme vertices mixture design," where the flux ingredients were varied simultaneously in CaO-MgO-CaF_2-Al_2O_3 flux systems. The aim is to develop satisfactory regression models involving proportions of flux ingredients and transfer of elements as shown in Fig. 1, so that the fluxes can be effectively used to achieve a desired level of weld metal chemical composition.

Planning of the Experiments

Extreme Vertices Design Algorithm

In experiments using a mixture of q components, a component (i^{th}) is expressed as a fraction x_i of the total mixture and the response is a function of the proportions of x_i, $i = 1, 2, \ldots q$, of the components and not the total amount of the mixture (Ref. 26). In practice, physical and chemical consideration often imposes lower (a_i) and upper (b_i) bounds $0 \le ai \le xi \le bi \le 1.0$; $i = 1, 2, \ldots q$, on the levels of all of the components of the mixture.

The extreme vertices design that was used for experimentation (Refs. 26–28)

P. KANJILAL (pra_kanj1@yahoo.co.in) *is Scientist, Mechanical Eng. Div., National Test House, Salt Lake, Kolkata, India.* T. K. PAL (t_k_pal@yahoo.com) *is Professor, Metallurgical Eng. Dept., Jadavpur University, Kolkata, India.* S. K. MAJUMDAR (skm@isical.ac.in) *is Professor, SQC & OR Division, Indian Statistical Institute, Kolkata, India.*

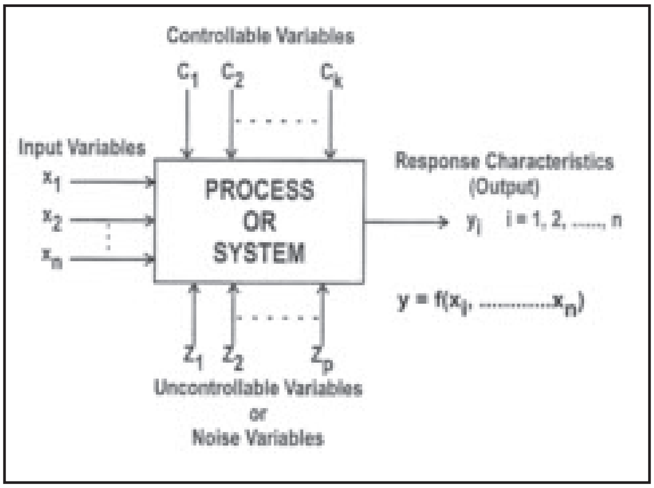

Fig. 1 — *General model of a process or system in a statistical mixture design experiment.*

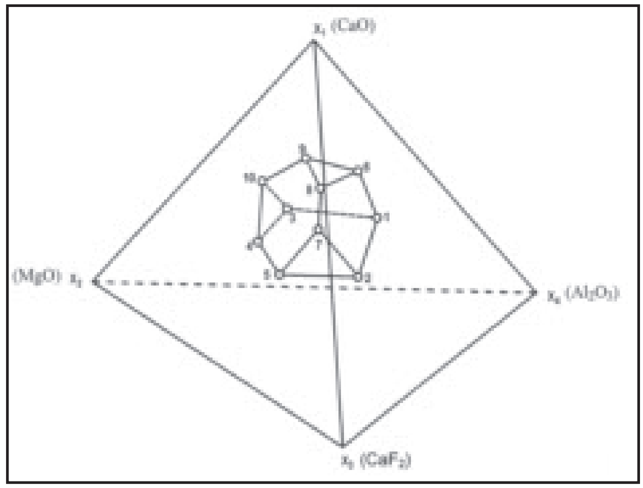

Fig. 2 — *The constrained factor space inside the tetrahedron describing the experimental space.*

Table 1 — Working Range of Flux Ingredients (Mixture Variable)

Flux Ingredients	Lower (wt-%)	Upper (wt-%)
Calcium oxide (CaO)	15	35
Magnesium oxide (MgO)	10	40
Calcium fluoride (CaF_2)	10	40
Aluminium oxide (Al_2O_3)	10	40

Table 2 — Design Matrix of Flux Used in the Experiment at Fixed Welding Parameters

	Mixture Variables Composition			Constants Composition	
Sample No.	CaO (wt-%)	MgO (wt-%)	CaF_2 (wt-%)	Al_2O_3 (wt-%)	SiO_2 (wt-%)
P1	15.00	15.00	10.00	40.00	10.0
P2	15.00	15.00	40.00	10.00	10.0
P3	15.00	32.40	10.00	22.60	10.0
P4	15.00	17.00	40.00	8.00	10.0
P5	15.00	32.40	24.60	8.00	10.0
P6	35.00	15.00	10.00	20.00	10.0
P7	17.00	15.00	40.00	8.00	10.0
P8	35.00	15.00	22.00	8.00	10.0
P9	29.60	32.40	10.00	8.00	10.0
P10	35.00	27.00	10.00	8.00	10.0
P11	24.43	23.14	24.43	8.00	10.0
P12	15.67	15.67	40.00	8.66	10.0
P13	25.92	24.36	10.0	19.72	10.0
P14	23.40	15.00	24.40	17.20	10.0
P15	19.87	32.40	14.86	12.87	10.0
P16	15.00	22.36	24.92	17.72	10.0
P17	35.00	19.00	14.00	12.00	10.0
P18	22.67	21.63	21.63	14.07	10.0

N.B.: Other additions to 18 flux samples. Fe-Mn = 4.0 wt-%, Fe-Si = 3.0 wt-%, bentonite = 3.0 wt-%

Table 3 — Chemical Compositions of Base Metal and Filler Metal Used for 18 Weld Metal Samples (P1-P18)

Sample	C (wt-%)	Mn (wt-%)	Si (wt-%)	S (wt-%)	P (wt-%)	O_2 (ppm)
Base metal	0.22	0.77	0.252	0.03	0.02	350
Filler metal	0.102	0.561	0.05	0.022	0.011	380

consisted of the 10 admissible vertices of the polyhedron, 7 centroids of the seven two-dimensional faces, and the overall centried. Thus, although 10 coefficients of the quadratic regression model for the response characteristics were required to be estimated, 18 design points were deliberately chosen for getting better estimates of the coefficients and error. The above design was obtained by following the two step procedures of Mclean and Anderson (Ref. 26). After having generated $4 \times 2^{4-1} = 32$ possible combinations of the four components, it was found that there were 10 admissible vertices, which satisfied the constraint for the mixture total as also the lower and upper bounds of each component proportion. The seven two-dimensional faces of the polyhedron were found by grouping the vertices of the polyhedron into groups of three or more vertices where each vertex had the same value x_i for one of the four components. Thus, the coordinates of the seven two-dimensional faces that satisfied the constraints are the design points sl. Nos. 11 to 17. The design point sl. No. 18 was the overall centroid, which was the average of all the 10 vertices. The transpose (x'x)–1, where x represents the complete design matrix of the given design, was also small. In three-dimensional space, the constraint design region is shown in Fig. 2, which represents the mixture space in the present experiment.

Snee (Ref. 29) also gave the algorithm for selecting the subsets of extreme vertices for fitting quadratic models of the following form in the constrained mixture spaces.

$$y = \sum_{i=1}^{q} \beta_i x_i + \sum_{i<j}^{q} \sum^{q} \beta_{ij} x_i x_j \qquad (1)$$

The regression coefficients β_i and β_{ij} are the least square estimates in the fitted model and y is the response variable.

The percentage variation of a given response characteristic is measured by the

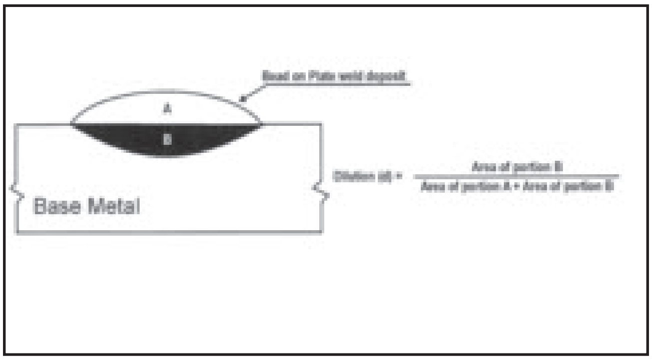

Fig. 3 — Schematic of weld deposit showing measurement of dilution.

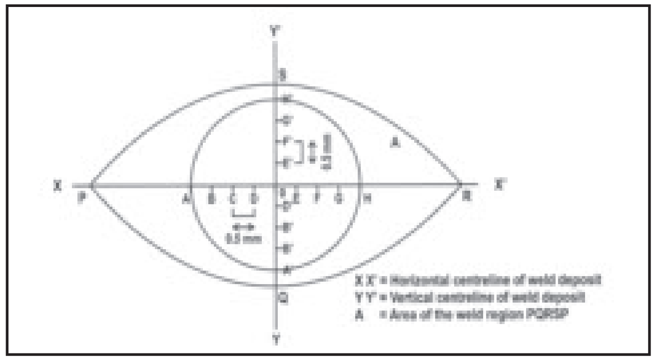

Fig. 4 — Weld metal region for EPMA analysis (shown within the circular area).

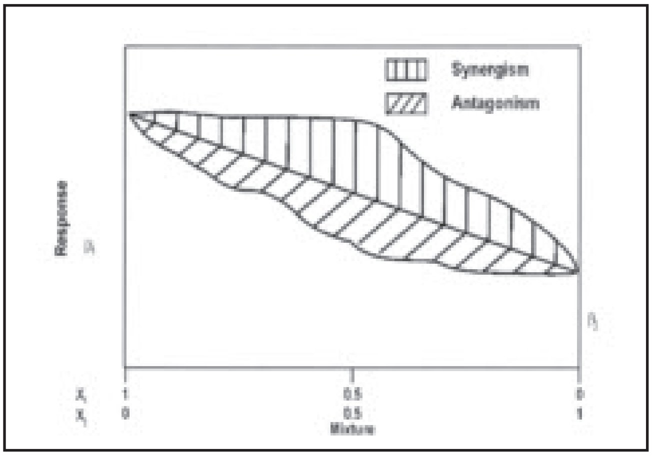

Fig. 5 — Synergism and antagonism of binary mixtures.

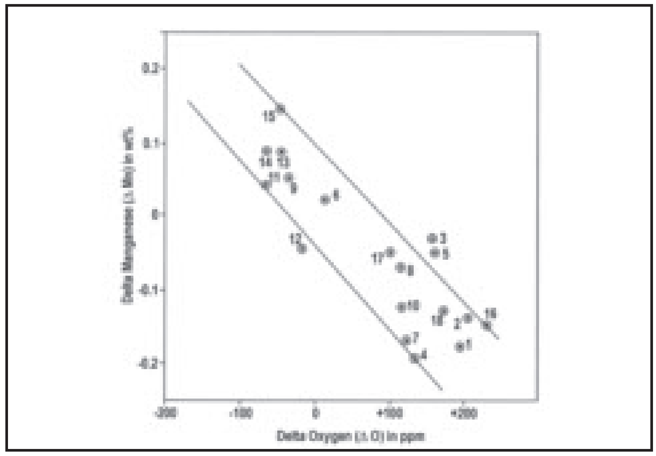

Fig. 6 — Variation of weld metal delta manganese with delta oxygen content.

term 'R', which is evaluated from the relation

$$R^2 = 1 - \frac{SSE/(N-P)}{SST/(N-1)} \quad (2)$$

Where, N is total number of observations, P is number of parameters, SSE is sum of square of errors, and SST is total sum of square.

Experimental Procedure

Formulation of Submerged Arc Fluxes

In the present study, the main aim was to investigate the effects of flux ingredients such as CaO, MgO, CaF_2, and Al_2O_3 on the transfer of metal during submerged arc welding. In order to prepare fluxes as per statistical design of experiments for mixture, the working range of each variable flux ingredient was found out by trial runs. Each ingredient viz CaO, MgO, CaF_2, and Al_2O_3 was varied from 5 to 50% at increments of 5%, with corresponding adjustment in other ingredients for each trial agglomerated flux. In the trial experiments, these fluxes were then used in making bead-on-plate weld deposits at prefixed welding parameters of 400 A, 26 V and 4.64 mm/s speed. After completion of each weld deposit, it was inspected at low magnification (5X) for any weld defects. In addition, slag detachability was also observed. The range of each flux ingredient, where satisfactory weld deposits were obtained, was noted. The working range of each variable of flux ingredients (CaO, MgO, CaF_2, Al_2O_3) for satisfactory weld deposits is given in Table 1. Within this working range, the agglomerated fluxes used in the actual experiment were prepared from the flux ingredients, as per formulations developed by statistical experiments for mixture design. The details of 18 fluxes are given in Table 2.

Submerged Arc Welding

Single pass, bead-on-plate weld deposits were made with direct current electrode positive (DCEP) polarity using 18 experimental fluxes (Table 2) on 16-mm-thick low-carbon steel plate with 3.15-mm-diameter low-carbon steel welding wire. The parameters used during welding of these 18 samples were maintained as the same as that used during standardization of experiments on fluxes.

Chemical Composition Analysis

The chemical compositions of steel plate and welding wire are given in Table 3. Chemical compositional analysis of base metal, filler metal, and the weld metal for constituents such as carbon, manganese, silicon, sulfur, phosphorus, and nickel contents were analyzed by optical emission spectra (OES) method. Weld metal oxygen and nitrogen contents were determined by Leco interstitial analyzer. Cylindrical samples of 3-mm diameter and 9-mm length prepared by machining the weld deposits were used for oxygen and nitrogen estimates. Chemical compositions were determined at four different locations of the same weld deposits. Microphotographs were taken on the weld metal samples for measurement of weld bead parameters such as width w, transverse cross-sectional area A, and dilution d, as shown in Fig. 3.

EPMA Analysis

Transfer of elements in the weld region have been studied by electron probe micro analyzer (EPMA) for selected weld metal samples. The spot of probe analyzer on the weld bead is shown in Fig. 4.

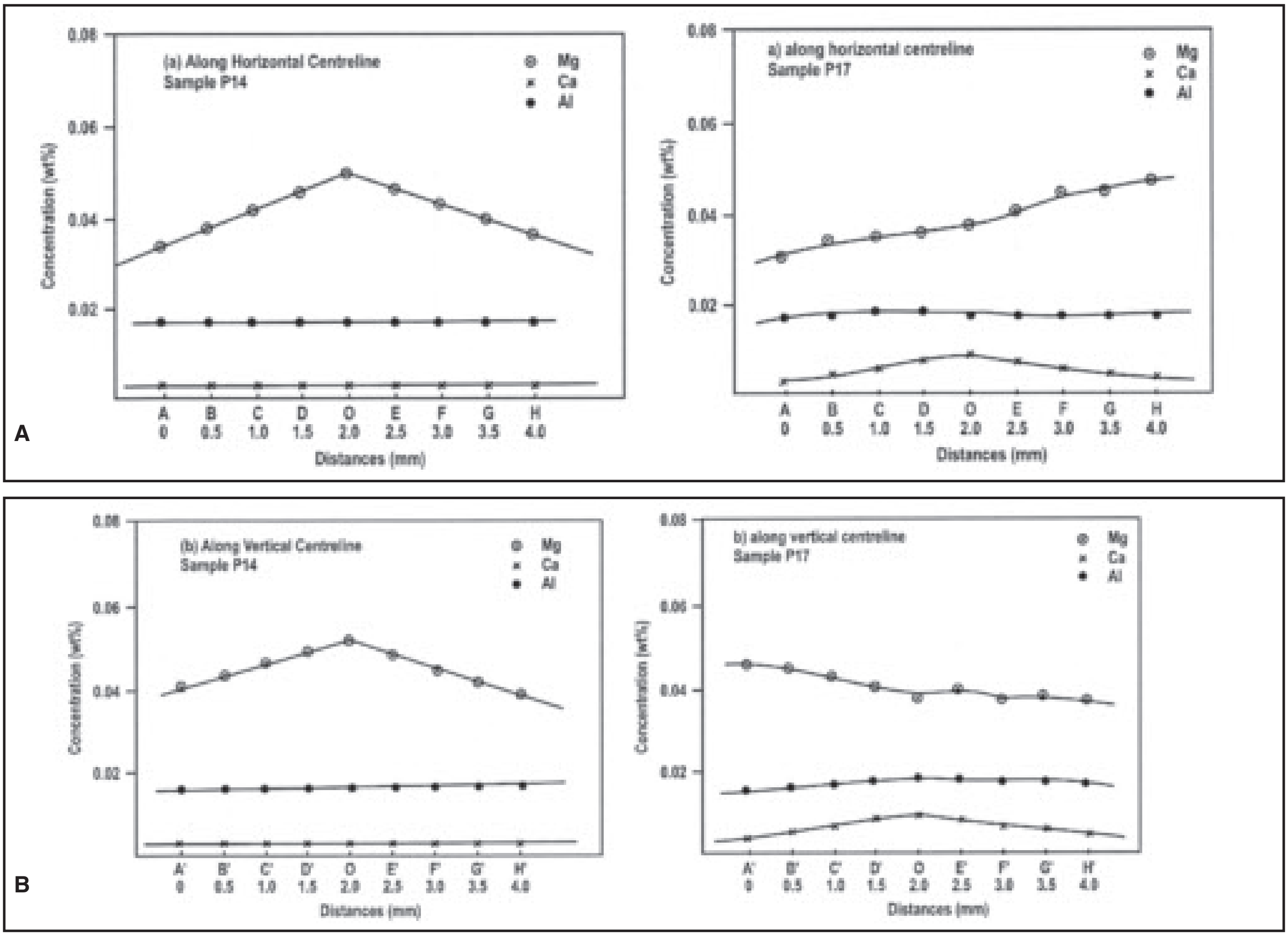

Fig. 7 — Distribution of magnesium, calcium, and aluminum along the weld metal samples P14 and P17. A — Along the horizontal centerline of the weld; B — the vertical centerline of the weld.

Results

The final weld metal composition is generally made of contributions from the welding electrodes, the base metal, and the molten metal-flux (slag-metal) reactions (Ref. 23). In the present experiment, welding parameters were not varied and flux height was kept on the base metal to a height of 0.35 mm along the path of the nozzle. Furthermore, the ratio of flux to wire melted varied within the small zone, i.e., 1.85 to 2.05. Therefore, the composition changes affected by the ratio of flux to wire melted may be assumed to be small in magnitude.

The chemical behavior of flux on element transfer is expressed in terms of a quantity delta (Δ), which is the difference between the composition of a particular element determined analytically and the amount of that element that could be present in the weld, if no elemental transfer for the weld pool to the flux or vice versa has taken place (Refs. 22, 24). This has been accomplished by taking the effect of dilution (d), which is the ratio of base plate to weld metal melted. The dilution of 18 welded samples is given in Table 4. Since the aim of the present experiment was to study the effect of flux ingredients on element transfer, the delta quantities were considered for further analysis and discussion. Chemical compositions were determined at four different positions of the weld and delta quantities were measured corresponding to the four sets of chemical constituents. These four sets of chemical constituents and corresponding weld metal delta quantities are given in Table 5A and B, respectively.

Development of Prediction Equations for Weld Metal Elemental Transfer

Extreme vertices design algorithm (XVERT) were applied on the experimentally determined values of responses, viz. weld metal delta oxygen (ΔO), delta manganese (ΔMn), delta silicon (ΔSi), delta sulfur (ΔS), and delta carbon (ΔC) as given in Table 5B in order to develop prediction equations for the responses. The predictors are the flux ingredients such as CaO, MgO, CaF_2, and Al_2O_3,and their binary mixture eg. CaO-MgO, CaO-CaF_2, CaO-Al_2O_3, MgO-CaF_2, MgO-Al_2O_3, and CaF_2-Al_2O_3.

The prediction equations are as follows:

$$\Delta O_2 = 58.9318\ CaO - 17.2406\ MgO + 2.6522\ CaF_2 + 12.7800l Al_2O_3 - 0.9086\ CaO.MgO - 1.5406\ CaO.\ CaF_2 - 2.0416\ CaO.Al_2O_3 + 0.8562\ MgO.\ CaF_2 + 0.7966\ MgO.\ Al_2O_3 + 0.3661\ CaF_2.\ Al_2O_3. \quad (3)$$

$$\Delta Mn = -0.029867\ CaO + 0.05574\ MgO - 0.004323\ CaF - 0.002228\ Al_2O_3 - 0.000474\ CaO.MgO + 0.001225 CaO.\ CaF_2 + 0.001361\ CaO.Al_2O_3 - 0.001352\ MgO.CaF_2 - 0.001532\ MgO.\ Al_2O_3 + 0.000204\ CaF_2.Al_2O_3 \quad (4)$$

$$\Delta Si = 0.012176\ CaO + 0.055635\ MgO + 0.006303\ CaF_2 + 0.013559\ Al_2O_3 - 0.001364\ CaO.MgO - 0.000063\ CaO.CaF_2 - 0.000190\ CaO.Al_2O_3$$

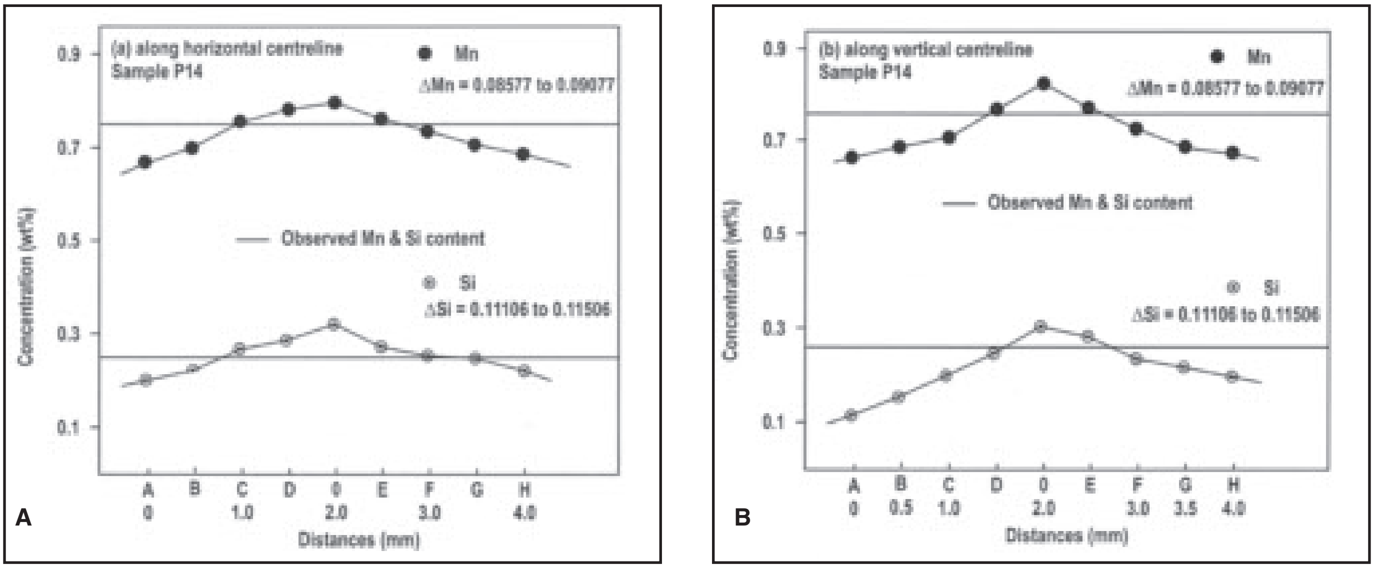

Fig. 8 — Distribution of manganese and silicon in weld metal sample P14. A — Along horizontal centerline of the weld; B — along the vertical centerline of the weld.

$$-0.001332\ MgO.CaF_2 - 0.001429\ MgO.Al_2O_3 + 0.000220\ CaF_2.Al_2O_3 \quad (5)$$

$$\Delta S = 0.002927\ CaO + 0.004700\ MgO + 0.001642\ CaF_2 + 0.002072\ Al_2O_3 - 0.000159\ CaO.MgO - 0.000070\ CaO.CaF_2 - 0.000079\ CaO.Al_2O_3 - 0.000102\ MgO.CaF_2 - 0.000119\ MgO.\ Al_2O_3 - 0.000019\ CaF_2.Al_2O_3 \quad (6)$$

$$\Delta C = -0.001712\ CaO + 0.007264\ MgO + 0.001276\ CaF_2 - 0.000432\ Al_2O_3 - 0.000125\ CaO.MgO + 0.000072\ CaO.CaF_2 + 0.000174\ CaO.Al_2O_3 - 0.000193\ MgO.CaF_2 - 0.000182\ MgO.Al_2O_3 - 0.000029\ CaF_2.Al_2O_3 \quad (7)$$

The model summary, coefficients, and level of significance of regression models are given in Appendices 1 and 2.

Nature of Variation of Weld Metal Delta Quantities with the Flux Ingredients

It is observed from the above prediction results (Equations 3–7) that flux ingredients have two types of effect on weld metal delta quantities, viz. 1) individual effect (x_i), and 2) interaction effect of binary mixtures(x_ix_j). It is to be noted here that for each response characteristics in the prediction equations developed by the regression model, only statistically significant variables and/or their binary synergism and/or binary antagonism will be considered to have a predominant effect on the given response characteristics. The concept of binary synergism and antagonism is quite different from the individual effect. The binary synergism/antagonism implies that the response value (weld metal delta quantities) obtained due to binary mixture is more than/less than the average of that response produced by two pure ingredients forming the same binary mixture. This is shown schematically in Fig. 5. The positive sign of the coefficients of individual flux ingredient in the prediction Equations 3 to 7 implies a gain of elements from flux to weld metal, and the negative sign implies a loss of elements from weld to slag. Similarly, a positive sign of the coefficients of binary flux mixtures on each response (i.e. binary synergism) implies a gain of elements from flux to weld, and the opposite effect (binary antagonism) implies a loss of elements from weld metal to slag. Among the flux ingredients, only those ingredients and/or their binary synergic/antagonism are considered significant, when their corresponding values given in the last column (sign) of the tabular form of coefficients (under Appendixes 1 and 2) are nearly equal to 0.05 (equivalent to 95% confidence level). The statistically significant variables for flux ingredients and their binary synergism/antagonism equivalent to 95% confidence level are summarized in Table 6. The other nonsignificant variables, although they constitute a part of the prediction equations, were not considered to have predominant effect on the response because these effects were not distinguishable from the random noise generated in the experiments.

Finally, the prediction equation for the response delta sulfur (ΔS) (Equation 6) is not a good fit as evident from R^2 values, given in Appendixes 1 and 2, and hence, this response is not considered for detailed discussion. However, the effect of each flux ingredient and its binary mixtures are stated in Table 6.

Table 4 — Dilution for 18 Weld Metal Samples in Model 1 Experiment at Fixed Welding Parameters

Sample No.	Dilution (d)	1-d
P1	0.41	0.59
P2	0.47	0.53
P3	0.45	0.55
P4	0.47	0.53
P5	0.43	0.57
P6	0.43	0.57
P7	0.46	0.54
P8	0.43	0.57
P9	0.39	0.61
P10	0.49	0.51
P11	0.47	0.53
P12	0.41	0.59
P13	0.46	0.54
P14	0.47	0.53
P15	0.45	0.55
P16	0.46	9.54
P17	0.42	0.58
P18	0.43	0.57

Discussion

The transfer of elements across the weld pool in submerged arc welding is attributed to the combined actions of several reactions that take place simultaneously in the molten weld pool. It has already been stated (Refs. 1–4, 19) that physical as well as chemical properties of fluxes are responsible for the transfer of elements in submerged arc welding. Among the transfer of elements in these studies, oxygen is the most important element of concern, because, beside its effect on the transfer of other elements like manganese, silicon, carbon, etc., oxygen in weld metal has a significant effect on weld metal microstructure and mechanical properties.

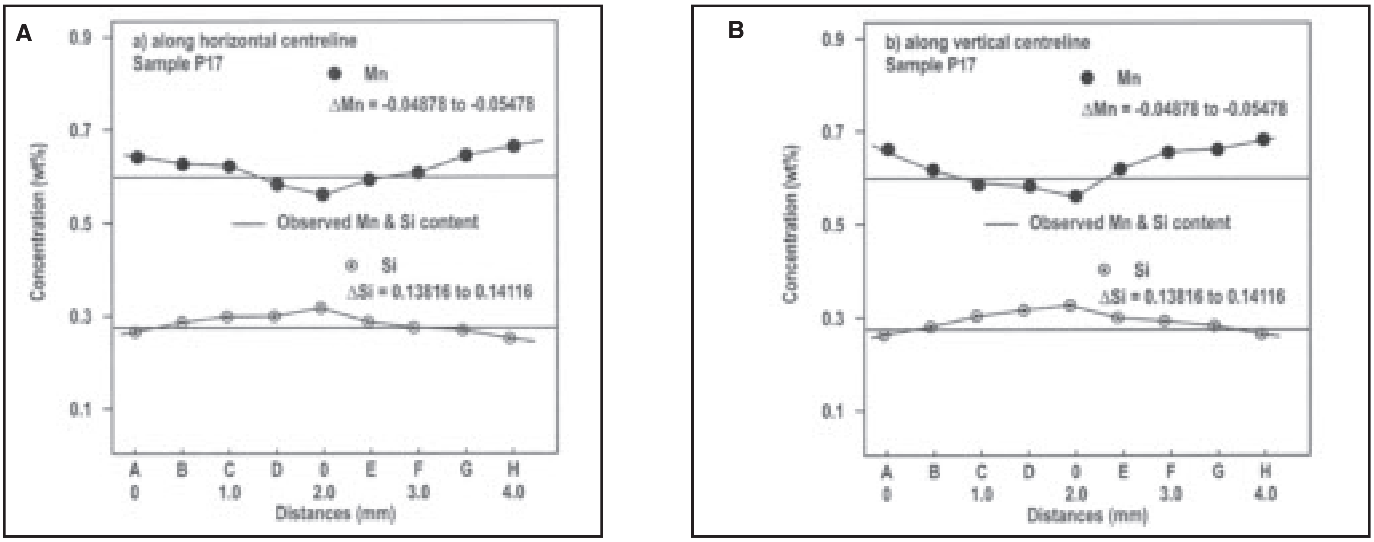

Fig. 9 — Distribution of manganese and silicon nickel in weld metal sample P17. A — Along horizontal centerline of the weld; B — along the vertical centerline of the weld.

Table 5a — Chemical Composition of 18 Weld Metal Samples at Four Different Locations of the Weld Deposits

Sample No.	Oxy (ppm)	Oxy (ppm)	Oxy (ppm)	Oxy (ppm)	Mn (wt-%)	Mn (wt-%)	Mn (wt-%)	Mn (wt-%)	Si (wt-%)	Si (wt-%)	Si (wt-%)	Si (wt-%)
P1	560	555	557	550	0.56	0.563	0.55	0.558	0.340	0.337	0.341	0.341
P2	568	563	564	558	0.52	0.522	0.521	0.524	0.21	0.211	0.212	0.208
P3	524	525	515	516	0.62	0.624	0.622	0.614	0.28	0.282	0.281	0.282
P4	500	496	505	490	0.47	0.468	0.466	0.478	0.17	0.169	0.173	0.174
P5	528	524	526	520	0.6	0.588	0.594	0.595	0.248	0.244	0.245	0.243
P6	380	370	377	375	0.67	0.673	0.674	0.672	0.229	0.227	0.228	0.230
P7	488	486	482	480	0.488	0.49	0.494	0.485	0.27	0.269	0.271	0.265
P8	481	482	476	484	0.58	0.583	0.582	0.581	0.2	0.202	0.201	0.202
P9	332	335	338	343	0.69	0.691	0.693	0.685	0.26	0.262	0.264	0.257
P10	484	470	477	468	0.54	0.541	0.539	0.536	0.193	0.195	0.191	0.190
P11	300	306	306	310	0.7	0.702	0.703	0.710	0.12	0.124	0.124	0.122
P12	352	351	348	360	0.601	0.6	0.601	0.610	0.15	0.153	0.15	0.153
P13	319	327	323	330	0.62	0.624	0.619	0.614	0.16	0.163	0.159	0.156
P14	302	310	300	316	0.748	0.745	0.75	0.750	0.258	0.256	0.255	0.260
P15	320	315	318	314	0.8	0.806	0.803	0.798	0.37	0.368	0.372	0.364
P16	595	594	593	590	0.507	0.509	0.505	0.502	0.2	0.204	0.203	0.205
P17	468	475	470	482	0.595	0.596	0.594	0.600	0.273	0.273	0.274	0.276
P18	541	530	545	525	0.517	0.513	0.519	0.516	0.16	0.161	0.163	0.168

Table 5a — Continued

Sample No.	S (wt-%)	S (wt-%)	S (wt-%)	S (wt-%)	C (wt-%)	C (wt-%)	C (wt-%)	C (wt-%)
P1	0.042	0.038	0.04	0.040	0.07	0.068	0.069	0.067
P2	0.042	0.04	0.042	0.039	0.07	0.071	0.068	0.068
P3	0.04	0.036	0.041	0.042	0.07	0.07	0.071	0.073
P4	0.034	0.036	0.033	0.036	0.06	0.061	0.062	0.059
P5	0.044	0.044	0.046	0.041	0.068	0.067	0.07	0.065
P6	0.028	0.028	0.03	0.030	0.098	0.096	0.095	0.093
P7	0.04	0.043	0.039	0.037	0.072	0.076	0.072	0.070
P8	0.028	0.03	0.03	0.026	0.07	0.069	0.078	0.072
P9	0.027	0.025	0.027	0.026	0.068	0.070	0.069	0.070
P10	0.034	0.033	0.034	0.030	0.063	0.067	0.066	0.060
P11	0.021	0.022	0.023	0.025	0.073	0.072	0.074	0.075
P12	0.037	0.035	0.036	0.034	0.095	0.092	0.091	0.091
P13	0.016	0.018	0.018	0.020	0.084	0.08	0.082	0.085
P14	0.031	0.029	0.032	0.030	0.089	0.085	0.087	0.091
P15	0.02	0.022	0.023	0.025	0.094	0.095	0.093	0.092
P16	0.024	0.025	0.027	0.027	0.061	0.062	0.059	0.057
P17	0.015	0.016	0.018	0.021	0.082	0.082	0.082	0.078
P18	0.023	0.023	0.025	0.022	0.058	0.057	0.055	0.060

Transfer of Oxygen

The positive and negative values of delta oxygen as given in Table 5B indicate both gain and loss of oxygen in weld metal had taken place during welding. The summarized results in Table 6 show that flux ingredients CaO and Al_2O_3 resulted in gain of oxygen for flux to weld metal. However, all binary mixtures of CaO viz. $CaO-CaF_2$, $CaO-Al_2O_3$, and CaO-MgO have binary antagonistic effect i.e., which means in all three cases, a loss of oxygen has taken place. Although CaO is considered to be a stable oxide (Ref. 23), the other characteristics of CaO, such as hygroscopic nature and reduction in viscosity of the slag (Refs. 2, 6, 14, 15, 24), increase the chances of contamination with air and moisture, which might be respon-

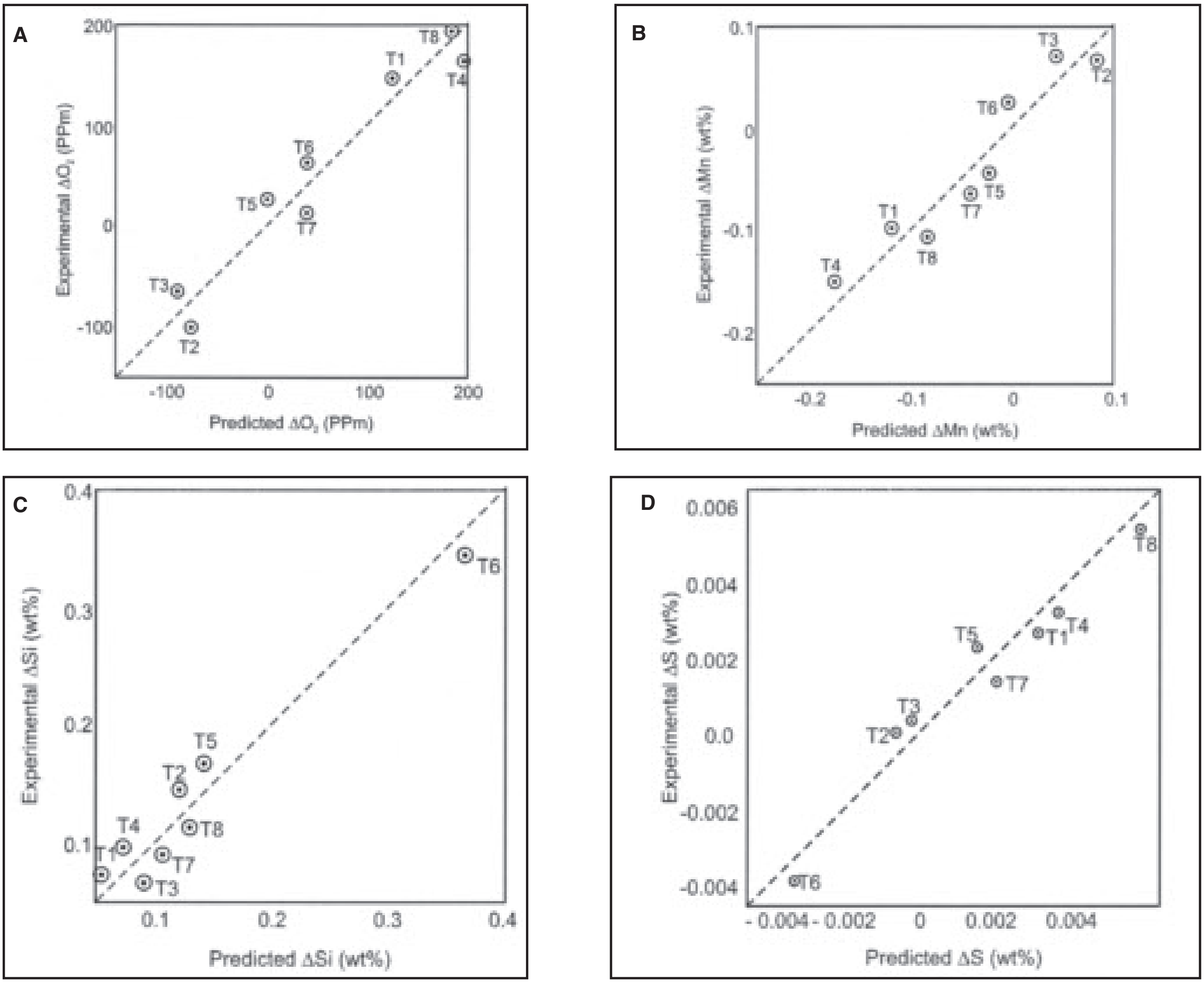

Fig. 10 — Comparison between experimental and predicted results for weld metal delta (Δ) quantities. A — ΔO_2; B — ΔMn; C — ΔSi; D — ΔS.

sible for an increase in oxygen content in the weld. The other flux ingredient Al_2O_3 can increase the oxygen content by liberating oxygen into the weld pool by suboxide formation (Ref. 6).

However, for the binary mixture of CaO, it is important to mention that CaF_2 being a nonoxide reduces the oxygen level by diluting the oxygen active species (Ref. 6). CaF_2 also increases viscosity of slag, particularly when CaO content is above 15 wt-% as observed by Mills and Keene (Ref. 15). CaF_2 may also reduce the hygroscopic nature of CaO by the following reaction:

$$2CaF_2 + 2H_2O = 2CaO + 4HF \quad (8)$$

Therefore, binary antagonistic effect of CaO-CaF_2 mixture on oxygen transfer is not unexpected. Similarly, in the case of CaO-Al_2O_3 mixture, it is the networking capability of Al_2O_3 in basic slag that ultimately increases the viscosity of the slag (Ref. 30), resulting in minimum oxygen entrapment in the weld metal by atmospheric contamination. Furthermore, CaO may reduce the activity of Al_2O_3 through the formation of stable calcium aluminate, (Ref. 15), which will reduce the tendency of suboxide formation of Al_2O_3. The result is lesser chance of oxygen liberation in molten weld pool by suboxide formation of Al_2O_3. Mixture of CaO-MgO, to a lesser extent, also has a binary antagonistic (loss of oxygen) effect, as evident from its coefficient of estimate given in Equation 3. The probable reason may be that MgO is not reported to contribute oxygen in the weld by atmospheric contamination associated with reduction in viscosity. Furthermore, Mg has higher deoxidation characteristics (Ref. 31). Therefore, with the addition of MgO to CaO, the increased deoxidation characteristics of flux reduce the oxygen content of weld metal, and thus helps to transfer oxygen from weld metal to slag.

An interesting result emerges from Table 6 that the effect of binary mixture of MgO, i.e., MgO-CaF_2 and MgO-Al_2O_3, is opposite to that of CaO-CaF_2 and CaO-Al_2O_3 as far as transfer of oxygen is concerned. Regarding binary synergism, i.e., (gain of oxygen) by MgO-Al_2O_3 mixture, we may say that unlike CaO, MgO is not observed to decrease the activity of Al_2O_3 by formation of complex compound, since MgO-Al_2O_3 compound has a higher boiling point (2130°C) compared to the boiling point (1600°C) of $CaO+Al_2O_3$ compound (Ref. 32). Therefore, activity of Al_2O_3 is not decreased and hence no such

Table 5b — Delta (Δ) Quantities of Weld Metal Constituents at Four Different Locations of Same Weld Deposit

Sample No.	ΔO_2 (ppm)	ΔO_2 (ppm)	ΔO_2 (ppm)	ΔO_2 (ppm)	ΔMn (wt-%)	ΔMn (wt-%)	ΔMn (wt-%)	ΔMn (wt-%)	ΔSi (wt-%)	ΔSi (wt-%)	ΔSi (wt-%)	ΔSi (wt-%)
P1	192.3	187.3	189.3	182.3	–0.08669	–0.08369	–0.09669	–0.08669	+0.20718	0.20418	0.20818	0.20818
P2	202.1	197.1	198.1	192.1	–0.13923	–0.13723	–0.13823	–0.13523	+0.06506	0.06606	0.06706	0.06306
P3	157.5	158.5	148.5	149.5	–0.03505	–0.03105	–0.03305	–0.04105	+0.1391	0.1411	0.1401	0.1411
P4	134.1	130.1	139.1	124.1	–0.18923	–0.19123	–0.19323	–0.18123	+0.02506	0.02406	0.02806	0.0296
P5	160.9	156.9	158.9	152.9	–0.05087	–0.06287	–0.05687	–0.05587	+0.11114	0.10714	0.10814	0.10614
P6	12.9	2.9	9.9	7.9	+0.01913	0.02213	0.02313	0.02113	+0.09214	0.09014	0.09114	0.09314
P7	121.8	119.8	115.8	113.8	–0.16914	–0.16714	–0.16314	–0.17214	+0.12708	0.12608	0.12808	0.12208
P8	113.9	114.9	108.9	116.9	–0.07087	–0.06787	–0.06887	–0.06987	+0.06314	0.06514	0.06414	0.06514
P9	–36.3	–33.3	–30.3	–25.3	+0.04749	0.04844	0.05049	0.04249	+0.13122	0.13322	0.13522	0.12822
P10	118.7	104.7	111.7	102.7	–0.12341	–0.12341	–0.12441	–0.12741	+0.04402	0.04602	0.04202	0.04102
P11	–65.9	–59.9	–59.9	–55.9	+0.04077	0.04277	0.04377	0.05077	–0.02494	–0.02094	–0.02094	–0.02294
P12	–15.7	–16.7	–19.7	–7.7	–0.04569	–0.04669	–0.04569	–0.03669	+0.01718	0.02018	0.01718	0.02018
P13	–47.2	–39.2	–43.2	–36.2	–0.03714	–0.03314	–0.03814	–0.04314	+0.01708	0.02008	0.01608	0.01308
P14	–63.9	–55.9	–65.9	–49.9	+0.08877	0.08577	0.09077	0.09077	+0.11306	0.11106	0.11006	0.11506
P15	–46.5	–51.5	–48.5	–52.5	+0.14494	0.15094	0.14794	0.14294	+0.2291	0.2271	0.2311	0.2231
P16	228.8	227.8	226.8	223.8	–0.15014	–0.14814	–0.15214	–0.15514	+0.05708	0.06108	0.06008	0.06208
P17	100.6	107.6	102.6	114.6	–0.05378	–0.05278	–0.05478	–0.04878	+0.13816	0.13816	0.139.16	0.14116
P18	173.9	162.9	177.9	157.9	–0.13387	–0.13787	–0.13187	–0.13427	+0.02314	0.02414	0.02614	0.03114

Table 5b — Continued

Sample No.	Δs (wt-%)	ΔS (wt-%)	ΔS (wt-%)	ΔS (wt-%)	ΔC (wt-%)	ΔC (wt-%)	ΔC (wt-%)	ΔC (wt-%)
P1	0.01672	0.01272	0.01472	0.01472	–0.08038	–0.08238	–0.08138	–0.08338
P2	0.01624	0.01424	0.01624	0.01324	–0.08746	–0.08646	–0.08946	–0.08946
P3	0.0144	0.0104	0.0154	0.0164	–0.0851	–0.0851	–0.0841	–0.0821
P4	0.00824	0.01024	0.00724	0.01024	–0.09746	–0.09646	–0.09546	–0.099846
P5	0.01856	0.01856	0.02056	0.0156	–0.08474	–0.08574	–0.08274	–0.08774
P6	0.00256	0.00256	0.00456	0.00456	–0.05474	–0.05674	–0.05774	–0.05974
P7	0.01432	0.01732	0.01332	0.01132	–0.08428	–0.08028	–0.08428	–0.08628
P8	0.00256	0.00456	0.00456	0.00056	–0.08274	–0.08374	–0.07474	–0.08074
P9	0.00408	–0.00208	0.00408	0.00308	–0.08002	–0.07802	–0.07902	–0.07802
P10	0.00808	0.00708	0.00808	0.00408	–0.09682	–0.09282	–0.09382	–0.09982
P11	–0.00475	–0.00376	–0.00276	–0.00076	–0.08446	–0.08546	–0.08346	–0.08246
P12	0.01172	0.00972	0.01072	0.00872	–0.05538	–0.05838	–0.05938	–0.05938
P13	–0.00968	–0.00768	–0.00768	–0.00568	–0.07228	–0.07628	–0.07428	–0.07128
P14	0.00524	0.00324	0.00624	0.00424	–0.06846	–0.07246	–0.07046	–0.06646
P15	–0.0056	–0.0036	–0.0026	–0.0006	–0.0611	–0.0601	–0.0621	–0.0631
P16	–0.00168	–0.00068	–0.00132	–0.00132	–0.09528	–0.09428	–0.09728	–0.09928
P17	–0.00836	–0.00936	–0.00376	–0.00736	–0.06956	–0.06956	–0.06956	–0.07356
P18	–0.00244	–0.00244	–0.00044	–0.00344	–0.09474	–0.09574	–0.09774	–0.09274

chances of reduction of oxygen content. Regarding the mixture CaF_2-Al_2O_3, it is important to mention that formation of such complex compound of CaF_2-Al_2O_3 has not been reported, so the chances of decrease in oxygen content by complex compound formation does not arise for the mixture CaF_2-Al_2O_3.

Transfer of Manganese and Silicon

The manganese transfer data (ΔMn) in Table 5B show that gain in weld metal Mn (i.e., ΔMn +ve) occurs in samples P6, P9, P11, P14, and P15. Among these samples, P9, P11, P14, and P15 show loss of oxygen and sample P6 shows very low level of gain of oxygen (Δ = 2.9 to 12.9 ppm). It is also pertinent to note the majority of samples that show a loss of Mn (Δ Mn = ¯ve) also show a gain of oxygen (ΔO = +ve). This phenomenon suggests that manganese transfer is also related to the transfer of oxygen in weld metal. With the increase of oxygen transfer into the weld metal, loss of manganese in the weld metal by oxidation was also observed by previous investigators (Refs. 4, 8, 14). The variation of ΔMn with ΔO_2 in weld metal, as shown in Fig. 6, supports such observation. A close look on the summarized result in Table 6 indicates two important aspects. Flux ingredient CaO increases (gain) oxygen transfer and expectedly decreases (loss) manganese transfer in weld metal. Flux mixtures CaO-CaF_2 and CaO-Al_2O_3 have binary antagonistic effect (loss) on oxygen transfer, whereas the same mixtures have binary synergistic (gain) effect on manganese transfer. The other two mixtures, viz. MgO-CaF_2 and MgO-Al_2O_3, have reverse effects i.e., binary synergistic (gain) effect on oxygen transfer and binary antagonistic (loss) effect on manganese transfer. The relationship between ΔMn and ΔO_2, as shown in Fig. 6, supports such behavior of flux mixtures as predicted in Table 6. Contrary to ΔMn, all samples except P11 recorded a gain of Si in the weld metal i.e. (ΔSi +ve). Since the flux system has SiO_2 as one of the constituents (10 wt-%), gain in Si (ΔSi +ve) may be possible due to the transfer of Si from flux to weld metal by thermochemical dissociation (Refs. 33, 34) and electrochemical reaction mechanism (Ref. 19). Flux ingredient Al_2O_3 may allow silicon in the flux to transfer into the weld metal by replacement of silica in silicate slag (Ref. 1).

The gain of manganese and silicon by MgO is reported in Equations 4 and 5. Table 6 may be explained by electrochemical reaction. In DCEN welding, Mg dissociates from MgO deposited at the base metal cathode by electrochemical reduction reaction of the filler metal. Manganese and silicon will form MnO and SiO_2, respectively, and dissolve in the weld pool. Due to limited solubility in molten metal (Ref. 33), Mg will react with these oxides (MnO and SiO_2) and form again as MgO. As a result, Mn and Si are expected to increase in the weld metal. However, difficulties may arise if Ca and Al are picked up from the slag by electrochemical reaction at the cathode, since CaO and Al_2O_3 are more stable than MgO at the high temperature encountered in submerged arc welding (Ref. 20). The higher the concentration of magnesium in the weld metal, the lower are Ca and Al, as observed by EPMA studies of weld metal samples (refer to P14 and P17) shown in Fig. 7. They probably support the hypoth-

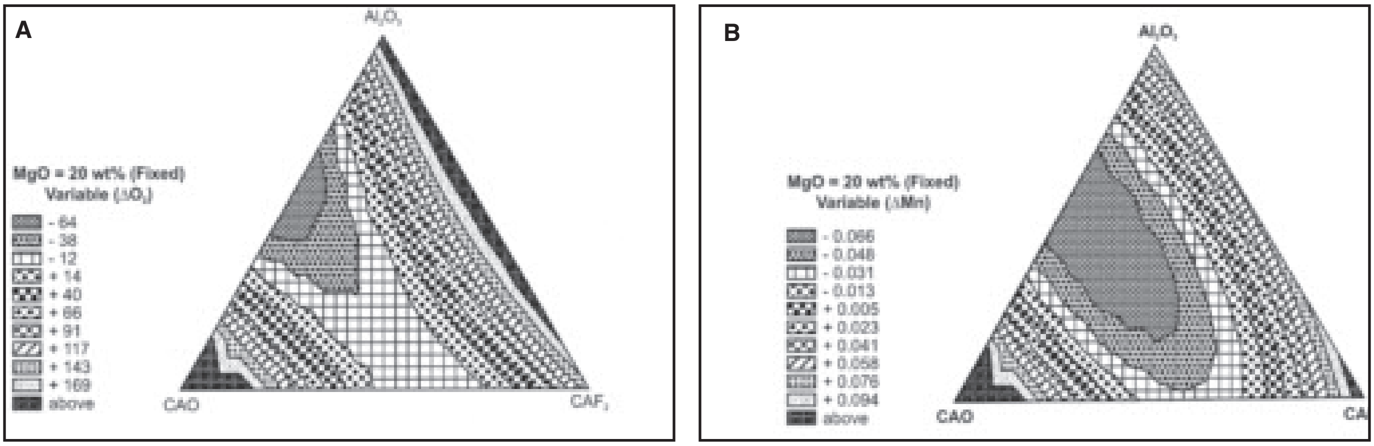

Fig. 11 — Fillet surface contour of weld metal. A — ΔO_2; B — ΔMn.

esis of more Mg pick-up from the slag.

It is also observed from Table 5B that sample P14 recorded a gain of Mn. The EPMA analysis of sample P14 along the horizontal and vertical centerline of weld (Fig. 8) shows maximum transfer of Mn occurs at the central region of the weld deposit. This may be due to the fact that weld metal remained liquid and solidified last, therefore giving more chances of both thermochemical and electrochemical reaction. Similarly, the maximum transfer of Si was observed for sample P14 at the central region of the weld deposit as evident in EPMA analysis silicon in Fig. 8. Interestingly sample P17 recorded loss of Mn (ΔMn from –0.04878 to –0.05478) but gain of Si (ΔSi from 0.13816 to 0.14116) as shown in Fig. 9. However, the transfer process (loss and gain) was mostly restricted along the central region of the weld deposit, similar to that observed in sample P14.

The loss of ΔMn and ΔSi by MgO-CaF_2 mixture could be justified as the addition of MgO in CaF_2 increases density and decreases conductivity of the melt (Ref. 15), which may hinder the transfer of Mn and Si across slag-metal interface. The other mixture CaO-MgO has a binary antagonistic (loss) effect on Si content. This behavior is associated with the reduction of SiO_2 activity by formation of complex silicates (Ref. 32). With the reduction of SiO_2 activity, the transfer of Si into the weld metal also decreased.

Table 6 — Predominant Effect of Flux Ingredients and Their Binary Mixtures on Weld Metal Delta (Δ) Quantities

(Responses) Weld Metal Delta (Δ) quantities	Predominant Effects: Pure Flux Ingredient — Increase	Pure Flux Ingredient — Decrease	Binary Mixtures of Flux Ingredient — Synergism	Binary Mixtures of Flux Ingredient — Antagonism
ΔO_2	CaO, Al_2O_3	—	Mgo-CaF_2 MgO-Al_2O_3 CaF_2-Al_2O_3	CaO-MgO, CaO-CaF_2, CaO-Al_2O_3
Δ Mn	MgO	CaO	CaO-CaF_2, CaO-Al_2O_3	MgO-CaF_2 MgO-Al_2O_3
Δ Si	CaO, MgO, CaF_2, Al_2O_3	—	—	CaO-CaF_2, MgO-CaF_2 MgO-Al_2O_3 CaO-MgO,
Δ S	MgO, CaF_2, Al_2O_3	—	—	CaO-CaF_2, CaO-Al_2O_3 MgO-MgO, MgO-Al_2O_3
Δ C	MgO, CaF_2	—	CaO-CaF_2, CaO-Al_2O_3	CaO-MgO, MgO-CaF_2 MgO-Al_2O_3
O_2	CaO, $CaF_2Al_2O_3$	—	MgO-CaF_2, MgO-Al_2O_3 CaF_2-Al_2O_3	CaO-MgO, CaO-CaF_2, CaO-Al_2O_3

Transfer of Sulfur

The prediction results given in Table 6 show that individual flux ingredients CaO, MgO, CaF_2, and Al_2O_3 are responsible for the gain of sulfur in the weld metal. Whereas, the binary mixtures, viz. CaO-MgO, CaO-CaF_2, CaO-Al_2O_3, MgO-CaF_2, and MgO-Al_2O_3 causes loss of sulfur (desulfurization) from the weld metal. It has been observed by U. Mitra and T. W. Eagar (Ref. 8) that apart from flux basicity, type of flux also has a significant influence on sulfur transfer. In steel making, sulfur is removed by reduction reaction. Desulfurization is promoted by high-basicity and low-oxygen potential of the flux. In order to find out the effect of flux ingredients as well as their binary mixtures on weld metal oxygen content, prediction equations were developed for oxygen content as given below.

$$\text{Oxygen } (O_2 \text{ ppm}) = 63.305 \text{ CaO} - 12.420 \text{ MgO} - 6.457 \text{ CaF}_2 - 16.775 \text{ Al}_2\text{O}_3 - 0.945 \text{ CaO.MgO} - 1.557 \text{ CaO.CaF}_2 - 2.061 \text{ CaO. Al}_2\text{O}_3 + 0.835 \text{ MgO.CaF}_2 + 0.767 \text{ MgO.Al}_2\text{O}_3 + 0.378 \text{ CaF}_2\text{.Al}_2\text{O}_3 \quad (9)$$

The predominant effects of flux ingre-

Table 7 — Randomly Designed Submerged Arc Flux Composition

Sample No.	Mixture Variables Composition: CaO (wt-%)	MgO (wt-%)	CaF_2 (wt-%)	Al_2O_3 (wt-%)
T1	17	20	30	13
T2	30	15	15	20
T3	25	30	15	10
T4	15	25	10	30
T5	20	28	12	20
T6	23	27	15	15
T7	19	18	11	32
T8	16	17	25	22

N.B.: Other additions to flux samples. SiO_2=10 wt-%, Fe-Mn=4.0 wt-%, Fe-Si=3.0 wt-%, bentonite=3.0.

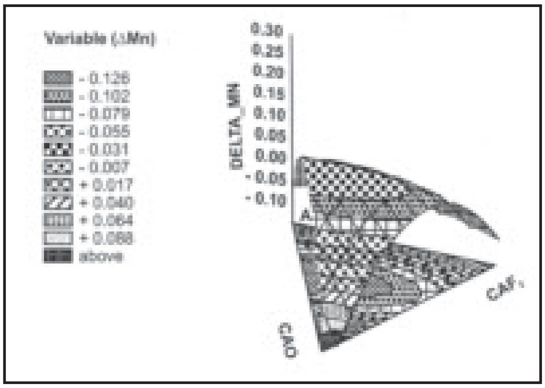

Fig. 12 — Fillet surface contour in three dimension for weld metal ΔMn.

dients and their binary mixtures are also incorporated in Table 6. The statistical details of the equations are given in Appendixes 2 and 3.

Since CaO, CaF_2, and Al_2O_3 increase weld metal oxygen content, as given in Table 6, desulfurization reaction will not be favored by these ingredients due to the reason that sulfur is removed by reduction reaction (Refs. 8, 9), therefore these three ingredients will help the gain of sulfur in the weld metal. However, MgO was not reported to increase weld metal oxygen content (Table 6). In spite of that, the gaining of sulfur by MgO indicates MgO is not capable of desulfurization. The probable reason may be 1) the radius of Mg^{2+} ions (0.78°A) is less than that of Ca^{2+} ions (1.06°A), 2) the stability of MgS is less than that of CaS, and 3) the solubility of desulfurization product MgS in weld metal is more than that of CaS (Ref. 34). All these phenomena probably reduce the sulfur absorbing capacity of MgO in the flux.

The loss of sulfur by CaO-MgO flux mixture (Table 6) could be due to an increase in free oxygen ion with addition of basic oxide and a decrease in the content of Fe^{++} by dilution. Both of these circumstances are favorable to the desulfurization process (Ref. 35). On the other hand, loss of sulfur by flux mixtures MgO-Al_2O_3 and CaO-Al_2O_3 could be due to the formation of oxygen ion in the slag, which results in the formation of a complex compound by the reaction of aluminate ion (or silicon aluminate ion) with the sulfur ion (Ref. 35). Furthermore, since CaO-CaF_2 and CaO-Al_2O_3 mixtures decrease (binary antagonism) oxygen content (Table 6), desulfurization reactions will be favored by these two mixture also, leading to loss of sulfur in the weld metal.

Adequacy of the Developed Prediction Equation

The adequacy of the prediction equations for weld metal delta quantities was checked by performing submerged arc welding using randomly designed fluxes — Table 7. The experimentally determined and theoretically predicted results of ΔO_2, ΔMn, ΔSi, and ΔS are compared graphically in Fig. 10. It is observed from Fig. 10 that there is reasonably good agreement between the experimental and predicted results. Therefore, we may infer that the prediction model is quite adequate in describing weld metal delta (Δ) equation, viz. ΔO_2, ΔMn, ΔSi, and ΔS.

Occasionally experiments are planned to be performed in some reasonably well-defined region of interest, centered about the operating conditions. The reason for exploring the region of interest is to see if there are other blends (mixture) in the vicinity of current conditions that can produce a response similar to or better than those currently being produced (Ref. 36). These response contour plots will be a useful tool for the designer in selecting the proper flux ingredient (composition) ranges in order to achieve their desired target value of that response.

The iso-response contour plots for selected responses, such as weld metal delta oxygen content and delta manganese content, were developed in the present experiment as an example. These are shown in Fig. 11A and B, respectively. The iso-response contour plots in three dimensions has been developed for the selected response (ΔMn), as shown in Fig. 12. The shades in each of these iso-response contour plots represent the value of the responses that may be achievable at different combinations of flux ingredients in the present set of experiments.

Conclusions

Following conclusions can be drawn from this study:

1) The transfer of elements, viz oxygen, manganese, silicon, and sulfur across the weld pool in submerged arc welding (SAW) can be predicted by developing suitable regression models with the help of statistical design of mixture experiments.

2) The variation of transfer of elements across the weld pool is primarily due to chemical reactions associated with SAW fluxes at fixed levels of the welding parameters.

3) Increase in viscosity by CaO and suboxide formation properties by Al_2O_3 are also the reason for oxygen transfer from flux to weld.

4) The interaction of CaO with CaF_2 and Al_2O_3 results in the loss of oxygen (refining) and a gain of manganese (alloying) content in the weld metal. However, the interaction of MgO with CaF_2 and Al_2O_3 shows an opposite effect toward oxygen and manganese transfer.

5) Gain of manganese in the weld metal resulted from an electrochemical reaction in the weld pool.

6) Gain of silicon in the weld metal was due to thermochemical dissociation and electrochemical reaction in the weld pool.

7) Transfer of sulfur from weld to flux is affected by an increase in oxygen in the molten weld pool. Low carbon is mainly due to the oxidation of available oxygen in molten weld pool.

References

1. Davis, M. L. E., and Bailey, N. 1980. How submerged arc flux composition influences element transfer. *International Conference on Trends in Steels and Consumables for Welding*. The welding Institute, London, UK: Paper 34, pp. 289–302.

2. Davis, M. L. E., and Bailey, N. 1978. Have we the right ideas about fluxes? *Proceedings of the International Conferences on Trends in Steels and Consumables for Welding*. The Welding Institute, London, UK: Paper 19, pp. 231–247.

3. Olson, D. L. 1989. Keynote address. The fundamentals of welding consumables. *Proceedings of the 2nd International Conference on Trends in Welding Research*, Gattlinburg, Tenn., pp. 551–562.

4. Davis, M. L. E., and Coe, F. R. 1977. The chemistry of submerged arc welding fluxes. The Welding Institute Research Report: 39/1977/M, May, pp. 1–61.

5. North, T. H., Bell, H. B., Nowicki, A., and Cray, I. 1978. Slag/metal interaction, oxygen and toughness in submerged arc welding. *Welding Journal* 57: 63–75.

6. Chai, C. S., and Eagar, T. W. 1982. Slag metal reactions in binary CaF_2 — metal oxide welding fluxes. *Welding Journal* 61(7): 229–232.

7. Indacochea, J. E., Blander, M., Christensen, N., and Olson, D. L. 1985. Chemical reactions during submerged arc welding with FeO – MnO – SiO_2 fluxes. *Metallurgical Transactions* B, Vol. 16 B, pp. 237–245.

8. Mitra, U., and Eagar, T. W. 1984. Slag metal reactions during submerged arc welding of alloy steels. *Metallurgical Transactions* A, Vol. 15A, pp. 217–227.

9. Mitra, U., and Eagar, T. W. 1991. Slag metal reactions during welding, Part III, verification of the theory. *Metallurgical Transactions* B, pp. 83–100.

10. Lau, T., Weatherly, G. C., and Mclean, A. 1985. The source of oxygen and nitrogen contamination in submerged arc welding using CaO-Al_2O_3-based fluxes. *Welding Journal* 64(12): 343–347.

11. Natalie, C. A., Olson, D. L., and Blander, M. 1990. Weld-pool pyrometallurgy. *Welding: Theory and Practice*, Ed. D. L. Olson,

— continued on page 146-s

Appendix 1 — Standard Error, t Statistic, Level of Significance and Confidence Interval for the Responses (Dependent Variables)

Response: Weld Metal Delta Oxygen (ΔO_2) Content

Effect	Std. Error	t Statistic	P Significance	Confidence Interval (95%) Lower	Confidence Interval (95%) Upper
CaO	6.651202	8.86032	0.000000	45.6362	72.22735
MgO	9.177225	–1.87863	0.064999	–35.5856	1.10441
CaF_2	2.708845	0.97910	0.331337	–2.7627	8.06713
Al_2O_3	3.385175	3.77529	0.000360	6.0131	19.54688
CaO.MgO	0.272755	–3.33137	0.001460	–1.4539	–0.36342
$CaO.CaF_2$	0.193945	–7.94330	0.000000	–1.9282	–1.15287
$MgO.CaF_2$	0.248777	3.44178	0.001040	0.3589	1.35354
$CaO.Al_2O_3$	0.211295	–9.66250	0.000000	–2.4640	–1.61926
$MgO.Al_2O_3$	0.264115	3.01597	0.003711	0.2686	1.32452
$CaF_2.Al_2O_3$	0.175454	2.08681	0.041024	0.0154	0.71687

Response: Weld Metal Delta Manganese (ΔMn) Content

Effect	Std. Error	t Statistic	P Significance	Confidence Interval (95%) Lower	Confidence Interval (95%) Upper
CaO	0.006001	–4.97699	0.000005	–0.041862	–0.017871
MgO	0.008280	6.73601	0.000000	0.039223	0.072326
CaF_2	0.002444	–1.76890	0.081829	–0.009209	0.000562
Al_2O_3	0.003054	–0.72955	0.468413	–0.008334	0.003877
CaO.MgO	0.000246	–1.92738	0.058517	–0.000966	0.000018
$CaO.CaF_2$	0.000175	7.00053	0.000000	0.000875	0.001575
$MgO.CaF_2$	0.000224	–6.02449	0.000000	–0.001801	–0.000904
$CaO.Al_2O_3$	0.000191	7.14100	0.000000	0.000980	0.001742
$MgO.Al_2O_3$	0.000238	–6.42759	0.000000	–0.002008	–0.001055
$CaF_2.Al_2O_3$	0.000158	1.28571	0.203325	–0.000113	0.000520

Response: Weld Metal Delta Silicon (ΔSi) Content

Effect	Std. Error	t Statistic	P Significance	Confidence Interval (95%) Lower	Confidence Interval (95%) Upper
CaO	0.004538	2.68324	0.009336	0.003105	0.021247
MgO	0.006261	8.88579	0.000000	0.043119	0.068151
CaF_2	0.001848	3.41049	0.001146	0.002609	0.009997
Al_2O_3	0.002310	5.87068	0.000000	0.008942	0.018175
CaO.MgO	0.000186	–7.32795	0.000000	–0.001736	–0.000992
$CaO.CaF_2$	0.000132	–0.47717	0.634916	–0.000328	0.000201
$MgO.CaF_2$	0.000170	–7.84564	0.000000	0.001671	–0.000992
$CaO.Al_2O_3$	0.000144	–1.31626	0.192834	–0.000478	0.000098
$MgO.Al_2O_3$	0.000180	–7.92859	0.000000	–0.001789	–0.001068
$CaF_2.Al_2O_3$	0.0000120	1.83448	0.071365	–0.000020	0.000459

Response: Weld Metal Delta Sulphur (ΔS) Content

Effect	Std. Error	t Statistic	P Significance	Confidence Interval (95%) Lower	Confidence Interval (95%) Upper
CaO	0.000495	5.91035	0.000000	0.001937	0.003917
MgO	0.000683	6.87823	0.000000	0.003334	0.006066
CaF_2	0.000202	8.13973	0.000000	0.001239	0.002045
Al_2O_3	0.000252	8.22036	0.000000	0.001568	0.002576
CaO.MgO	0.000020	–7.83173	0.000000	–0.000200	–0.000118
$CaO.CaF_2$	0.000014	–4.86116	0.000008	–0.000099	–0.000041
$MgO.CaF_2$	0.000019	–5.53316	0.000001	–0.000140	–0.000065
$CaO.Al_2O_3$	0.000016	–5.03865	0.000004	–0.000111	–0.000048
$MgO.Al_2O_3$	0.000020	–6.03380	0.000000	–0.000158	–0.000079
$CaF_2.Al_2O_3$	–0.000019	–1.48386	0.142913	–0.000045	0.000007

Response: Weld Metal Delta Carbon (ΔC) Content

Effect	Std. Error	t Statistic	P Significance	Confidence Interval (95%) Lower	Confidence Interval (95%) Upper
CaO	0.001039	–1.64773	0.104468	–0.004399	0.000365
MgO	0.001433	5.06798	0.000004	0.004399	0.010129
CaF_2	0.000423	3.01568	0.003714	0.000430	0.002121
Al_2O_3	0.000529	–0.81781	0.416599	–0.001489	0.000624
CaO.MgO	0.000043	–2.93944	0.004615	–0.000210	–0.000040
$CaO.CaF_2$	0.000030	2.38676	0.020062	0.000012	0.000133
$MgO.CaF_2$	0.000039	–4.96770	0.000006	–0.000271	–0.000115
$CaO.Al_2O_3$	0.000033	5.25772	0.000002	0.000108	0.000239
$MgO.Al_2O_3$	0.000041	–4.41123	0.000042	–0.000264	–0.000100
$CaF_2.Al_2O_3$	0.000027	0.93231	0.354781	–0.000080	0.000029

Appendix 2 — Text of Whole Mixture Model for the Responses (Dependent Variables)

Dependent Variable	R^2	SS Model	df Model	MS Model	SS Residual	df Residual	MS Residual	F Value	P Significance
Delta O_2	0.686865	467971.5	9	51996.84	213343.9	62	3441.031	15.11083	0.000000
Delta Mn	0.648355	0.370643	9	0.041183	0.201023	62	0.003242	12.70159	0.000000
Delta Si	0.682053	0.212610	9	0.023623	0.099110	62	0.001599	14.77791	0.000000
Delta S	0.382705	0.005212	9	0.000579	0.008406	62	0.000136	4.270905	0.000242
Delta C	0.528908	0.006010	9	0.000668	0.005353	62	0.000086	7.734355	0.000000
Oxygen content	0.680338	476622.7	9	52958.02	223945.3	62	3612.02	14.66162	0.000000

Appendix 3 — Standard Error, t Statistic, Level of Significance, and Confidence Interval for the Responses

Response: Weld Metal Oxygen Content

Effect	Std. Error	t Statistic	P Significance	Confidence Interval (95%) Lower	Upper
CaO	6.814592	9.28970	0.000000	49.6834	76.92770
MgO	9.402668	–1.32095	0.191373	–32.2161	6.37522
CaF_2	2.775389	2.32653	0.023273	0.9061	12.00495
Al_2O_3	3.468333	4.83663	0.000009	9.8420	23.70816
CaO.MgO	0.279456	–3.38446	0.001241	–1.5044	–0.38718
CaO.CaF_2	0.198709	–7.83541	0.000000	–1.9542	–1.15975
MgO.CaF_2	0.254888	3.27729	0.001720	0.3258	1.34486
CaO.Al_2O_3	0.216486	–9.52158	0.000000	–2.4940	–1.62854
MgO.Al_2O_3	0.270603	2.83515	0.006177	0.2263	1.30813
CaF_2.Al_2O_3	0.179764	2.10640	0.039224	0.0193	0.73800

— continued from page 144-s

R. Dixon, and A. L. Liby, chapter 5, Elsevier Science publishers, B.V., pp. 151–173.

12. Moor, M. A. B, North, T. H., and Bell, H. B. 1978. Characteristic properties of flux formulations used in submerged arc welding, *Welding and Metal Fabrication*, (4): 193–199.

13. Eagar, T. W. Oxygen and nitrogen contamination during arc welding. *Weldments: Physical Metallurgy and Failure Phenomena*, also E. J. Charistofel, et al., p. 31, Schenectady, N. Y., General Electric Co.

14. Schwemmer, D. D., Olson, D. L., and Williamson, D. L. 1979. The relationship of weld penetration to the welding flux. *Welding Journal* 58(5): 153-s to 160-s.

15. Mills, K. C., and Keene, B. J. 1981. Physicochemical properties of molten CaF_2-based slags. *International Metals Review*, No. 1, pp. 21–69.

16. Indacochea, J. E., and Olson, D. L. 1983. Relationship of weld metal microstructure and penetration to weld metal oxygen content. *Journal Materials for Energy Systems*, ASM Iinternational, Vol. 5, No. 3, pp. 139–148.

17. Polar, A., Indacochea, J. E., and Blander, M. 1990. Electrochemically generated oxygen contamination in submerged arc welding. *Welding Journal* 69(2): 68–74.

18. Chai, C. S., and Eagar, T. W. 1981. Slag-metal equilibrium during submerged arc welding. *Metallurgical Transactions B*, Vol. 12B, (9): 539–547.

19. Polar, A., Indacochea, J. E., and Blander, M. 1991. Fundamentals of the chemical behavior of select welding fluxes. *Welding Journal* 70(1): 15–19.

20. Indacochea, J. E., Blander, M., and Shah, S. 1989. Submerged arc welding: Evidence for electrochemical effects on the weld pool. *Welding Journal* 68(3): 77–83.

21. Kim, J. H., Frost, R. H., Olson, D. L., and Blander, M. 1990. Effect of electrochemical reactions on submerged arc weld metal compositions. *Welding Journal* 69(12): 446–453.

22. Blander, M., and Olson, D. L. 1986. Electrochemical effects on weld pool chemistry in submerged arc and D.C. electroslag welding. *Proceedings of the International Conference on Trends in Welding Research*, Gatlinburg, Tenn., ASM International, 8605-007, pp. 363–366.

23. Dallam, C. B., Liu, S., and Olson, D. L. 1985. Flux composition dependence of microstructure and toughness of submerged arc HSLA weldments. *Welding Journal* 64(5): 140–150.

24. Dunn, P. S., Natalie, C. A., and Olson, D. L. 1986. Sol-gel fluxes for flux cored welding consumables. *Journal of Materials for Energy Systems*. Vol. 8, No. 2, pp. 176–184.

25. Burck, P. A., Indacochea, J. E., and Olson, D. L. 1990. Effects of welding flux additions on 4340 steel weld metal composition. *Welding Journal* 69(3): 115–122.

26. Mclean, R. A., and Anderson, V. L. 1966. Extreme vertices design of mixture experiments. *Technometrics*, Vol. 8, pp. 447–454.

27. Snee, R. D., and Marquardt, D. W. 1976. Screening concepts and designs for experiments with mixture. *Technometrics*, Vol. 18, pp. 19–29.

28. Snee, R. D., and Marquardt, D. W. 1974. Extreme vertices designs for linear mixture models. *Technometrics*, Vol. 16, pp. 399–408.

29. Snee, R. D. 1979. Experimental designs for mixture systems with multicomponent constraints. *Communications in Statistics: Theory and Methods*, Vol. A8, No. 4, pp. 303–326.

30. Moore, J. J. *Chemical Metallurgy*, Chapter 5, slag chemistry, 2nd edition, pp. 152–172.

31. Surian, E. 1997. ANSI/AWS E7024 SMAW Electrodes: The effect of coating magnesium additions. *Welding Journal* 76(10): 404–411.

32. Dean, J. A. *Langes Handbook of Chemistry*, formerly compiled and edited by N. A. Langi, thirteenth edition, McGraw Hill Book Co., Sec. 9: 13–14, Sec 4, pp. 15, 35, and 71.

33. Davis, M. L. E., and Bailey, N. 1991. Evidence from inclusion chemistry of element transfer during submerged arc welding. *Welding Journal* 70(2): 57–66.

34. Oiks, G. Converter and open hearth steel manufacture. *Fundamentals of Theory and Technology*, MIR Publishers, Moscow, pp. 97–200, 324–334.

35. Herasymanko, P., and Speight, G. E. 1950. Ionic theory of slag metal equillibria, Part-II, applications to the basic, open hearth process. *Journal of Iron and Steel Institute*, (12): 289–303.

36. Cornell, J. A. *Experiments with Mixtures, Designs, Models and the Analysis of Mixture Data*, John Willey & Sons, Chapter 3, The use of independent variables, pp. 65–109.

OMEGA™ and MB - Air-Cooled Guns designed for industrial durability...

OMEGA™ MIG-GUNS - Light-Medium-Heavy Industrial - Removable neck

- 250, 350 and 450 amperes
- Full 360° positionable and removable swannecks
- One - piece rigid swannecks with covered armor jackets for operator comfort
- Tight tolerance interface, direct crimped torch body, and neck locking screw enable optimal current transfer
- Slip-on and threaded nozzles
- Optional neck liners for gun liner cost savings

MB MIG-GUNS - Industrial Fixed Neck

- 180 and 350 amperes
- Fixed swanneck design
- Multiple handle options
- Proven design for durability and operator appeal

ABICOR BINZEL®

Alexander Binzel Corporation
650 Research Drive, Suite 110
Frederick, Maryland 21703
Phone: 800.542.4867
Fax: 301.846.4497

INDUSTRIAL DURABILITY - for any application

Circle No. 1 on Reader Info-Card

www.abicorusa.com